Deltares

An Analysis of the Physical Coastal System along East Coast Park, Singapore

Daniel Martens

1203082-000

Deltares

Title
An Analysis of the Physical Coastal System along East Coast Park, Singapore

Client	Project	Pages
EcoShape	1203082-000	136

Keywords
Singapore, East Coast Park, coastal erosion, structurally controlled coast, headland control, conceptual model, temporal and spatial morphological scales, cross- and longshore sediment transport, waves, tide, monsoons, eustatic sea level rise, land subsidence

Abstract
The Republic of Singapore, or commonly referred to as Singapore, is the smallest nation in Southeast Asia and it is well protected from the open oceans by the surrounding land masses. Its total surface area has increased by more than 20% since the 1960s due to intensive land reclamations, for which the main reason was to create more accommodation space for the increasing population. Along the southeast coast of Singapore, some 1.85 km^2 was reclaimed for recreational purposes, resulting in a 15 km long coastal park called *East Coast Park*.

East Coast Park is built on entirely reclaimed land and comprises a sandy shoreline. The beaches along this shoreline are formed due to the implementation of anthropogenic structures all along this stretch of coast through so-called *headland control*. These structures were meant to stabilise the newly reclaimed land, which was placed on top of an unconsolidated thick layer of marine clay. In time, however, several phenomena have occurred along this new stretch of coast, indicating coastline retreat due to erosion and in some cases also flooding of the coastal area. Researchers of the EcoShape Consortium have therefore decided to investigate the possibility of applying the so-called *Building with Nature* principles in solutions to coastline retreat along East Coast Park, resulting in the *East Coast Park design pilot*. A key aspect in this investigation is the understanding of the underlying coastal processes, which has resulted in the study before you.

In this study an analysis is made of knowledge to date and a conceptual model is developed to analyse coastal processes on both a small and a large scale. Driving forces underlying these processes are waves, the tide, monsoons and relative sea level rise. On the large scale the influence of waves, the tide and relative sea level rise on the coastal morphology is assessed (semi-)quantitatively using numerical modelling tools Delft3D, Unibest-TC and Unibest-LT, but also using nautical charts and satellite imagery. On this scale the presence of anthropogenic structures is neglected. On the small scale the presence of structures is included. Due to insufficiently readily available data the assessment is made more quantitatively, using satellite imagery and photographs.

Version	Date	Author	Initials	Review	Initials	Approval	Initials
	may 2013	D. Martens		M.C.J.L. Jeuken		T. Schilperoort	

State
final

AN ANALYSIS OF THE PHYSICAL COASTAL SYSTEM ALONG EAST COAST PARK, SINGAPORE

by

Daniel Martens

A thesis submitted in partial fulfillment of the

requirements for the degree of

Master of Science

in the field of

Civil Engineering

at

Delft University of Technology

Delft, The Netherlands

Submitted for approval on

May 14, 2013

Graduation committee

Prof.dr.ir. M.J.F. Stive	Chairman, Delft University of Technology
Dr. M.C.J.L. Jeuken	Deltares / EcoShape
Dr.ir. J.S.M. van Thiel de Vries	Deltares / Delft University of Technology
Dr.ir. G.J. de Boer	Deltares / Delft University of Technology
Dr. S.K. Ooi	National University of Singapore / Singapore-Delft Water Alliance
Dr. D.K. Raju	National University of Singapore / Tropical Marine Science Institute

An Analysis of the Physical Coastal System along East Coast Park, Singapore
D. Martens / May 14, 2013

This research was carried out at:
Deltares
Rotterdamseweg 185
2600 MH Delft
The Netherlands

and

Singapore-Delft Water Alliance (SDWA)
EW1 02-05
2 Engineering Drive 2
Singapore 117577
Singapore

January 19, 1822

At twelve o'clock to-day we passed the narrow channel of the Rabbit and Coney, the western entrance of the Straits of Singapore, and soon found ourselves surrounded in every direction by beautiful verdant islands. The sea was smooth, the sky clear, and the whole prospect equally novel and pleasing. From the deck there could be counted between fifty and sixty green and woody islands of various dimensions, and from the mast-head above seventy. I do not believe there is any part of the world which can afford a prospect, in its way, of superior beauty, and this indeed has been observed and confessed by all voyagers. The prospect we had on entering the Singapore coast was beautiful and unexpected. We found ourselves completely landlocked, in every direction, by the green and woody shores of the islands surrounding us; and the sea, though considerably ruffled without, was here as smooth as glass.

John Crawfurd (1783 - 1868)

From *Journal of an Embassy from the Governor-General of India to the Courts of Siam and Cochin China, Vol. 1,* 1830, page 64, dated 19 January 1822

Abstract

The Republic of Singapore, or commonly referred to as Singapore, is the smallest nation in Southeast Asia and it is well protected from the open oceans by the surrounding land masses. Its total surface area has increased by more than 20% since the 1960s due to intensive land reclamations, for which the main reason was to create more accommodation space for the increasing population. Along the southeast coast of Singapore, some 1.85 km^2 was reclaimed for recreational purposes, resulting in a 15 km long coastal park called *East Coast Park*.

East Coast Park lies along the southeast coast of Singapore and it is characterised by a range of sandy beaches, which have been formed after to the implementation of anthropogenic structures all along this stretch of coast. These structures were meant to stabilise the newly reclaimed land, which consists of relatively coarse fill material on top of an unconsolidated thick layer of marine clay. In time, however, several phenomena have occurred along this new stretch of coast, indicating coastline retreat due to erosion and in some cases also flooding of the coastal area. Researchers of the EcoShape Consortium have therefore decided to investigate the possibility of applying the so-called *Building with Nature* principles in solutions to coastline retreat along East Coast Park, resulting in the *East Coast Park design pilot*. A key aspect in this investigation is the understanding of the underlying coastal processes, which has resulted in the study before you.

Due to the fact that only limited data was readily available throughout this study, the (relative) influence of coastal processes has mainly been addressed qualitatively, but where possible quantitatively. In order to assess these processes two scales were analysed separately, namely (1) a (coastal) cell system scale, with a *coastal cell* being a beach enclosed by two adjacent anthropogenic structures, and (2) the ECP system scale, comprising all of the coast along East Coast Park. On these scales different processes contribute to changes in the coastal morphology. These processes are induced by different driving forces, of which we identified (a) waves, (b) tide, (c) monsoon-induced wave variability and (d) relative sea level rise.

Looking at the large-scale system of East Coast Park, we mainly addressed the influence of relative sea level rise on the southeast coast of Singapore. Relative sea level rise consists of both local sea level rise and land subsidence. Local sea level rise is assumed to follow global projections of sea level rise, see also NCCS (2012). Land subsidence, however, is found to be of the same order of magnitude as eustatic sea level rise at the present day, resulting in a local *relative* sea level rise twice as large as the eustatic sea level rise. This has been observed through subsidence of both the land and anthropogenic structures along East Coast Park over the past decades. The effect of land subsidence decreases asymptotically in time, but due to the fact that East Coast Park is relatively young the effect is assumed to be still significant for the upcoming years to decades.

From the analysis of the small-scale system of coastal cells it was found that the influence of waves is mainly felt in the cross-shore direction rather than the longshore direction. Waves contain too little energy to transport *coarse* sediments alongshore in deeper waters, but are able to cause alongshore drift along the waterline at the beach. This alongshore drift is shown to be varying in time, depending on the angle of wave incidence, which changes due to changing monsoons and wind directions throughout the year. In cross-shore direction sediment is lost due to wave action on the beach berm and beach profile, leading to the

formation of scarps along the beach planform. These results have been obtained using the numerical modelling tools Unibest-TC and Unibest-LT, satellite imagery, bathymetrical charts and photographs. For the influence of the tide on the coastal morphology use has been made of a nested Delft3D model, from which resulted that the influence of the tide is negligible in the nearshore region, since tidal currents pick up (fine) sediments only at a distance of about 200 m offshore.

Relating the small- and the large-scale systems, it can be concluded that the influence of relative sea level rise affects the entire coast, including the small-scale coastal cells, although on relatively large time scales. On shorter time scales *waves* mainly lead to distribution of sediment along the coastal profile, with the effect of the *monsoons* being the dominant contributor. During the more energetic northeast (N.E.) monsoon sediment is distributed over larger distances along the profile, flattening the profile, whereas during the calmer southwest (S.W.) monsoon a steepening of the profile occurs. Angles of wave incidence also change throughout the year, both in between as within the monsoon periods, leading to a (re-)distribution of sediment along the beach profile.

Acknowledgements

Hereby I would like to thank everyone who has supported me throughout this thesis and my studies.

From Deltares I would especially like to thank Claire Jeuken for involving me into the project and for her patience and guidance throughout my thesis. It has been a great opportunity and experience and I am grateful to have been part of it. I want to thank Jaap van Thiel de Vries for his guidance as well, and especially for his inexhaustible positive energy, which has given me a motivating push ahead every time I talked to him. Many thanks go out to Julia Vroom, Jamie Lescinski and Bas van Maren, for making me feel part of the team and for helping me along the way.

I would like to show my gratitude to my supervisors in Singapore, dr. Seng Keat Ooi from the Singapore-Delft Water Alliance for making me feel at home at SDWA and dr. Durairaju Kumaran Raju from the Tropical Marine Science Institute for guiding me during my stay there. Many thanks to Balaji Vaithyanathan, for assisting me and getting soaked with me in the rain during the fieldwork.

I would also like to thank prof. Teh Tiong Sa, whom I hope to meet in person some day, for his advice as a long-time expert on East Coast Park and his permission to re-use his photographs.

Tatjana, thank you for always being there for me, in good and bad times. I cannot imagine my life without such a loving sister, you have made it beautiful and meaningful. I thank my parents for everything they have taught me in life, and most importantly for their unconditional love. Mom, thank you for also being my best friend.

Feng Xue, thank you for being part of my life and for your love and affection. You are an incredible source of inspiration to me. Near or far, you brighten my every day and I look forward to be reunited with you every single second.

I am very grateful to be able to say that there are too many friends I would like to thank personally, for being part of my life, for the inspiration, honesty, laughs, talks, drinks, and so on. As my friend, old or new, you will know that that goes for you as well.

Contents

Appendices

1 Introduction

1.1 Background

Often referred to as the *Little Red Dot* on any map of the world, the Republic of Singapore - or shortly Singapore - is located at the tip of Peninsular Malaysia, along the shortest sea route between China and India. Mainly due to this strategic position Singapore has been able to flourish and establish its position as one of the wealthiest nations in the world, currently having the highest GDP per capita (Knight Frank Research, 2012).

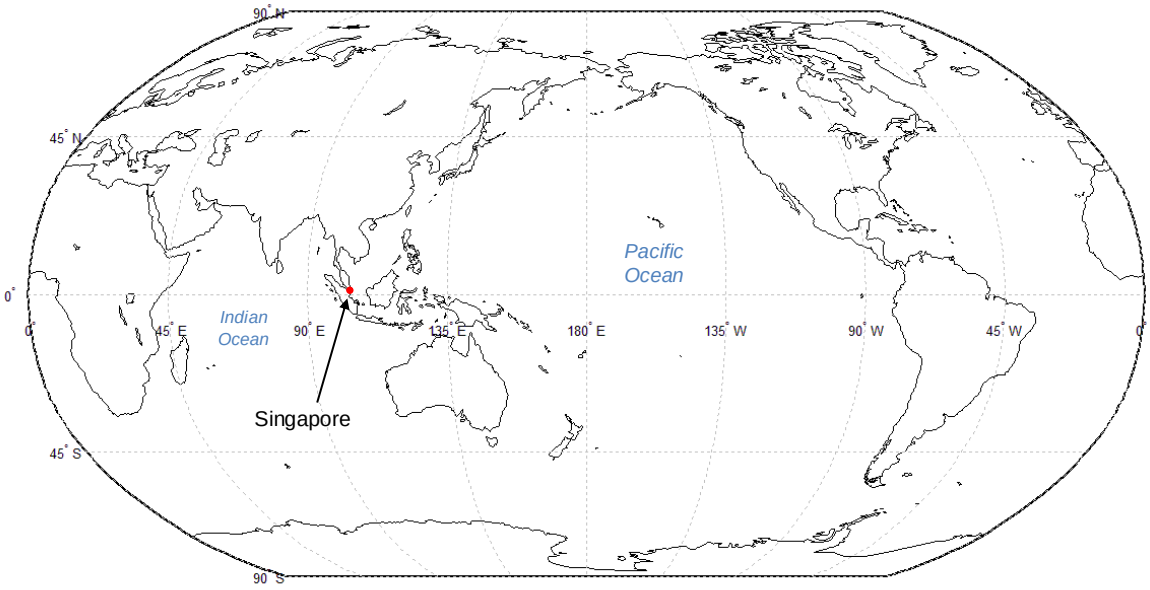

Figure 1.1 Singapore and its location on the globe, indicated according to its epithet 'Little Red Dot'

This ability to flourish also comes with a downside, as economic growth has attracted many foreigners to work and even live on the small island over the past decades, increasing the demand for housing while land availability is scarce. As of 2012, the population of Singapore amounts over 5.3 million people, of whom 62% are citizens and the remaining 38% are permanent residents or foreign workers. With a population density of 7422 people per square kilometre it is currently the third most densely populated country in the world (Department of Statistics, 2012). To get a feeling for the meaning of such numbers a simple comparison can be made, for instance with the Netherlands, one of Europe's most densely populated countries. The total land area of the Netherlands is currently 58 times the total land area of Singapore, while the population amounts *only* three times that of Singapore.

To answer the demand of space and at the same time provide enough space for recreational purposes, some major land reclamation works have been carried out during the second half of the past century. These reclamation works have increased the total land area from 581.5 km^2 in the 1960s to 714.3 km^2 in 2011, an increase of more than 20% in half a century (Department of Statistics, 2012). Nevertheless, land availability remains scarce and the Singaporeans are still actively looking for possible solutions.

Among the reclamation works that have been carried out in previous decades, a series of reclamation works called the East Coast Reclamation Scheme have resulted in the subject of this study. East Coast Park is a beach park of 1.85 km^2 reclaimed land and it is located along the southeast coast of Singapore, see Figure 1.2. East Coast Park serves as a recreational hideout for both locals and tourists, offering a myriad of amenities, such as sporting, dining, public barbecue pits, picnic and camping spots, and beaches all along the 15 km stretch of coastline.

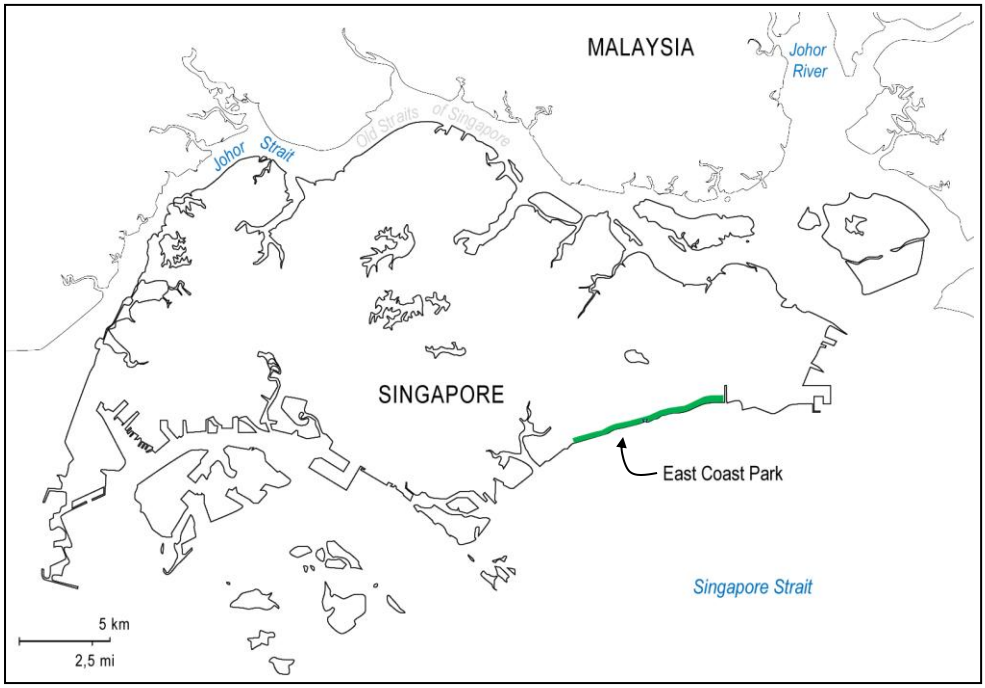

Figure 1.2 Outline map of the islands of Singapore and the tip of southern Peninsular Malaysia. East Coast Park is indicated in green along the southeast coast.

To create an aesthetically attractive and sandy coastline along the southeast, the Singaporeans brought sands from inland hills and from abroad. When the first phases of the reclamation works had been completed in the early 1970s, a series of structures was implemented to protect the newly reclaimed land and to encourage formation of bay-shaped beaches. Despite some changes the structures have undergone in the past decades, both in type as in dimension, they have remained an icon in the worldwide application of structures to stabilise sandy coastlines. Presently a variety of sandy beaches can be found all along the coastline of East Coast Park, where one can enjoy the equatorial waters of the Singapore Strait while looking out over the Indonesian Riau Archipelago to the south.

1.2 Problem description

As mentioned in the previous section, the implementation of structures along East Coast Park was meant to guarantee stability of the coastline, while at the same time stimulating the formation of bay-shaped beaches. Over the past two decades, however, unforeseen erosional phenomena have been observed on several locations along this coastline, as well as occasional inundation landward of the high water mark. Figure 1.3 present a few examples of such phenomena.

Figure 1.3 Photographs all re-used with permission from Teh Tiong-Sa, professor at the National University of Singapore and researcher at the Tropical Marine Science Institute in Singapore: (a) cliff erosion westward of headland 19, 1992; (b) undermining and failure of path due to berm erosion, 2002; (c) berm erosion in the lee of headland 3, 2004; (d) inundation landward of the high water mark during extreme high tide, 2001; (e) inundation and erosion in the lee of a headland, date and location unknown; (f) scarp retreat near McDonald's, 1991. All photographs were taken along East Coast Park. For the locations of the photos reference is made to Figure 3.7. (source: http://geogallers.com/geo/geoteachers.php)

Despite ample studies on the formation of bay-shaped beaches on sandy coasts, on which the implementation of structures along East Coast Park has largely been based, little is still known on the processes and dynamics affecting and reshaping this coastline and causing it to erode. Many of the current arguments given when trying to explain the observed phenomena have a more suggestive character, while concrete evidence remains insufficient or completely absent.

Without a proper understanding of the system, beach management will be based on short-term reactive solutions rather than long-term proactive solutions. Simultaneously, beach management activities might be inefficient or even invoke adverse effects where not applied properly. Therefore care should be taken in the application of new solutions for proper beach management, so that the initial philosophy of working *with* rather than *against* nature is maintained.

1.3 Research objectives

For the reasons mentioned above, researchers of the EcoShape Consortium[i] have decided to build upon the initial ideas of the Singaporeans and investigate alternative methods for working with nature in a tropical coastal environment such as in Singapore, based on the so-called *Building with Nature* principles (Waterman, 2010). In short, the principles aim to integrate natural values and its strengths in engineering solutions.

Applied to East Coast Park, a so-called eco-dynamic design pilot has been initiated, in which various alternatives are proposed, based on the integration of the following fundamental aspects, which are illustrated in Figure 1.4: (1) physics, (2) ecology and (3) socio-economics. A thorough understanding of all three aspects is paramount in order to effectively apply new solutions. In light of that, this study focuses on one of these aspects, namely the physical system.

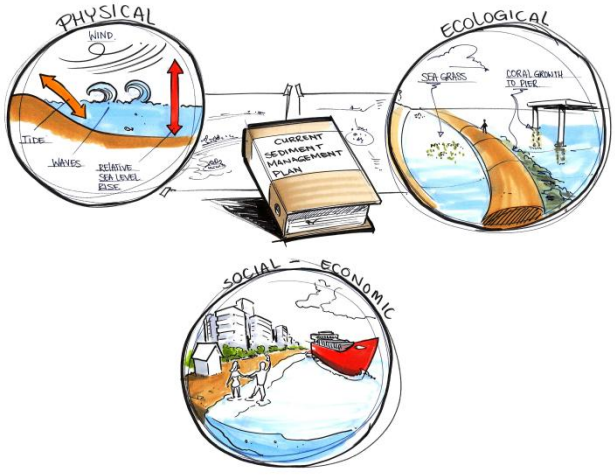

Figure 1.4 Building with Nature key points

[i] *EcoShape Consortium is a collaboration of a variety of parties in the Netherlands, among which Deltares and Delft University of Technology, which aims towards research on and application of the Building with Nature program. For more information visit http://www.ecoshape.nl/*

Following the aforementioned lack of understanding of the physical processes, the study described in this report aims to build upon the knowledge to date and expand this knowledge where possible. Given the fact that raw data is not readily available for East Coast Park, and for Singapore in general, the focus of this study lies mostly on *qualitatively* assessing the various processes influencing the coastal morphology, on both short and long time scales, in order to narrow down knowledge gaps and create a starting point for further research. Where available, a variety of tools has been used to substantiate these assessments *quantitatively*.

To properly carry out the suggested analysis, both a research question and objectives need to be clearly formulated. The research question for this study is:

What are the dominant physical processes causing erosion along the coastline of East Coast Park, Singapore?

The objectives following from this research question are then:

- *To identify the alongshore variation of coastline retreat*
  Based on literature and visual observations retreat seems to occur to different extents along the coast;

- *To qualitatively assess the causes of this alongshore variation*
  Alongshore differences in coastal retreat might be caused by local deviations in bathymetry, coastline orientation, structure orientation, beach-structure interaction and sediment availability. In that case, hydrodynamic boundary conditions and the corresponding coastal processes leading to erosion might vary in alongshore direction as well;

- *To qualitatively assess what happens to eroded material*
  An important aspect is whether there is a structural loss of sediment out of the system, or whether sediment is merely redistributed within the system.

1.4 Thesis outline

Throughout this report some basic knowledge of coastal dynamics is expected from the reader. There is an abundance of literature available through many sources, on both hydrodynamic and morphodynamic processes in general. In this report, a brief explanation is given to substantiate hypotheses where thought necessary, but no chapter is dedicated to repetition of theories. Instead, reference is made to the designated literature.

In Chapter 2 a comprehensive overview of the system considered is given, which is deemed necessary to perform a valid analysis of the presently occurring processes. Firstly, some major geological and geophysical aspects are presented, which can then be related to the climate we observe around Singapore and near the southeast coast in particular. From there on, in Chapter 3, a step will be made to our area of interest: East Coast Park. In this chapter firstly an introduction will be given into the historical changes that have formed the southeast coast of Singapore over the past decades. Thereafter, the coastline at its present state will be presented, which forms the starting point for the further analysis.

Chapter 4 describes the methodology used in this study. The methodology starts with a conceptual model which describes the approach taken in the analysis, using a schematisation of the physical system and its processes. Based on this conceptual model then some research questions and hypotheses are formulated, which form the basis of the analysis in the subsequent chapters. Finally, a concise overview is given on the available tools used in the analysis of Chapters 5 and 6.

In Chapter 5 and 6 the results of the analysis are presented, building upon the hypotheses as described in Chapter 4. Chapter 5 focuses on the large-scale analysis, treating large-scale changes in the coastline and long-term coastal processes. From thereon a step is taken to a smaller scale, assessing short-term processes. From the results of both analyses, finally in Chapter 7 the relation between the different scales is given, relating the processes to the morphological evolution. The chapter ends with concluding remarks and recommendations for further research.

2 Physical system description

2.1 Geological and geophysical aspects

2.1.1 Physical setting

Southeast Asia

Located at the southernmost tip of Peninsular Malaysia, at a latitude of 1° north of the equator, Singapore is the smallest nation in Southeast Asia by area and the second smallest in all of the Asian continent, the first being the Maldives. Contrary to the Maldives, Singapore finds itself sheltered from the larger, open oceanic systems by a range of archipelagos, such as the Indonesian islands relatively nearby and the Philippine archipelago farther eastward, see Figure 2.1. Tectonic activity is common along western Sumatra, note the extensive mountain range, but the activity is too far away to have any substantial effect on Singapore (Chia, Khan, & Chou, 1988). Sumatra has also protected Singapore from any serious impact from the Boxing Day Tsunami that occurred less than a decade ago in the Indian Ocean, and tsunamis occurring in the Pacific Ocean are usually absorbed by the Philippine Archipelago. The coastline of Singapore is thus tectonically stable and resides in a low energy environment. Based on plate tectonics, this coastline can then be classified as a *marginal sea coast* (Bosboom & Stive, 2011). The effect of seismic activity in the Earth's lithosphere is considered negligible in this analysis.

Figure 2.1 Topographic view of part of Southeast Asia, with some of the major cities and the larger seas. The Sunda Shelf, coloured in white blue, averages depths of less than 100 metres and the continental slope marks the 200 metre depth contour. Adapted from http://maps.ngdc.noaa.gov/viewers/bathymetry/

A major part of Southeast Asia is founded on the Sunda Shelf, a stable continental shelf and a southward extension of mainland Southeast Asia, see Figure 2.1. The Sunda Shelf is covered by shallow seas with water depths smaller than 200 m. Locally water depths can exceed 100 metres, but most depths do not exceed 50 metres, particularly in nearshore regions. These relatively small water depths result directly from an extensive build-up of the low-density, quartz-rich underlying crust of which the Sunda Shelf is made of (Gupta, 2005).

Singapore, Malaysia and the Riau Archipelago

The Republic of Singapore consists of 63 islands, of which the main island is the largest and the one comprising our area of interest, East Coast Park. The islands together make up for an area of more than 700 km^2 (Section 1.1) and plans to increase this area even more, albeit not as rapidly, are still ongoing. Most of the land surface of Singapore is less than 15 m above mean sea level, especially along the coasts, with exceptional hills exceeding 100 m in the centre of the main island (Chia et al., 1988).

The borders of Singapore with adjoining countries are roughly indicated in Figure 2.2. The main island, which commonly is referred to when mentioning *Singapore*, bears no *natural* connections with mainland Malaysia, only two man-made crossings. The island is separated from Malaysia by the Johor Strait, formerly known as the *Old Straits of Singapore*.

To the south, the nearest landmasses are part of the Riau Archipelago, a group of islands within the Riau Islands Province of Indonesia. The Singapore Strait separates the Indonesian islands from the Singaporean ones, and forms a narrow connection from the Strait of Malacca in the west to the South China Sea in the east, with widths varying from 5 km at its narrowest cross-section to less than 20 km elsewhere. The Strait of Malacca in its turn flows out into the Andaman Sea, a basin of the Indian Ocean, and the South China Sea in the east forms a basin of the Pacific Ocean (Figure 2.1). Water depths in the Strait of Singapore are on average less than 30 m, while only in certain parts depths larger than 50 m are found. In the narrower part of the strait, just south of Saint John's Island, a deep trench is found with a maximum depth of about 714 m (Chia et al., 1988). The shipping route from the South China Sea to the Malacca Strait and back passes this narrow part of the Singapore Strait.

When comparing the geographical position of Singapore on a more regional scale, such as in Figure 2.2, to its sheltered position from the open oceans as visible in Figure 2.1, it becomes clear how well located the small nation is within Southeast Asia. Also on a more regional scale the nearby landmasses seem to shelter the main island from the surrounding waters, though not excluding it from their benefits such as international navigation. Being a relatively young country, Singapore has undeniably profited from its location. Figure 2.2 shows how the tip of Peninsular Malaysia embraces Singapore from the north, sheltering its northern as well as its western and eastern coastlines, whereas the archipelago to the south forces passage of the strait along the main island and simultaneously reduces the possibility of a large fetch from more southern waters.

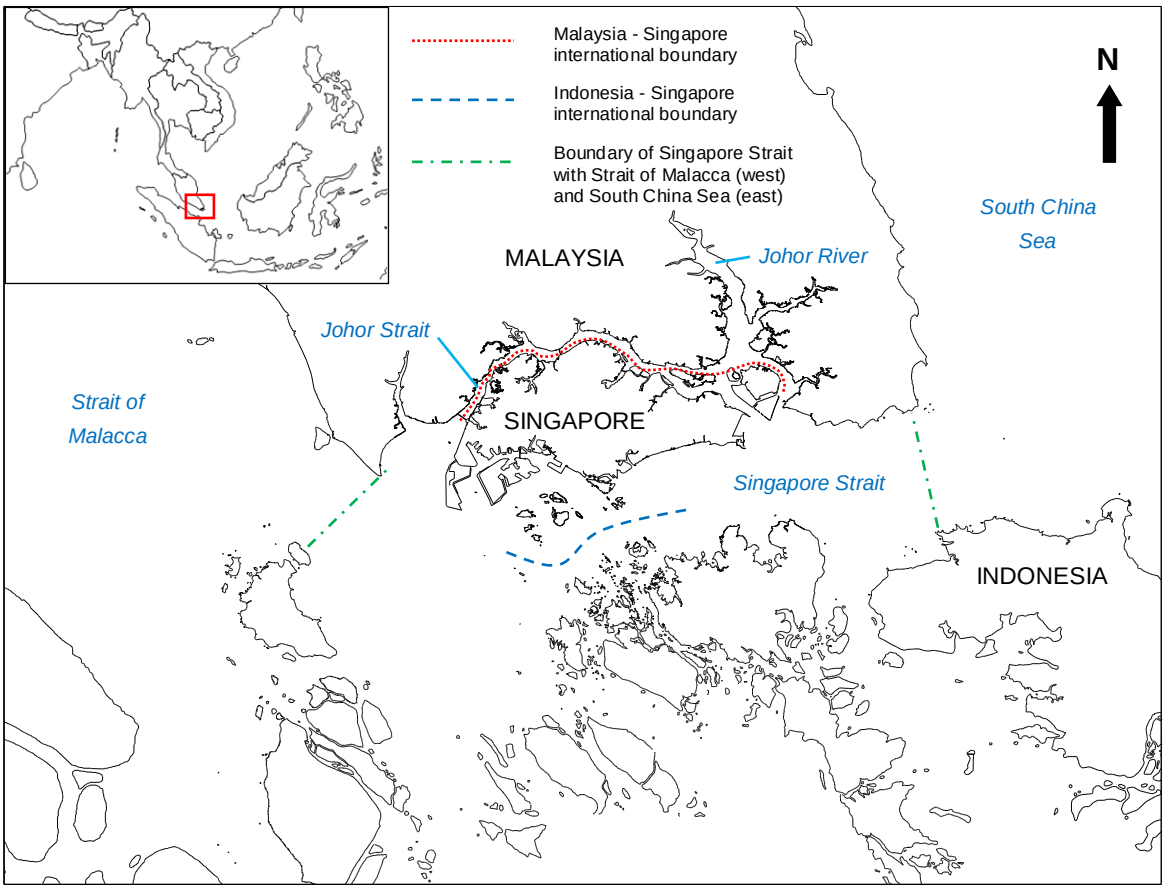

Figure 2.2 Outline map of Singapore and nearby landmasses, and its position in Southeast Asia (mini map).

East Coast Park

As shown earlier in Figure 1.1, East Coast Park covers a significant part of the southeast coast of Singapore. Landward it is bordered by the East Coast Parkway, which serves as a main connection from central Singapore to Changi Airport in the east. In the west, East Coast Park borders Marina East and in the east it borders Tanah Merah, see Figure 2.3. These sections are divided by runoff channels. This stretch of coast is nearly 15 kilometres long, and contrary to Marina East and Tanah Merah it lacks a shore-parallel submerged breakwater offshore of the coastline. Therefore, the shore along East Coast Park remains in direct contact with the waters of the Singapore Strait, both during high and low tidal water levels.

The entire south-eastern coastline of today is built on reclaimed land. An initial intertidal flat had been transformed completely into a sandy shoreline, more on which is discussed in subsequent chapters. The shoreline is under direct influence of the Singapore Strait, and thus also of storms occurring on the South China Sea, which generate swell waves that reach East Coast Park. The climatology is described in more detail in Section 2.2.

Looking at Singapore's geophysical setting, the island nation seems to be ideally located in an environment with high tectonic activity relatively nearby. It is free of volcanic hazards, free of tsunamis, though entirely enclosed by water.

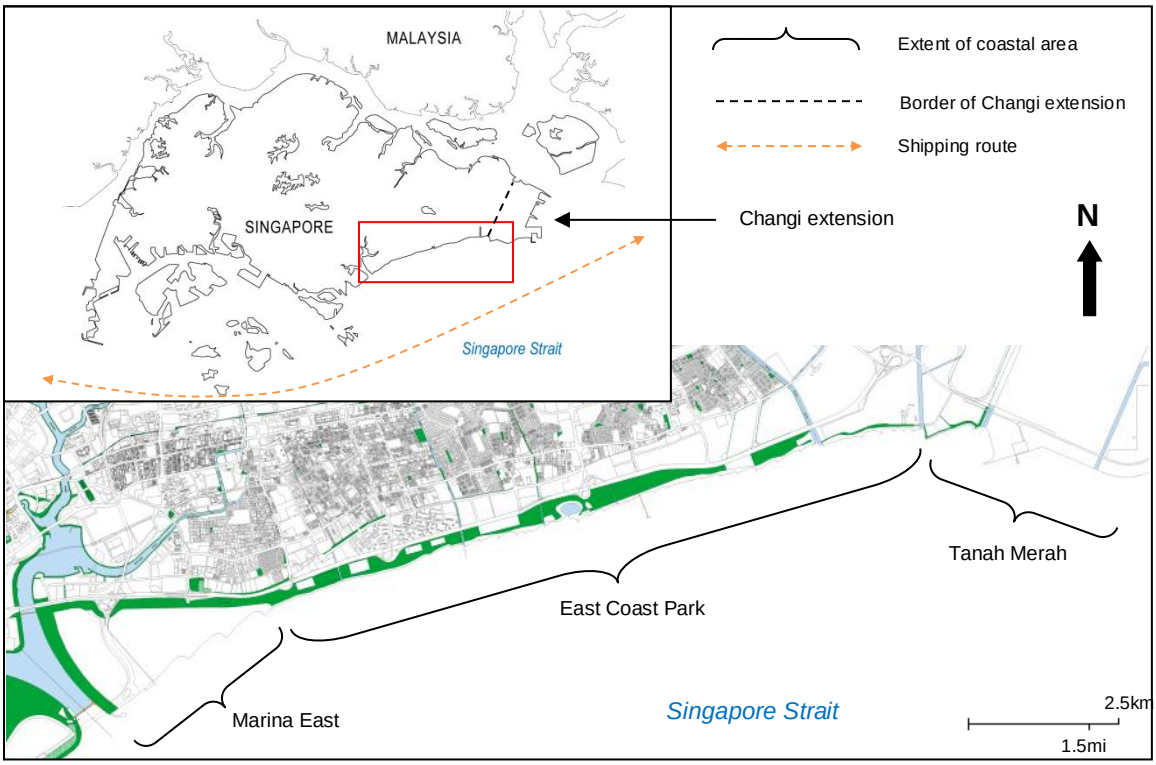

Figure 2.3 The extent of East Coast Park (in green) and an indication of its lateral boundaries which separates it from adjacent Marina East and Tanah Merah

2.1.2 Geological deposits

Historically, six major formations have contributed to the geological deposits on Singapore island to date. These formations are known locally as the Kallang Formation, Old Alluvium, Jurong Formation, Bukit Timah Granite, Gombak Norite and the Sahajat Formation (Chong, 2004). Each formation has its own characteristics and together they have resulted in a large variety in sediment deposits on the island. In our area of interest, the southeast coast of Singapore, the Kallang Formation and the Old Alluvium have been the main contributors to the bottom foundation.

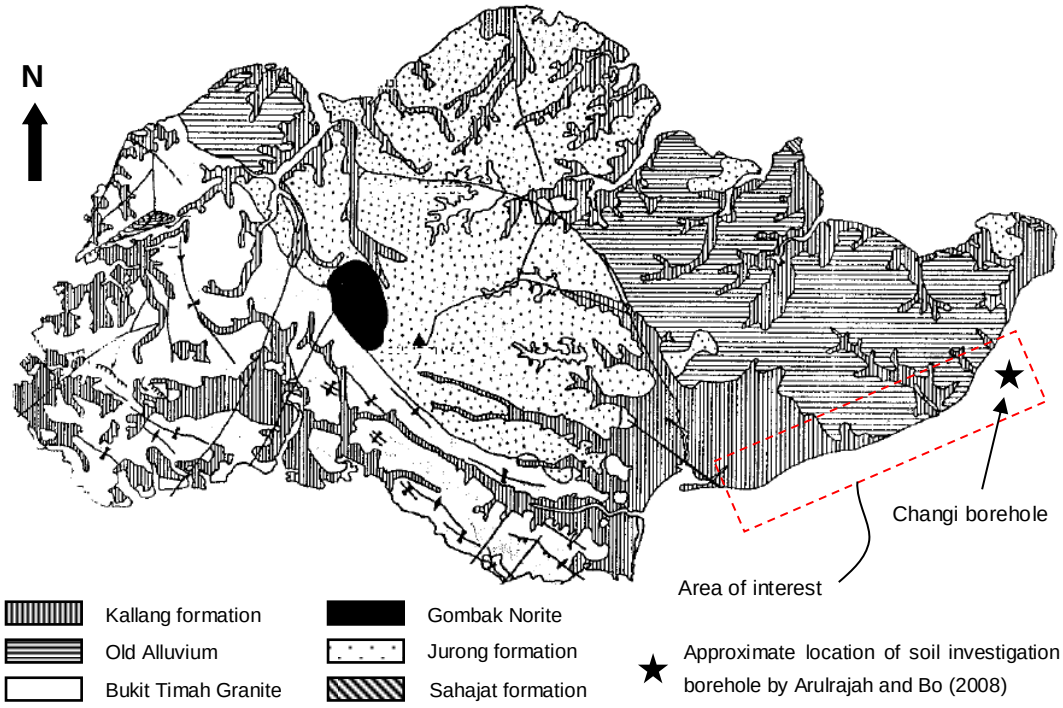

Figure 2.4 Geological map of the main island of Singapore (Adapted from Chong (2004))

The Kallang Formation, which is the more recent formation, is composed of marine, alluvial, littoral and estuarine sedimentary deposits. These deposits cover nearly 25% of the total land surface of the main island of Singapore and support most of the reclaimed land along the southeast coast. The Kallang Formation is generally divided into the Upper and Lower Marine Clay. These two layers are separated by a stiffer intermediate layer, consisting of sandy silt or sandy clay, which in fact is the dried-out layer of the Lower Marine Clay. This drying out is caused by exposure of the seabed to the atmosphere due to falling and rising sea levels in the geological past, starting approximately 75.000 years ago (Arulrajah & Bo, 2008).

Figure 2.5 depicts a soil investigation borehole profile at the Changi extension, of which the approximate location is indicated in Figure 2.4. The profile serves as a good representation of the soil underlying the East Coast Park landfill, where probably only the thickness of the sand fill layer differs from that at Changi. Thicknesses of the underlying Kallang Formation can vary considerably, from 10 to 15 m near estuaries to 40 m elsewhere. The results from Arulrajah and Bo (2008) show that the latter is also the case along the southeast coast of Singapore.

The Upper Marine Clay layer is generally 10 to 20 m thick, and has a high water content and liquid limit, with values ranging from 70% to 88% and 80% to 95%, respectively. The intermediate layer is about 2 to 5 m thick, and the bottom of the Lower Marine Clay reaches depths from 30 to 50 m below the seabed. The water content and liquid limit of this layer are typically less, ranging from 40% to 60% and 65% to 90%, respectively. High water contents commonly tell something about consolidation characteristics of the soil layer, namely the higher the water content the larger the consolidation (rate) of the soil.

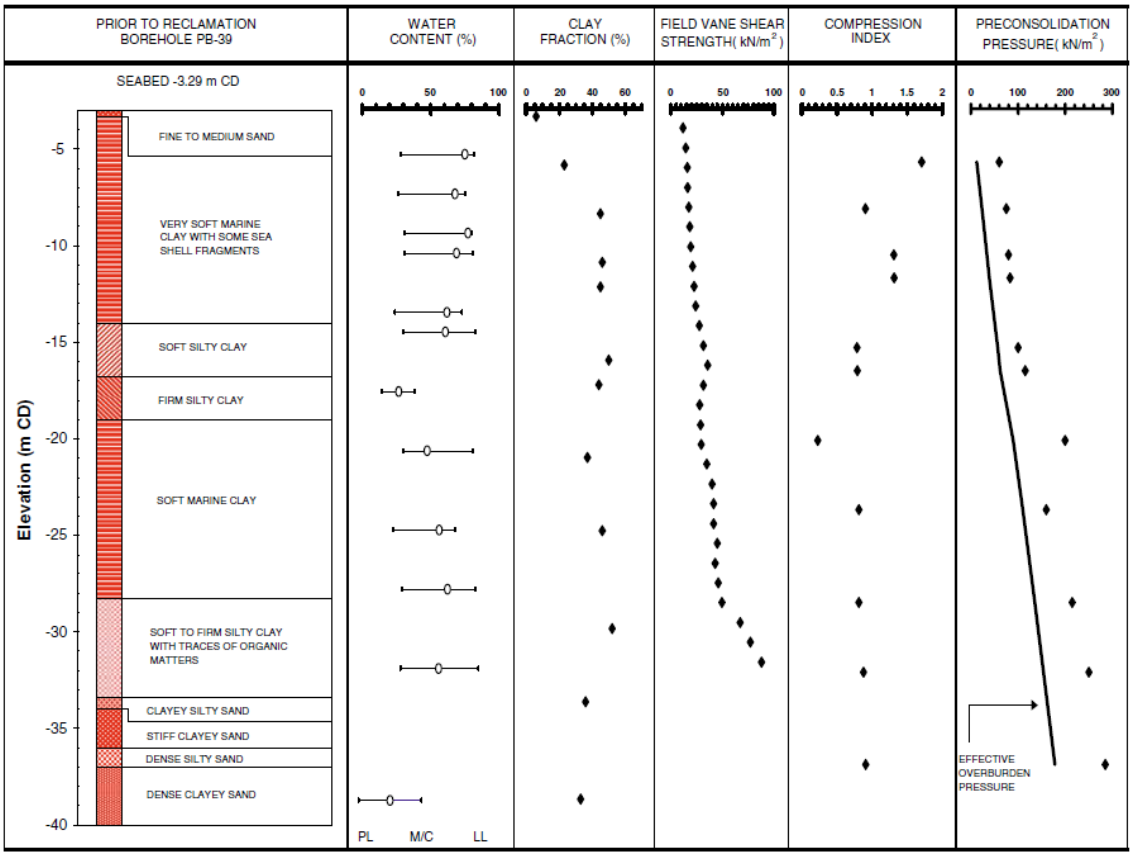

Figure 2.5 Typical soil profile and geotechnical parameters of a soil investigation borehole at Changi (Arulrajah and Bo (2008))

From the foregoing values and in analogy with conclusions drawn in the study of Arulrajah and Bo (2008), it can be concluded that the fill material along the southeast coast of Singapore is underlain by an unconsolidated substratum formed during the Kallang Formation, of which the more recent upper layer is less consolidated than the lower one.

Underlying the Upper and Lower Marine Clay layers of the Kallang Formation are deposits from the Old Alluvium, which mainly consist of a mixture of sand and clays, and support most of the younger formations, although uninterrupted sheets at the surface are found as well.

2.1.3 Coastal landforms and features

Prior to the land reclamations of the past decades, the coastline of Singapore had been identified as low-lying. Along the south-eastern shores two prominent cliffs were present, which have been identified as the *large* and *small red cliff*. The large and small cliff were located at Tanah Merah Besar and Bedok, respectively, see Figure 2.6. According to early references, these cliffs were of no substantial elevation. They had been levelled to provide fill and construction material as soon as the nation's economy and population started to grow after the British set foot on the island (Chia et al., 1988).

The coastline along the southeast originally had a mildly sloping sandy shore, bordered by a intertidal flat. Beaches were common, consisting mainly of fine sand and mud. The supply of these fine sediments came from the Johor River up north and from local, though smaller, rivers such as the Geylang and Kallang rivers, also see Figure 2.2. Near the red cliffs some pebble beaches had been observed, but these were only found directly adjacent to the rocky outcrops. Due to the supply of sediments from the Geylang and Kallang rivers, sand bars at the mouths of these rivers were occasionally observed. A predominantly westward directed longshore current along the southeast coast, described in the next section, has made the formation of a large spit at Tanjong Rhu (*lit.* Cape Rhu) possible (P.P. Wong, 1973, 1985). Also, an intertidal coral reef was present south of Bedok, seaward of the small red cliff, at the edge of the intertidal flat (Figure 2.6).

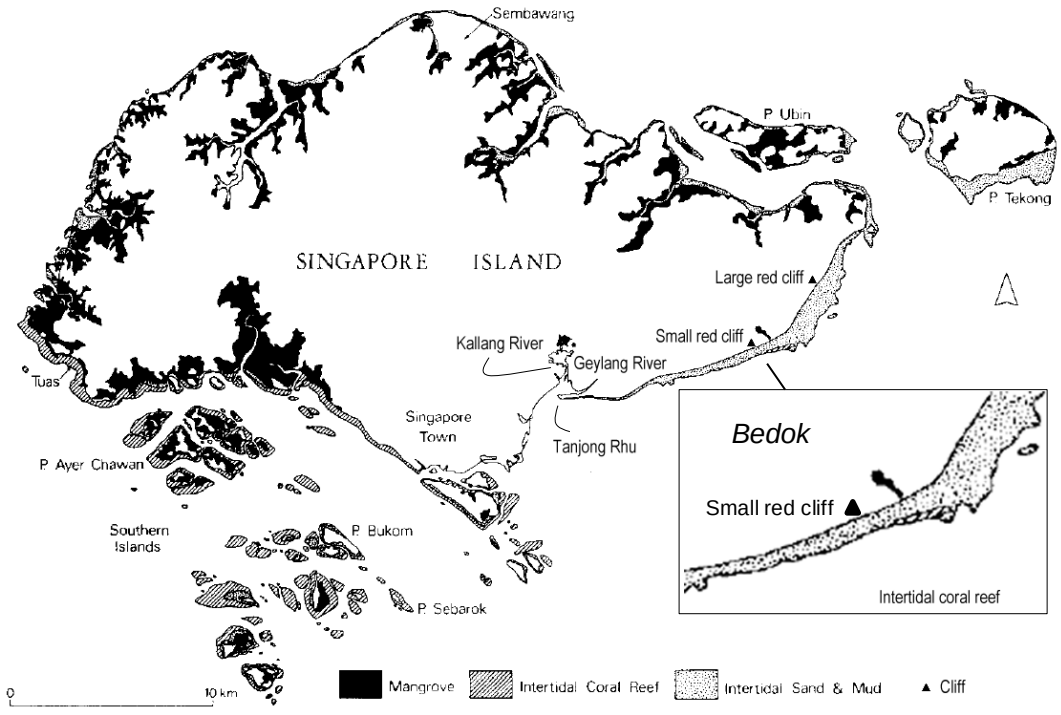

Figure 2.6 Extent of mangroves, intertidal coral reefs and intertidal sand and mud around Singapore in 1953 (Adapted from Hilton and Manning (1995)).

At the present day, the southeast coastline is located several hundreds of metres seaward of the original coastline, leaving no trace of the former coastline and its features. The intertidal flat has been entirely covered by fill material and the same is assumed for the formerly present coral reef, of which no recent data is available. The current coastline consists entirely of sand, of which the fill material has been obtained from inland hills and foreign resources. Figure 2.7 clearly depicts the transformation of the southeast coastline, which has changed its orientation from a convex to a concave shape.

This new coastline is stabilised by a series of anthropogenic structures, which are described in more detail in Section 3.2. Between these structures a variety of sandy beaches are found. Due to this seaward shift of the coastline, the shore is not mildly sloping anymore, but instead rather steep, with less distance to the deeper parts of the Singapore Strait.

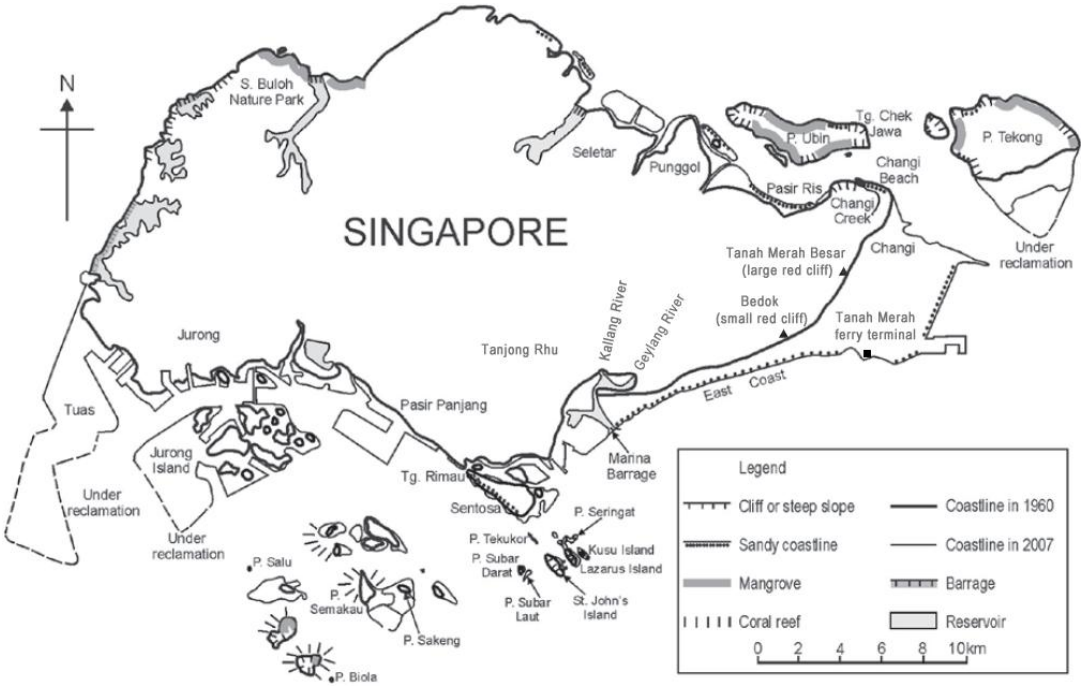

Figure 2.7 Singapore coastline features and changes from 1960 to 2007. The coastline in 1960 corresponds with the coastline in 1820, as described in P.P. Wong (1985). Note how the plan form of the southeast coast has been transformed from a convex to a concave shape. The surface of the current shoreline along the southeast consists entirely of sand (Adapted from Bird (2010)).

2.2 The coastal climate

2.2.1 General

The climate of Singapore is categorised as a tropical rainforest climate and is fairly constant throughout the year. Temperatures vary from about 23 to 32 °C. Mean monthly temperatures are 25.5 °C in December and January and 27.3 °C in May and June and the yearly average temperature is 26.8 °C. Humidity is high all over the year, with average monthly values ranging from 80% to 90% (Chia et al., 1988).

The amount of precipitation is generally determined by the seasonality caused by the monsoons, discussed in more detail in Section 2.2.3. Mean monthly averages vary from 158.5 mm in July to 287.9 mm in December. In comparison with the Netherlands, which is considered a rainy country with average monthly rainfall ranging from 42.3 mm to 82.8 mm, this is significantly more, especially when considering the average amount of precipitation days in both countries (178 days for the Netherlands versus 183 for Singapore).[ii] Naturally, differences in precipitation intensity matter a lot, as well as local wind patterns, as in Singapore precipitation has a more torrential behaviour, whereas in the Netherlands it is more evenly spread out over the day.

Tropical storms and typhoons are uncommon near Singapore, and mainly follow paths along the Philippine Archipelago, which subsequently absorbs most of the energy. In December 2001, however, the first recorded tropical cyclone Typhoon Vamei developed some 60 km northeast of Singapore. According to a study performed by Tay (2010) such extreme events could induce an additional water level rise of 1.6 m around Singapore, depending on the location. Nevertheless, the probability of occurrence of such extreme events is estimated to be once every 100 to 400 years (Chang, Liu, & Kuo, 2003).

Impacts of El Niño and La Niña events on Southeast Asia have been evident in the late 1990s, leading to periods of severe droughts which especially affected inland regions of Peninsular Malaysia and Indonesia, and the Philippine Archipelago (Gupta, 2005). Other than a strong reduction in rainfall, a worldwide coral bleaching event during 1997 and 1998 also affected corals in the Singaporean waters. Besides these events no significant impacts on Singapore and its shorelines have been recorded since.

2.2.2 Coastal waters

The surface temperature of the waters in the Singapore Strait varies from about 27 to 31 °C annually and averages almost 29 °C, with negligible variations along the vertical. Turbidity and light penetration have changed drastically since the land reclamations, with measured visibility up to 10 m in the early 1960s versus less than 2 m on a clear present day. This is mainly caused by fine sediment particles that are stirred up from the muddy seabed, which then remain in suspension for a long time. Increased exposure of the shoreline to waves contributes to these longer suspension times, contrary to the former situation where waves would dissipate over the intertidal flat. Surface salinity can fall to 21.6 ‰ during periods of heavy rainfall, but annual values generally vary from 28.5 ‰ to 32 ‰ (Chia, Rahman, & Tay, 1991). The wave and current environment in the Singapore Strait is predominantly driven by monsoon winds and the tide, which are discussed in the next section.

[ii] *Data retrieved from the National Environment Agency of Singapore (http://app2.nea.gov.sg) and the Koninklijk Nederlands Meteorologisch Instituut of the Netherlands (http://www.knmi.nl/)*

2.2.3 Winds

The monsoon wind system

Monsoons in Southeast Asia also affect the climate of Singapore. Monsoons are seasonally reversing wind patterns occurring in the tropics and subtropics. This reversal is caused by changes in the heating of continents and oceans during the year, which is related to the difference in heat capacity of land and water. Since the heat capacity of land is in general smaller than that of water, less energy is needed to heat or cool down land. Consequently, differences in atmospheric pressure over the land and water masses then determine the direction of wind flow.

In Southeast Asia monsoons are prominent due to, amongst others, a combination of the presence of the large landmass of the Asian continent and a large temperature range over the year. So during Northern Hemisphere winter, when cold surges arrive from Siberia, the land cools more quickly than the seas, creating a high-pressure zone over the Asian continent which in turn causes winds to blow in the direction of the low-pressure equatorial seas. During Northern Hemisphere summer this pattern reverses, with winds blowing from the equatorial seas towards the Asian continent. The former period lasts from about November to March/April and is referred to as the northeast (N.E.) monsoon, wheras the latter lasts from about March/April to October and is referred to as the southwest (S.W.) monsoon. Near continents, the monsoon winds generally overrule the moderate trade winds (Bosboom & Stive, 2011; Gupta, 2005; Van Maren & Gerritsen, 2012).

In Figure 2.8 a schematisation of these monsoon wind patterns is given, including mean rainfall over the distinct periods. The rainfall, as well as winds, is considerably larger during the N.E. monsoon than during the S.W. monsoon. These effects are felt through increased wave heights and currents in the Singapore Strait, and changes in both direction as magnitude can be almost directly related to the reversal of the monsoons (Ooi, Sisomphon, Kurniawan, & Gerritsen., 2011).

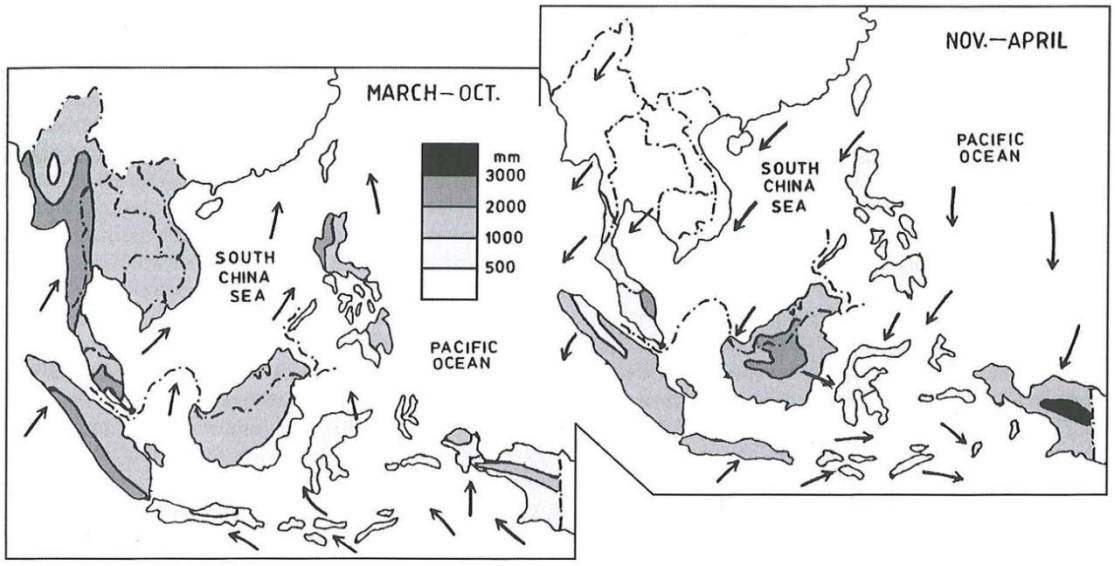

Figure 2.8 The southwest (S.W.) and northeast (N.E.) monsoon wind patterns in Southeast Asia (Gupta, 2005).

Sumatra squalls

Besides monsoons, during the S.W. monsoon so-called *Sumatra squalls* tend to occur occasionally. These squalls are lines of thunderstorms coming from Sumatra and the Strait of Malacca, that cause rapid increases in wind speeds and precipitation. Although mean daily wind speeds are larger during the N.E. monsoon, the highest short-term (10 minutes) wind speeds are commonly experienced during the S.W. monsoon.

Wind speeds were measured by Chew, Wong, and Chin (1974) and these showed strong variations in both speed and direction for both of the recorded periods. During the N.E. monsoon winds are generally smaller than 5 m/s, with daily averages of 1.8 to 2.5 m/s and exceptional gusts up to 8 m/s. During the rest of the year, daily averages vary from 1.3 to 1.9 m/s [iii], occasionally reaching up to 3 m/s (Chia et al., 1988).

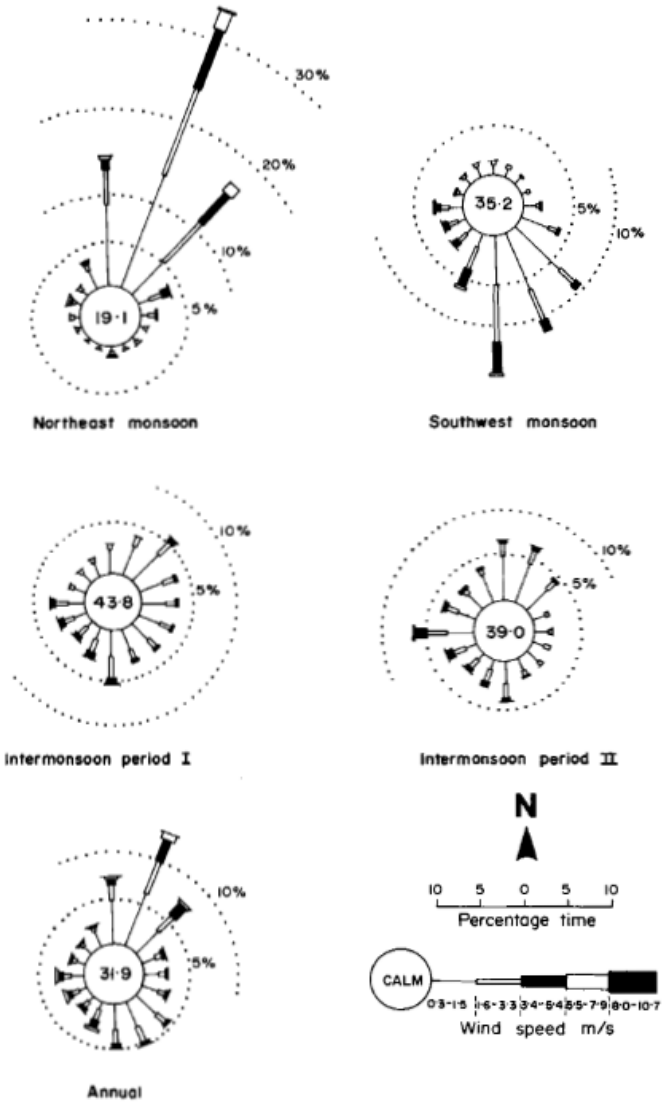

Figure 2.9 Annual and seasonal wind roses for Singapore (Chia et al., 1988)

[iii] *From the National Environment Agency of Singapore (http://app2.nea.gov.sg)*

2.2.4 Waves

Wind waves and swell

Considering the relatively short length of the almost uniform coastline at East Coast Park, the offshore wave climate is assumed to be similar along the length of this coast. Nearshore variability in approaching waves will mainly be caused by the interaction between waves, local bathymetry and structures.

Wave fetch in the Singapore Strait is generally short and the directions of maximum fetch rarely coincide with those of the strongest winds. Therefore, the waves approaching the southeast coast of Singapore are mainly swell waves entering the Singapore Strait from the South China Sea in the east, that refract towards the southeast coast on approaching the main island of Singapore. They refract to become about 20° to the control lines[iv] connecting the structures along the southeast coast (Chia et al., 1988; Silvester & Ho, 1972; Silvester & Hsu, 1997). Due to the reclamation of the Changi East Reclamation phases, eastward of East Coast Park (Figure 2.3), the eastward bathymetry has been altered extensively and subsequently the approach angle has been influenced as well, now being larger than 20° with respect to the control line of the structures (Figure 5.8).

During several periods in 1972 and 1973 wave measurements were carried out at Bedok by Chew et al. (1974), after land reclamations at East Coast Park had already initiated. These measurements were carried out at the end of an open jetty in 3.5 m water depth. Using the data from the measurements, through linear wave theory and refraction diagrams deep water waves were calculated.

The deep water wave results showed that 55% of the significant wave heights H_s = 0.2 - 0.4 m during the N.E. monsoon and H_s = 0.1 - 0.2 m during the rest of the recorded period. The mean zero-crossing period T_z = 2.5 - 3 s for about 50% of the time during the N.E. monsoon and T_z = 3 - 3.5 s 40% of the time during the rest of the recorded period (Figure 2.10). The maximum recorded wave height H_{max} = 1.1 m with a period T_{max} = 3 seconds. During the S.W. monsoon, strong winds resulting from the aforementioned Sumatra squalls can generate sea waves of approximately 1 m in height in open waters. At the coast however, breaker heights (H_b) are generally found to be less than 0.2 m, because of refraction and dissipation by shallow waters, islands and coral reefs (Chia et al., 1988). During studies performed by Chew and Wei (1980) for the reclamations of Marina South and Marina East, maximum wave heights of 1.14 m were recorded, with T_z of 3 seconds.

What is noticeable in Figure 2.10 is the angle of wave approach during the different periods. During the S.W. monsoon there seems to be a more even distribution in wave direction, with waves predominantly approaching the coast from both the south and the southeast. Due to the orientation of the coast, which is also illustrated in the above figure, waves then approach the coast from almost opposite angles. During the N.E. monsoon there is a clear dominance from the southeast.

[iv] *A control line is a line connecting the nearest tips of two adjacent headlands and is, depending on the layout of the structures, parallel to (part of) the enclosing shoreline. See also Silvester, Tsuchiya, and Shibano (1980).*

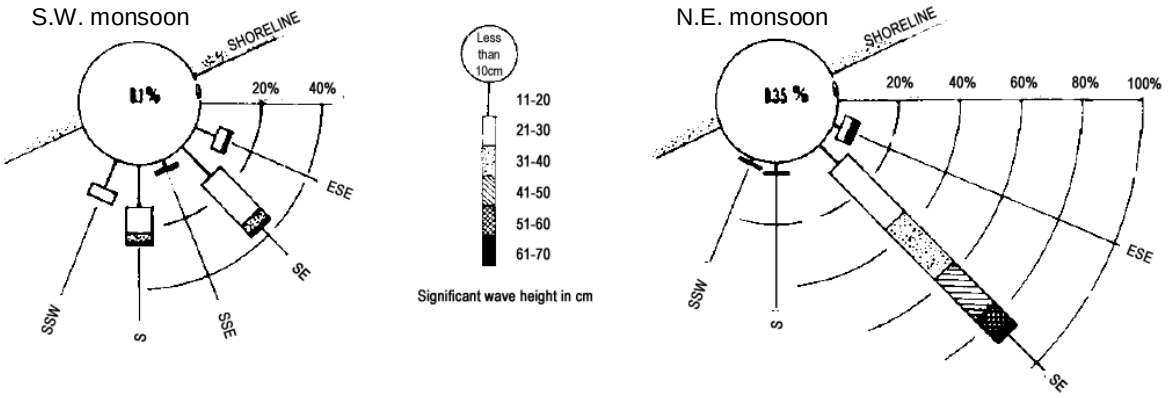

Figure 2.10 Significant wave heights in cm and dominant direction of approach at East Coast Park, resulting from measurements performed during periods from August to November 1972 and April to July 1973 (S.W. monsoon, left panel) and from December 1972 to March 1973 (N.E. monsoon, right panel) (After Chew et al. (1974))

Unfortunately, besides the measurements from Chew and Wei (1980), no wave records have been published since the 1970s, and with the coming of the digital age numerical models are nowadays used to predict wave characteristics. These models are based on wave buoy measurements far offshore of the southernmost tip of Peninsular Malaysia, and do generally not include locally induced waves. Assuming that the wave climate has not changed significantly in the past decades, the use of the wave characteristics as given by Chew et al. (1974) seems defendable for the purpose of this analysis. See also Appendix A for additional information on the wave climate.

Ship waves

The presence of vessels in the Singapore Strait has raised the question whether ship waves influence the southeast coast of Singapore. Seaborne traffic in the Singapore Strait mainly consists of container vessels and high-speed ferries. While large container vessels can generally induce rather long primary waves, navigation speed for large vessels in the Singapore Strait is restricted to 12 knots (= 6.17 m/s) in the fairway located approximately 3500 m off of East Coast Park.[v] This restriction is due to high traffic intensities and narrowing of the fairway towards the west. According to Schroevers, Huisman, Van der Wal, and Terwindt (2011) large vessels can generate long primary waves of about 0.3 m or more in height with periods of more than 20 s, and much shorter but higher secondary waves. In general, such low-crested long waves can induce a large run-up on the beach profile, increasing hydraulic loads and saturation of the beach, which could eventually lead to erosion (Katoh & Yanagishima, 1992). Seaward of the 10 m depth contour, at an approximate distance of 1000 m offshore, anchorage areas for waiting vessels are found, see Figure 2.11. Despite the high traffic intensities observed in the Singapore Strait and the long waves large vessels can generate, the available wave measurements used in this analysis date back to a period when seaborne traffic was less than observed today.

[v] *Rule 7 from "Rules for Vessels navigating through the Straits of Malacca and Singapore", adopted by the International Maritime Organization (IMO)*

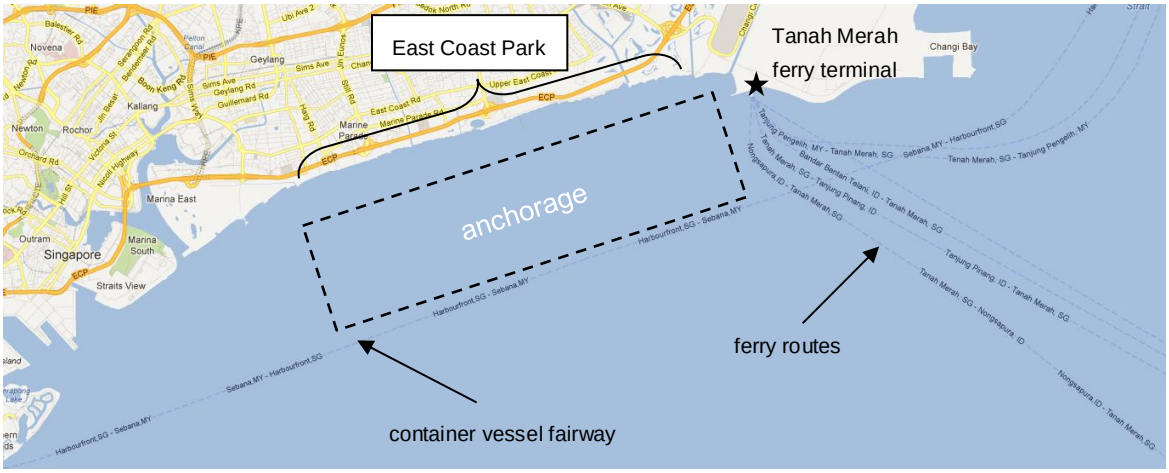

Figure 2.11 Top view of the southeast coast of Singapore and its coastal waters, indicating the ferry routes to and from the Tanah Merah ferry terminal. The area north of the container vessel fairway is used for anchorage of vessels waiting to enter the harbour area. See also http://www.mpa.gov.sg/.

Besides these large container vessels, smaller, high-speed ferries sail to and from the Tanah Merah ferry terminal east of East Coast Park. These sail to and from the terminal around 50 times a day [vi], and could invoke waves that reach East Coast Park. However, when looking at the ferry routes as shown in Figure 2.11, it can be seen that these routes are located at least 2 km away from East Coast Park and that waves would only propagate towards the coast on arrival of the ferry.

The ferries cross the fairway of the Singapore Strait at speeds of 25 knots (= 12.86 m/s) (Qu, Meng, & Suyi, 2011), and well before approaching the terminal they slow down. Using the depth-based Froude number in equation 2.1 it can be determined whether the generated waves are subcritical (Fr < 0.6 – 0.7), transcritical (Fr ≈ 0.9 – 1.1) or supercritical (Fr > 1.1), see also Kirkegaard, Kofoed-Hansen, and Elfrink (1998), and Maritime Navigation Commission (2003). For water depths h of at least 30 to 40 m in the fairway of the Singapore Strait and the above vessel speed V_s we then obtain Fr = 0.65 – 0.75, which lies at the limit of the subcritical range. According to Kirkegaard et al. (1998) the corresponding wave heights can then reach up to 0.6 m near the vessel, with periods T of about $0.27V_s$. Such periods have also been found by Torsvik and Soomere (2008). If these relatively short waves reach the coast, they are found to contribute to onshore rather than offshore sediment transport at beaches, possibly leading to steepening of beach profiles (Kirkegaard et al., 1998). However, the waves decay exponentially with increasing distance from the vessel track, generally described by ω^{n}, with ω the distance to the vessel track and n a constant ranging from -0.33 to -0.55 (Maritime Navigation Commission, 2003). Considering a distance of 2000 m from the ferry routes to the shore of East Coast Park, these waves are then of little influence on the coast. Near Tanah Merah the influence might be larger and could have contributed to the construction of the intertidal seawall just eastward of it.

$$Fr = \frac{V_s}{\sqrt{gh}} \qquad 2.1$$

[vi] *Based on daily average amounts of ferry arrivals and departures, see http://www.singaporecruise.com.sg/*

2.2.5 Tide

The tide in the Singapore Strait results from a combination of tidal characters in both the South China Sea and the Bay of Bengal, a bay in the Indian Ocean. In the South China Sea, the tidal character is mixed and predominantly diurnal. In the Bay of Bengal the tidal character is predominantly semi-diurnal. In the Singapore Strait, then, mixture of these tides invokes a complex regime with considerable tidal asymmetry, consisting of a predominantly semi-diurnal vertical tide and a predominantly diurnal horizontal tide.

Figure 2.12 clearly illustrates the different tidal regimes present along the Malay Peninsula and in the Singapore Strait, based on the so-called *form factor F* (Van Maren & Gerritsen, 2012).

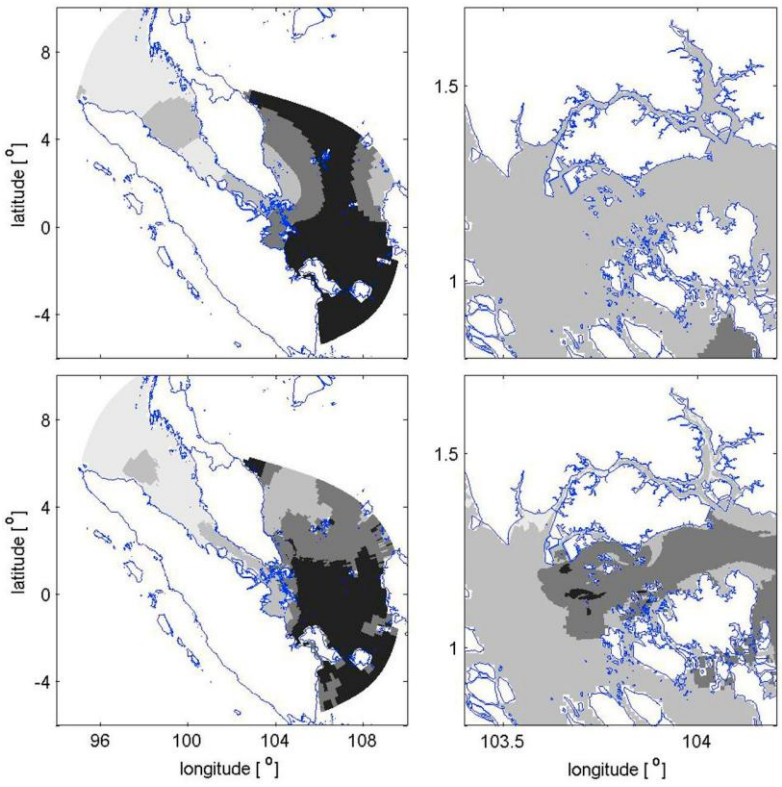

Figure 2.12 Tidal regime, based on the tidal form factor F ($F = (A_{K1} + A_{01})/(A_{M2} + A_{S2})$) for (top) water levels and (bottom) currents in (left) the whole model domain and (right) in detail near Singapore. Black is diurnal (F > 3), light gray is semidiurnal (F < 0.25), greyshades in-between are mixed, dominantly semidiurnal (F = 0.25 – 1.5) to diurnal (1.5 -3). From Van Maren and Gerritsen (2012).

In terms of the *form factor F*, which is determined as the ratio of the amplitudes of the main diurnal components K1 and O1 and the sum of the main semi-diurnal components M2 and S2 (Bosboom & Stive, 2011), the mixed and predominantly semi-diurnal tidal character around Singapore would have a form factor ranging from $0.25 < F < 1.5$. Van Maren and Gerritsen (2012) have confirmed that, generally, $F = 0.25$ in the west of the Singapore Strait and $0.5 < F < 1$ in the east. The expression for F is given below.

$$F = \frac{K_1 + O_1}{M_2 + S_2} \quad 2.2$$

Vertical tide

The mean spring tidal range generally exceeds 2 m, being 2.3 m on average. Mean High Water Spring (MHWS) is usually around CD + 2.8 m (Chart Datum) and Mean Low Water Spring (MLWS) around CD + 0.5 m, but peaks up to CD + 3.0 m occur from time to time[vii]. The shoreline is defined as CD + 2.515 m, which is equal to MSL + 0.863 m (Raju, Santosh, Chandrasekar, & Tiong-Sa, 2010). Chart Datum is defined equal to Lowest Astronomical Tide (LAT). The tidal regime around Singapore can thus be classified as a *meso-tidal regime*, which generally have mean spring tidal ranges around 2 - 4 m (Bosboom & Stive, 2011).

To assess the relation between tide and wave influence, the so-called *relative tidal range* (RTR) is often used, see equation 2.3:

$$RTR = \frac{MSTR}{H_b} \quad 2.3$$

in which *MSTR* is the mean spring tidal range (m), which is on average 2.3 m, and H_b is the wave height before breaking (m), which was observed to be less than 0.2 m (Section 2.2.4). This results in RTR = 11.5, which indicates a tide-dominated environment (Masselink & Hughes, 2003). The breaking wave height, however, is affected by local parameters and by the wave climate and can therefore be varying around 0.2 m. Assuming the breaking wave height to be in the range of 0.15 – 0.25 m, this gives us a RTR in between 9.2 and 15.3. Since RTR < 3 for wave-dominated beaches and RTR > 15 for a pure tidal flat, the coast along East Coast Park falls in the intermediate relative tidal range (Bosboom & Stive, 2011). This can be observed from the fact that the surf zone shifts with falling and rising water levels, and because of the large tidal range this gives waves under normal circumstances only relatively limited time to affect different zones in the beach profile.

Horizontal tide

Currents caused by tidal flow are generally measured and calculated further offshore of the coasts of Singapore, in larger water depths. Nevertheless, several data are available to provide sufficient insight into the currents occurring along the southeast coast, and they can easily be translated to nearshore currents through a simple expression applicable to shallow waters. Such a relationship is given in equation 2.4. The assumption is that the current velocity magnitude linearly depends on the water depth and alongshore water level gradient, assuming that the effect of inertia in shallow waters is minor. In equation 2.4, v_1 and v_2 are the tidal current velocities at the cross-shore positions with depths h_1 and h_2, respectively (Bosboom & Stive, 2011).

$$v_2 = v_1 \sqrt{\frac{h_2}{h_1}} \quad 2.4$$

[vii] *Tide information was obtained from long-term (1996-2008) tidal gauge measurements at the Tanah Merah ferry terminal, made available by the Maritime and Port Authority of Singapore (MPA)*

A significant variety in measured and calculated currents is found in literature, ranging from 0.1 to 0.5 m/s in nearshore regions, depending on the location. There is some doubt, however, about the validity and applicability of certain values to our own area of interest, especially because many of these values are measured in the vicinity of submerged breakwaters or near the mouth of Marina Bay. During float track observations for the study of the Marina South and Marina East reclamations performed by Chew and Wei (1980), for instance, current velocities were measured offshore of the reclaimed land and found to be of the order 0.36 to 0.38 m/s. At other locations they were found to be of the order 0.42 to 0.47 m/s. However, these currents were measured along a submerged breakwater, just offshore of the western end of Marina East, in the vicinity of the channel mouth where water flow converges and therefore flow in that region is expected to be larger than along East Coast Park.

From numerical model calculations large current velocities, in the order of 1 to 2 m/s, are found at certain locations in the Singapore Strait (Van Maren & Gerritsen, 2012). Near the coast, however, results from numerical calculations in the nearshore region of East Coast Park have provided values of about 0.3 m/s at the 5 m depth contour in the west and about 0.25 m/s at the 2 m depth contour in the east, see also Appendix F.[viii] Taking this range as a starting point for our analysis, according to equation 2.4 the nearshore tide-induced current velocity chosen at a water depth of 1 m then becomes about 0.13 - 0.18 m/s, which seems to be a reasonable value considering the observed mild climate along East Coast Park.

Direction of flood flow is generally from east to west, and due to the tidal asymmetry this flow usually prevails longer than the ebb flow.

2.2.6 Non-tidal currents

Besides tidal flow, the monsoon winds also generate currents in the coastal waters of Singapore, which can reach up to a maximum speed of about 0.26 m/s in the eastern and southern part of the open waters of the Singapore Strait during the S.W. monsoon, and about 0.36 m/s during the N.E. monsoon (Chia et al., 1988). Nearshore, the wave-induced longshore currents should be superimposed on the currents caused by local winds and tidal flow. To date, no records on wave-induced currents along East Coast Park have been published.

2.2.7 Sediment transport

Considering the mild wave and current environment along the southeast coast of Singapore, sediment transport is expected to occur mainly for fine sediments. Tracer experiments have been performed in the past to measure sediment transport along this coast, from which values of sediment transport rates were estimated to be around 4.5 tonnes/day (1000 m^3/yr) going from west to east during the S.W. monsoon, and 12 tonnes/day (2800 m^3/yr) from east to west during the N.E. monsoon. The net average transport rate was estimated at 2 tonnes/day (500 m^3/yr) in southwest direction (P.P. Wong, 1985). However, no indication is given on whether these transports were assessed for fines or for the coarse fill material along East Coast Park. The validity of such transports is also impeded by the fact that these

[viii] *Velocity retrieved from numerical modelling calculations of tidal flow in front of the southeast coast of Singapore, using a nested model in the 2D Singapore Regional Model, which is discussed in Chapter 5.4 (Julia Vroom, Deltares)*

measurements were made in the initial stages after the land reclamations, and no records of more recent measurements or calculations have been found since.
The complex and reversing hydrodynamic environment, together with the influence of anthropogenic structures and frequently performed beach nourishments, make it difficult to accurately assess sediment transports along the southeast coast. This forms a major knowledge gap in the current analysis, as the sediment budget along East Coast Park cannot be assessed quantitatively. However, after the reclamation of Changi East in the eastern part of the southeast coast, together with the implementation of a large variety of shore-parallel structures and on both sides of East Coast Park, it seems plausible to assume that no input of medium to coarse sediments are present in the system we observe. This makes a semi-quantitative analysis still possible, using readily available data and numerical models to perform sensitivity analyses.

2.3 Conclusions

The main island of Singapore is surrounded by landmasses, sheltering it from the surrounding seas and oceans. The low energy environment and tectonic stability classifies its coastline as a marginal sea coast. East Coast Park is located along the southeast coast of the main island of Singapore, being under direct influence of the Singapore Strait. It is built on reclaimed land, which basically consists of a sand layer underlain by a thick layer of unconsolidated marine clay, reaching up to 30 or even 50 meters locally. The original coastline had a mildly sloping sandy shore bordering a tidal flat, with beaches consisting mainly of fine sand and mud, of which the supply came from the Johor River and the more local Geyland and Kallang rivers. Nowadays a steep beach profile is found all along East Coast Park and coarse sands rather than fine sands are found on its beaches.

Located at latitude 1° north of the equator, Singapore experiences high temperatures all year round, varying from 23 to 32 °C. Precipitation is characterised by relatively short showers of high intensity. Tropical storms and typhoons, however, are uncommon near Singapore. Winds are generally mild and governed by the N.E. monsoon and S.W. monsoon. During the S.W. monsoon *Sumatra squalls* cause stronger gusts of wind. The wave climate in the Singapore Strait varies accordingly, with swell predominantly approaching the coast of the main island from the southeast during the N.E. monsoon and from the south *and* southeast during the S.W. monsoon. Wave heights rarely exceed 1 m, and 55% of the significant wave height H_s is 0.2 to 0.4 m during the N.E. monsoon and 0.1 to 0.2 m during the rest of the year. The corresponding mean zero-crossing period varies from 2.5 to 3 s during the N.E. monsoon and from 3 to 3.5 s during the rest of the year. Large vessels induce low-crested long waves which can occasionally reach the coast as well.

The tide is characterised by a mixed and predominantly *semi-diurnal* vertical tide and a predominantly *diurnal* horizontal tide. The mean spring tidal range is on average 2.3 m, with MLWS at CD + 0.5 m and MHWS at CD + 2.8 m (CD + 0 m = MSL – 1.652 m). The horizontal tide induces currents in the order of 1 to 2 m/s in the Singapore Strait, but at a depth of 1 m off the coast of East Coast Park the current velocity is around 0.13 m/s.

In order to assess the influence of all these external forces on the coastline evolution along East Coast Park, it is necessary to have a basic insight into the structures protecting it, as well as the sedimentology of the beaches. This will be addressed in the following chapter.

3 East Coast Park: a structurally controlled coast

3.1 Introduction

With some basic knowledge of the physical environment and climate along the (southeast) coasts of Singapore, we can now take a closer look at our study area. This chapter is meant to give a concise overview of the reclamation works that have resulted in the coastline we observe today, and of the structures that have been implemented to stabilise it. From this historical perspective we then take a look at the present-day situation, identifying coastal cells and their characteristics.

3.2 Anthropogenic influences

As has been previously mentioned and is assumed to be a well known fact by now, Singapore has undergone some major land reclamations during the past several decades, and plans for future reclamations are on the table. Due to these reclamations the length of natural shorelines has decreased considerably, from about 507 km or 96% of the total coastline in 1953, to 192 km or 40% of the total coastline in 1993 (Hilton & Manning, 1995).

To validly assess the physical coastal system and its processes at East Coast Park, some basic knowledge of the anthropogenic influences along this coast is indispensable. Therefore, in this section an overview of all known human-induced adaptations along East Coast Park during the past several decades is presented. This excludes beach nourishments, of which no records are available publicly.

3.2.1 East Coast Reclamation Scheme

Implementation

The East Coast Reclamation Scheme refers to a series of land reclamation phases that have been implemented from the late 1960s to the mid-1980s along the southeast coast of Singapore. Note that this scheme does not refer to land reclamation for East Coast Park only. The initial purpose of these reclamations were (1) to alleviate the shortage of suitable land for development near the city, (2) to provide space for new housing estates, (3) to construct a new highway to relieve traffic congestion on the existing East Coast Road, which was the main connection from Tanjong Rhu to the northeast, going along the coast, and (4) to create attractive artificial beaches along the new shoreline (P.P. Wong, 1973).

Following a pilot project in 1962, during which 19 ha of land was reclaimed from the Singapore Strait, between 1968 and 1985 the southeast coast of Singapore was extended in seaward direction in seven reclamation phases, see Figure 3.1. The reclamation of Changi Airport during the Changi East Reclamation Scheme consisted of two separate phases which were implemented in between 1976 and 1986 (Chia et al., 1988).

The phases of the East Coast Reclamation Scheme have resulted in an additional 1525 ha of land by 1985, translating the coastline more than 600 m seawards at Bedok and about 240 m at Tanjong Rhu. See Table 3.1 for an overview of the different reclamation phases.

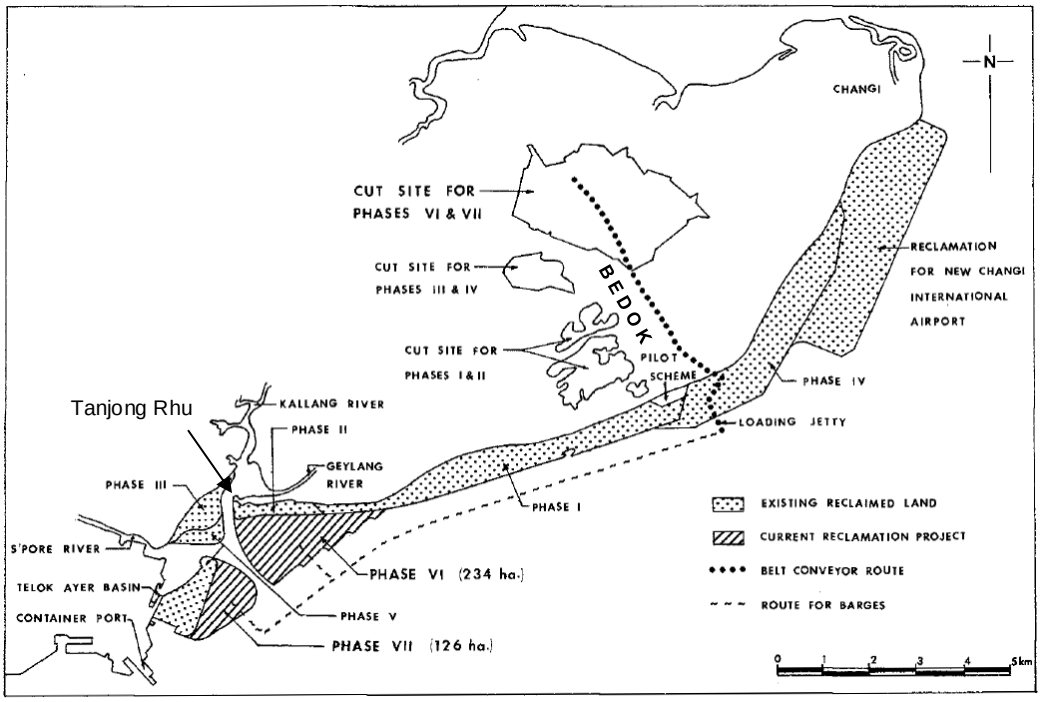

Figure 3.1 The layout of various phases of the East Coast Reclamation Scheme (Chew & Wei, 1980)

Table 3.1 Phases of the East Coast Reclamation scheme (after P.P. Wong (1973); (1985))

Phase	Area (* 10^4 m^2)	Period
Pilot Scheme	19	1962
I	405	1968 - 1970
II	53	1970 - 1971
III	67	1971 - 1975
IV	486	1971 - 1976
V	154	1974 - 1977
VI	234	1979 - 1985
VII	126	1979 - 1985
Total	1544 ha	23 years

The implementation of phases I and II was carried out in several stages, starting from the Pilot Scheme at Bedok in the east and going in westward direction towards Tanjong Rhu, the tip of the aforementioned spit (Figure 2.6 and Figure 2.7). To protect the newly reclaimed land, in the first phases a seawall was constructed. Also, a strip of fill material was placed seaward from the seawall to be transformed into beaches by hydrodynamic forces. Not long after, the fill material had already been carried away and undermining of the seawall due to wave action followed. From the eroded fill material shoals were being formed west of Tanjong Rhu, blocking the passage to the Kallang and Geylang Rivers. Due to high construction and maintenance costs, further elongation of the seawall was brought to a halt and a breakwater system was implemented to entrap the sediments. In Figure 3.2 a schematic overview is given of all structures implemented after reclamation phases I and II.

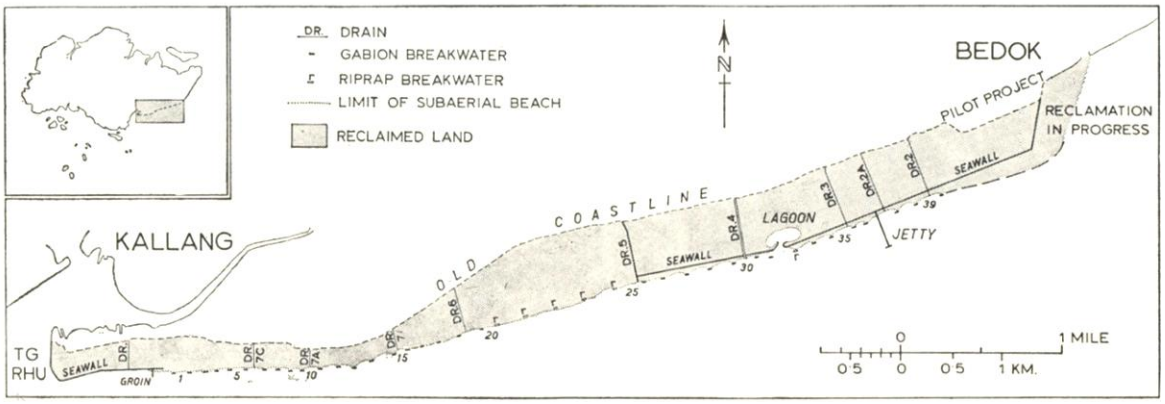

Figure 3.2 Reclaimed land during phases I and II of the East Coast Reclamation Scheme. The numbers indicate the stretches of coast, or cells, enclosed by two adjacent breakwaters present after implementation (P.P. Wong, 1973).

What is remarkable in Figure 3.2 is the presence of the seawall, of which the construction had been halted halfway through the construction phase when undermining started to occur at the eastern offshore facing corner. The seawall is still visible today, see Figure 3.3.

Figure 3.3 Crest of the old seawall still visible along East Coast Park. Left: photo taken by Teh Tiong Sa, 2001. On the image the crest of the seawall is visible, reaching above the ground level. In fact, this ground level had lowered as a result of land subsidence, for which on both sides of the seawall the ground level is lower than the crest of the seawall. Right: Photo taken by author, December 2012

Fill material

In Figure 3.1 the cut sites for fill material during the different phases of the reclamation works are indicated. The cut sites for phases I & II and VI & VII were initially natural hills at Siglap and Tampines respectively, while the cut site for phases III & IV was a sand quarry, which was turned into the Bedok Reservoir after the reclamations were completed (Chia & Chou, 1991). The sediments from all of the cut sites dated from the Old Alluvium, consisting mainly (~70%) of coarse sand, but also of clays and gravels (P.P. Wong, 1973).

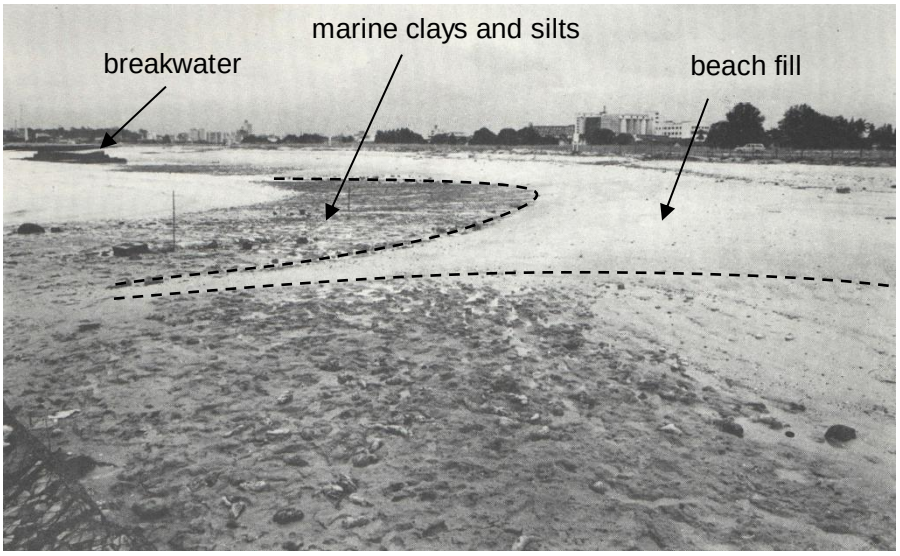

Figure 3.4 Sand projection overlying marine clays at the lee of the downdrift breakwater of cell 22. The dashed lines indicate the transition zone from fill material, consisting mainly of coarse sand, to the underlying marine clays and silts (Adapted from P.P. Wong (1973))

The original marine sedimentary deposits along the southeast coast consisted of Holocene sediments, mainly marine clays and silts, dating from the Kallang Formation. Along East Coast Park, the fill material was directly projected on top of the original deposits, see the photograph in Figure 3.4. In this figure a clear transition from fill material to original material is visible. Since the fill material consisted of a mixture of sediments, wave action in time caused the finer sediments to be washed out, leaving behind beaches consisting of coarser sands and gravels. The net direction of transport of the washed out fines was in westward direction, which had lead to the formation of the spit at Tanjong Rhu indicated in Figure 2.6, see also P.P. Wong (1973).

3.2.2 Headland control

As described in the previous section, during the phases of the East Coast Reclamation initially a seawall was implemented, which lead to erosion of the fill material and undermining of the seawall, especially at the eastern tip. To prevent further erosion and create stable beaches, a new approach was adopted, originating from Silvester (1960), who described stabilization of sedimentary coastlines by means of hard structures. The idea was to implement a series of breakwaters along the coast, in order to improve shoreline stability and simultaneously alleviate the construction and maintenance costs the seawall brought along with it, see also Figure 3.5. The concept finds it basis in the fact that longshore sediment transport depends on the angle of wave incidence. This angle is determined relative to a normal through the coastline, where waves approaching the coast perpendicularly (at an angle of 0°) or traveling parallel to the coast (at ± 90°) induce no longshore sediment transport. Commonly, waves approach a coast under an angle in between 0° and 90°, because of which headlands can be implemented perpendicular to the predominant angle of wave incidence, in order to reduce this wave angle and diminish possible sediment transport.

With the adoption of these ideas, the implementation of the breakwater series along the southeast coast of Singapore became the first large-scale application of such a system, which later became known as *headland control* (J. Hsu, Silvester, and Xia (1989); Silvester and Hsu (1997); Wang, Tan, and Cheng (2009)).

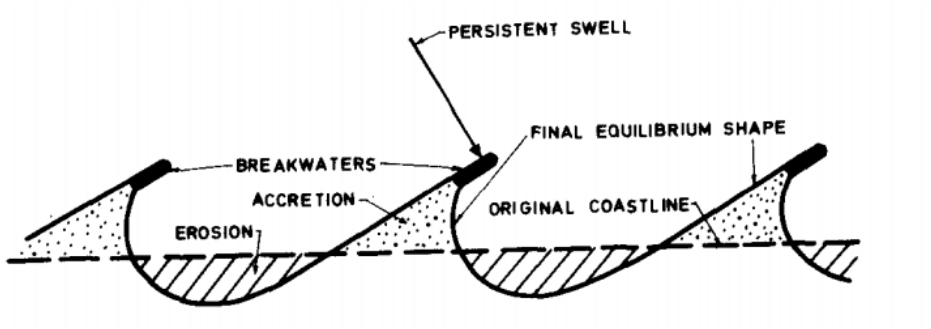

Figure 3.5 Design of the breakwaters and beaches at East Coast Park (Chew et al., 1974)

Before the method was internationally defined as headland control, many analyses had already been done on the implementation breakwaters and the consequent developments of so-called *crenulate shaped bays*, or also J-shaped bays[ix], between them (Figure 3.5).

In the initial years after the breakwaters were constructed, the coastal morphology developed rapidly, with waves and currents reshaping the new coastline towards equilibrium. Not all breakwaters along East Coast Park were implemented according to the concept of headland control, which is seen in the subsequent section. However, for the locations where headland control *was* implemented, beach planforms seemed to follow the theoretical predictions relatively accurately.

Initially, riprap breakwaters were implemented along a part of the coast, but due to the high construction costs gabion breakwaters were constructed at the remaining locations. The riprap breakwaters were constructed in the dry, in the fill material, while the gabion breakwaters were constructed on the foreshore. An example of both construction methods is shown in Figure 3.6.

Since the application of headland control along the southeast coast of Singapore some additional land reclamations and other man-made changes have been executed. When phase VI was executed, many of the implemented structures were either buried or removed, see Figure 3.1 and Figure 3.2, and in the years following many of the gabion breakwaters seemed to fail due to instability. One contributing factor was the cutting of steel wires that were supposed to keep the stones in place, because fishermen were eager to obtain the mussels that clammed themselves in between the stones (Silvester & Hsu, 1997). This has led the gabion breakwaters to all be replaced by riprap breakwaters.

[ix] *In literature a variety of names is found, among which crenulate-shaped bay, J-shaped beach, zeta bay, half-heart bay, spiral beach, hooked beach, pocket beach, headland-bay beach, headland-embayed beach, structurally controlled beach and topographically-bound beach (J. R. C. Hsu, Yu, Lee, & Benedet, 2010).*

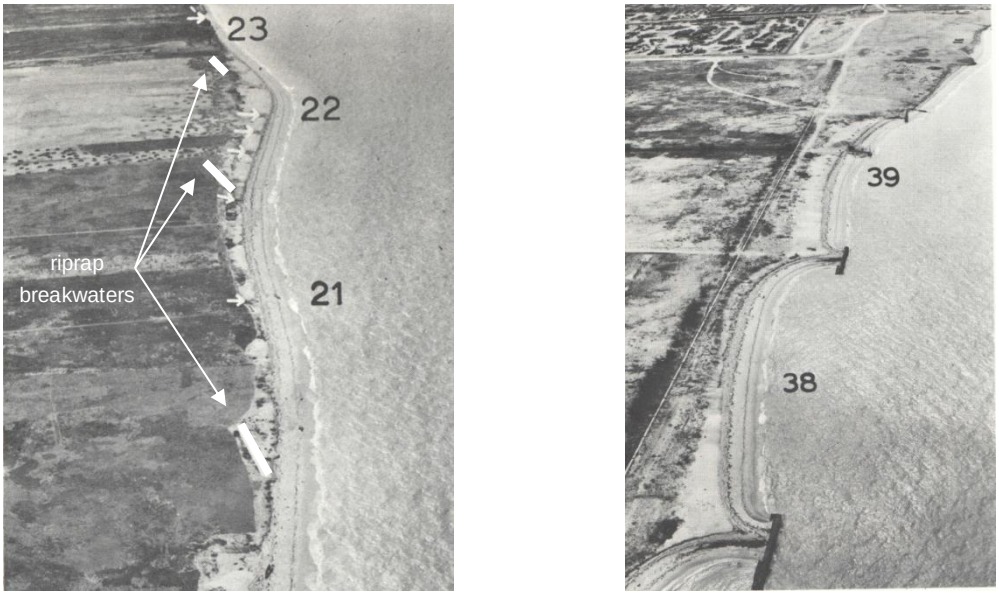

Figure 3.6 Left: low aerial oblique of East Coast Park, looking east, showing how riprap breakwaters were placed in the reclamation fill material. The breakwaters are indicated by white lines. Right: aerial oblique further eastward along the coast, still looking east, showing gabion breakwaters on the foreshore and the development of bay-shaped beaches in the initial years. After P.P. Wong (1973)

3.3 Coastal cells

3.3.1 Cell classification

With the implementation of structures along the coast came the morphological changes that shaped the beaches. In analogy with P.P. Wong (1985) the same nomenclature will be used to define these individual beaches, namely *cells*. Cells, or coastal cells, are here defined as coastal segments that are enclosed by two adjacent breakwaters or headlands hereupon. This enclosure is of course not literal, but merely defines the lateral boundaries in between which hydrodynamic forces shape the beach.

Not all headlands have been constructed with the same dimensions or orientation, nor are all implemented according to the concept of *headland control*, and this has resulted in different beach profiles and planforms for different coastal cells. Today, a variety of coastal cells is found along East Coast Park, making up a total of 31 cells. These cells are usually identified by the headlands that enclose them. Figure 3.7 gives an overview of the present-day headlands and beach cells found along East Coast Park.

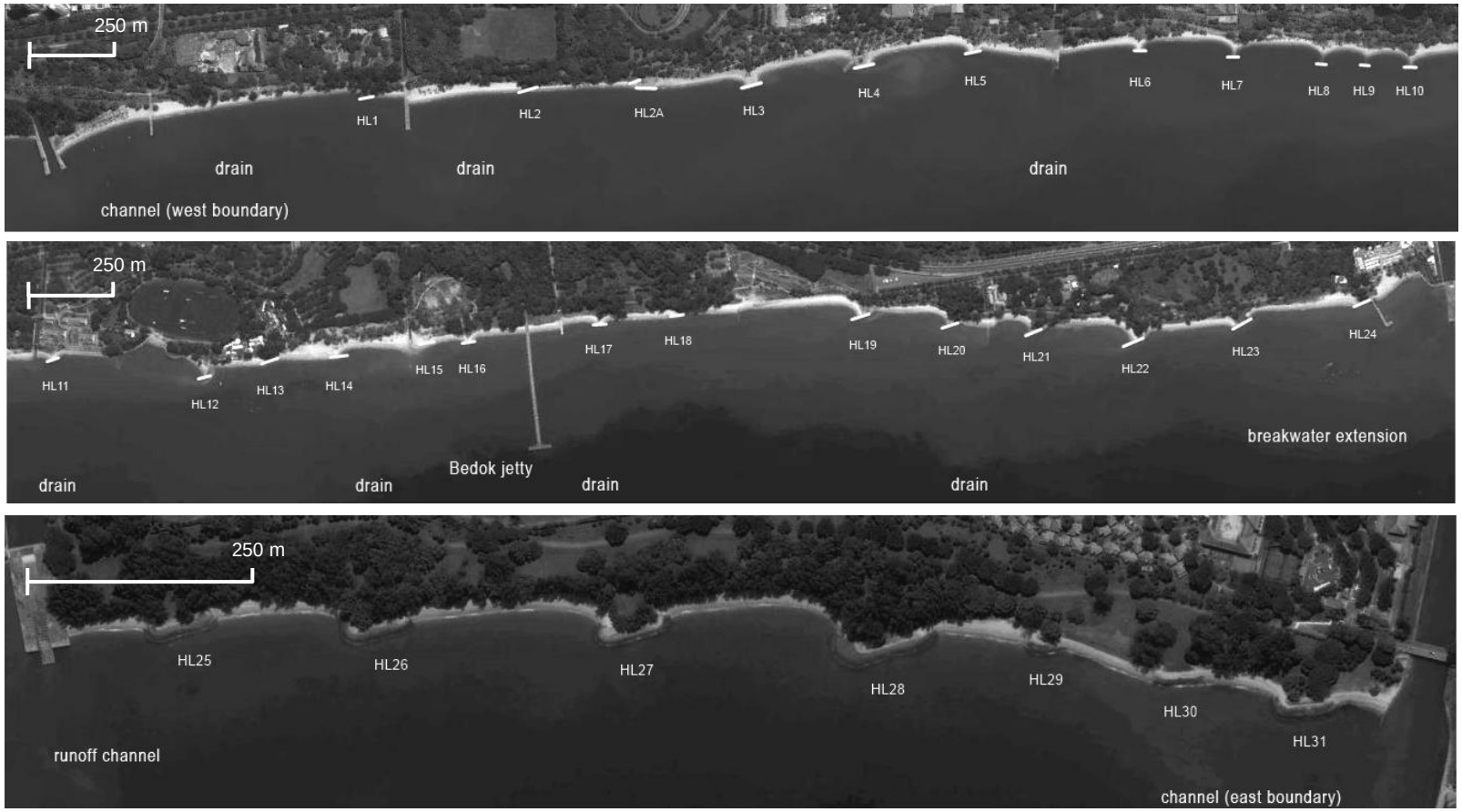

Figure 3.7 Headlands, coastal cells and large drains along East Coast Park, according to the stretch defined in Figure 2.3. Headlands are marked in white (top panels). Different scalings are used in the different satellite photos, so that separate images are not in proportion with each other. ***Top****: from the westernmost end of East Coast Park in eastward direction, including headlands (HL) 1 to 10;* ***Middle****: the central part, including headlands 11 to 24. The Bedok jetty is indicated, where the wave measurements were performed by Chew et al. (1974), as well as a breakwater extension at headland 24, which had been developed after 2002;* ***Bottom****: the easternmost part of East Coast Park, including headlands 25 to 31.*

From the above figures it becomes clear to what extent both structures and beaches vary along the coast. In the top panel of Figure 3.7, a clear distinction can be seen between the western headlands and the ones towards the east, the spacing between them being much smaller for the latter. Headland 2A is a recently (2009) developed headland, which was built after the original headland became exposed to the sea from the fill material. Most of the headlands in this stretch have been altered in the past decade, mainly increasing the dimensions and especially the crest level, which had become insufficient.

Continuing from headland 11, there is an interruption by a small lagoon, and the Bedok jetty further eastward. A difference in beach formation from headlands 19 to 24 is visible, in comparison with the more westward headlands. Whereas the latter are more or less in line with each other along the coast, the former are not, creating highly asymmetric beaches. Also noticeable is their similar orientation. Headlands 25 to 31 make up of the most eastward breakwater series along East Coast Park. Commonly these headlands and their beaches are left out of focus, due to the fact that major erosion problems are found to occur in the sections from headland 1 to 24. This is also related to the fact that in these sections most (recreational) infrastructure lies close to the shore.

For all of these headlands, as well as for the beaches enclosed by them, certain specific parameters have been measured using Google Earth satellite imagery. Based on these parameters, a simple classification of each cell has been made based on the beach type occurring in each cell. Three different types have been identified, namely straight beaches, pocket beaches and J-shaped beaches. Straight beaches are beaches in which the larger part of the beach is considered straight and curvature is mainly found in the lee of structures only, see for instance the sections in between headlands 1 to 8 in Figure 3.7. Pocket beaches have more profound symmetric curvature all along the beach line, which is mainly determined by the smaller spacing in between two headlands, see the beaches in between headlands 8 and 10. In J-shaped beaches the profound curvature is asymmetric, and thus found on one side of the coastal cell only (e.g. the beaches between headlands 25 to 28).

Although coastal cells are here defined as being enclosed by two adjacent headlands, in the parameter analysis these cells were defined as being enclosed by any type of structure which influences the local morphology. In this way a total of 31 coastal cells has been identified, see also Appendix B. The distribution of the cell types is given in Figure 3.8.

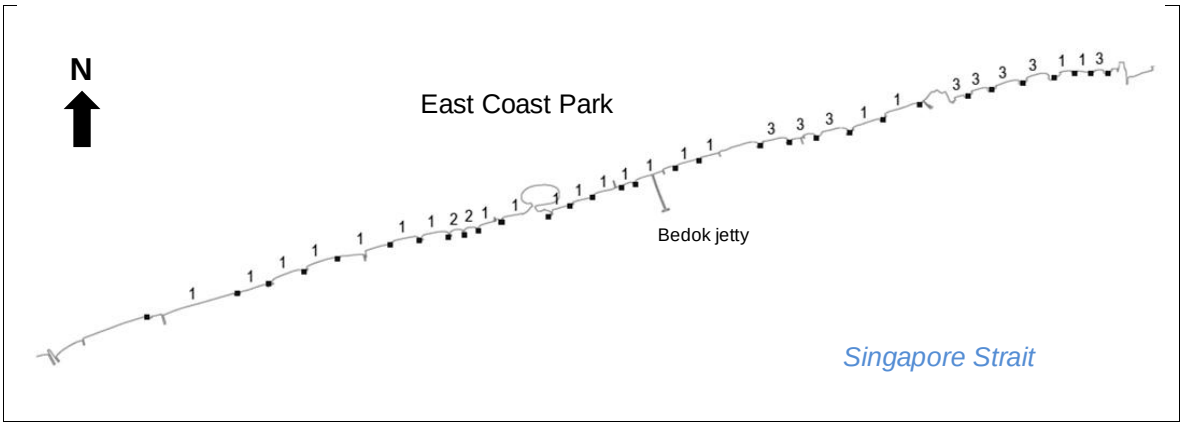

Figure 3.8 Coastal cell type classification along East Coast Park, starting from headland 1 up to the channel defining the eastern boundary. The type numbers are according to (1) straight beaches, (2) pocket beaches (symmetric), and (3) J-shaped beaches (asymmetric). Headlands are indicated as black cubes.

From this simple classification it becomes clear that most beaches along East Coast Park are rather straight, while only in two cells pocket beaches are found, namely between headlands 8, 9 and 10. Two zones of J-shaped beaches are found, namely in between headlands 19-22, 25-28, and in between headlands 30 and 31. These zones are characteristic in the sense that they occur along more curved sections of the coastline. Because of the asymmetry in these beaches, erosion is generally more profound in the beach section which is sheltered from the predominantly present waves.

3.3.2 Beach sedimentology

In order to properly analyse the morphodynamics in a coastal cell, clear insight in the sediment distribution in these cells is paramount, as sediment distributions often tell something about past processes. In literature some data on sediment characteristics on the shoreface is available. During different periods in 1972 and 1973, just after the first two reclamation phases, sediment samples had been analysed at different locations on the shore. Samples from in between the headlands in July 1972 averaged 0.19 mm. In May 1972, just after the N.E. monsoon had ended, the average grain size was found to be 0.97 mm at mid-tide. In August 1973 an average of 0.3 mm was observed on the upper foreshore, 0.63 mm at mid-tide and 0.76 mm at the lower foreshore. Near the headlands sediment seemed to be coarser than in between the headlands, see
Figure 3.9 for the alongshore distribution of the mean grain size (Chew et al., 1974). In an unpublished study by Tan, Goh, and Wang (2007) mention was made of an average grain size diameter D_{50} of 1.25 mm.

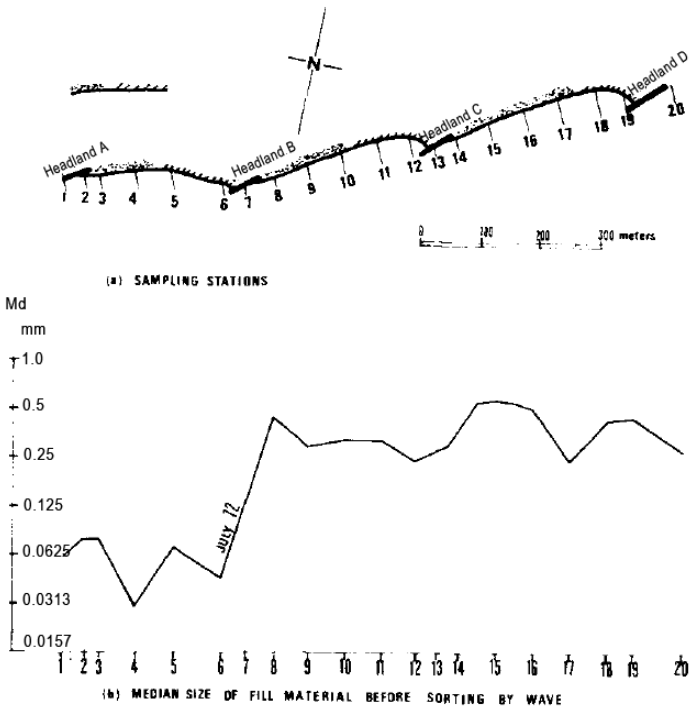

Figure 3.9 Initial grain size characteristics of fill material before sorting by waves, measured during 1972 and 1973. The upper panel shows the sampling locations along a stretch of 3 coastal cells. The lower panel shows the resulting alongshore mean grain size distribution (After Chew et al. (1974)).

Due to the rather high variability in sediment sizes in literature and the lack of up-to-date sediment analyses, some sediment samples have been collected from two beaches at East Coast Park, namely the two pocket beaches enclosed by headlands 8, 9 and 10. More details on this sediment analysis can be found in Appendix C. The results from this analysis are shown in Figure 3.10, and show coarse values of D_{50} at mid- and low-tide, and also at high-tide behind the breakwaters. In the centre of the coastal cells, on average, D_{50} = 0.5 mm at high-tide level, D_{50} = 1.3 mm at mid-tide level and D_{50} = 1.4 mm at low-tide level. In the lee of the headlands, D_{50} = 1.4 mm at the high-tide and D_{50} = 1.1 mm at low-tide level. The mean diameter on the beach face is 1.3 mm, with a particle density of 2.66 kg/m^3 (Appendix C).

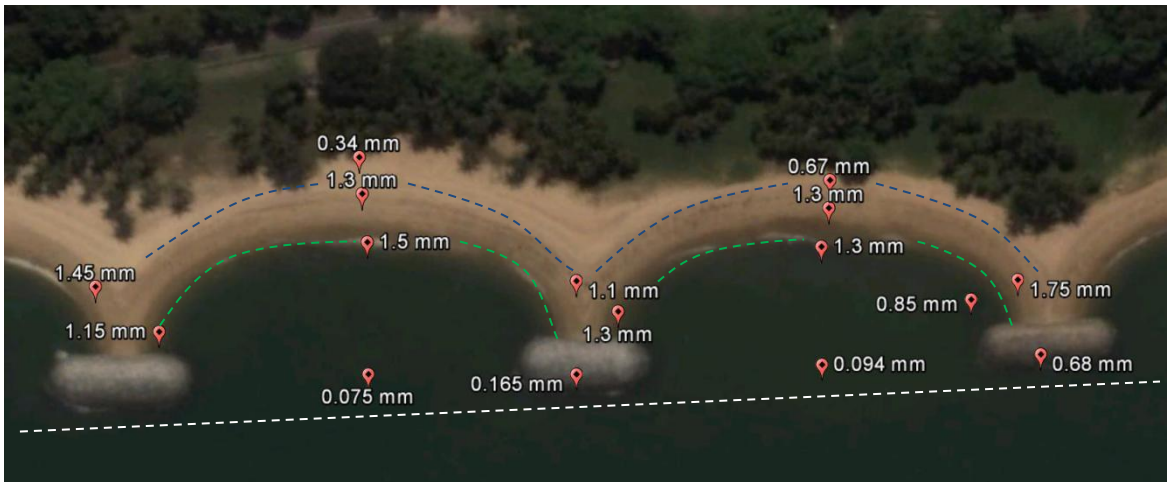

Figure 3.10 Mean sediment grain sizes (D_{50}) and the locations where sediment samples were collected in between headlands 8, 9 and 10 at East Coast Park, on 13 December 2012 during Low Water Spring tide. The blue dashed line indicates the high water line, the green dashed line indicates the low water line, and the white dashed line indicates the upper shoreface. In the centre of the coastal cells, samples were also collected at mid-tide. Indicated locations might deviate from exact locations.

This large mean diameter on the beach face is consistent with the mean value mentioned in Tan et al. (2007). These coarse grains are sand grains, which are present mainly on the lower part of the beach face and in the lee of the headlands. Towards the beach berm, above the high water mark, as the slope of the beach flattens the sediment diameter seems to gradually become less coarse. Going seaward from the low water mark to the upper shoreface, one will soon notice a change in bottom surface sediment composition. Not too far from the beach foot a rather rapid transition to the underlying clayey substratum is observed. In the cells considered, at this transition sand seems to encroach the substratum. Along the upper shoreface mainly mud is found, consisting of a mixture of silt and clay.

3.3.3 Beach state

The beach profile commonly found along East Coast Park is rather steep, ranging from 1:5 to 1:15 depending on the location and time, and the shoreface is mildly sloping, ranging from 1:30 to 1:100 towards the lower shoreface. According to Wright and Short (1984) three morphodynamic beach states can be distinguished in natural systems, namely reflective beaches, dissipative beaches and intermediate beaches (Bosboom & Stive, 2011).

Reflective beaches have a relatively steep and narrow beach face with slopes generally in between 1:5 and 1:10. These beaches have a berm and a narrow surf zone. Sediment is usually coarse and no breaker bars are present. Reflective beaches commonly result from mild wave conditions, transporting sediment onshore, and are most oftenly found in low-energy swell and monsoon wave climates. Waves at the beach face are mostly in the range of plunging to surging.

Dissipative beaches form the other extreme morphodynamic state and have a relatively flat and wide beach and shoreface, with nearshore slopes in the range of 1:20 to 1:100. Landwards commonly dunes are found, and the surf zone is wide. Sediment is relatively fine and usually multiple breaker bars are present in the cross-shore profile. Dissipative beaches result from high energy wave environments, which are mainly found in storm wave environments. Waves at the beach are generally of the spilling type. An important difference between reflective and dissipative beaches is the variability in morphodynamic behaviour, which is most prominent on dissipative beaches.

Intermediate beaches are the beaches with characteristics of both extreme morphodynamic beach states. Waves in this range usually vary from spilling to plunging or collapsing, depending on the tendency of the beach state, and features on intermediate beaches are generally strongly three-dimensional (Bosboom & Stive, 2011).

To determine the beach state at a particular coast, usually (one of) two parameters are used, namely the so-called *Dean number* and the *Irribarren number*.

Dean number

According to Dean (1973), the beach state can be expressed as follows:

$$\Omega = \frac{H_b}{w_s\, T} \tag{3.1}$$

in which H_b is the breaking wave height (m), w_s the sediment fall velocity (m/s) and T the wave period (s). Reflective beaches typically have a *Dean number* $\Omega < 1$, and for dissipative beaches $\Omega > 6$. The intermediate morphodynamic states thus have a value $1 < \Omega < 6$. Thus, from this it can be seen that for larger wave periods and for smaller grain sizes, and consequently smaller sediment fall velocities, larger values are found for Ω, identifying a dissipative beach state.

The sediment fall velocity mainly depends on the grain size, and a general expression is given as (Van Ieperen, 1987):

$$\mathrm{w_s} = \sqrt{\frac{\rho_s - \rho_w}{\rho_w} \cdot \frac{4 g D_{50}}{3 C_D}} \tag{3.2}$$

in which ρ_s is the particle density of the sediment (kg/m^3), ρ_w the water density (kg/m^3), g the acceleration of gravity (m/s^2), D_{50} the mean particle diameter (m) and C_D the so-called drag coefficient (-). The drag coefficient is determined by the roughness of the sediment particle and can be assessed through iteration, using the particle Reynolds number:

$$\mathrm{Re} = \frac{w_s D_{50}}{\nu} \qquad 3.3$$

with ν the kinematic viscosity coefficient (m^2/s), which has a characteristic value of 10^{-6} m^2/s for water (Bosboom & Stive, 2011).

To assess the Dean number for beaches along East Coast Park, we will firstly have to determine the sediment fall velocity w_s. For this, the drag coefficient C_D needs to be assessed, which can be done through iteration using a curve describing the relation between the drag coefficient C_D and the particle Reynolds number *Re*, see Figure 3.11.

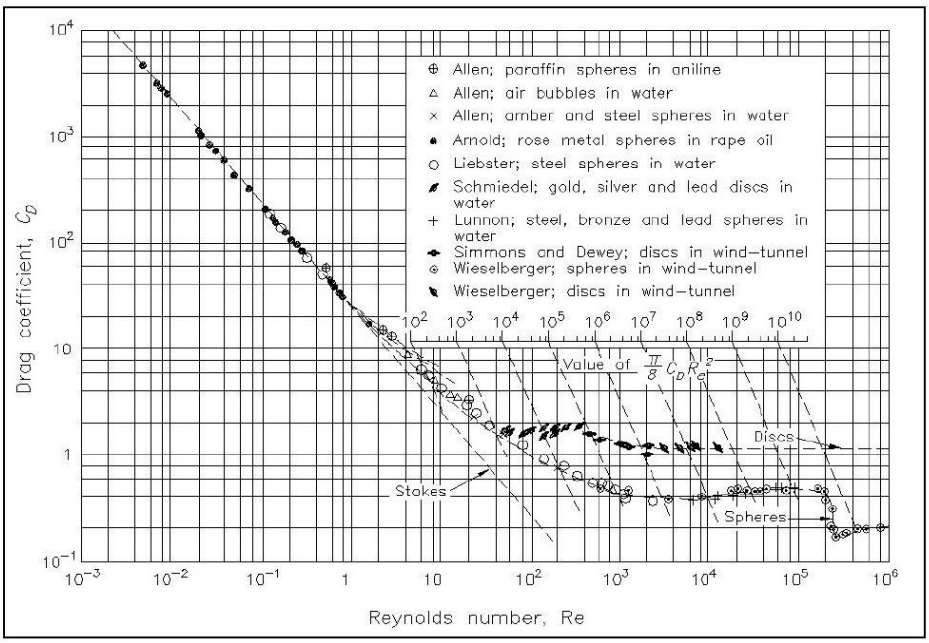

Figure 3.11 Drag coefficient as a function of the Reynolds number (Vanoni, 1975)

The below values are used, of which D_{50} and ρ_s follow from our sediment analysis:

- D_{50} = 0.0013 m
- ρ_s = 2.66 kg/m^3
- ρ_w = 1018 kg/m^3 [x]
- g = 9.18 m/s^2

Using these values and Figure 3.11, and re-writing equation 2.6 to

$$\mathrm{w_s} = \frac{Re \cdot \nu}{D_{50}} \qquad 3.4$$

the iteration then results in a particle Reynolds number Re ≈ 250, a drag coefficient C_D = 0.7 and accordingly a sediment fall velocity w_s = 0.2 m/s. Since this fall velocity seems rather high, a validation is made using alternative equations to assess the sediment fall velocity (Cheng, 1997). These alternatives are given in equations 3.5, 3.6 and 3.7.

[x] *Based on an average sea surface temperature of 29°C and an average salinity of 30‰, see Section 2.2.2, the water density was calculated using an online calculator, at http://www.csgnetwork.com/h2odenscalc.html*

Concharov (Ibad-Zade, 1987):

$$w_s = 67.6\Delta D_{50} + 0.52\Delta\left(\frac{T}{26} - 1\right) \quad for\ D_{50} = 0.015 - 0.15\ cm \qquad 3.5$$

Van Rijn (1990):

$$w_s = 1.1\sqrt{\Delta g D_{50}} \quad for\ D_{50} > 0.1\ cm \qquad 3.6$$

Cheng (1997):

$$w_s = \frac{\nu(\sqrt{25 + 1.2D_*^2} - 5)^{1.5}}{D_{50}} \quad with\ \ D_* = D_{50}(\frac{\Delta g}{\nu^2})^{1/3} \qquad 3.7$$

in which *T* is the average sea surface temperature (= 29 °C, see Section 2.2.2), *Δ* is 1.66 and all other parameters are known. Using equations 3.5, 3.6 and 3.7 to calculate the sediment fall velocity, we then obtain fall velocities of w_s = 0.147 m/s, w_s = 0.16 m/s and w_s = 0.13 m/s, respectively. Considering the fact that no limitations are given on the applicability of these formulations, a range will be taken to give us a band of possible beach states, using w_s = 0.13 to 0.20 m/s.

The wave height before breaking was found to be H_b = 0.2 m in Section 2.2.4. However, to stay consistent with Section 2.2.5, in which an uncertainty range was chosen for possible breaker heights, we choose the same range of breaker heights in our calculation of the beach state. This range is H_b = 0.15 – 0.25 m/s, and with T = 3.5 s (Appendix A), we can apply equation 3.1 for each combination of H_b and w_s, to find Ω = 0.21 - 0.55 < 1, clearly indicating a reflective beach state along East Coast Park disregarding the selected uncertainty range of the parameters. However, it should be kept in mind that this state refers to the beach face only, because during lowest spring tides the upper shoreface becomes exposed and this shoreface has a far gentler slope and is composed of finer surface sediment, which would eventually result in higher Dean numbers according to equation 3.1.

Irribarren number

The Irribarren number, or surf similarity parameter, is an expression relating the beach slope to the wave steepness:

$$\xi = \frac{tan\ \alpha}{\sqrt{H_0/L_0}} \qquad 3.5$$

in which *α* is the angle of the beach slope, H_0 the deep water wave height and L_0 the deep water wave length. In fact, $\sqrt{(H_0/L_0)}$ expresses the wave height over wave period, but the deep water wave length is used in order to obtain a dimensionless parameter (Battjes, 1974; Schiereck, 2004).

Using this expression, an indication can be given on the wave breaker types occurring at the beach. Thus, assuming constant offshore hydrodynamic conditions, the slope of the beach would then determine the type of wave breaking. But notions of gentle or steep slopes are in fact relative, as hydrodynamic conditions are hardly constant. Spilling breakers are commonly found for values of ξ < 0.3; plunging breakers occur for values of 0.5 < ξ < 3; collapsing

breakers lie in the transition zone between breaking and non-breaking, 2.5 < ξ < 3; for values of 3 < ξ < 5 surging breakers occur, with waves surging up and down the slope (Schiereck, 2004).

With the wave characteristics as obtained from Chew et al. (1974), see Section 2.2.4 and Appendix A, we can then calculate the Irribarren number for East Coast Park, with the expression for the deep water wave length (Bosboom & Stive, 2011; Holthuijsen, 2007):

$$L_0 = \frac{gT^2}{2\pi} \qquad 3.6$$

Based on occurrence an offshore wave height of H_0 = 0.25 m is taken, with a wave period of around T = 4 s. This results in a deep water wave length L_0 = 25 m. According to equation 2.8 and beach slopes ranging from 1:5 to 1:15 the Irribarren is then found to be 0.67 < ξ < 2, which states that the predominant waves breaking on the beaches along East Coast Park are theoretically of the plunging type. In reality, however, the breaking type depends much on the local wave climate and water level. During lower water levels the waterline recedes back to the upper foreshore, which has a gentler profile and thus mainly spilling breakers are found then. During high water levels, however, waves break either directly on the beach when waves are large enough or surge up and down the beach slope during milder conditions. The breaking waves are then of the plunging and surging type.

3.4 Conclusions

Over the past decades the southeast coast of Singapore has undergone some major transformations, with the natural shoreline turned into an entirely man-made one by the land reclamations that have been carried out during the East Coast Reclamation Scheme. Besides creating accommodation space for housing estates, the coastal area was intended to serve as a recreational coastal park with attractive beaches, called East Coast Park. For the reclamations a formerly present intertidal flat was covered with a layer of fill material. The surface of the intertidal flat consisted mainly of marine clays and silts, whereas the fill material consisted of a mixture of coarse sands and fines, which were taken from inland hills on the main island.

In order to protect the newly reclaimed land from wave action and to stimulate the formation of beaches along the coast, a series of structures was implemented based on the concept of *headland control*. Headland control is characterised by the placement of headland breakwaters perpendicular to the normal of the predominant wave climate. In this way asymmetric, J-shaped embayments were formed where the concept was applied, and elsewhere other types of beaches were found. A total of 31 so-called *coastal cells* was created, which are categorised as being either straight (20 cells), pocket beach (2 cells) or J-shaped (8 cells).

During formation of the beaches in the coastal cells, waves sorted out the sediments, washing out the fines and leaving behind coarse-grained beaches. The average grain size diameter D_{50} on the beach slope is nowadays around 1.3 mm, based on literature and on fieldwork that has been performed during this study. With a mild wave climate present, beaches along East Coast Park are of the reflective type according to the classification of beach states by Dean (1973). This seems especially true when regarding the large beach profile slopes, which vary from 1:5 to 1:15. A variety of wave breaker types is found along the

coast, because of different beaches in alongshore direction but also because of a cross-shore varying beach profile. During low water levels spilling waves are observed, whereas during high water levels waves are either plunging or surging on the beach.

In this chapter some basic characteristics of East Coast Park and its beaches have been addressed, in order to provide some background knowledge of the system to be analysed. The next step is then to build upon this knowledge and assess the processes influencing the coastal morphology. Before doing so, firstly a clear approach needs to be formulated. By defining a simple and schematic conceptual model some research questions and hypotheses can be formulated, which form the basis of the subsequent chapters. This approach, the conceptual model and the research questions and hypotheses are described in the methodology in the next chapter.

4 Methodology

4.1 Introduction

In this chapter the methodology that has been followed in the analysis of the physical coastal system in front of East Coast Park is described. Before any analysis is further elaborated, it is helpful to create a conceptual model, which is the first step in this methodology. The conceptual model can be regarded as the backbone of the analysis presented in Chapters 5 and 6. It basically consists of a system schematisation, with the system comprising the coastal zone along East Coast Park. To reduce the complexity of the analysis of such a relatively large system, in which various processes prevail on different temporal and spatial scales, the schematisation is meant to discretise the system and treat different scales separately. Since in reality a continuous interaction exists between processes prevailing on different scales, the integrity of the conceptual model can only be guaranteed when this interaction is included in the analysis.

Based on the conceptual model some research questions and hypotheses are formulated, which form the framework for the subsequent chapters and are validated and elaborated on by means of the study. Following these research questions and hypotheses, at the end of this chapter a short overview is given on the tools used to assess the coastal processes and on the outline of the following chapters.

4.2 Conceptual model

4.2.1 Objective

With only limited readily available data at hand, one's options to perform an adequate quantitative analysis become limited as well. It is therefore paramount to ensure the clarity of the study objective and the feasibility of the analysis. Considering the limited amount of resources and short timeframe for this study, a quantitative analysis is not always feasible and in that case a qualitative analysis is deemed sufficient in light of the Building with Nature design pilot.

A conceptual model is an encouraging tool because of its simplicity, and it has been indispensable in the process and progress of the analysis. The objective of the conceptual model is to serve as a tool to facilitate the analysis of the dynamics of the coastal system in a qualitative way, which can then be substantiated quantitatively where (future) readily available data allows for more thorough analyses. It can be regarded as the foundation of the analysis, which is set up in a very basic way so that it can be complemented, adjusted and applied to similar coastal systems.

4.2.2 Approach

Before setting up a conceptual model it is important to have a clear approach, which can be used as a guide and reference throughout the setup and analysis. In this study, the approach has been simplified to some basic steps, which are deduced from various spatial scales on which morphological changes take place in the system considered. Temporal scales of

morphological changes, however, still form an uncertainty and are presumed to increase with increasing spatial scales. Superimposed on these scales are the processes that then occur on these different scales. In Figure 4.1 such different scales have been illustrated.
The idea behind this approach is basic and straightforward, namely to visualise the system to consist of smaller, interdependent subsystems. The entire stretch of East Coast Park and its coastal zone can be regarded as the large-scale system, whereas the small-scale subsystems comprise the previously defined coastal cells, thus each subsystem representing an individual cell.

Before carrying out the steps of the analysis, the two scales and their boundaries need to be defined carefully. The large-scale contains the broadest area of interest and a buffer for future evolutions. Initially local, small-scale characteristics, which might not have a direct impact on the large-scale, are neglected. One can think of the presence of structures along the coast and the occurrence of runoff channels within a coastal cell, or local irregularities in the coastal profile. After defining the large scale and its characteristics, the subsystems can be defined based on criteria that ought to specify the boundaries of such a system. In order to avoid ambiguities, such criteria should be generally applicable to coastal cells along East Coast Park.

In the foregoing chapter three different types of coastal cells had been identified, based on different characteristic parameters from both the cells as the enclosing structures. In our domain decomposition, then, local characteristics *within* a subsystem (e.g. cell type, structure orientation, spacing...) do not necessarily need to be similar for each subsystem, even though we define generally applicable criteria to specify the *boundaries* of subsystems. This means that initially the same boundary conditions can be applied to each subsystem, irrespective of differences in beach cell characteristics, so that an efficient analysis is made possible.

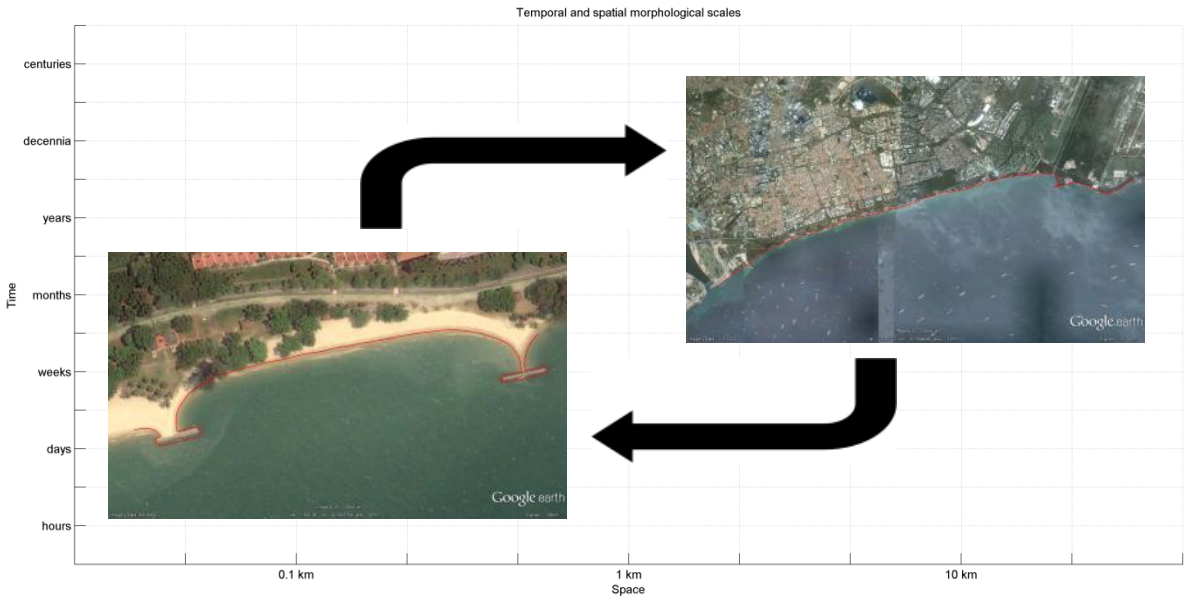

Figure 4.1 Spatial and temporal morphological scales of the coastal system in front of East Coast Park. Temporal scales are indicated on the vertical axis and spatial scales on the horizontal. In this study, two system scales are defined: a large-scale system, comprising all of East Coast Park, and a small-scale system, comprising an individual coastal cell.

The two spatial and temporal morphological scales depicted in Figure 4.1 are thus characterised as follows:

1 The large-scale system, which is part of a global system and comprises all of East Coast Park, is affected by long-term processes and the residual effect of short-term processes, while morphological changes are visible on large time scales only. Small-scale characteristics, such as structures, are neglected on this scale; only their effects on the large-scale morphology are considered, e.g. due to long-term interaction between coastal cells;

2 The small-scale system, which comprises beaches enclosed by two adjacent headlands (i.e. coastal cell), in which the morphology is largely determined by relatively short-term processes. Processes occurring on the large-scale system scale determine the boundary conditions of the small-scale system.

Both scales are interlinked with each other and can therefore not be regarded as entirely independent systems. Processes occurring on a small scale might not be directly visible on a large scale, but on the longer term small-scale processes might lead to noticeable effects on the large scale as well. The arrows in Figure 4.1 indicate this dependency.

4.2.3 Orthogonality hypothesis

When assessing the geomorphologic evolution of beaches along East Coast Park, a typical approach as described by Gonzalez, Medina, and Losada (2010) can be used. They define a practical method to make valid, preliminary beach planform and profile analyses, according to the *orthogonality hypothesis*. The orthogonality hypothesis states that complex, three-dimensional morphological scales and their processes can be broken down into two-dimensional scales which can be treated independently of each other. The *orthogonality* then refers to the fact that the scales are orthogonal to each other, comprising of a transversal and a longitudinal scale, the former referring to cross-shore and the latter to longshore profiles. This is illustrated in Figure 4.2 below.

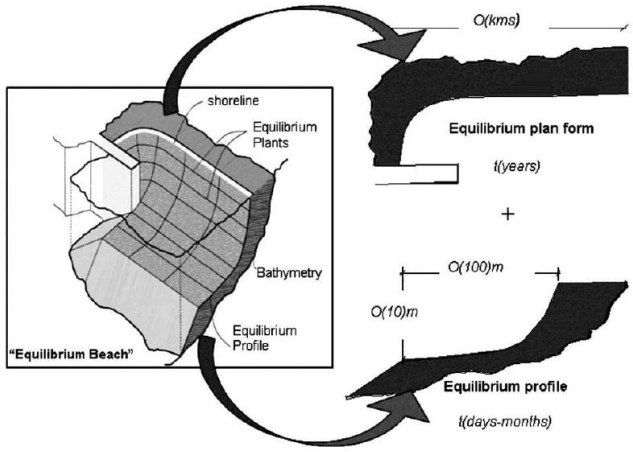

Figure 4.2 Sketch of an "equilibrium beach" (beach plan + beach profile). Orthogonality of the longitudinal and transversal movements of a beach (Gonzalez et al., 2010)

This method was already addressed earlier by Silvester and Hsu (1993), and provides a great advantage to the qualitative assessment in this study and to the use of fast and simple numerical modelling tools.

Applying the above method to our study, we can thus assess cross-shore and longshore morphodynamics independent of each other. In a cross-shore analysis we look at morphological evolution of a beach profile, whereas in a longshore analysis we look at the coastline and the beach planform. In analogy with the domain decomposition from Figure 4.1, the independent analyses of cross-shore and longshore morphodynamics do not imply that both scales are independent in reality as well. It is therefore paramount to find a relation between the analyses of both scales, in order to assess the three-dimensional behaviour of the coastal zone as much as possible.

4.2.4 System schematisation

In order to set up a comprehensible and generally applicable conceptual model, schematising the coastal system along East Coast Park is inevitable. The coastal system along the entire stretch of East Coast Park, hereupon referred to as *ECP system*, consists of a series of subsystems, namely the coastal cells as described in Chapter 3.3. Each individual subsystem will from hereon be referred to as a *cell system*. Regarding the relatively small dimensions of the coastal cells, the basic assumption is here that all cells are subject to the same driving forces. This does not infer that the processes determining the morphology within a cell are identical for all cells, as these depend on local parameters as well.

If we consider a coordinate system with its origin at the western most point of the system, located on the shoreline, with the x-axis perpendicular to the coast and positive in offshore direction and the y-axis parallel to the coast and positive in eastward direction, the subsystems can be schematised as in Figure 4.3. Along each of these subsystems boundary conditions ought to be specified, which can be both hydrodynamic and morphodynamic conditions. Below schematisation forms the starting point for any step in the analysis of the system as a whole.

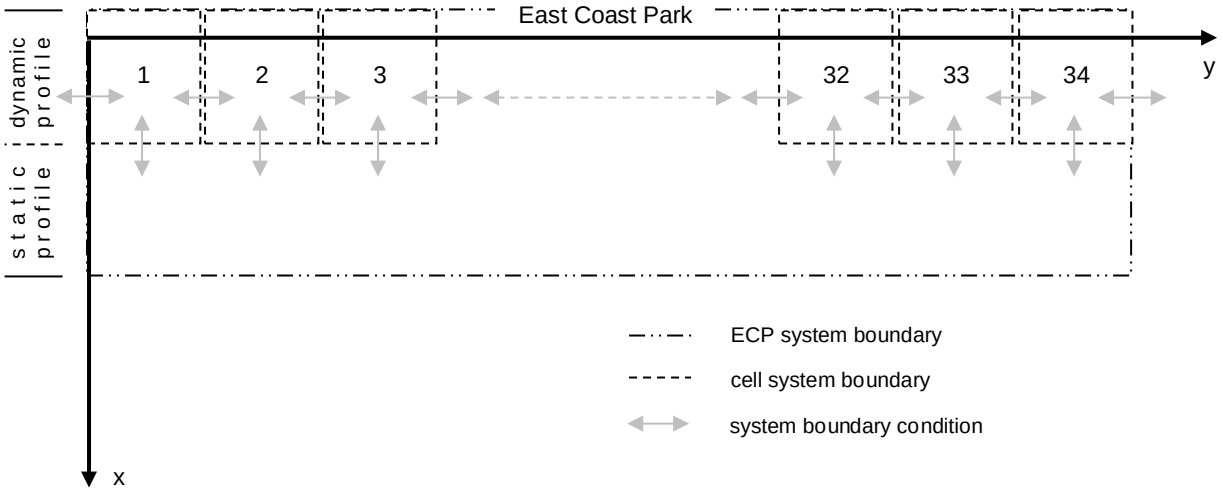

Figure 4.3 System schematisation of the coastal system of East Coast Park, consisting of the full ECP system and its cell systems. The x-axis coincides with the westernmost boundary of the system and is positive in offshore direction. The y-axis coincides with the current shoreline and is positive in eastward direction.

4.2.5 Boundary conditions

As stated above, the boundary conditions consist of hydrodynamic and morphodynamic conditions. Performing an analysis with a lack of data forces one to look at the considered system as part of a larger system, because many of the conditions affecting neighbouring coastal systems might affect our system as well, and cross-boundary interactions exist in reality. In this analysis we will consider the large scale ECP system and the small scale cell system separately. Thereafter, based on both analyses, the interactions between the different system scales are addressed. In this way the cell system is regarded as part of the ECP system, which in its turn is part of a global system as mentioned before.

ECP system

As shown in Figure 4.3, the ECP system profile is divided into a dynamic and a static part. The dynamic zone is assumed equal to the littoral zone, of which the seaward limit is determined by the depth of closure. The depth of closure or closure depth is defined as the depth beyond which no significant longshore or cross-shore sediment transport occurs due to littoral transport processes. It is generally defined as the depth at the seaward limit of the littoral zone. The static zone is the part of the profile where no significant changes in morphology occur. Due to tide-induced water level variations the position of the seaward limit of the dynamic zone shifts in cross-shore direction, as waves start to feel the bottom further offshore during lower water levels. The boundaries of the ECP system in x-direction are taken sufficiently far enough on- and offshore, well beyond the seaward limit of the littoral zone and far enough landwards. In this way, the shifting of the seaward dynamic limit and ongoing shoreline retreat at the coastline is also taken into account. The seaward boundary of the static zone and thus ECP system lies far enough offshore, though shoreward of the previously mentioned anchorage zone, which starts at the 10 m contour line, approximately 1000 m offshore (Section 2.2.4). The offshore boundary condition consists of hydrodynamic conditions only. Namely, as the seaward boundary of the static zone is assumed to be well beyond the littoral zone, the assumption here is that cross-shore sediment transport is equal to zero at the seaward limit of the ECP system. The hydrodynamic conditions consist of offshore wave conditions and possibly tidal currents and wind conditions.

In y-direction, the western and eastern boundaries coincide with the western boundary of the first cell system and the eastern boundary of the last cell system, respectively. As it is still unknown whether there is a sediment input and output across the boundaries of the system, these boundary conditions are assumed to consist of both sediment transport in and out of the littoral zone and longshore currents caused by waves and the tide. In Figure 4.3 this is indicated by the arrows crossing the western and eastern boundaries of the littoral zone. Possible long-term cross-boundary transport due to shifting of the seaward dynamic limit is indicated as well. In the ECP system the coastline is initially schematised as an uninterrupted coastline, under the *initial* assumption that anthropogenic structures mainly affect the small-scale processes and can thus be neglected in the large-scale system. The validity of this assumption will be addressed when looking at the interaction between the different system scales.

Cell system

In x-direction, cell systems share the same landward boundary as the ECP system, but not the same seaward boundary. Cell systems comprise the aforementioned dynamic part of the ECP system profile. The boundary conditions at the seaward boundary consist of nearshore wave, tide and wind conditions. Sediment distribution in the cross-shore profile predominantly occurs within this dynamic profile, whereas on the long-term exchange of sediment through the seaward boundary might occur as well.

In y-direction, adjacent cells share boundaries and therefore boundary conditions at coinciding boundaries will be similar for both cells. Regarding the scope of the study, the boundary conditions are assessed in a qualitative way rather than in a quantitative way, meaning that the cell systems will be generalised in analogy with the classification as depicted in Figure 3.8. There we defined three beach types, namely straight beaches, pocket beaches and J-shaped beaches. The morphological interaction between adjacent cells, and thus the possibility of sediment transport, then depends on the type of cell, the sediment availability and the sediment transport capacity, and is therefore not necessarily guaranteed for every cell along the coast. Contrary to the ECP system, on cell system scale anthropogenic structures are not neglected, as their dimensions and orientations strongly influence the processes occurring within these systems.

Even though the boundary conditions for the large-scale and the small-scale systems are not necessarily identical, the structure of both is the same. In x-direction we have a land boundary and hydrodynamic conditions, whereas in y-direction we have both hydrodynamic conditions and sediment in- and outputs, see Figure 4.4 below.

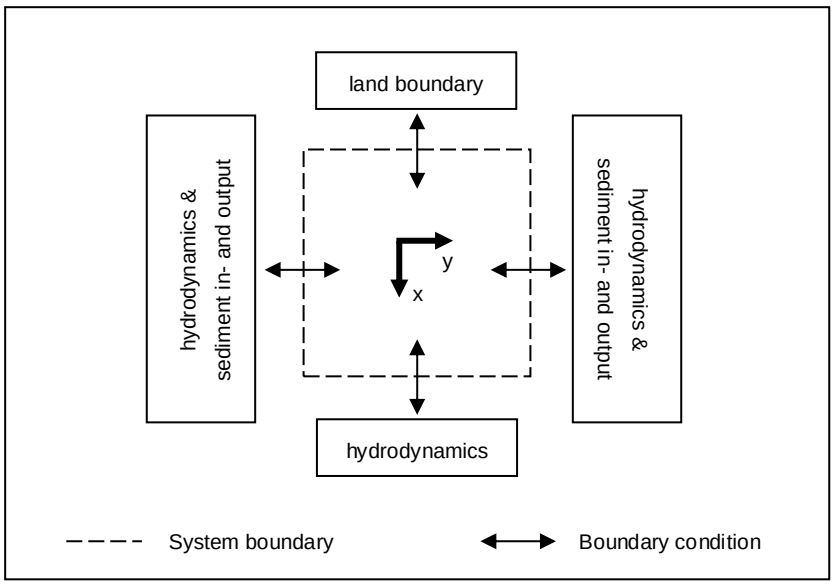

Figure 4.4 System boundary conditions

4.2.6 Coastal processes

In the conceptual model we generally focus on two possible directions of sediment transport: *cross-shore* and *longshore sediment transport*. Prior to this study it was still unknown which of these transport modes is dominant over the other, where dominance is defined by the (long-term) transport magnitudes that each of these transport modes induce. The possibility of a combination of both transport modes or the existence of complex processes such as turbulent eddies is hereby not excluded, but will for the sake of simplicity and applicability be neglected at this stage.

Next, it is important to define the driving forces we will take into account in the conceptual model. These can be derived from Section 2.2, in which the coastal climate is described. There are several processes that could contribute to shoreline retreat, be it on the ECP system scale as on the cell system scale.

The following drivers are considered to be of importance:

- (monsoon-generated) swell waves;
- (locally generated) wind waves;
- tide;
- relative sea level rise (sea level rise combined with land subsidence).

Using the same approach as depicted in Figure 4.1, we can now visualise the processes in a similar manner, based on the temporal scales and the extent of the spatial scales on which they occur. In Figure 4.5 these processes are shown.

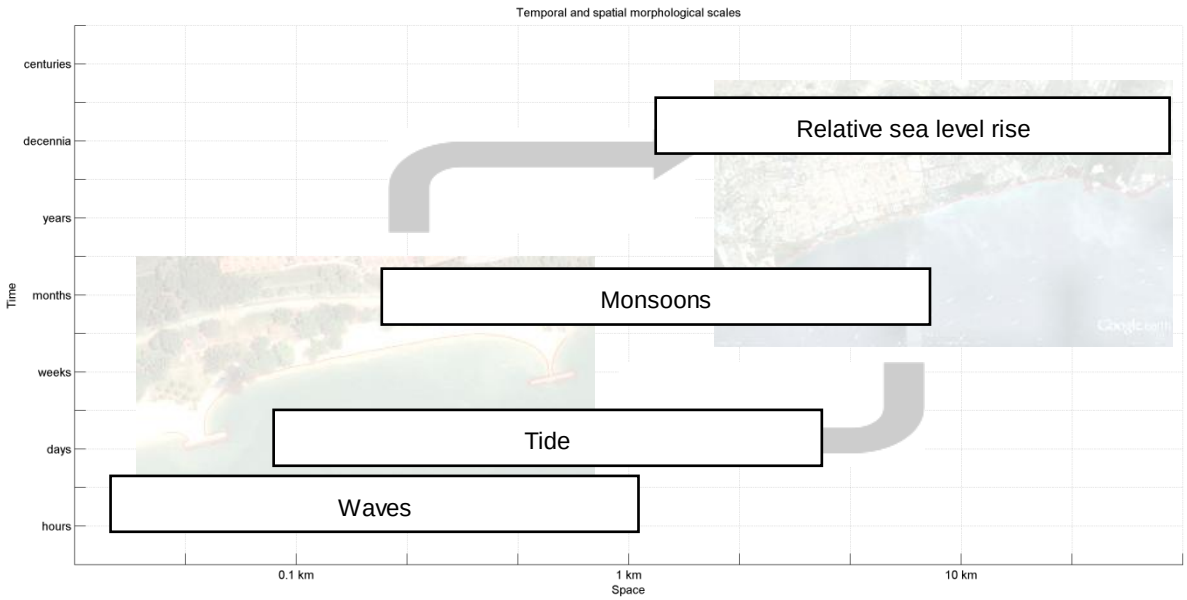

Figure 4.5 Processes affecting the morphological evolution of the coastline

Of the above processes, currently only accurate data on (monsoon-generated) swell waves and the tidal regime is available. In the figure above, the monsoons are mainly meant to

indicate the variability of the wave climate throughout the year. Relative sea level rise consists of eustatic sea level rise in combination with local land subsidence. In the following analysis the focus will thus be narrowed down to the influence of waves, the tide, monsoon variability and the effect of relative sea level rise. Together with the possibility of having cross- and longshore sediment transport, we can create a simple table to use for reference during the analysis, see Table 4.1.

In this table we can indicate which combination of driving force and direction of transport seems to be significant in the morphological evolution of our system, and cross out those combinations that are unlikely to occur or are insignificant. In this first step of the analysis we can already leave out the combination of tide and cross-shore transport, as the tide itself mainly causes water level changes and thus negligible cross-shore flows in the dynamic profile. Alongshore, on the other hand, both the tide and the waves might induce large enough longshore currents to transport sediment. Waves breaking on the shoreface might also move sediment cross-shore.

Whether any of the remaining combinations is significant depends on both the contribution to morphological changes and the ratio between each of the combinations. The effect of monsoon variability and relative sea level rise is accounted for as well, as these can affect cross-shore and longshore processes on longer time scales. In Table 4.1 the border between the ECP and cell scale processes is not definite, as the influence of monsoons and the tide crosses the boundary of the cell scale, thus affecting both the cell scale on the short-term as the ECP scale on the relatively long scale, see also Figure 4.5. Table 4.1 can be applied to both the present-day processes as to the processes of before the land reclamations, of which the latter would have an assumptive character due to lack of readily available data. In this way the significance of coastal processes can be expressed as a function of time, to see how they have changed and to assess what has caused this.

Table 4.1 Significance of coastal processes in the morphological evolution.
RSLR = relative sea level rise. The dashed-dot line indicates that the effect of monsoons is not restricted to the ECP system scale only.

		cross-shore transport	longshore transport
ECP scale	RSLR		
	monsoons		
cell scale	tidal currents	– –	
	waves		

Indication of significance, negative less significant: – – , – , + , + +

Note that the use of pluses and minuses to assess the significance of the various processes is one of many ways to do so, and will just as likely be affected by subjectivity of the author as any other method would, regarding the semi-quantitative approach of this analysis. The goal of this method is merely to indicate the *relative* importance of each coastal process.

Hereafter we will look at the coastal processes occurring on both the cell system scale and the ECP system scale, separately.

Cell system

If we take a symmetric cell system as an example for illustration, we can visualise the coastal processes occurring on a smaller scale for explanatory purposes, as is done in Figure 4.6. In this figure the dynamic and static profile are separated into three zones, (1) a zone within a coastal cell where only wave action is significant in the transport of sediment; (2) a zone where waves and the tide both contribute to currents that might bypass sediment around the structures in longshore direction; (3) a zone where waves have no or hardly any influence and only the tidal currents dominate. Because the dynamic profile was assumed equal to the littoral zone, the seaward boundary has been defined by the depth of closure. The location of this depth of closure is not fixed in time, but is approximated as the point where waves start to 'feel' the sea bottom. Therefore the dynamic profile is assumed to comprise the zones where waves have any influence. Seaward of the dynamic profile (at the transition from 2 to 3) waves are negligible and only the tide plays a role. Note that here structures are included in the analysis, because the effect of structures on local processes is significant on a cell scale.

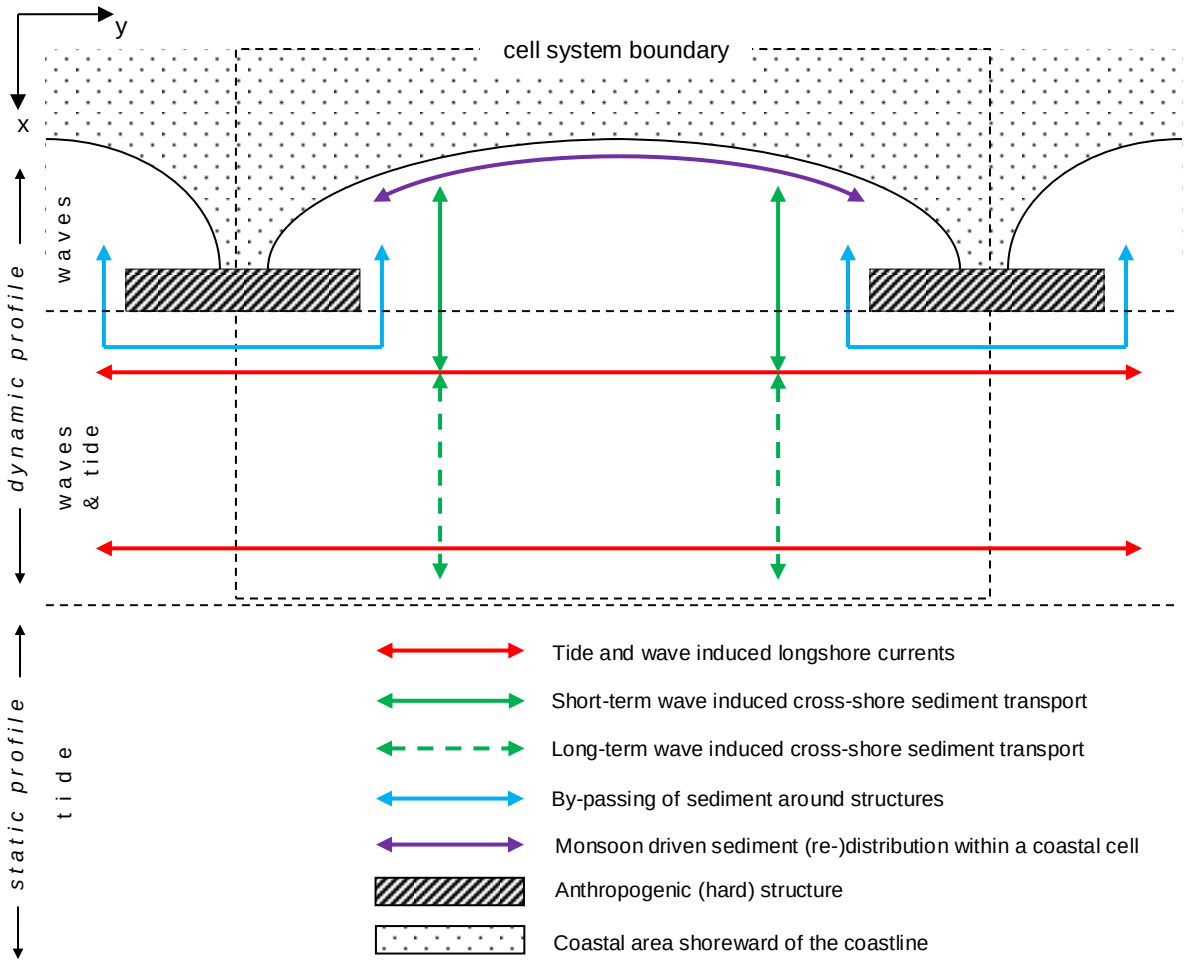

Figure 4.6 Schematisation of the plan view of a cell system with the zones of influence for waves and tide

In the figure four major coastal processes are distinguished, indicated by different colours, although these do not necessarily occur independently of each other. Below each of these processes is concisely described.

- *Wave induced cross-shore sediment transport*

  Cross-shore sediment transport occurs perpendicular to the shoreline, which in this schematisation coincides with the x-direction. Sediment can be brought both off- and onshore, depending on beach profile, grain diameter and wave climate. Since the wave climate is dependent on the time of the year, also the cross-shore sediment transport will be. If this is also the case along East Coast Park, indications of monsoon-varying profiles should be visible throughout the year, similar to winter and summer profiles in more temperate environments.

  During the N.E. monsoon, with more energetic waves, a more gentle profile is then expected because of offshore directed sediment transport. During the S.W. monsoon a steeper profile is expected, due to the milder wave climate that occurs, consisting mainly of short waves that build up the beach profile. In general, losses due to cross-shore sediment transport are the result of the balance between these onshore and offshore directed sediment transports. In case offshore directed sediment transport dominates over onshore directed sediment transport, (temporary) shoreline retreat is to be expected;

- *Tide and wave induced longshore sediment transport*

  Longshore sediment transport occurs if wave and tide induced longshore currents are strong enough to carry sediment alongshore. With obliquely incident waves approaching the coast a wave induced longshore current can be generated, which occurs within the dynamic profile. The point at which waves start to break depends on the water level and local bathymetry.

  Because of a steep beach face, during high water a narrow surf zone exists, contrary to a wider surf zone on the gentler shoreface during low water levels. In combination with tidal currents along the shore, the wave induced currents might then transport sediment in alongshore direction, parallel to the y-axis, due to alongshore gradients in sediment transport. Besides these currents the grain diameter plays an important role in the actual transport as well, since larger grain sizes are more difficult to transport than fines;

- *Sediment redistribution within a beach cell*

  With waves penetrating the beach cell under different angles throughout the year, sediment might be distributed within the cell without it necessarily contributing to structural erosion. This will mainly depend on the orientation and position of headlands and of course wave climate. Thus a seasonality might also be found in the sediment distribution within a cell. Such phenomena have been observed around the world, such as along the Mediterranean coasts of Spain, see Valdemoro and Jiménez (2006), where seasonal changes in wave climate invoke changes in sediment distribution and thus different orientations of the beach throughout the year. This is often referred to as *beach rotation*, and typically occurs on embayed beaches enclosed by (natural) headlands. Some study examples on beach rotation along the Spanish Mediterranean coasts can

be found in, amongst others, Bowman, Guillén, López, and Pellegrino (2009), Ojeda and Guillén (2008) and Turki, Medina, Gonzalez, and Coco (2012);

- *By-passing of sediment around structures*

  By-passing of sediment around a structure is a combination of cross-shore and longshore sediment transport. As mentioned above, the breaker zone will shift with the tidal range. Knowing that the beach face along East Coast Park is relatively steep and the upper shoreface relatively gently sloping, sediment can thus be eroded from the beach face during high water levels and transported to the upper shoreface, in the zone where both waves and the tide influence the morphology. If the wave- and tide-induced current is then strong enough, sediment could be carried in alongshore direction during lower water levels. Finer sediments might then be transported back into a cell during rising water levels; for coarse sediment this seems unlikely to occur. Such (hypothetical) interaction between coastal cells raises the question whether by-passing then is a uni- or bidirectional phenomenon. In other words, if by-passing of sediment occurs, is there a balance in westward and eastward directed sediment transport, keeping the sediment within a certain alongshore margin, or is there a dominant direction which eventually leads to a loss of sediment from the system? By-passing of sediment can be regarded as an intermediate step, linking the cell system scales to the larger ECP system scale.

These processes, and especially by-passing of sediment and relative sea level rise, have been visualised in the figures below, in order to better illustrate the expected processes occurring along the coast.

Figure 4.7 Illustrative sketch of a part of East Coast Park and a cross section, indicating different sediment layers and contour depths. Created by JAM visual thinking (http://www.jam-site.nl/)

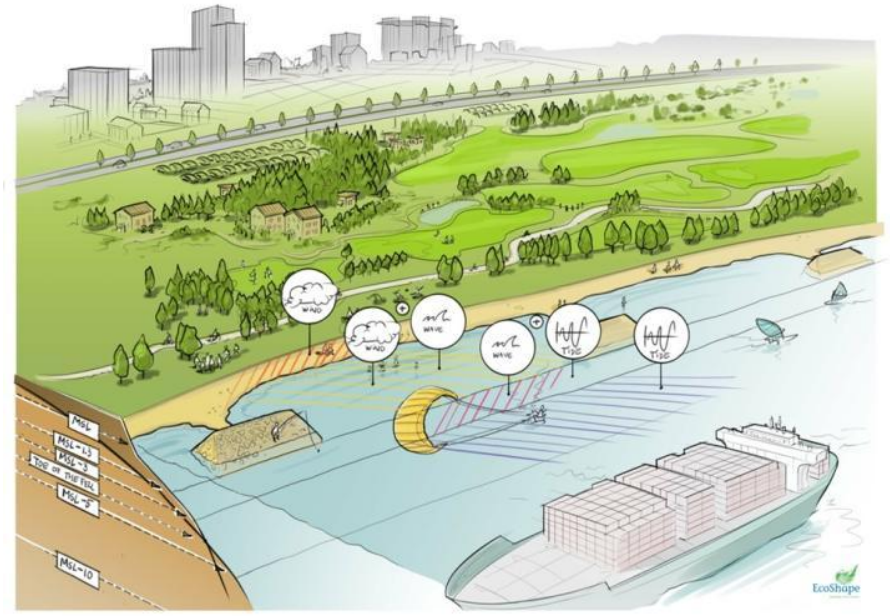

Figure 4.8 Indication of driving forces for sediment transport occurring in different zones along the cross-shore profile. In order, from the shore in seaward direction: (1) wind induced transport; (2) wind and wave induced transport; (3) wave and tide induced transport; (4) tide-dominated transport. Created by JAM visual thinking (http://www.jam-site.nl/)

Figure 4.9 An illustration of processes contributing to a structural loss of sediment. Sediment by-passing around structures is shown in the top view of the sketch, and sea level rise and land subsidence in the cross-shore transect. Created by JAM visual thinking (http://www.jam-site.nl/)

ECP system

Using Figure 4.3 and complementing it with the processes that we would observe when looking at the large ECP system scale gives Figure 4.10 below. In this schematisation the presence of anthropogenic structures is neglected on the ECP scale. The influence of these structures is treated on the cell scale as mentioned before. On the ECP scale, the shoreline movement will mainly be determined by long-term processes. By neglecting the presence of structures on the ECP scale we only take into account the long-term residual effect of short-term processes, such as interaction between coastal cells due to by-passing of sediment around structures. Since these short-term processes are in fact influenced by the presence of structures on the cell scale, structures are thus indirectly accounted for on the ECP scale through the residual effect of these processes. In the figure below the residual effects are indicated as a combination of short-term wave and tide induced cross-shore and longshore sediment transport, possibly leading to an exchange of sediment between adjacent coastal cells and sediment input/output across the longitudinal ECP system boundaries. Together with relative sea level rise these processes then determine whether the coastline as a whole will be advancing or retreating.

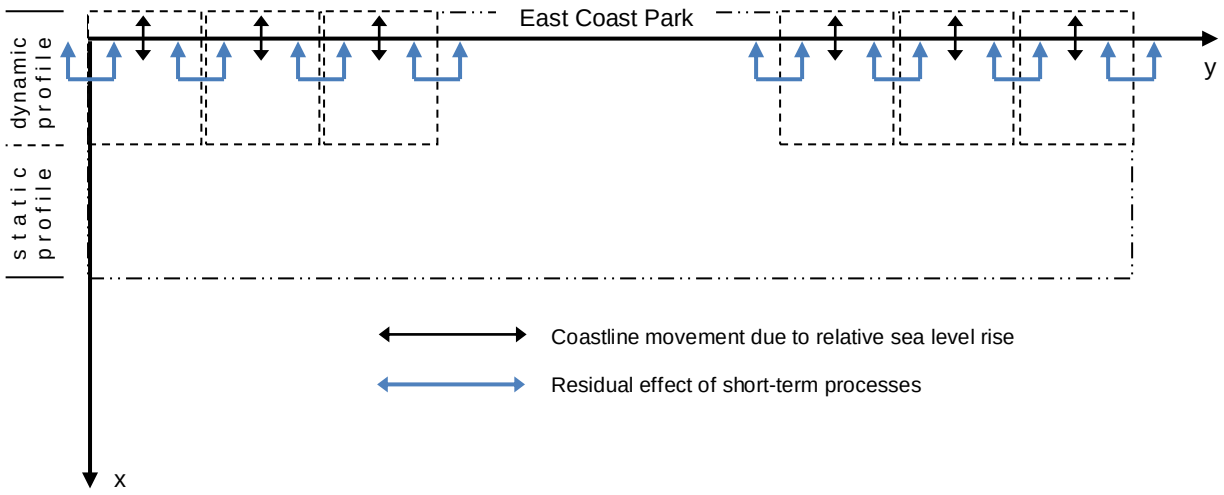

Figure 4.10 ECP system scale processes

4.2.7 Interaction of scales

After having defined the different morphological scales and the processes that define the coastline evolution on each scale, finally the interaction between the two different scales should be assessed, as depicted in Figure 4.1. This interaction has in fact already been mentioned several times, using by-passing of sediment as a possibility to distribute sediment within and perhaps even beyond the ECP system. This is an example of small-scale processes influencing the large-scale system. Long-term processes dominating on the large-scale in their turn affect the small-scale systems, such as the long-term effects of relative sea level rise. The arrows in Figure 4.1 show these bilateral influences of both scales. In this way a complete picture will be created of the coastal system at East Coast Park.

4.3 Research questions and hypotheses

Following the conceptual model we can formulate some research questions and hypotheses which form the framework of Chapters 5 and 6. The analysis described in the subsequent chapters is meant to validate the hypotheses defined in this section, by using the approach as described in the conceptual model. Behind each research question the scale it refers to is mentioned in between brackets, with the scales being the previously defined *ECP* and *cell* scales.

1 How have the land reclamations of the past decades affected the nearshore morphodynamic processes? (ECP)

Two separate reclamations are considered of influence here. The largest impact has been caused during the East Coast Reclamation Scheme, during which the original coastline and coastal profile have been altered drastically, transforming the natural environment into a man-made one. External (hydrodynamic) forces have responded to this disturbance of the natural environment by reworking the disturbed system towards an equilibrium which is in accordance with the new system characteristics, such as a steep coarse-grained beach profile versus a former mildly sloping intertidal flat. An equilibrium is commonly reached exponentially, and so are the largest changes expected to have occurred in the initial stages after the land reclamations.

The other impact is expected to have been caused by the extension of Changi Airport east of East Coast Park, which has changed the southeast coastline from a convex to a concave shape, sheltering East Coast Park more from hydrodynamic forces from the east. Due to this extension the propagation path of swell waves coming from the South China Sea has been affected, causing a stronger refraction of the waves towards the coast. This has subsequently altered the angle of wave incidence, leading to a less oblique wave approach to the coast. Such a change in wave approach directly affects the wave conditions at the shoreline and the corresponding morphodynamic processes.

2 How does relative sea level rise affect the coastline of East Coast Park? (ECP)

Relative sea level rise is the result of eustatic sea level rise and land subsidence. Sea level rise is a global phenomenon, and in combination with local land subsidence the effect could be even more significant, leading to a cross-shore translation of the coastline. In literature numerous times the presence of an unconsolidated substratum along the southeast coast has been mentioned, supporting the possibility of land subsidence (e.g. Arulrajah and Bo (2008) in Chapter 2). Relative sea level rise is generally a long-term process, but can be more noticeable when land subsidence is significant. Looking at East Coast Park, which is still relatively young, we can then expect land subsidence to have been significant over the past decades, especially with increasing surface loads.

3 To what extent does the tide contribute to sediment transport in the nearshore region along East Coast Park? (ECP)

In Chapter 2 the tidal characteristics have been treated concisely. Two aspects can be distinguished when regarding the tide, namely the vertical tidal range and the tide-induced currents. The former mainly affects the active zone of waves and is therefore

treated in the next research question. The latter has already been investigated thoroughly for the more central part of the Singapore Strait, although mostly the effect on fine sediments has been treated rather than the effect on (coarse) sands. Due to the changed coastal profile after the land reclamations the ratio between tide and wave influence on the nearshore morphology is expected to have changed significantly.

Because of a steeper beach profile water levels on the upper foreshore are relatively large compared to the formerly present intertidal flat, reducing the influence of tidal currents on the bed topography. In Chapter 2 a preliminary calculation showed the tidal current to be in the order of 0.1 m/s at a water depth of 1 m. Considering the fact that nowadays coarse sand is found on the beach, such currents seem to contain too little energy to transport sediment in alongshore direction.

4 Are waves able to stir up and transport sand? If so, where in the profile? (ECP/cell)

The wave climate at Singapore is generally mild, see also Chapter 2, and might contain too little energy to produce significant orbital and current velocities. Again considering the fact that the sediments we currently observe on the beach face mainly consist of coarse sands, transport of these coarse grains becomes questionable. Bearing in mind the large tidal range, however, the surf zone is expected to shift during different water levels, increasing the active width of the profile.

As the profile slope changes in cross-shore direction, different parts of the profile are affected in time, and due to different processes. On the steep beach profile coarse sediments are expected to be stirred up during high water levels and transported in cross-shore direction due to undertow and gravity-driven flow. Further seaward the profile is gentler and the bottom surface is covered by finer sediments, which are picked up by wave-induced longshore currents (in combination with tide-induced longshore currents) and transported in alongshore direction. The presence of structures in the profile adds another criterion to the longshore sediment transport capacity, limiting the possibility of longshore transport of coarse sediments. The latter aspect is to be treated on a smaller, cell scale, where structures are included in the analysis.

5 What is the seasonal effect of monsoons on the coastal morphology? (cell)

With both the N.E. monsoon and the S.W. monsoon leading to different wave climates during several months of the year, it is expected that the coastal morphology changes accordingly. As mentioned earlier a different angle of wave incidence results in different morphodynamic processes. This means that different equilibrium profiles and planforms exist for the different monsoon periods and that sediment might be re-distributed within a coastal cell during these periods, rather than being entirely lost from the cell. Regarding the more energetic wave climate during the N.E. monsoon, the net effect is then expected to be determined by this monsoon period.

6 Are waves able to by-pass sand around headlands to adjacent coastal cells? (cell)

Building upon the aforementioned shifting of the surf zone, a longshore current might exist seaward of the headlands. In case sand is transported far enough offshore from te beach it might end up in the zone where a longshore current is present and, if possible, be transported alongshore. The possibility of this by-passing effect should result from the analysis of hypothesis 4. During rising water levels the sand might be carried back

into a coastal cell, leading to a possible exchange of sediments between adjacent cells, or even a loss of sediment from the entire system if there is a predominant direction of transport, see also Figure 4.10.

4.4 Further analysis

4.4.1 Available sources of information

To make a qualitative assessment of the physical processes influencing the coastline, it is necessary to know which sources of information are available, and which tools might be helpful in providing more insight into the system. Below a short overview is given of the different sources of information in this study.

Literature

Literature is an indispensable source of information in any analysis. Fortunately a decent amount of literature dating back to the early stages of the East Coast Reclamation Scheme is publicly available, see also Section 3.2.1. Unfortunate, on the other hand, is the lack of technical detail on certain aspects and lack of clarity about the origin of data or assumptions in much of this literature. This does not imply that this literature is outdated in any way, as they provide reasonable insight into the system before and after the reclamations.

Rather recently a study has been conducted on the morphological evolution of the beach cells along East Coast Park, by Tan et al. (2007). Their study includes both analytical and numerical analyses and provides much insight into shoreline evolution or equilibrium profiles and planforms within the beach cells, but less insight into actual driving forces and processes. The solutions they provide to counteract shoreline erosion are therefore not substantiated from a solution-oriented point of view, but more from a problem-oriented point of view. Also, the solutions they provide (e.g. increasing dimensions of headlands) are not sustainable and do not allow for growth with relative sea level rise. These solutions seem to be in conflict with the Building with Nature principles on which an eco-dynamic coastal protection would be based. Therefore, the objectives and thus conceptual model of *this* study are different and will be carried out qualitatively instead of quantitatively.

Nautical charts

Nautical charts can give insight into nearshore bathymetry as well as coastline changes as a function of time. The most recent charts, from the last decade, have been provided by the Maritime and Port Authority of Singapore (MPA). Older charts dating back to before the East Coast Reclamation Scheme were provided by the National Archives of Singapore, and also some charts in the chart database at Deltares in the Netherlands have been found.

Aerial images

Satellite imagery today is available at such high quality that analysis of even coastal cells is possible, especially through freeware such as Google Earth. Since Google Earth is relatively new, older satellite imagery needs to be obtained elsewhere. Luckily, the United States

Geological Survey (USGS) has provided an online tool, called EarthExplorer [xi], to search through worldwide databases regarding aerial imagery.

Numerical models

Numerical models may help to gain insight into complex hydrodynamic and morphodynamic processes and evolution. Where data is sufficiently available, these models can be validated and used to make predictions for e.g. different coastal zone management strategies. Unfortunately, accurate data has either been lacking or not readily available during this study, creating limitations when it comes to defining boundary conditions of models.

Any expert on numerical modelling will admit that *rubbish in = rubbish out*, and therefore the focus of this study has not been on the calibration and validation of numerical modelling tools to investigate morphodynamic processes, but rather on carrying out sensitivity analyses in order to gain insight into the importance of different morphodynamic processes. In this way one is 'restricted' to common sense and basic insight into coastal dynamics, which is regarded as a much more valuable lesson than merely letting models do the work.

The numerical modelling tools used in this study were Unibest-LT and Unibest-TC for the influence of waves on the nearshore morphology, for longshore and cross-shore calculations respectively, and Delft3D was used to calculate tidal currents. [xii] In all of these models the presence of structures has been omitted.

In Table 4.2 below an overview is given of the tools used in this study to assess different processes.

Table 4.2 Sources of information used for the analysis of various processes

		cross-shore transport	longshore transport
ECP scale	RSLR	Literature	Literature
	monsoons	Charts, Literature	Aerial images
cell scale	tide	Delft3D, Charts	Delft3D
	waves	Unibest-TC, Charts	Unibest-LT

4.4.2 Validation of hypotheses

Finally, we will close off this chapter by shortly indicating how the aforementioned hypotheses will be analysed in the subsequent chapters. Chapter 5 and 6 both follow the domain decomposition of our conceptual model, in which we treat the ECP scale and cell scale separately. For each of these scales the morphological evolution is analysed by means of the available tools as shown in Table 4.2.

In Chapter 5 firstly the ECP system is treated, addressing the large-scale coastline and profile changes due to the land reclamations of previous decades and the long-term effect of relative sea level rise, see research questions 1 and 2. The effect of these changes on the physical processes has been analysed using literature, nautical charts and aerial images. Besides

[xi] *http://earthexplorer.usgs.gov/ and http://glovis.usgs.gov/*

[xii] *See for more information: http://www.deltaressystems.com/hydro/products*

that, the influence of the tide as well as waves on the nearshore bottom topography is treated as well (research questions 3 and 4), where the presence of structures is neglected in the large-scale analysis. For this analysis readily available literature and the numerical models Delft3D, Unibest-TC and Unibest-LT have been used.

Thereafter we go into more detail on the smaller cell scale in Chapter 6, in which the cell system is treated. The effect of waves on the shoreline is now assessed with the inclusion of structures along the coast. On this scale we mainly look at wave- and tide-induced sediment transport, but also take the seasonal effect of monsoon variability into account, as described by research questions 4, 5 and 6. The hypotheses are analysed using numerical models, nautical charts and aerial images.

5 ECP system analysis

5.1 Introduction

Following the approach described in the previous chapter, the following chapter presents the analysis results of the large-scale ECP system, see Figure 5.1.

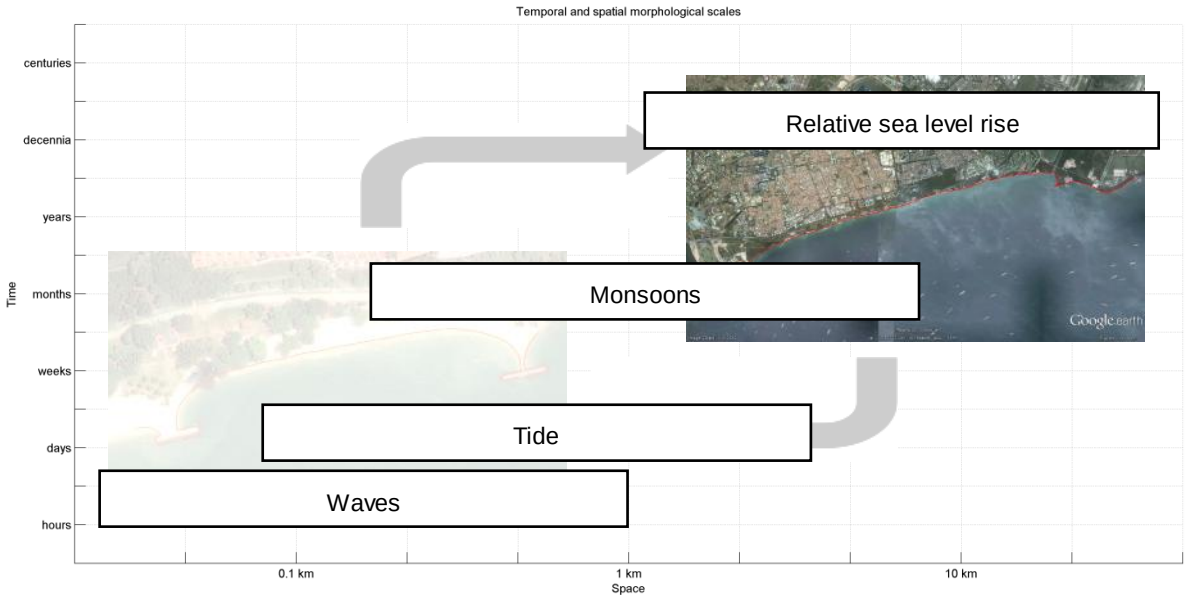

Figure 5.1 Spatial and temporal morphological scales of the coastal system in front of East Coast Park, with the large-scale system highlighted

Similar to Figure 4.5, in the above image dominant processes in the nearshore evolution have been indicated. Of these processes mainly relative sea level rise and the monsoon-induced variability in wave climate contribute to long-term changes in morphology, but also the tide plays a role in the nearshore region. The morphological changes and processes have been assessed in the study and are presented in this chapter.

The layout of this chapter is straightforward, as a chronological order is maintained in the assessment of man-made changes along the southeast coast of Singapore. Firstly the man-made changes over the past decades are discussed. Following these changes, their effect on the coastal processes is touched upon, to gain insight into how these processes have changed since the beginning of the land reclamations. This then brings us to the present-day coastal processes, which are treated from a large-scale and long-term perspective. An important aspect in this large-scale assessment is the fact that the presence of headlands along the newly reclaimed land is neglected. East Coast Park is then regarded to have an uninterrupted and nearly uniform coastline. In the next chapter the presence of headlands is included in the cell scale analysis. Throughout this chapter the first three hypotheses as narrowed down in Section 4.3 are answered.

5.2 Man-made historical changes

In this section man-made changes over the past decades are treated in two parts. In the first part the focus is on large-scale morphological changes in the coastal profile, while the second part focuses on the coastal shape and coastline orientation. This approach is merely used for illustrative purposes and it needs to be addressed that these different perspectives do not imply that the cross-shore and alongshore profiles are morphologically independent in reality.

5.2.1 Changes in the coastal profile

In Chapter 3, and section 3.2 in particular, we have already given an introduction into the land reclamations that have been performed over the past decades. For details on the implementation phases and applied stabilisation methods reference is made to that section. In this section the effect of the changes on the overall coastal profile is analysed, using (historical) nautical charts.

To start with an analysis of the coastal profile it is insightful to know what the system looked like *before* the land reclamations. Figure 5.2 shows part of a chart from 1927, in which the southeast coast of Singapore is depicted long before the land reclamations were carried out. The more convex shape of the initial coastline can be recognised, which confirms the illustrations shown earlier in Figure 3.1 and Figure 3.2. More noticeable, however, is the presence of an intertidal flat and intertidal reef along the former coastline. The intertidal flat represents an entirely different coastal profile than we observe today. At the present day, no trace of either the intertidal flat or the intertidal reef is visible at the surface.

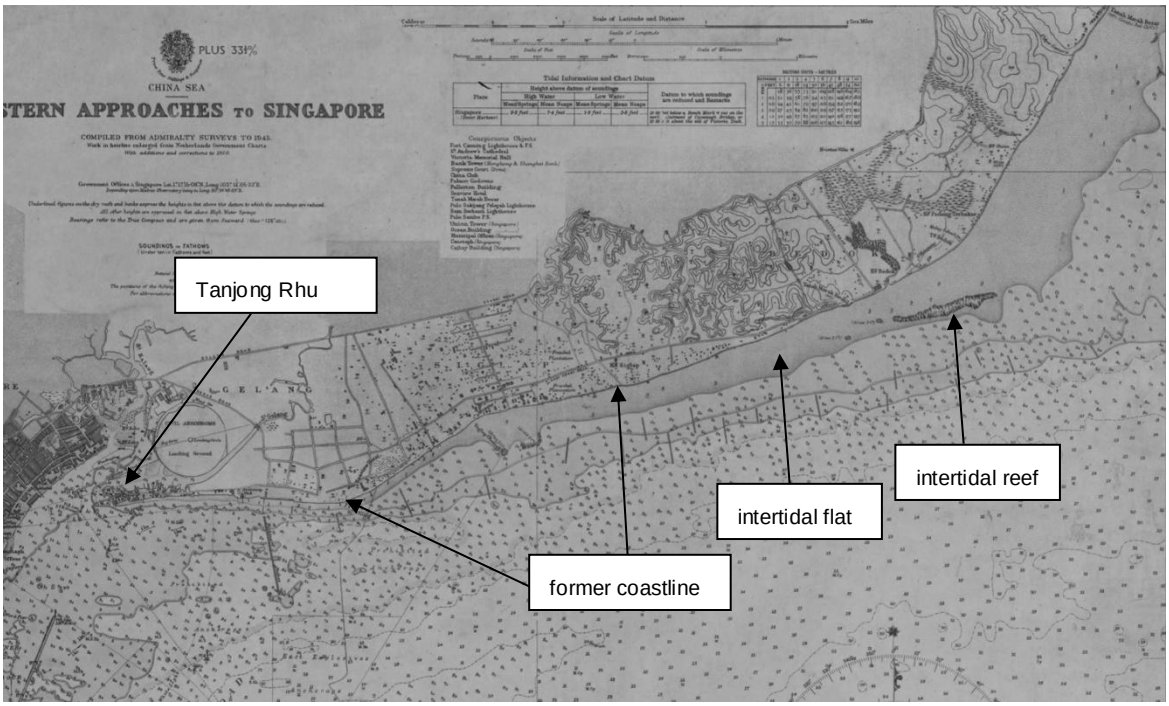

Figure 5.2 British Admiralty Chart 2556 (cropped), Eastern Approaches to Singapore, 1927, showing the southeast coast several decades before the land reclamations (Obtained from the National Archives of Singapore)

To illustrate this, an overlay has been made of the former coastal zone over the present-day coast, see Figure 5.3 below. In the upper panel of Figure 5.3 polygons are created to represent the former coastal area along the southeast of Singapore (brown), as well as the intertidal flat and intertidal reef (white and matte, respectively). With the implementation of the land reclamations both the intertidal flat and intertidal reef have been buried under the fill material. This becomes more clear when looking at a cross-section along this coast, such as along the red line in the *upper* panel of Figure 5.3.

In the *lower* panel of Figure 5.3 this cross-section is illustrated, showing how the coastal profile has changed since the land reclamations. Here the extent of the land fill is indicated, as well as the extent of the former intertidal flat. The former foreshore was much wider and more gently sloping than is the case today. The original profile had a slope of about 1:200 in the nearshore zone, whereas currently a slope of varying from 1:15 to 1:100 is found. The extent of the intertidal flat ranged from several tens of metres in the west to several hundreds of metres going east, being around 500 m at the chosen profile below. Currently the intertidal zone averages 'only' 60 metres in width.

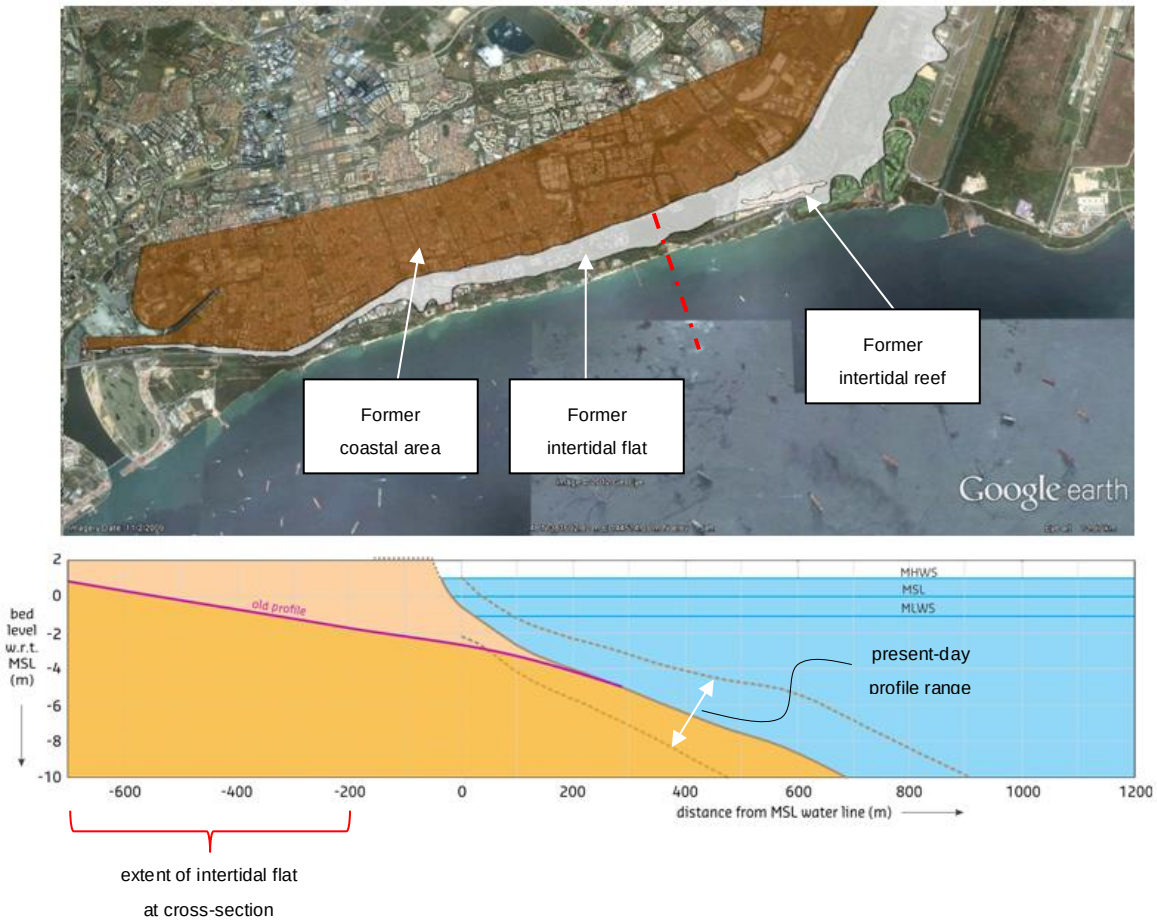

Figure 5.3 Comparison of the former and present-day coastal profile. The upper image shows an overlay of the 1927 coastline and tidal flat over the present-day coastal area, and the red dashed-dot line is the intersection along which both the historical and current profiles are measured. The lower image depicts the result of both cross-shore profiles, showing the old marine clay substratum (yellow) and the sandy fill layer on top of it. The two dotted profiles indicate the range of profiles along East Coast Park, the lower being the most shoreward and the upper being the most seaward profile.

The former intertidal area consisted of fine sand and mud at the surface, underlain by a marine clay layer. On top of this a layer of coarse-grained fill material of several metres thick had been placed to serve as the foundation of present-day East Coast Park. It should be noted however that every bottom material has its own sediment characteristics, and thus different equilibrium profiles are found for different bottom material. In general, the coarser the sediment material, the larger the angle of repose and the steeper the profile. Thus, it is not necessarily 'unnatural' to have a much larger sloping foreshore in comparison with the original profile. An important aspect, however, is the response from the (hydrodynamic) forces driving morphological evolution along the coast. This is treated later on in this chapter.

Besides changes in the slope of the foreshore, it is important to realise that the fill material does not extend far offshore. As observed during the fieldwork, which is described in more detail in Appendix C, the transition from coarse sand to mud occurred relatively near the lower beach face in the coastal cells where sediment was collected. From there on the presence of the substratum becomes more noticeable, which consists of very fine sediments, see also Figure 3.10. In some cases in the past even, some of the marine clay has appeared at the waterline after being washed out from the underlying layer (Changsha, 2011a). This is an important aspect when trying to assess equilibrium profiles, for which many of the present methods are not directly applicable. Namely, a two-layered vertical profile is present due to the fact that the zone comprising of sand is relatively narrow compared to the extent of the harder substratum and the latter thus shows up at the bottom surface relatively close to the shoreline. Also, the upper fill layer is relatively thin in comparison to the underlying substratum.

Besides the chart dating from before the land reclamations several nautical charts have been obtained, dating from 1977, 1985 and 2001. Using these charts the nearshore bathymetry can be simply illustrated as a function of time. This is done in Figure 5.4, in which the bathymetry of the three different charts (1977, 1985 and 2001) is shown. In order to distinguish significant changes in the nearshore zone between each of these charts, an overlay is made as shown in Figure 5.5, which is a larger crop than the images in Figure 5.4 to indicate Changi in the east and the presence of the so-called Outer Shoal in the west. What can be seen from the figures is that the depth contours of 1977 and 1985 seem to align in most of the nearshore zone, which is indicated by the combined blue and yellow line in the overlay (i.e. light green line in Figure 5.5). Compared to the bathymetry of 2001 the former 1977 and 1985 contour lines seem far more irregular than the latter in the nearshore region (approx. 1 km from the shoreline).

Especially in the eastern part of East Coast Park, the contour lines seem to have smoothened out and become more uniform in alongshore direction by 2001, while the bathymetry westward is still irregular. Note that the largest changes are found nearshore, while the shape of the Outer Shoal southwest of East Coast Park has hardly changed over a period of more than two decades. On average, the contour lines seem to align reasonably well. Nevertheless, some differences in depth contour reach up to several tens of metres in horizontal direction locally. On the chart from 2001, some shallower parts near the coast are indicated. Considering possible changes in precision (e.g. surveying precision might have increased over the years) used for these charts it cannot be directly concluded that this indicates a seaward shift of the depth contours on the upper foreshore, even though this seems a fairly plausible conclusion if assumed that sediment has been transported offshore. Changes on this scale will be dealt with in the next chapter.

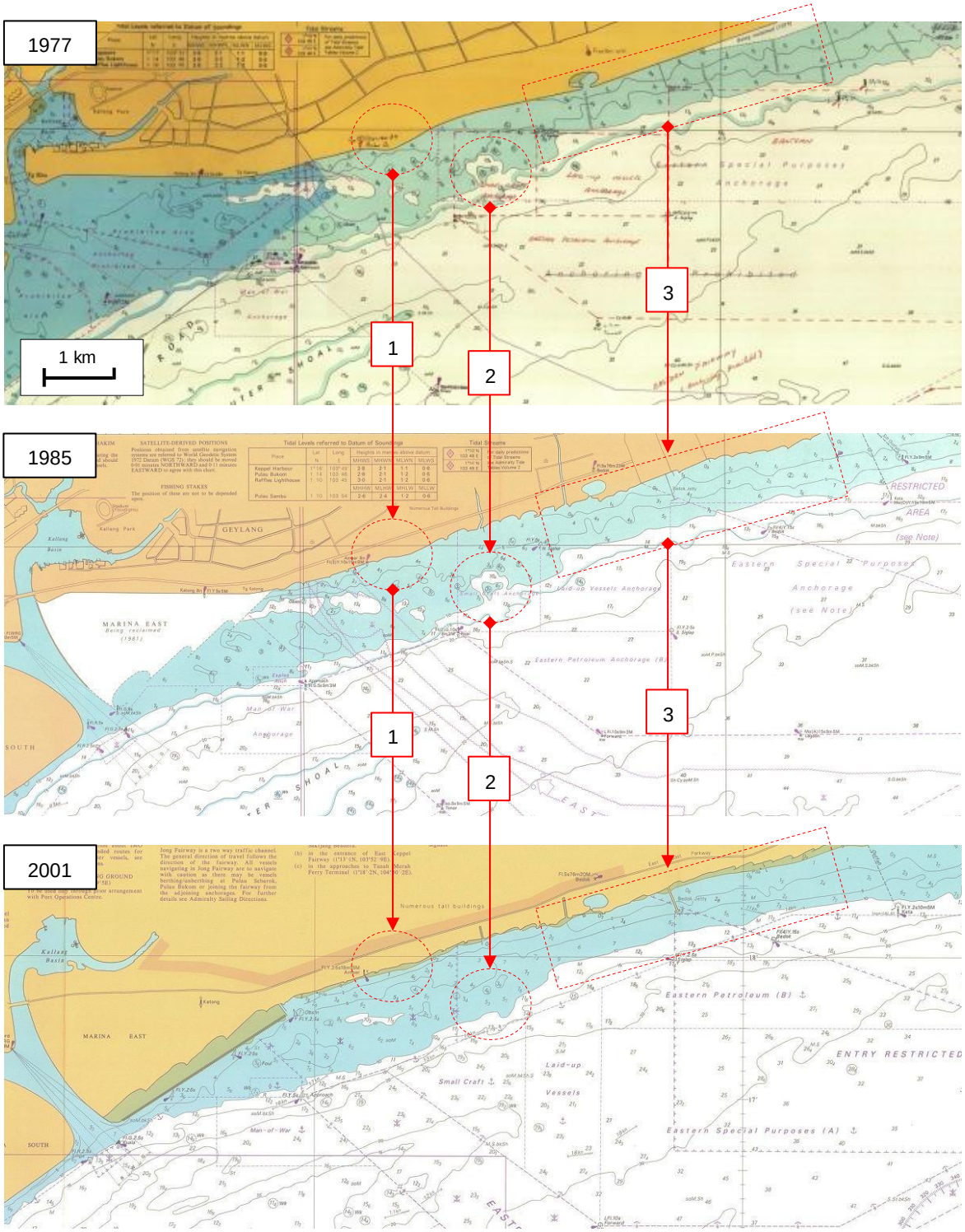

Figure 5.4 Comparison of 1997, 1985 and 2001 nearshore bathymetry along southeast Singapore. The three panels show the (cropped) nearshore depth contour lines for each chart. The original charts all have a scale of 1:27500. The arrows indicate some examples of locations in the coastline and nearshore bathymetry where significant changes are visible: (1) indicates the disappearance of a bulge in the coastline over time; (2) indicates the disappearance of an irregularity in the bathymetry in between 1985 and 2001; (3) marks a change in contour lines, becoming more uniform in between 1985 and 2001.

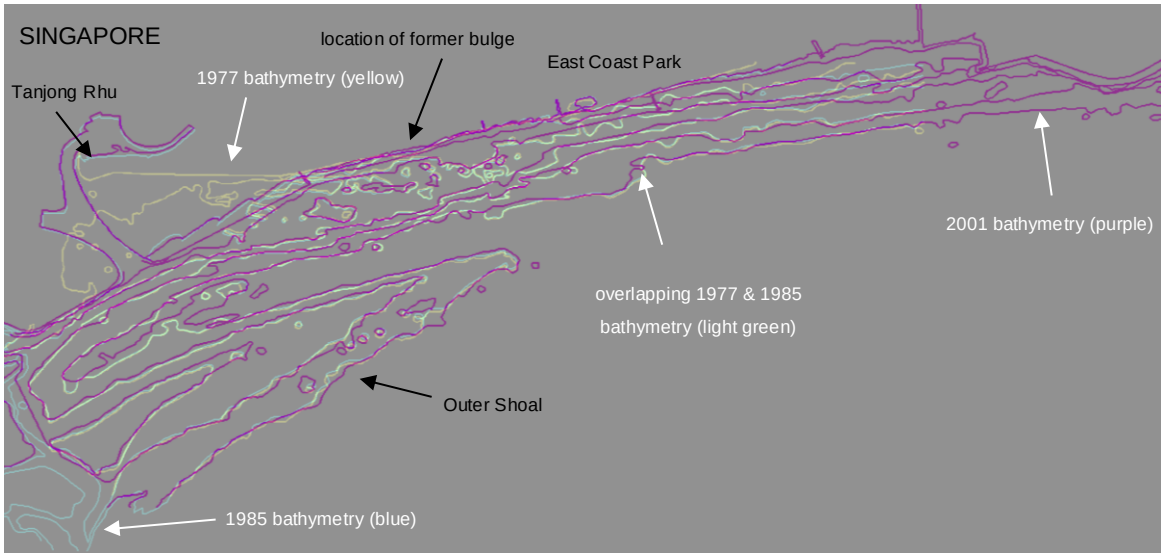

Figure 5.5 Overlay of contour lines along the southeast coast of Singapore for 1997, 1985 and 2001, after digitalisation. The contour lines of the 1977, 1985 and 2001 charts are coloured in yellow, blue and purple, respectively. The contour map comprises of the 0, 2, 5, 10, 15 and 20 m contour lines.

The changes in bathymetry in Figure 5.4 and Figure 5.5 are generally located at least a hundred metres from the coastline. At this scale it can therefore not be concluded that these changes are *directly* caused by human-induced changes along the coast or whether they follow from a response of coastal processes to the new coastal profile, which can be regarded as an *indirect* cause of human-induced changes.

Besides changes in the bathymetry, also changes in the coastline are seen for the different charts, of which the most obvious one is indicated in Figure 5.4. Again, certain differences could be caused by differences in precision of the various charts. These changes in the coastal shape and coastline, as well as the so-called *bulge* in Figure 5.4, are treated next.

5.2.2 Changes in the coastal planform

To start with an analysis of the coastline we reflect back on Figure 5.2, in which we confirmed the convex shape of the coast before the land reclamations. To build upon this observation, some satellite images have been obtained which show the coastal development over the past decades, see Figure 5.6. The earliest (clear) satellite image for Singapore dates back to the early 1970s, which is *after* the implementations of the first reclamation phases. Nevertheless, the images in Figure 5.6 clearly illustrate the changes the southeast coast of Singapore has undergone since the first phases of the East Coast Reclamation Scheme.

Note however that the initial reclamation phases had already been implemented before 1973, so that the land on which East Coast Park is built is already visible on the satellite image in Figure 5.6a. Less than two decades later the addition of Marina South and Marina East westward of East Coast Park is already visible, as well as the first addition for Changi Airport eastward of East Coast Park (Figure 5.6b). From thereon the only major changes have occurred at Changi, which was extended seawards and transformed the southeast coast into a more concave shape, see Figure 5.6c and Figure 5.6d. Along East Coast Park, however,

only minor changes are observed after 1973, where ‘minor’ is of course relative to the above scales.

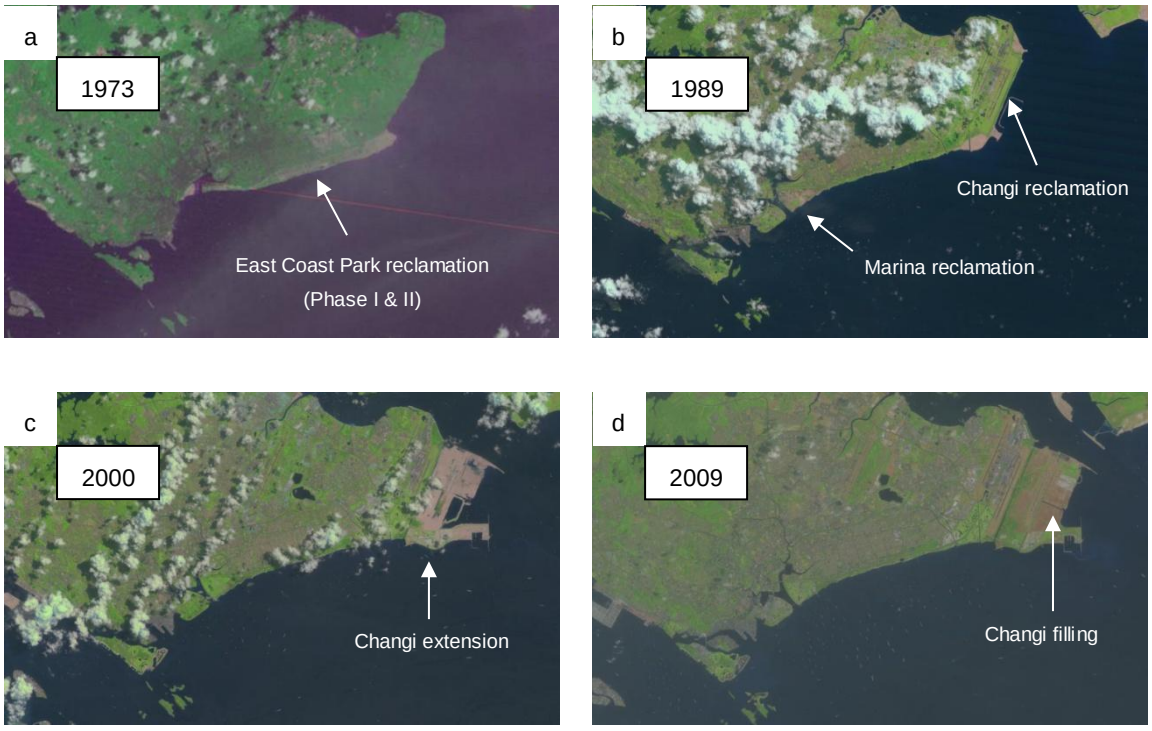

Figure 5.6 Satellite images of Singapore (cropped) for different times. (a) Landsat 1 MSS L1G, 17-10-1973, (b) Landsat 4 TM L1T, 01-06-1989, (c) Landsat 7 ETM+ L1T, 28-04-2000, (d) Landsat 5 TM L1T, 08-02-2009 (Imagery obtained at http://glovis.usgs.gov/)

If we take a closer look at East Coast Park on the satellite images of 1989 and 2009 some of the changes along East Coast Park can be observed. In Figure 5.7 few of these have been pointed out. Going from west to east along the southeast coast in this figure, we firstly observe a bulge present in 1989, which is indicated by the dashed ellipse and seems to correspond to the bulge we observed in Figure 5.4. In 2009, however, this bulge seems absent. The locations L1 and L2 point out certain indents that are present in 1989 but not visible in 2009. At the eastern tip of the mouth of the East Coast Lagoon, see L3, there seems to have been some sediment loss over the years. Finally, and most obviously, the transformation of the easternmost part of East Coast Park is indicated at L4, which is caused by the reclamation and extension of land for present-day Changi Airport.

As indicated earlier, the coastal planform and profile are not independent characteristics of the coast. Also, due to the fact that the land for East Coast Park and Marina East has been reclaimed some decades ago, it is expected that these human-induced changes have only altered the nearshore bathymetry in the initial stages after the land reclamations. Because of the alteration of the coastal profile a disturbance in the equilibrium profile had been created, even though the new equilibrium profile is different from the original one (see Figure 5.3). This has resulted in a response from coastal processes, which try to rework the disturbed profile to an equilibrium state.

It then seems logical to realise the importance of interactions between the coastal profile (and planform) and nearshore coastal processes. Frequent beach nourishment works might have contributed to disturbances and sediment availability in the coastal profile as well, however no information is readily available on such works and thus not much can be said about their influence on the coast quantitatively.

Disregarding this shortcoming, it is still possible to assess the interaction between the land reclamations and the coastal processes as a function of time, be it semi-quantitatively, based on available data and some basic knowledge on coastal dynamics. In the next section we will firstly assess the effect that the aforementioned changes have had on processes occurring along the coast. From this interaction between hydrodynamic forcing and nearshore morphology we are then able to obtain a more thorough understanding of the coastal evolution to date, which is paramount in understanding the present-day situation.

Figure 5.7 Changes along the southeast coast of Singapore in between 1989 and 2009. Satellite images from Landsat 4 TM L1T, 01-06-1989 (upper panel) and Landsat 5 TM L1T, 08-02-2009 (lower panel), cropped and zoomed to approximately 270% of the original. The dashed ellipse indicates the area where a bulge is visible in 1989. L1 and L2 indicate locations of visible indents along the 1989 coastline, which are absent in 2009. At L3 a change in the tip at the mouth of the lagoon is visible. L4 indicates the changes in the east due to the seaward extension of Changi (Imagery obtained at http://glovis.usgs.gov/)

5.3 Implications of man-made changes

5.3.1 Implications for processes

In general three processes are expected to have been affected the most by the land reclamations, namely processes resulting from

1 the tide;
2 (monsoon-induced) wave action on the shoreline;
3 relative sea level rise.

Below, the effect on each of the above driving forces is assessed qualitatively.

The tide

From the comparison of the cross-shore profile from 1927 with the current profile we could see how the extent of the intertidal zone has changed drastically due to the land reclamations. Where the intertidal flat used to extend up to approximately 350 metres offshore, the present-day intertidal zone is 'only' 60 metres wide (Figure 5.3). Before the land reclamations, the water would thus draw much further back, causing waves to affect the coast during high water levels only. Due to shallower water depths in front of the former coastline, tidal currents might have been able to pick up the (fine) sediments on the foreshore more easily. With the new profile, however, wave action on the beach is more frequent, despite the still large tidal range. Tide-induced sediment transport on the other hand has become more limited, as larger depths are reached closer to the shore and tidal currents contain too little energy to pick up the coarse sediment we observe today.

(Monsoon-induced) wave action on the shoreline

With the presence of the wide and gently sloping intertidal flat, waves would start dissipating further offshore, losing much energy before reaching the coast. Keeping in mind the fact that waves could only reach the coast during high water levels, the effect of wave action on the shoreline was less prominent than is the case nowadays, where waves break directly on the beach and do so during longer time intervals. Other than that, the extension of Changi Airport has affected the exposure of the southeast coast and the angle of wave incidence. This can be illustrated as in Figure 5.8 below.

Before the seaward extension at Changi the predominant waves approached the southeast coast almost directly from the east, and refraction occurred relatively close to the shore. Due to the presence of the Changi extension the coastline along East Coast Park is somewhat more sheltered from waves from the east. Also, because of changes in bathymetry that have been caused by the land reclamations, wave refraction nowadays occurs farther offshore around the tip of the Changi extension. This means that the angle of wave incidence to the coast has decreased, where the angle is taken relative to the normal of the (local) coastline.

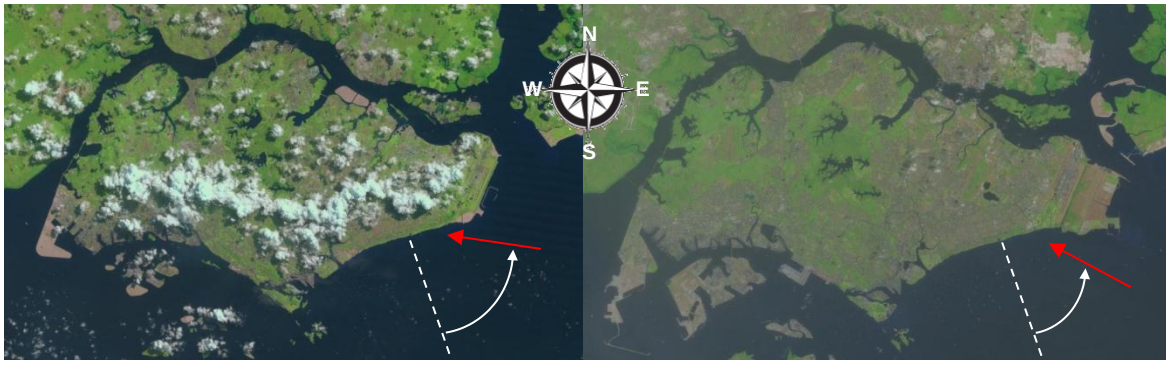

Figure 5.8 Satellite images of Singapore from 1989 (left) and 2009 (right), clearly showing the extension of Changi East in the east. The red arrows schematically illustrate the increase in wave incidence towards East Coast Park, with the angle of wave incidence taken relative to the normal of the East Coast Park coastline. The indicated angles are merely for illustration purposes.

A change in wave approach results in a change in sediment transport. This can be explained by use of the so-called S-φ curve, see Figure 5.9. The curve below is merely used for explanatory purposes and does not reflect the exact S-φ curve for East Coast Park. The S-φ curve relates the longshore sediment transport rate S to the angle of wave incidence φ to the coast. It basically states that S increases as φ increases, which was addressed already in the description of headland control in Chapter 3. Thus, waves propagating parallel to the coast induce no longshore sediment transport, nor do waves approaching the coast perpendicularly. Somewhere in between, ideally around 42°, S is at its maximum. Only one quadrant of the S-φ curve is illustrated In Figure 5.9.

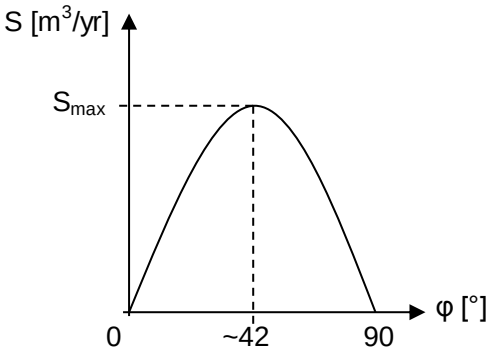

Figure 5.9 S-φ curve

Reflecting back on the changes in wave approach along East Coast Park, we can then say that the sediment transport along this coast has changed as well. With the knowledge of waves nowadays approaching the coast under an angle of about 20° (Chia et al., 1988), it is then assumed that this angle used to be larger before the extension of Changi. In other words, longshore sediment transport is assumed to have been larger before the land reclamations, although this difference might only be minor and have mainly had an effect on fine sediments.

Relative sea level rise

Prior to the land reclamations, relative sea level rise (RSLR) is expected to have been dominated by absolute or eustatic sea level rise and less by land subsidence. In Section 2.1.2 we have seen from vertical bottom profiles that the originally present bottom is built up of two relatively thick layers of *unconsolidated* marine clay. By reclaiming land coarse fill material has been used to cover part of the original bottom, thus adding a load on top of the clay layer. This load has increased the effect of land subsidence, causing it to become of the same order of magnitude as the eustatic sea level rise.

The above implications on coastal processes have triggered the interaction between the coastal morphology and hydrodynamic forces, where the latter try to rework the system towards a 'natural' equilibrium, causing the coastline to erode or accrete over time. The most evident example is the bulge that has been mentioned several times already in the previous sections. Based on this example, a study has been performed on shoreline retreat along this part of East Coast Park, which is described hereafter.

5.3.2 Shoreline retreat

Risk mapping

Below the disappearance of the aforementioned bulge will be treated, for this is the only location along East Coast Park where shoreline retreat has been studied more extensively. Researchers of the Tropical Marine Science Institute (TMSI) in Singapore have assessed this shoreline retreat using geographic information system (GIS), comparing the coastline of 1972 with that of 2007 using cadastral maps in order to create a risk map with predictions of future coastline developments, see the left panel in Figure 5.10 (Raju et al., 2010).

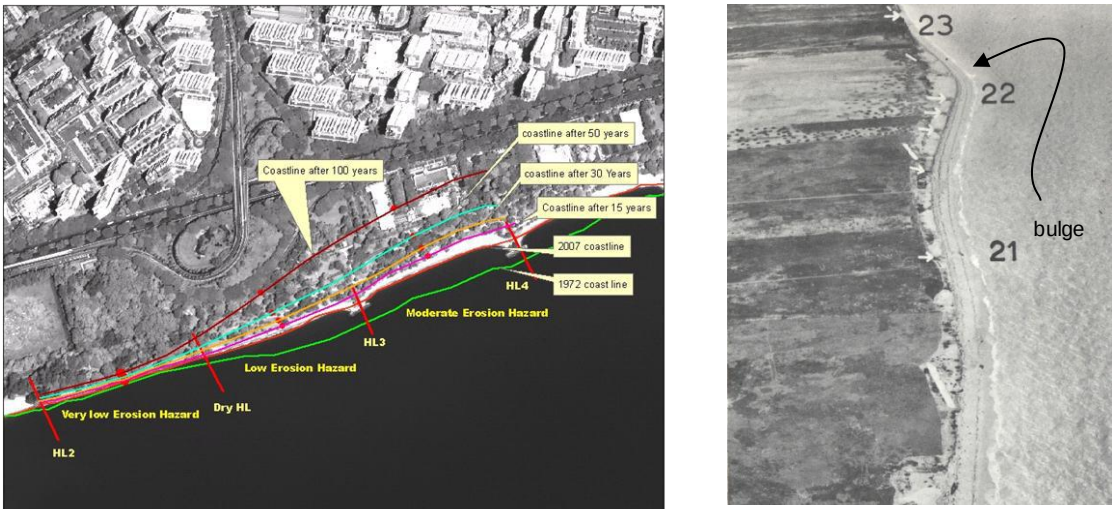

Figure 5.10 ***Left panel****: risk map by Raju et al. (2010), in which the green line is the 1972 coastline and the red line the 2007 coastline. The purple, orange, blue and dark-red lines are the expected coastlines after 15, 30, 50 and 100 years, respectively.* ***Right panel****: low aerial oblique of East Coast Park, looking east, showing how riprap breakwaters were placed in the reclamation fill material. The numbers indicate beach numbers as formerly defined by P.P. Wong (1973), which are located in between present-day headlands 2 and 4, see also Figure 3.6.*

The coastline is defined at CD + 2.515 m (MSL + 0.863 m). Their study focused on the location of the formerly present bulge mentioned in Section 5.2, because this section of the coast showed the largest erosion in preceding decades compared to other locations along East Coast Park. In the left panel of Figure 5.10 the coastline for different years is drawn. The green line indicates the coastline in 1972, the next red line coincides with the 2007 coastline, and all other lines are linearly extrapolated lines for based on the data from 1972 - 2007. These extrapolations indicate predictions of future coastline positions and thus erosion rates along this section, which resulted in a variation of an average of -0.187 m/yr to -1.29 m/yr elsewhere. The risk map that resulted from their results was based on the assumption that the rate of coastline retreat is linear and continues to occur with a similar trend.

Interpretation of findings TMSI

In Section 3.2.2 already mention was made on the construction of riprap breakwaters in the dry. For ease of reading, Figure 3.6 has been repeated in the right panel of Figure 5.10, now with an indication of the bulge present in the 1970s. From a coastal engineering perspective, the presence of this bulge can be regarded as a disturbance along this coast, which seems to have been a singular phenomenon, see also Figure 5.4. This disturbance was in fact the location along the coast where sediment was located offshore of the headland breakwaters, thus having no protective measures to stabilise the sediment. Then, with waves predominantly approaching the coast under an angle, gradients in alongshore sediment transport occur along the bulge. On the side facing the wave crests positive transport gradients will occur, whereas on the side opposite of the incoming waves negative transport gradients will occur. The transport gradients then lead to erosion of the disturbance in the shoreline, be it on a short or long time scale, depending on the wave environment. The erosion rate usually decreases in time, with the transport gradients decreasing as the bulge flattens out (Bosboom & Stive, 2011).

The study performed by Raju et al. (2010) focuses on mapping of the shoreline retreat only, not on the driving forces behind this retreat. The future retreat has been obtained through linear interpolation of their measurements, which results in an expected coastline retreat exceeding the actual retreat. To more accurately assess this retreat an approach as described above leads to a better understanding of the phenomenon. Namely, the erosion process has been induced by gradients in sediment transport along the coast, which were largest along the periphery of this bulge. In the initial stages after the reclamation these gradients were largest, leading to a relatively large erosion rate. In time the gradients and consequently the erosion rate decreased.

Nowadays the presence of this bulge is hardly noticeable and the shoreline has retreated shoreward of the breakwater that was constructed in the dry. This exposure has been depicted in
Figure 5.11, in which the retreat of the shoreline during 7 years is illustrated according to a reference line and some markers. With the exposure of the headland to wave action and the flattened out bulge, the assumption is then that the coastline section at the bump has reached a near state of equilibrium and will not retreat much further due to long-term processes. This assumption is supported by a lack of (coarse) sediment input into the coastal system along East Coast Park.

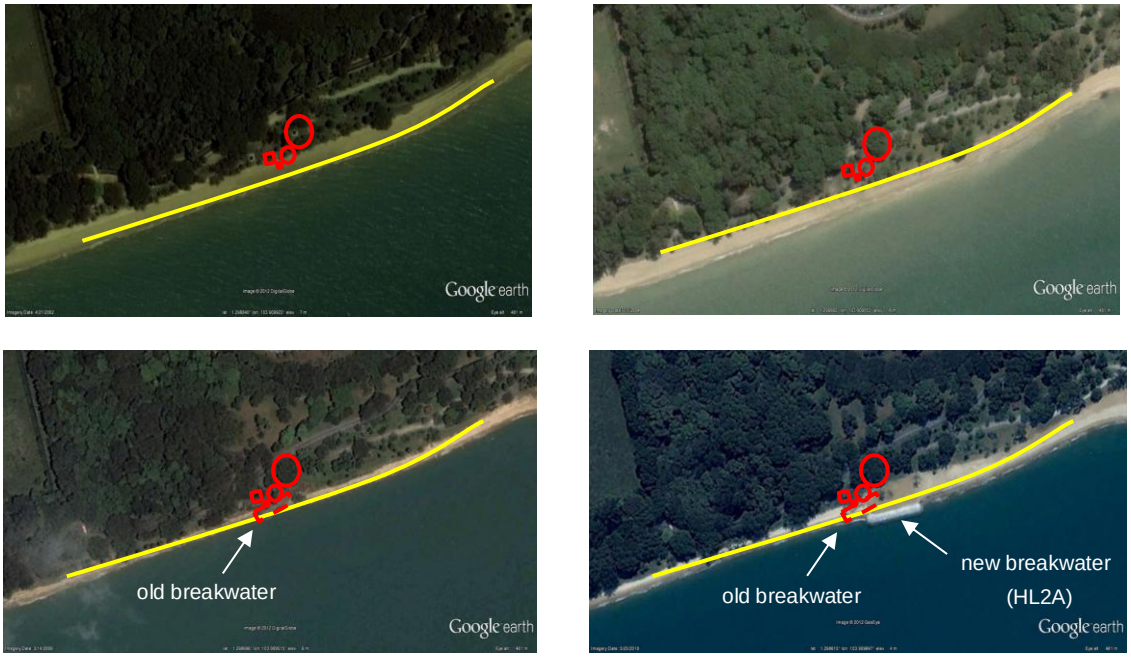

Figure 5.11 Shoreline retreat and exposure of buried riprap breakwater at headland 2A. (a) 2002: the red circles and yellow line are markers set according to this shoreline. (b) 2004: first signs of retreat visible. (c) 2006: first signs of breakwater exposure. (d) 2009: construction of headland 2A seaward of the previously exposed breakwater.

In the above section the effects of man-made changes on processes have been discussed, and an example has been given of the response of waves to such (local) changes. The discussed example comprises only a relatively small section of the coast and does therefore not necessarily represent the entire coastal stretch of East Coast Park. Besides waves, two other driving forces contribute to changes in the coastal morphology, as mentioned earlier. To understand the morphodynamics of the system today, the influence and the current state of each of these forces will be treated separately in the next section.

5.4 Present-day coastal processes

In this section the present-day coastal processes are described as accurately as possible, based on available data and on first order calculations. In Chapter 4 we defined several zones where different processes play a role. For illustrative purposes this zonation is repeated below, see Figure 5.12. In this figure the zonation is schematised based on the system scale we currently regard, namely that of the ECP system. On this scale we neglect the presence of structures, for which the actual coastline can be schematised as a (relatively) straight line that moves shore- or seaward depending on the balance between relative sea level rise and sediment supply. In the nearshore region the tide and (monsoon-induced) wave action affect the morphology on the long-term. Based on this zonation each morphological driver (tide, waves and RSLR) is treated consecutively.

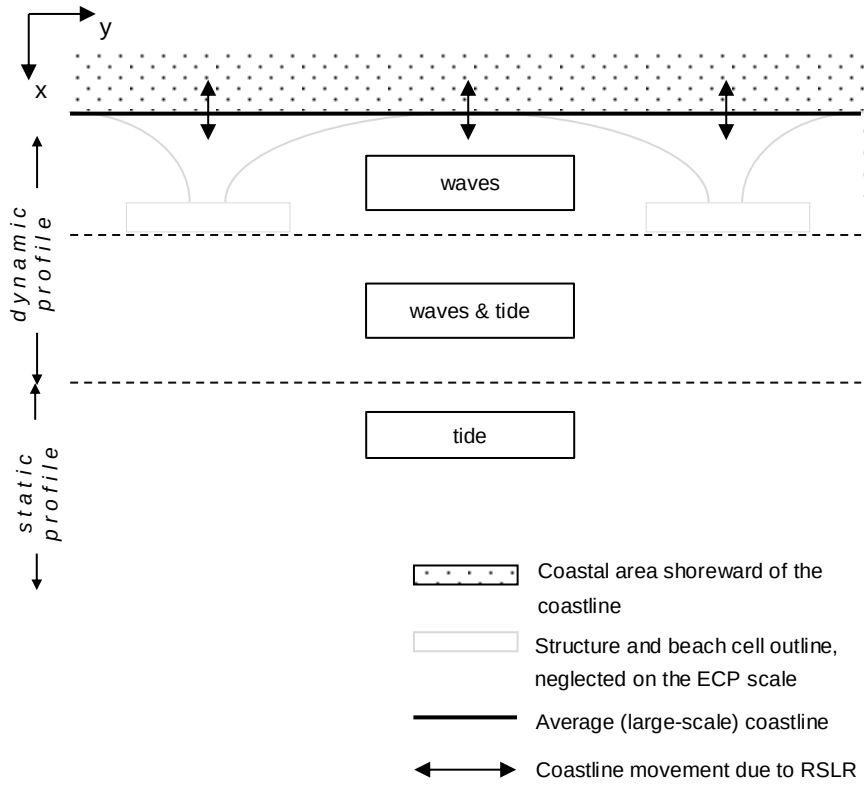

Figure 5.12 Zonation of driving hydrodynamic forces in the nearshore region for the large-scale analysis. Based on Figure 4.6.

For each of the processes described in the following sections different approaches have been used. The reason for this has mainly to do with the availability of data. Relatively accurate models are readily available on tidal fluctuations and currents, whereas boundary conditions to accurately implement waves in more complex models are absent. Therefore a trade off has been made and each of the processes has been investigated separately using various tools.

5.4.1 Tide

Starting with the tide, we regard both the vertical and the horizontal tide, of which characteristics for the Singapore Strait have already been described in Section 2.2.5. In this section, however, we will focus on the tidal influence on the nearshore region along East Coast Park. In Figure 5.12 it is indicated that the (horizontal) tide is expected to affect the morphology where the water depth is small enough for tidal currents to pick up sediment. Earlier it was already indicated that the vertical tide is 2.3 m on average, creating a relatively narrow intertidal zone of about 60 m on average, which was shown in Figure 5.3.

Using the numerical modelling tool Delft-3D[xiii], several computations have been performed which build upon the tidal computations of Van Maren and Gerritsen (2012), but with the focus on the coastal waters East Coast Park. A 2D model was used which is nested in the so-called 2D Singapore Regional Model (SRM)[xiv]. The nested model has a computational grid with cells of 30 by 30 metres, in which the presence of structures has been neglected. Nevertheless, some insight into the flow velocities in the nearshore region along the southeast coast of Singapore can be obtained, from which we can derive the contribution of the (horizontal) tide to changes in the nearshore morphology.

To assess flow velocities and sediment transport rates due to tidal currents in the nearshore region southeast of Singapore, several months have been chosen to represent the two distinctive monsoons we observe in the region. For the N.E. monsoon the months December and January were chosen, and for the S.W. monsoon June was chosen. For each of these months model calculations have been made. An example is shown in Figure 5.13, which shows the flow velocity vectors for the S.W. monsoon. Differences in flow velocities between the S.W. and N.E. monsoon are minor, and it therefore suffices to show the results of one period only. The remaining results are included in Appendix F.

In Figure 5.13 the maximum flow velocities in both eastward and westward direction are depicted, as well as the residual flow for that period. From the latter we see that the residual flow is divided into an eastward directed flow along the eastern part of East Coast Park and a westward directed flow along the western part of East Coast Park. The corresponding flow velocities increase in magnitude towards the deeper waters of the Singapore Strait. There they can reach up to 1m/s or more, which was shown by Van Maren and Gerritsen (2012). Our interest however is restricted to the coastal area in front of East Coast Park, and from the modelling results we can already see that flow velocities near the shore are generally less than 0.3 m/s.

In order to get a better feeling for these nearshore flow velocities, these have been illustrated for a part along East Coast Park in Figure 5.14. There it is seen that flow velocities near the shoreline are in order of 0.2 m/s, if not less. In Section 2.2.5 we have shown that flow velocities along East Coast Park vary from about 0.13 - 0.18 m/s at the 1 m depth contour. Again, it needs to be repeated that structures have not been included in these computations, and flow velocities near the shoreline might in reality be influenced by the presence of these structures and local bathymetry. However, the flow results seem to be valid as a first estimate for further analysis.

[xiii] *See for more information: http://www.deltaressystems.com/hydro/products*

[xiv] *The Singapore Regional Model (SRM) is a numerical model set up for hydrodynamic modelling of the waters surrounding Singapore, including large parts of the surrounding seas and with open boundaries in the Andaman Sea, South China Sea and Java Sea. See also Van Maren and Gerritsen (2012).*

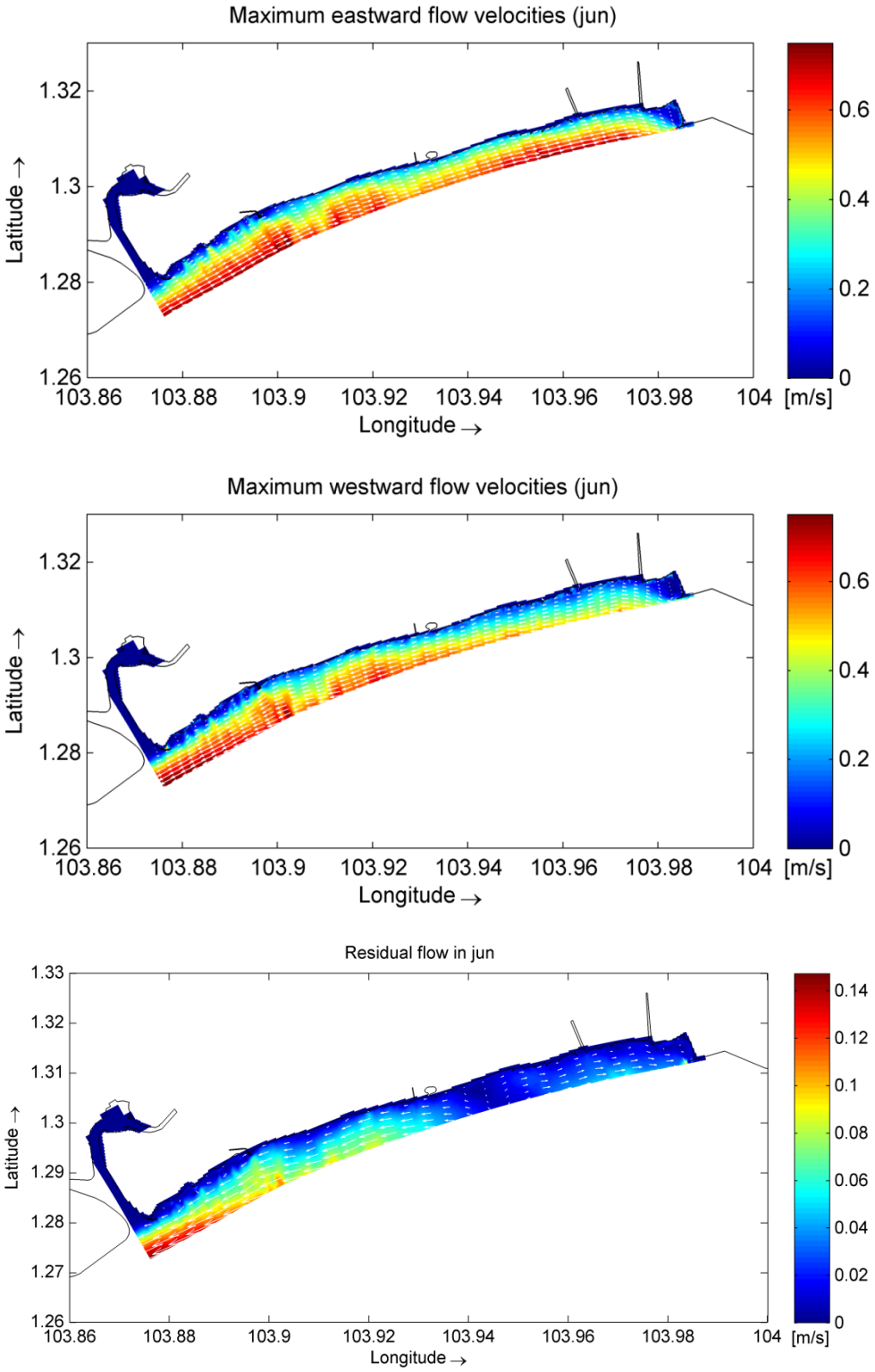

Figure 5.13 Flow velocities of tidal currents southeast of Singapore for June, representing the S.W. monsoon. The velocities have been computed using a nested Delft3D model in the 2D Singapore Regional Model. The results show maximum eastward and westward directed flow velocities in the upper and middle panel, respectively. The lower panel shows the residual flow velocities. The model results were obtained from Julia Vroom at Deltares.

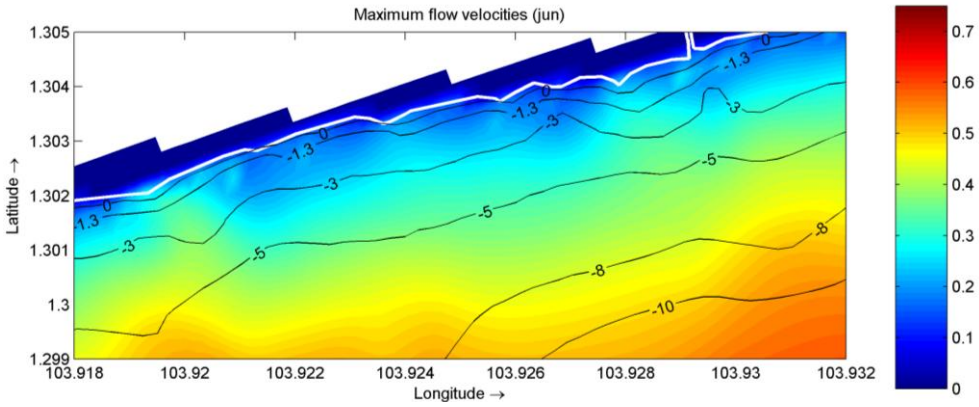

Figure 5.14 Nearshore flow velocities along a part of East Coast Park. The model results were obtained from Julia Vroom at Deltares.

Besides flow velocities also sediment transport as a result of the aforementioned currents has been modelled, again using Delft3D. These sediment transport calculations have been performed for a mean grain diameter D_{50} of 0.2 mm. In reality much coarser sediment is present on the beaches along East Coast Park, and much finer sediment is present at the bottom surface of the sea further offshore, based on findings from the fieldwork (Appendix C). In that case, however, the sediment transport calculations can still be used to gain some insight into the sediment transport capacity of tidal currents along East Coast Park. Compared to sediment present on the beach this capacity might then be an overestimation, and compared to the actual bottom surface sediments further offshore it might be an underestimation. Note however that a layer of cohesive sediment at the bottom surface might also create an additional resistance factor to the flow and thus sediment transport capacity. All in all it can give us insight into tide-induced sediment transports.

Results are shown in Figure 5.15 on the next page, in which vectors of annual sediment transports are shown for both the S.W. and the N.E. monsoon, by scaling of the model results to one year for June and December respectively. From these results it can be seen that the major difference between the two periods is found in the western part offshore of East Coast Park. During the S.W. monsoon (June) most of the sediment transport is directed towards the east, while during the N.E. monsoon (December) westward directed sediment transport is found along the western part offshore of East Coast Park. For January (see Appendix), the results are almost similar to those of December, except that already part of the westward directed transport in December has reversed into eastward directed transport.

In all of the results transport seems to occur mostly offshore of the coast, and transport becomes negligible towards the coast, even for the used grain diameter of 0.2 mm. It is then expected that the tide-induced sediment transport for grain diameters of 1.3 mm is near zero. It should be noted however that all computed transport rates are here the result of tide-induced flow only, while *in reality both waves and the tide combined contribute to current velocities along the coast*. In the next sections we will address wave-induced flow velocities along the coast.

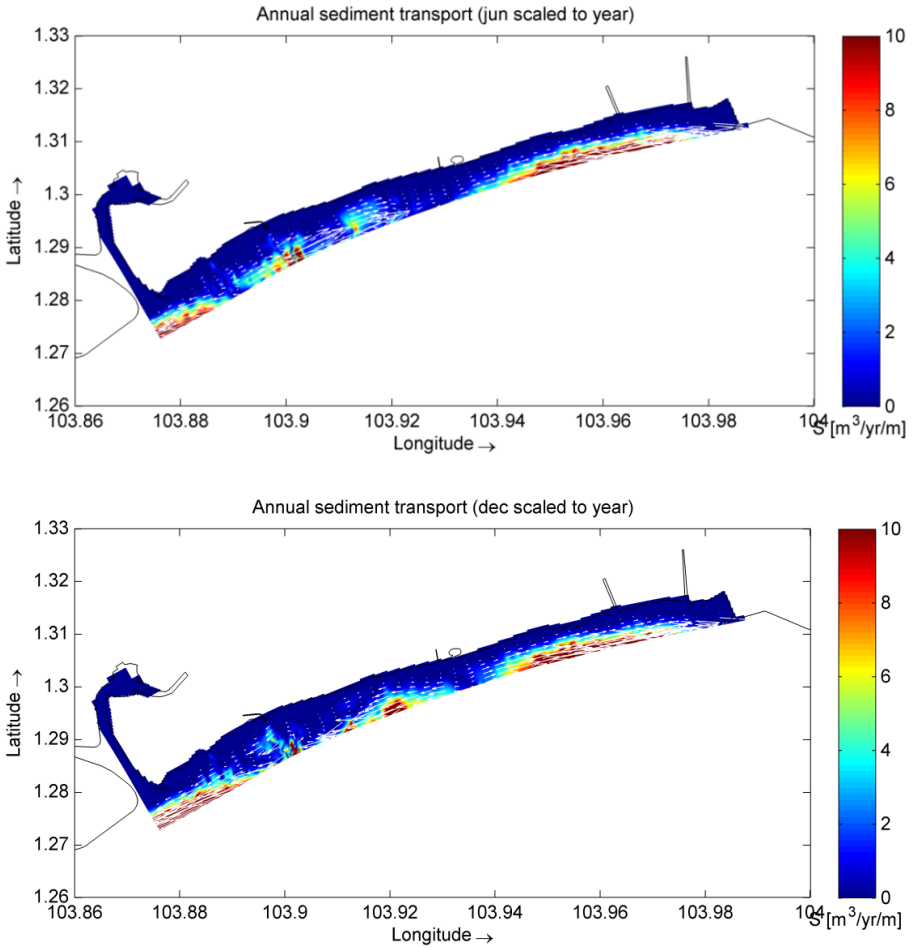

Figure 5.15 Sediment transports due to tidal currents southeast of Singapore for June (upper panel) and December (lower panel), representing the S.W. monsoon and N.E. monsoon, respectively. The model results were obtained from Julia Vroom at Deltares.

To illustrate the above results for flow velocities and sediment transports more clearly, several rays have been taken along East Coast Park to show the cross-shore distribution of both the cross-shore and longshore components, see Figure 5.16. The result for cross-section 200 is shown in Figure 5.17, confirming the aforementioned flow velocity magnitudes and the reversal of sediment transport direction along the cross-section.

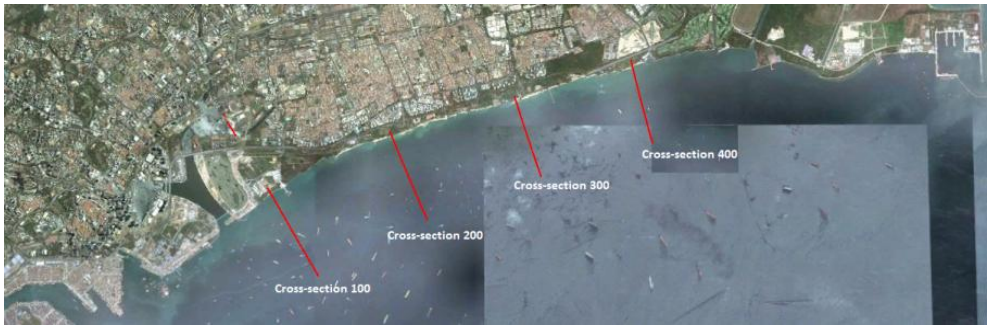

Figure 5.16 Cross-shore rays along the southeast coast, with no. 200, 300 and 400 along East Coast Park.

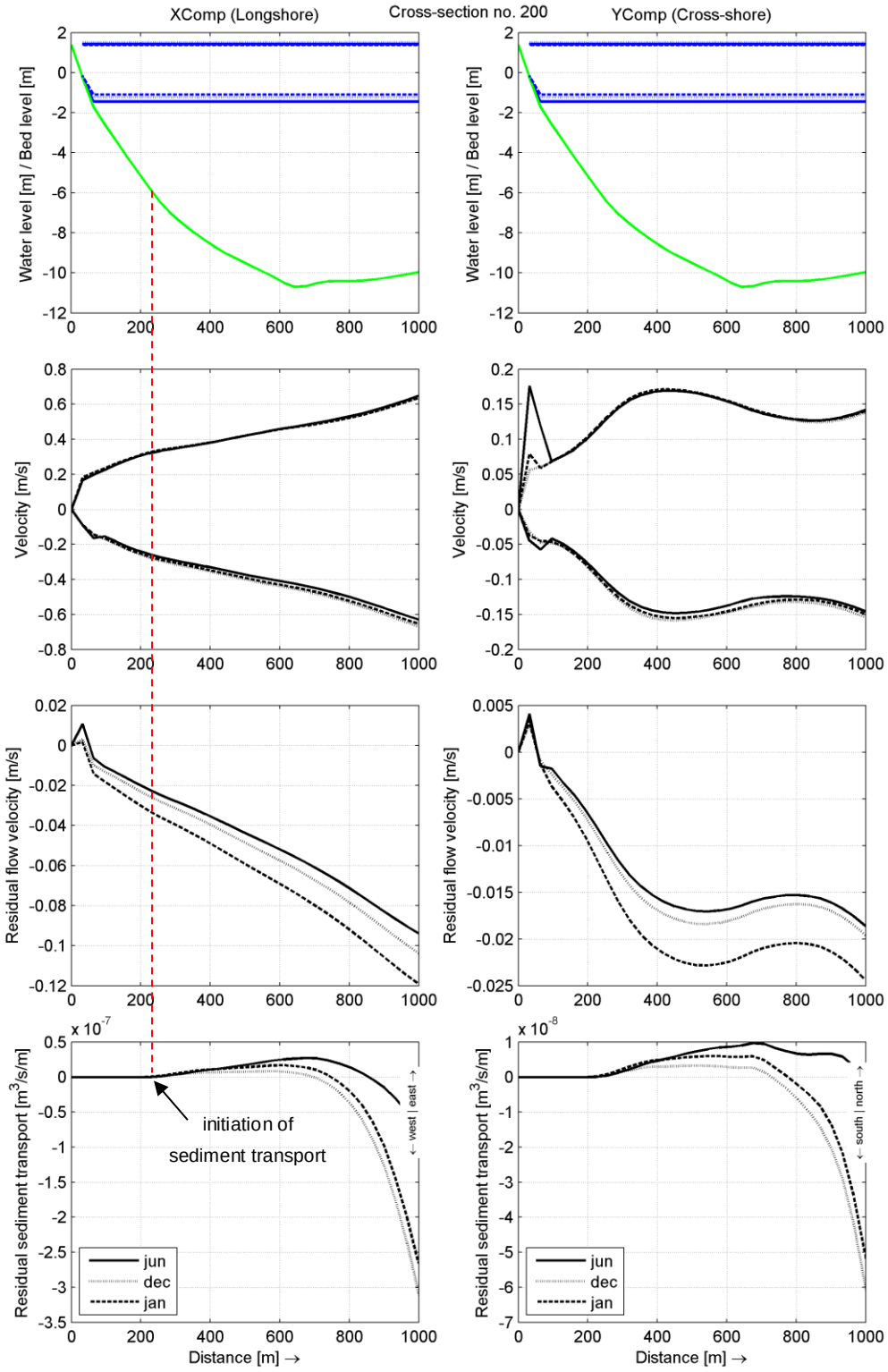

Figure 5.17 Cross-section 200: cross-shore distribution of in cross- and longshore flow velocities and sediment transport rates for the months June (S.W. monsoon), December and January (N.E. monsoon). In the left column the longshore components are illustrated, and in the right the cross-shore components.

5.4.2 Waves

Going from offshore in onshore direction, we enter the zone where waves start to feel the bottom and start affecting the morphology as well, see Figure 5.12. In this section several wave-induced morphological aspects are presented, in order to say something about the morphological evolution of the coastal profile and the sediment transport capacity. In order to do so use has been made of the 2D numerical modelling tools Unibest-TC and Unibest-LT. Unibest-TC is generally used to model cross-shore profile evolutions and sediment transports, whereas Unibest-LT is generally used to calculate longshore sediment transports for a variety of selected profiles.

In the ideal case, where sufficient data is readily available, both these models could be used to make a fully quantitative assessment of the coastal processes. In this study, however, this is not the case and therefore the choice is made to use these models as efficiently as possible. Doing so, the analysis of the model results then lies on the interpretation of the observed developments, rather than focusing on the output values.

In this analysis the use of Unibest-TC and –LT has been divided into different goals.
With Unibest-TC two aspects have been qualitatively (or semi-quantitatively) investigated:

- profile evolution and cross- and longshore sediment transport *distribution* for a year;
- morphological equilibrium timescale of the cross-shore profile.

With Unibest-LT the wave transformation towards the coast and the resulting wave-induced longshore current has been investigated, in order to say something about the actual sediment transport *capacity* rather than the *distribution* that is obtained with Unibest-TC. In both models the presence of structures is neglected at this stage.

For both models a range of profiles, 16 in total, along East Coast Park has been chosen. These profiles are illustrated in Figure 5.18, drawn over the bathymetry used to define the profiles. Note however that the numbering in Figure 5.18 does not coincide with the numbering used in the model results. The profiles 1 to 16 in Figure 5.18 coincide with profiles 9 to 24, respectively. To assess the present-day influence of waves on the coastal morphology we will start with results obtained from Unibest-TC for the profile development and distribution of sediment transports for one year. Thereafter the wave-induced longshore current and sediment transport capacity will be treated.

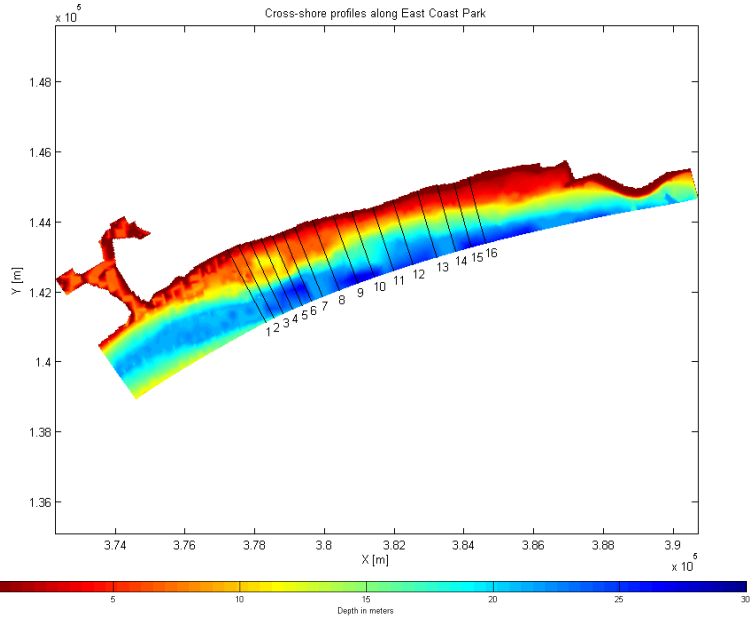

Figure 5.18 Bottom depth along the southeast coast of Singapore. The lines indicate the profiles used in the calculations using Unibest-LT. Profile 10 here coincides with the coastal cell where sediment was collected for analysis during this study, and profile 13 coincides with the profile used in Figure 5.3 to compare it with the profile belonging to the former intertidal flat.

Wave-induced profile evolution and sediment transport distribution (Unibest-TC)

For each of the above illustrated profiles the evolution of the cross-shore profile under influence of a wave climate as obtained from Chew et al. (1974) has been modelled. Two wave climates have been defined, one for the N.E. monsoon and one for the S.W. monsoon, see also Appendix A. For each of these wave climates evolutions have been modelled for a period of one year, to assess the relative influence of both wave climates on the profile. These calculations have been performed for sediment diameters of 200, 600 and 1300 µm, of which the latter is in accordance with the actual grain diameter found on the beach, which is our main area of interest in the profile. Due to the lack of readily available input data for this model, calibration of the model and validation with real-time measurements has so far not been possible.

Nevertheless, quite some insight can be obtained by use of such models, if properly applied. In Figure 5.19 and Figure 5.20 results are shown of two profiles, profile 4 and profile 10, respectively. Profile 10 falls within one of the coastal cells where the sediment for analysis (Appendix C) had been collected.

When interpreting these model results the reader should be aware that no attention should be given to the actual magnitudes on the axes of the figures. Due to insufficient accuracy of the model input and uncalibrated parameters, not much value can be given to output magnitudes. Despite that, we can still regard the results from a qualitative point of view. Looking at Figure 5.19 and Figure 5.20 we then firstly address the morphological evolution of the bed profile in the lower panel of each figure. For each profile both the bottom profile after one year is shown, formed under influence of the N.E. (the blue line) and S.W. monsoon (the red line).

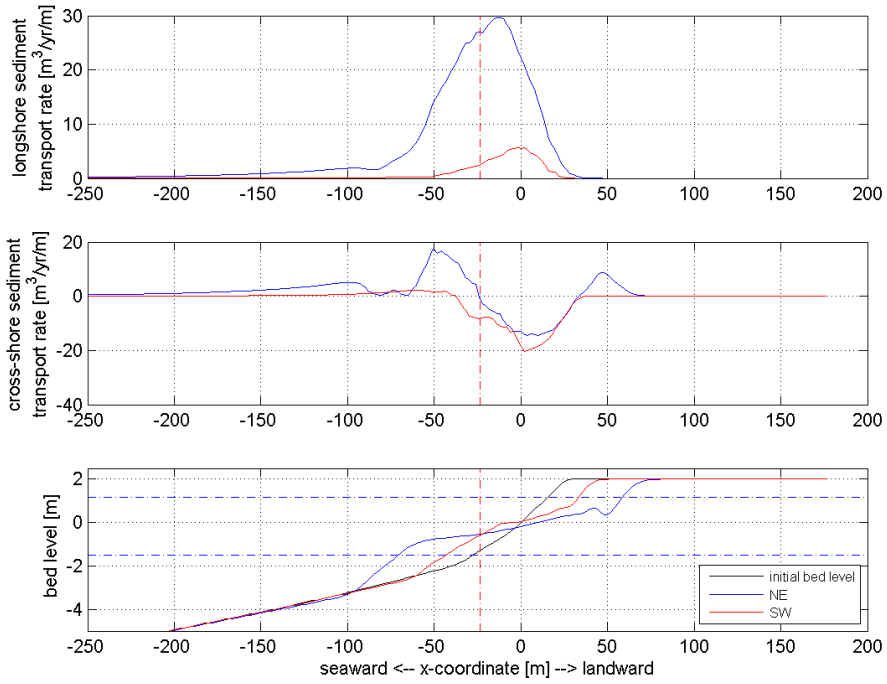

*Figure 5.19 Cross-shore profile evolution and sediment transport distribution for **profile 4** in Figure 5.18. Longshore sediment transport is positive in westward direction, cross-shore sediment transport is positive in offshore direction, and the bed level of the profile is illustrated with respect to MSL.*

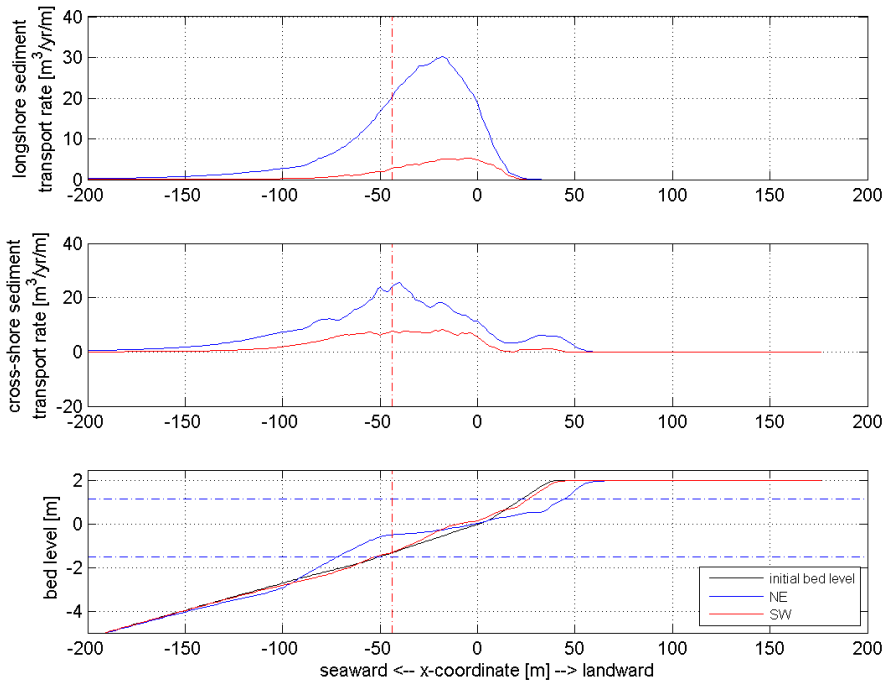

*Figure 5.20 Cross-shore profile evolution and sediment transport distribution for **profile 10** in Figure 5.18. Longshore sediment transport is positive in westward direction, cross-shore sediment transport is positive in offshore direction, and the bed level of the profile is illustrated with respect to MSL.*

In profile 4 the effect of both monsoon periods is more noticeable, showing more erosion in the upper berm and accretion in the lower beach profile during the N.E. monsoon, which corresponds to the more energetic wave climate. In profile 10 this is still visible, although less for the S.W. monsoon. What seems to happen is that the intertidal area flattens out during the rising and lowering of the water level (MLWS and MHWS are indicated by the horizontal blue dashed lines).

Looking at the distribution of the sediment transport, we observe westward and offshore directed sediment transport rates for each of the profiles. The westward direction sediment transport is due to the fact that waves refracting to the coast predominantly arrive at the coast under an angle from the east. What can also be seen in the figures is that most sediment transport occurs relatively near the shoreline, mostly in the intertidal zone. This is caused by the fact that waves approaching the coastline are generally small, due to which wave breaking occurs relatively near the shoreline. However, taking the tide-induced water level fluctuations into account, this wave breaking is dependent on both the water level at a certain time and the bottom profile. Namely, profile 4 in Figure 5.19 shows a steep beach profile and a much gentler upper foreshore. This then implies that during high water levels waves break closer to the shore, whereas during low water levels waves start feeling the bottom further offshore and thus also breaking occurs further away from the shoreline. The effect of these water level fluctuations then result in the distribution of sediment transport as shown in the upper panels of both Figure 5.19 and Figure 5.20.

When firstly looking at the model results in Figure 5.19 the conclusion would be that waves do affect the coastal profile rather significantly, trying to reshape it towards a certain equilibrium. What needs to be realised, however, is the fact that the profiles used in this model are not necessarily in dynamic or static equilibrium. It is then interesting to validate this based on a timescale to morphological equilibrium. In order to do so model runs have been performed for a period of 10 years, for each of the wave climates as used here.

Following the profiles used for illustration of transports and profile evolution, we follow these same profiles in the morphological timescale to equilibrium, see Figure 5.21 and Figure 5.22, which illustrate the profile evolution for profiles 12 (or 4 in Figure 5.18) and 18 (10 in Figure 5.18). Again, it should be noted that results should be interpreted carefully. In the upper panel of the figures the profile after 10 years is shown. This resulting profile, however, is not realistic and is the result of numerical instabilities in the model. What is interesting is to see after what time in the model run this instability occurred, which is visible by the sudden jumps in the profiles in the lower panel of Figure 5.21 and Figure 5.22. These two lower panels illustrate the morphological evolution in time until and after a dynamic equilibrium has been reached. It seems that after a period of about one or two years an equilibrium has been reached, being dynamic which can be seen by the ongoing fluctuations afterwards.

Based on this result and on the morphological timescales of other profiles (see Appendix E), a conclusion which can then be made is that waves *do* affect the coastal profile, but only significantly in the early stages of a disturbed equilibrium. It should be realised that in these model calculations only one sediment grain size has been used for the entire profile, whereas the bottom surface of the profile is non-homogeneous in reality. This short timescale to morphological equilibrium would indicate that wave-induced cross-shore sediment transport is not a dominant process in the long-term coastline retreat. This influence, however, depends on many other processes and can be more clearly assessed when more is known about the relative influence of wave-induced longshore currents and sediment transport *capacity*.

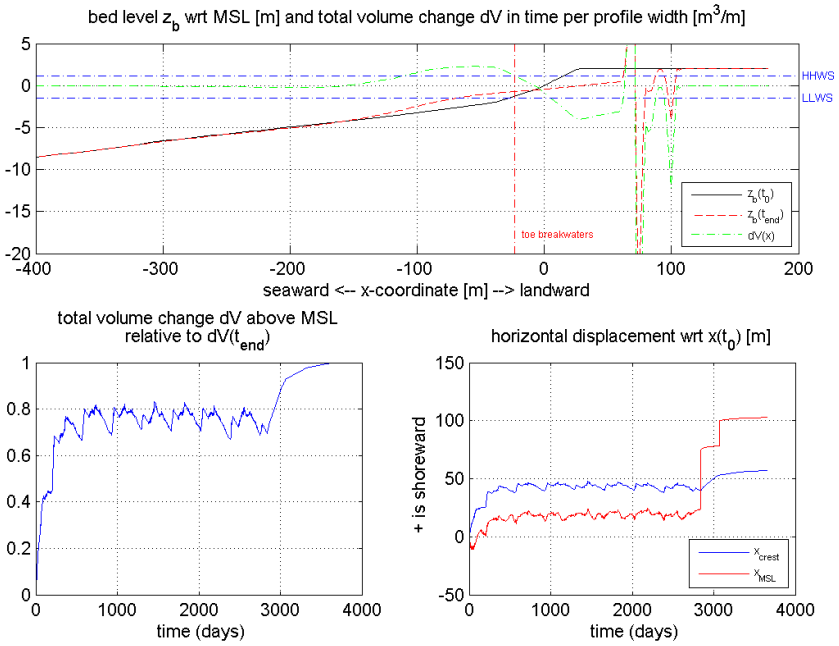

*Figure 5.21 Morphological equilibrium timescale for **profile 4** in Figure 5.18. The upper panel depicts the resulting profile after a period of 10 years. The lower left panel illustrates the change in total volume above MSL relative to the volume change at the last time step. The lower right panel depicts the horizontal displacement in time of both the berm (blue) as the point in the beach profile coinciding with MSL.*

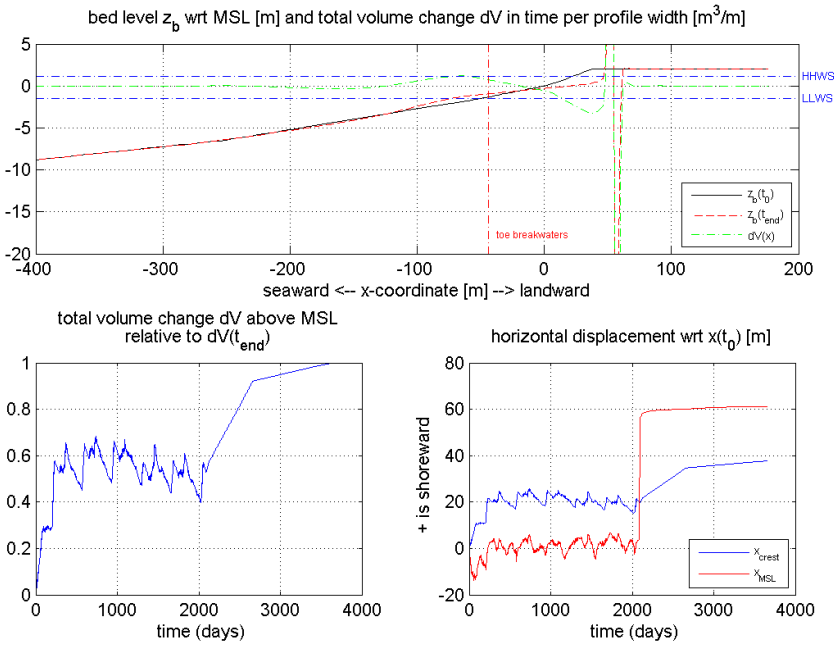

*Figure 5.22 Morphological equilibrium timescale for **profile 10** in Figure 5.18. The upper panel depicts the resulting profile after a period of 10 years. The lower left panel illustrates the change in total volume above MSL relative to the volume change at the last time step. The lower right panel depicts the horizontal displacement in time of both the berm (blue) as the point in the beach profile coinciding with MSL.*

Wave-induced longshore current and sediment transport capacity (Unibest-LT)

According to literature, longshore sediment transport has been a major factor in transporting sediment along and away from the coast (Chew et al., 1974; Tan et al., 2007; Wang et al., 2009; P.P. Wong, 1973, 1985). Yet, a clear distinction should be made in the alongshore transport of fine and coarse sediments. Sediments found on the beaches along East Coast Park are generally coarse, with a mean grain diameter of about 1300 µm.

According to the aforementioned literature, beach fill material consists of a mixture of coarse and fine sediments. Finer sediments are then said to be washed out from the beach, leaving behind the coarser grains. But from the observations made before of cross-shore sediment transport the question then arises what happens to the offshore transported coarse grains. Are they all brought back onshore under milder wave conditions during the S.W. monsoon, do they stay in the deposited offshore zone, or are they picked up by the wave- and tide-induced longshore current and then transported alongshore?

To validate this we regard two aspects determining the transport of sediment alongshore at East Coast Park:

- the zone in the cross-shore profile where longshore currents might occur;
- the capability of these currents for the alongshore transport of coarse grains.

The zone where cross-shore currents occur is generally referred to as the *active width* and can be estimated by determining the so-called *closure depth* or *depth of closure*. The depth of closure has been described by Hallermeier (1980), who defined three zones along the coastal profile: the littoral zone, the shoaling zone and the offshore zone. He defined the depth of closure at the transitions of all zones, thus coming up with an inner depth of closure and an outer depth of closure, of which the latter expression takes into account the sediment diameter, see equation 5.1 (Hallermeier, 1983):

$$\mathrm{h_d} = 0.018 H_m T_m \sqrt{\frac{g}{D_{50}(s-1)}} \qquad 5.1$$

in which H_m and T_m are the median wave height (m) and period (s), respectively, g is the gravitational acceleration (m/s^2), D_{50} the sediment diameter (m) and s the ratio of specific gravity (-). Now a rough estimation of the (outer) closure depth can be made. Using H_m = 0.35, T_m = 4.83 (Appendix A), D_{50} = 0.0013 m and s = 2.66 (Appendix C), we then obtain a closure depth h_d = 2.05 m. Considering the relatively large tidal range the location of this closure depth then shifts perpendicular to the coast.

If we take a typical profile along East Coast Park, see Figure 5.23, we can determine the width of the active zone L. With a closure depth of about 2 m, the width of the active zone becomes L = 55 to 75 m, depending on the water level. For MSL it is about L = 70 m. This then means that within a zone of 55 to 75 metres from the waterline waves contribute to longshore currents. This is true only in case structures in the cross-shore profile are absent, otherwise the actual width of the active zone is less. Note that the above extent of the active width follows from the profile in Figure 5.23. For different profiles, different active widths are found. Also, the location of the depth of closure is not static, but more an indication.

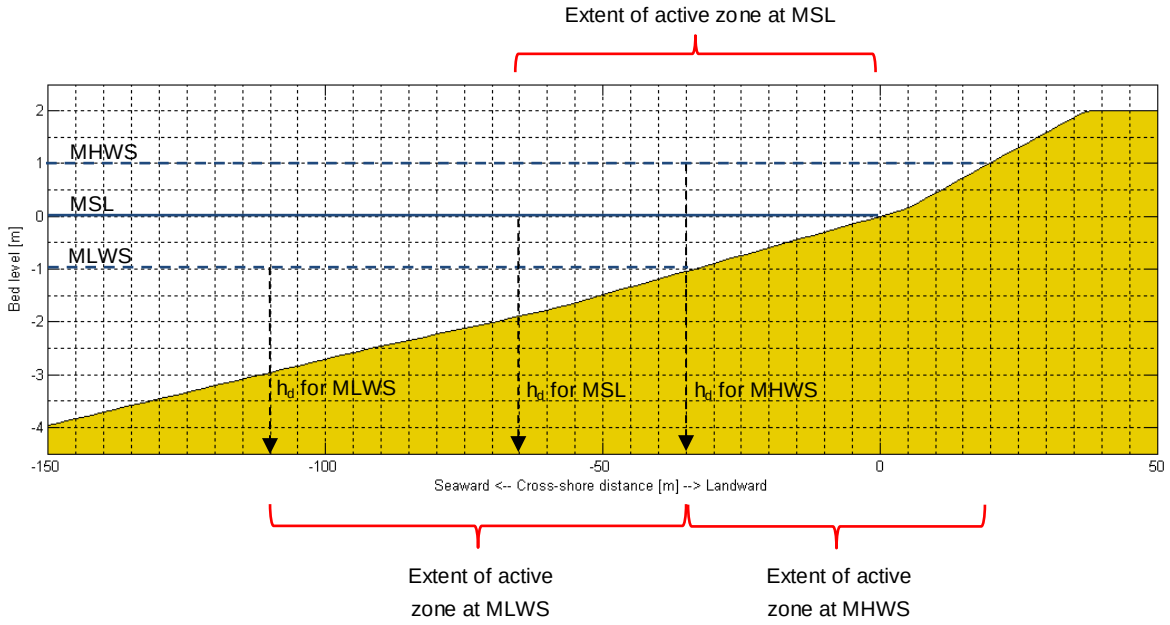

*Figure 5.23 Extent of active width for a typical cross-shore profile along East Coast Park, representing **profile 10**. This profile lies in the area where the sediment samples have been collected (Appendix C), in the vicinity of headland 10. The water lines for MHWS, MSL and MLWS are indicated, as well as the cross-shore locations of the corresponding closure depths (black arrows).*

Now that the extent of the active width is known, the next step is to find out whether these longshore currents are actually able to pick up sediment and carry it alongshore, so whether the sediment transport *capacity* is sufficient. To do so, use has been made of the 2D model Unibest-LT. With this model wave transformation has been calculated for each profile in Figure 5.18. From this wave transformation we have then been able to obtain cross-shore distributions of a variety of parameters, namely the significant wave height H_s (m), the wave orbital velocity U_{rms} (m/s), the wave angle (°) and the wave-induced longshore current velocity V (m/s).

The calculations were performed for both the S.W. and N.E. monsoon. An example is taken from the N.E. monsoon, which has the most energetic wave climate, see also Appendix A. Results for other profiles can be found in Appendix E, here one profile is used for illustrative purposes. The calculations have been performed for all wave heights given in the adapted wave climate found in Appendix A. The resulting Figure 5.24 shows the cross-distribution of the parameters mentioned earlier, with in the lower panel the bottom depth profile.

Looking at the results, it seems that the wave height at the waterline seems to be consistent with the values found in literature, where an average breaking wave height of about 0.2 m was observed along the coast (Chia et al., 1988). Then, looking at the wave-induced longshore current, the largest current occurring for the largest wave height reaches up to 0.3 m/s, whereas the most commonly occurring waves of 0.25 and 0.35 m/s induce a longshore current of about 0.1 and 0.15 m/s, respectively. In itself these values do not seem too large, but when adding the tide-induced longshore current as determined in Section 2.2.5, an additional 0.13 to 0.18 m/s should be added to the wave-induced current, giving an average range of about 0.23 - 0.33 m/s.

Water level fluctuations are not directly taken into account in the results, the results shown in Figure 5.24 represent wave transformation with a water level at MSL. What is interesting to see, however, is that the extent of the active zone at MSL, which we defined earlier in Figure 5.23 to be about 70 m, is visible by the extent of the distribution of the longshore current in cross-shore direction (fourth panel from the top in Figure 5.24).

It should be remarked that on this scale we neglect the presence of structures. In reality however, structures might impede longshore currents and consequently alter the above found values. The influence of structures is dealt with in the next chapter. Using the below results we can then make a first order calculation to determine the current necessary to carry sediment alongshore by calculating the initiation of motion for sediment along East Coast Park.

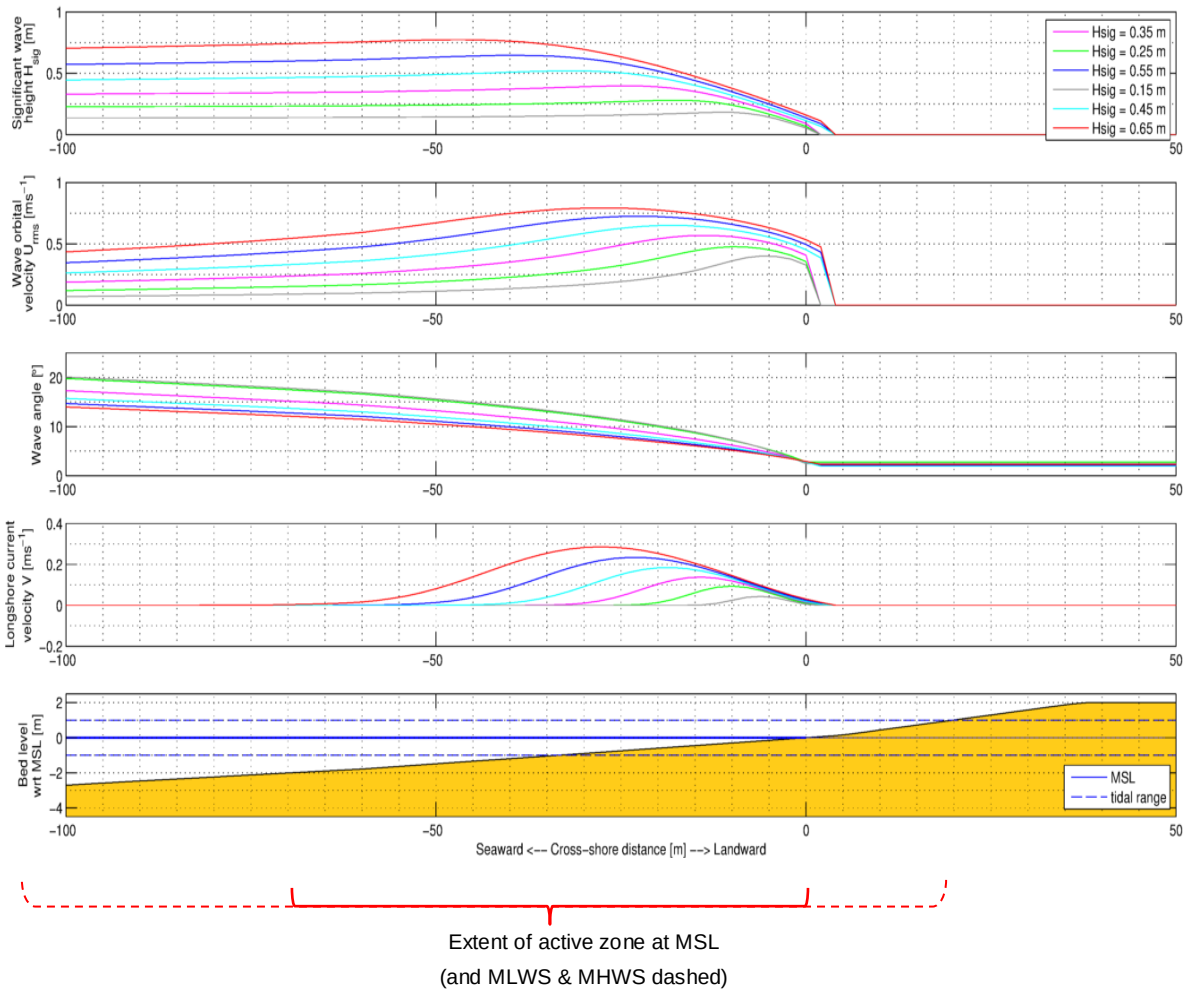

*Figure 5.24 Wave transformation and resulting current along **profile 10** in Figure 5.18 for H_s = 0.65 (red), 0.55 (navy), 0.45 (light blue), 0.35 (magenta), 0.25 (green) and 0.15 (grey) m during the N.E. monsoon. **From top to bottom**: the significant wave height H_s, the wave orbital velocity U_{rms}, the wave angle, the longshore current velocity V and the bed level. The vertical red line indicates the average location of the toe of headlands along East Coast Park.*

To determine initiation of motion use is made of the Shields parameter of motion, which is formulated as (Schiereck, 2004; Shields, 1936):

$$\Psi_c = \frac{\tau_c}{(\rho_s - \rho_w)g} = \frac{u_{*c}^2}{\Delta g D_{50}} = \frac{\bar{\bar{u}}^2}{C^2 \Delta D_{50}} \quad 5.2$$

in which Ψ_c is the so-called Shields parameter, which can be regarded as a stability parameters, τ_c is the critical shear stress, ρ_s the particle density, ρ_w the water density, u_{*c} the critical shear velocity and Δ the relative density of sediment particles in water, and D_{50} the mean grain diameter. To obtain the critical velocity necessary to initiate motion, we need to define the critical shear velocity (which is not an actual velocity), which is:

$$u_* = \bar{\bar{u}} \sqrt{\frac{g}{C}} \quad 5.3$$

in which $\bar{\bar{u}}$ is the velocity averaged over height and time, and *C* a 'smoothness' coefficient, which can be determined according with:

$$C = 18 log \frac{12h}{k_r} \quad 5.4$$

with *h* the local water depth and k_r the so-called equivalent roughness, which is generally taken as $2*D_{50}$ (Schiereck, 2004). With *h* taken at a water depth of -1.3 m, which is the average water depth at the toes of headlands along East Coast Park, and k_r = 0.0026 (for a sediment diameter of 1.3 mm), we obtain C ≈ 68. The two remaining unknowns are then Ψ_c and $\bar{\bar{u}}$. Using the below expression we can determine the Shields parameter from the graph in Figure 5.25.

$$D_* = D_{50} \left(\frac{\Delta g}{\nu^2} \right)^{1/3} \quad 5.5$$

with ν the kinematic viscosity, which is equal to 1.33 * 10^{-6} m^2/s for water (20°C).
Now, With Δ = 1.66 and D_{50} = 1.3 mm, D_* ≈ 33. Using the graph below, we then obtain a Shields parameter of Ψ_c ≈ 0.037 = 0.04.

Using this value to obtain $\bar{\bar{u}}$ from equation 5.2, we then get $\bar{\bar{u}}$ = 0.63 m/s. Thus, even with currents induced by the waves with H_s = 0.65 m, the wave- and tide-induced longshore current will not be able to transport the coarse sediment in alongshore direction. This critical velocity was calculated assuming a homogeneous sand bed, consisting of coarse grains over the entire profile. In reality the composition of the bottom surface material is non-homogeneous, consisting of finer sediments further offshore. These finer sediments might be picked up by the currents and carrier alongshore. This would substantiate claims in literature about the washing out of fines from the beaches.

Another aspect to keep in mind, however, is the fact that a bottom surface composed of mud and clay (which is assumed to occur offshore of the beach profile, see Appendix C) is more cohesive. If coarse grains are transported far enough offshore from the sandy beach (e.g. due to undertow, gravity driven flow) to be deposited in the more cohesive bottom surface material, an additional shear stress should be accounted for in the calculation of sediment

transport, making longshore sediment transport of *coarse* sand under normal wave conditions even more unlikely. The above assessment is a first order calculation with certain limitations. However, it serves well as a first estimate and gives basis for further analyses on wave-induced sediment transport along East Coast Park.

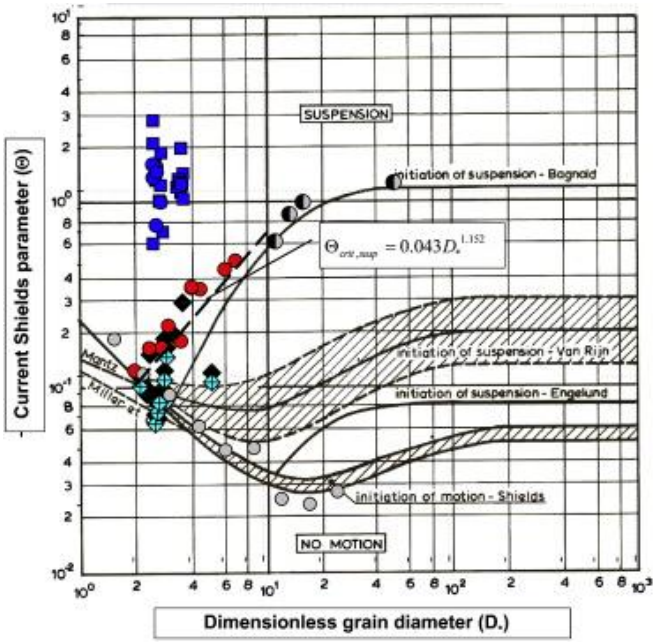

Figure 5.25 Critical shear stress according to Shields - Van Rijn (From Amos et al. (2010))

All in all, it can be concluded that waves *do* contribute to sediment transport along the coast, however the sediment transport of *coarse* sediment outside the beach profile is less likely than that of finer material. We need to bear in mind that in reality the wave climate does not always follow the climate found in literature (Appendix A). Extreme events occur from time to time, such as combinations of high winds and thus large waves with high water levels and even heavy rainfall. The combination of these processes is not accounted for in the above assessment, but will be touched upon in the next chapter.

5.4.3 Relative sea level rise

Eustatic sea level rise

Absolute sea level rise, or eustatic sea level rise, is a global phenomenon that has been studied extensively over the past decades. It is widely accepted as a long-term contributor to shoreline retreat. In the Fourth Assessment Report (AR4) of the Intergovernmental Panel on Climate Change (IPCC, 2007) different scenarios are modelled to predict sea level rises in metres at 2090-2099, relative to 1980-1999. According to these scenarios, a global rise in sea level ranging from 0.18 to 0.59 m is expected by 2100, excluding an uncertainty value of 0.2 m related to ice sheet flow. Most of the lower limits of the scenarios are about 0.2 m. From 1961 to 2003 the eustatic sea level rose at an average rate of 0.0018 mm/year and it is shown that this rate continues to accelerate in the future (Church & White, 2006). The sea level rise for Southeast Asia is expected to be similar to the global projections (NCCS, 2012).

Based on satellite measurements performed over the past decade, a further sea level rise at a rate of about 0.003 m/year is assumed for the next decade (Leuliette, Nerem, & Mitchum, 2004). At such a rate, if it were constant, the MHWS level would increase to over 3 metres during the next century.

For this study the interest is to estimate the influence of sea level rise on East Coast Park during the past decades, and how much it can affect the coastline in the future. During the last century, the average rate of eustatic sea level rise was about 0.002 m/year. To estimate shoreline retreat due to (absolute) sea level rise a quick-and-dirty approach can be used such as the Bruun Rule (Bruun, 1962), which is based on a simple two dimensional mass conservation principle. Bruun suggested that, under the influence of a rising sea level, the equilibrium profile would remain unchanged and translate upward and shoreward. He then considered eroded sediment from the upper profile to be deposited lower in the profile. The idea is illustrated in Figure 5.26.

In Figure 5.26 is depicted how a sea level rise (SLR) can lead to shoreline retreat (R), depending also on the depth of closure (h_d), the active width of the profile (L) and the berm crest height (B). He then formulated the following expression, which is commonly known as the Bruun Rule (Bruun, 1988):

$$\mathrm{R} = \frac{(SLR) * L}{(h_d + B)} \qquad 5.6$$

The parameters of this equation are represented in Figure 5.26.

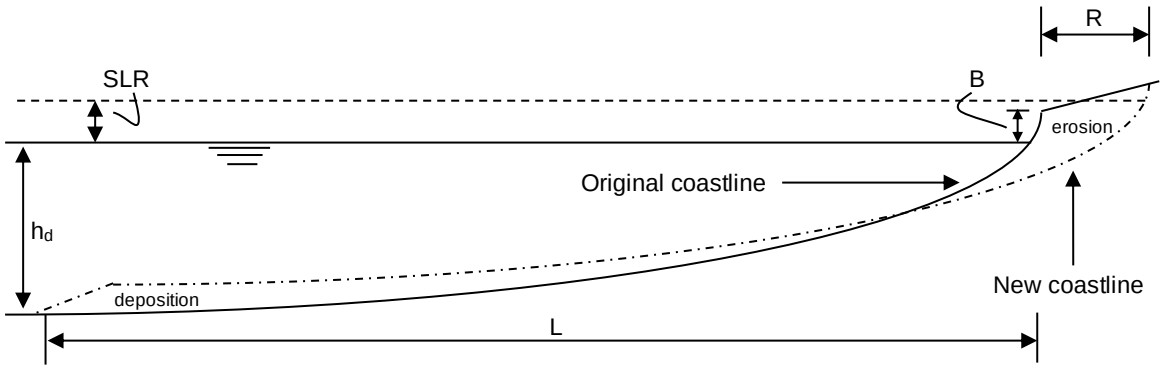

Figure 5.26 Schematisation of the Bruun Rule

In the previous section we found the depth of closure h_d to be 2.05 m and the corresponding extent of the active width at MSL is about 70 m. The berm crest lies at about CD + 4.0 m. With MSL at CD + 1.652 m the berm height B is then about (CD + 4.0 m - 1.652 m) = MSL + 2.348 m. Filling in these values in equation 5.6, assuming a sea level rise which is in accordance with the findings of the IPCC, say from 0.2 m to 0.6 m, the coastline retreat then becomes 3.18 m for SLR = 0.2 m and 9.55 m for SLR = 0.6 m, which is predicted to occur over a period of 100 years.

Note that the above hand calculation is a rough indication using the application of the Bruun Rule, which is a well-known deterministic method that is used mainly for first order estimates and should not be regarded as a tool on which sensitive engineering decisions should be based, as its simplicity comes with many limitations (Cooper & Pilkey, 2004). The found values for coastline retreat seem to be rather large. But to gain some insight into possible *extreme* values of coastline retreat due to sea level rise, the values found in this study are merely used as a first order estimate.

What is an important aspect of eustatic sea level rise is the fact that with increasing water levels depth-limited wave breaking will occur closer to or directly on the upper beach or berm and erode the berm. Also, during high water levels and storms there will be a higher probability of flooding (P. P. Wong, 1992).

Land subsidence

Besides eustatic sea level rise, vertical movement of the fill material and substratum can play a crucial role in the retreat of shorelines. Land subsidence has been observed along East Coast Park in the past decades, which has mainly been evident through the lowering crest heights of the headlands and the increased frequency in inundation of large areas of the park. Based on observations of land surface lowering along the old seawall, it was estimated that the land surface had lowered almost one metre in between 1972 and 2001 (Changsha, 2011b).

The main reason for land subsidence is the fact that the reclaimed land at East Coast Park and elsewhere along the southeast coast of Singapore is built on unconsolidated layers of marine clay. The findings of Arulrajah and Bo (2008) on bottom composition along the southeast coast of Singapore by, see Figure 2.5, confirm this fact. Due to the additional weight of the fill material consolidation of the substratum and creep in the subsurface layers is stimulated. Therefore land subsidence should be regarded as an important contributor to relative sea level rise.

Considering the fact that timescales of subsidence are in the order of decades, the largest subsidence has already occurred in the initial stages after the land reclamations, due to the asymptotic decay of subsidence rates. Since East Coast Park is still relatively young, ongoing land subsidence can still be of the same order of magnitude as eustatic sea level rise, which therefore doubles the expected rise in sea level along East Coast Park. This means that *relative* sea level rise until 2100 is then expected to be ranging from 0.4 to 1.2 m. The previously estimated values for coastline retreat are in that case in the order of 6.4 m to 19 m. Heightening and increasing the dimensions of headland breakwaters along the coast even further stimulate the consolidation process due to increased loads.

Following the above described present-day coastal processes it would then be interesting to determine an equilibrium profile under influence of all these processes, which could tell us something about the coastal profile we observe today. With a non-homogeneous composition of bed material in the profile, however, this is not as trivial as it sounds. This we be dealt with shortly in the next section.

5.5 Equilibrium profiles

In this section concisely mention is made qualitatively on the assessment of cross-shore equilibrium profiles along East Coast Park. To do so commonly Bruun's (1954) simple power law describing the relation between the water depth *h* and the offshore distance *x* is used:

$$\mathrm{h} = Ax^{2/3} \qquad 5.7$$

in which *h* is the total water depth, *A* is a dimensional shape parameter and *x* is the horizontal distance from the shoreline. The parameter A is usually determined empirically. In subsequent studies, an empirical relation between the shape parameter A and the sediment grain size (Moore, 1982), or fall velocity w_s (Dean, 1987), was found, from which could be concluded that a larger value for A generally indicates a steeper equilibrium profile. Tan et al. (2007) have applied this expression to determine equilibrium profiles, for the first 100 metres from the shoreline, along East Coast Park and at first sight seem to have achieved results that coincide reasonably with the present profiles. In their application, no mention has been made on the applied value for the shape parameter *A*, however, which depends on the stability characteristics of the seabed material and is found to be a site-specific parameter.

Following our knowledge on the cross-shore difference in sediment composition, recall Figure 5.3, and the observations made during the collection of sediment samples, the validity of the applicability of Bruun's (1954) expression needs to be questioned. For the coastal cells enclosed by headlands 8, 9 and 10, the transition from coarse sediment to mud was found to be near the low water line, say around halfway from the shore to the control line connecting the headlands. The headlands in their turn are located at about 30 to 50 metres from the shore, depending on the location, with the toe of headlands 8, 9 and 10 reaching the 0.6 m contour line, on average. Equation 5.7 dominates for h > 0.3 - 0.5 m for sandy beaches (Muñóz-Pérez, Tejedor, & Medina, 1999), meaning that the validity and applicability is dependent on the water depths in the sandy profile. However, in the coastal cells we consider a transition in sediment is found around 0.2 - 0.5 m water depth, with from there on mud and clay being predominant in offshore direction.

Pilkey et al. (1993) studied the general applicability of equation 5.7 and found some fundamental problems in the assumptions that (1) sediment is moved only by wave orbitals, (2) the underlying shoreface geology is unimportant, and (3) profile shape differences are caused only by variations in grain size, thus stating that the shape parameter A is a function of sediment grain size only. Following that, the importance of the underlying geology was studied for beaches on which sand is found only in some parts of the (upper) profile and areas of hard or muddy substrata are encountered along the profile. Such beach profiles are referred to as so-called *reef-protected beaches* (Muñóz-Pérez et al., 1999), see Figure 5.27, and the profile shape parameter A was found to be different from the one used in equation 5.7, being determined by the wave transformation and decay of waves approaching the hard substratum. This implies that along East Coast Park care must be taken with the choice of a value for this parameter, since there we observe a varying bottom composition along profiles as well.

Tan et al. (2007) used sediment grain size as found on the beach (D_{50} = 1.25 mm) to describe the equilibrium of the entire cross-shore profile, which seems to be an invalid approach when considering the cross-shore sediment variability *and* availability. From the three studied nautical charts in the previous section, only the later period showed deviations in contour

lines, possibly indicating that beach sediment has been transported in offshore direction, covering the underlying substratum. From this perspective, one could suggest the development towards a new cross-shore equilibrium, made up of sand on top of the marine clay layer, which in its turn has already formed an equilibrium profile over the past centuries.

However, the expressions for assessing equilibrium profiles assume a vertical uniformity in sediment, and the thickness of the sand layer on top of the substratum is relatively small, again limiting the applicability of equation 5.7 to profiles along East Coast Park. Therefore it is paramount to firstly obtain accurate insight into the cross-shore variability of bottom sediment composition and the corresponding shape parameter *A*, before regarding equilibrium profiles along East Coast Park.

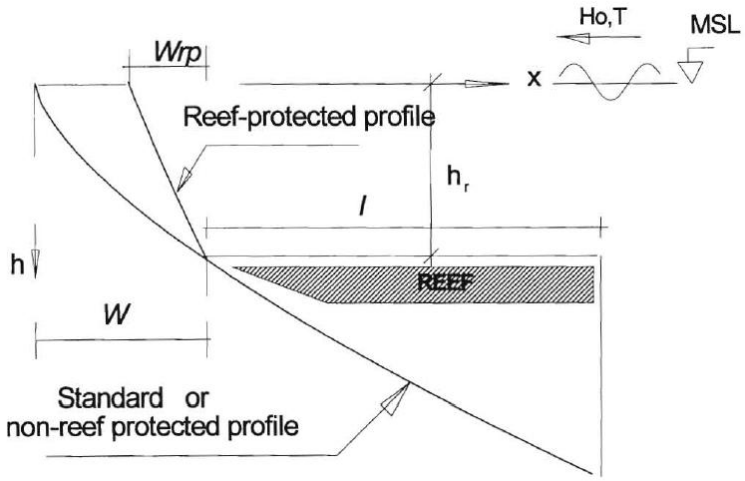

Figure 5.27 Sketch of protected and non-protected sections along the beach profile (Muñóz-Pérez et al., 1999)

5.6 Discussion and conclusions

Having addressed the larger temporal and spatial morphological scales, we have been able to make a semi-quantitative assessment of the coastal evolution and coastal processes along East Coast Park. Despite the roughness of first order calculations, they have given us more insight into the influence of some major contributing external forces on the nearshore morphology. With the foregoing analysis we are now able to validate some of the hypotheses that were defined in Chapter 4.

1 How have the land reclamations of the past decades affected the nearshore morphodynamic processes?

The hypothesis stated that the transformation of the coastline and coastal profile has caused a response from natural forces, the coastline being convex before the land reclamations and the profile being mildly sloping with the presence of the intertidal flat. In Section 5.2.1 we have illustrated how the coastal profile has changed by comparing the former profile with the present-day profile. From this comparison it has become clear that the coastal profile has changed drastically, having a slope of about 1:200 in the nearshore zone *before* the land

reclamations to a slope of about 1:15 to 1:100 nowadays. Despite the fact that different sediment materials lead to different equilibrium profiles, this transformation in profile shape has lead to a direct impact of waves at the waterline for a longer duration, regarding the narrow intertidal zone we observe today. Besides that, the extension of Changi Airport in the east of Singapore has influenced the angle of wave approach to East Coast Park. After the extension waves refract more towards the coast, having a larger impact directly at the waterline. Longshore transport (of fines), however, is expected to have decreased, since the incident wave angle has decreased as well.

2 How does relative sea level rise affect the coastline of East Coast Park?

As a first order assessment several hand calculations have been made to determine possible coastline retreat due to (relative) sea level rise. These calculations, however, are very rough and built upon many limitations. When it comes to the influence of relative sea level rise on East Coast Park, it suffices to conclude that the effect of land subsidence is a significant contribution to relative sea level rise along East Coast Park, the rate of land subsidence being of the same order of magnitude as *eustatic* sea level rise today (approximately 20 to 60 cm for the next century). In the past this rate has been higher, due to the asymptotic behaviour of the consolidation process. In the future this rate is then expected to decrease, but it can still have a major impact on an engineering timescale (several decades).

3 To what extent does the tide contribute to sediment transport in the nearshore region along East Coast Park?

In the hypothesis the effect of the tide on the nearshore morphology was said to be minor, based on the small current velocities that occur near the coast. From preliminary calculations using a numerical model (Delft3D) it was indeed seen that the effect of tidal currents on the nearshore morphology is negligible. Calculations were performed using a sediment diameter of 200 µm, which leads to an underestimation of sediment transports at the beach profile but can lead to an overestimation further offshore where finer sediments are present, especially considering the fact that currents can reach up to more than 0.5 – 1 m/s offshore. In our area of interest, which is the upper part of the coastal profile, sediment is too coarse to be transported by tide-induced currents.

4 Are waves able to stir up and transport sand? If so, where in the profile?

In the hypothesis we assumed the mild wave climate in the coastal waters of Singapore to contain too little energy to produce significant orbital and current velocities to transport sediment. Using 2D numerical models (Unibest-TC and –LT) we have been able to assess the influence of waves on the coastal morphology semi-quantitatively. Firstly we observed a flattening out of the coastal profile under influence of the wave climates of both the N.E. and S.W. monsoon. This flattening out is an indication of waves reworking the coastal profile towards an equilibrium. By looking at the timescale to morphological equilibrium we found that this dynamic morphological equilibrium was reached within two years of the start of the calculation. This short timescale would imply that ongoing coastal erosion along East Coast Park is not (only) predominantly caused by wave-induced cross-shore sediment transport. However, as mentioned earlier in reality a combination of processes exists. In this chapter we

mainly looked at relatively long timescales. On shorter time scales the influence of waves might be significant, especially in combination with water level fluctuations caused by the tide.

The width of the active zone at MSL was found to be about 70 m for one of the profiles along East Coast Park, ranging from 55 to 75 m when the tidal range is included. Waves start feeling the bottom at about 2 m water depth. The wave-induced longshore currents, however, are too small to transport *coarse* grains in alongshore direction, at least on the short-term based on the initiation of motion. With finer sediments found offshore of the beach profile such transport seems more likely, especially in combination with tide-induced currents. It should be noted that direct wave breaking on the beach can induce significant turbulent velocities to stir up sediment directly at the waterline. Depending on the intensity of the wave climate and the beach profile, even coarse sediment might in that case be stirred up and transported in cross-shore direction due to undertow and gravity driven flow.

In the assessment of the influence of tide and waves on the coastal morphology we have neglected the presence of structures in this analysis. However, in reality structures can affect nearshore coastal processes significantly, possibly resulting in different morphological behaviour. In the next chapter we therefore include these structures in our analysis and focus on the interaction of structures and their adjacent beaches, looking at the so-called *cell* system as defined in our conceptual model (Chapter 4).

6 Cell system analysis

6.1 Introduction

Building upon the approach as described in Chapter 4, we continue our analysis and focus here on the small-scale cell system, see Figure 6.1

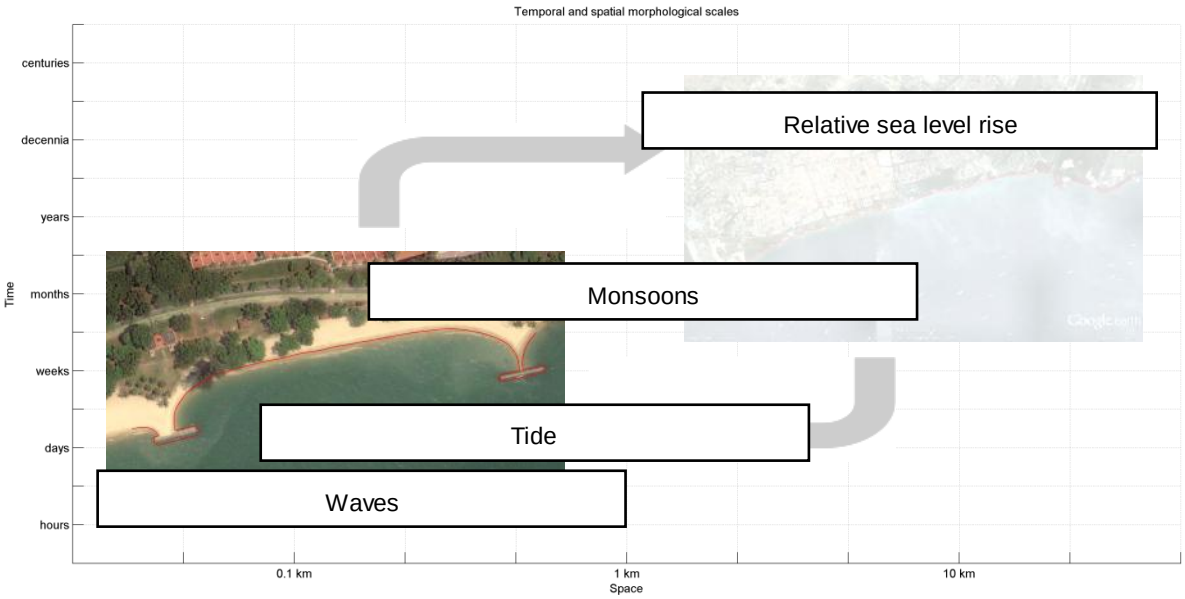

Figure 6.1 Spatial and temporal morphological scales of the coastal system in front of East Coast Park, with the small-scale system highlighted

Following the orthogonality hypothesis of Gonzalez et al. (2010), similarly as in the previous chapter the beach planform and the cross-shore profile are regarded separately in the analysis. Again, this does not imply independence of coastal planform and coastal profile. According to Gonzalez et al. (2010), the method is specifically applicable open coasts in an extreme morphodynamic state, following the beach state classification as defined by Wright and Short (1984). This is the case for the coastline we observe along East Coast Park. In Section 3.3.3 we had classified the beaches of East Coast Park to be reflective, with plunging waves and a meso-tidal regime.

The processes on this scale were said to be predominantly determined by wave forces, be it due to local winds or due to changing monsoons, and by the tide. Defining the zones on which various coastal processes take place, we can then illustrate the zonation in analogy with Figure 5.12, but then including the presence of structures, see Figure 6.2. This zonation is based on the analysis of the cell system, in which processes are influenced by structures along the coast. In the previous section we have treated the influence of the tide and waves on the nearshore morphology, going from offshore to onshore. On the cell system scale we now reach the zone closest to the shoreline, where waves are dominant and the tidal influence is mainly felt by water level fluctuations.

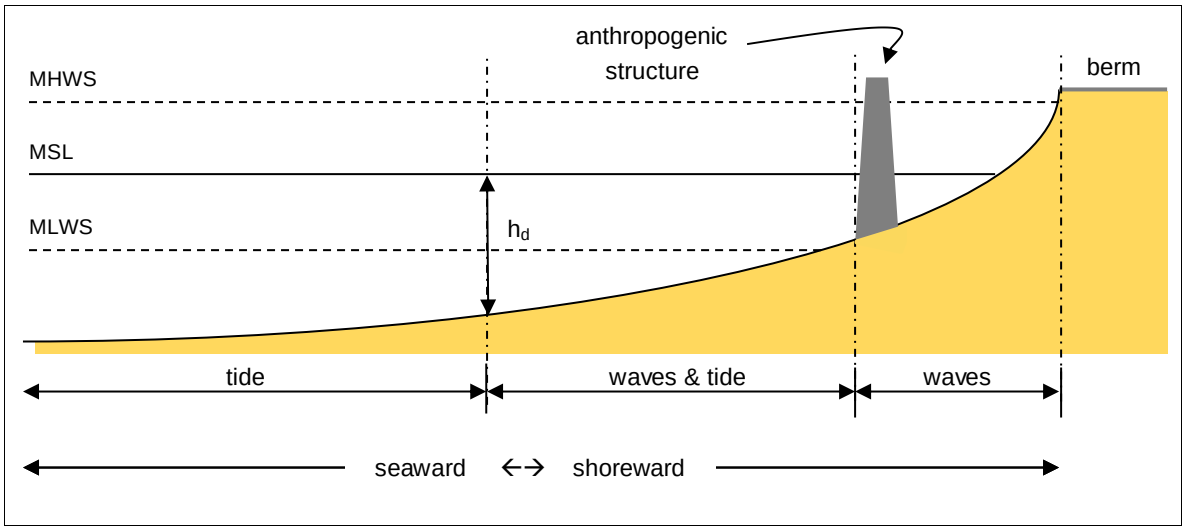

Figure 6.2 Zonation of driving hydrodynamic forces in the nearshore region for the small-scale analysis. Based on Figure 4.6 and Figure 5.12, looking in western direction, with the coast to the right (north). Note that this is a schematisation, actual locations might differ in reality.

The layout of this chapter is built upon the processes occurring within and around the coastal cells as defined in Chapter 3. Firstly we will discuss the different coastal cells we defined earlier and the expected interaction with the structures enclosing them. From thereon cross-shore and longshore sediment transport is discussed qualitatively, building upon the results obtained in the previous chapter. This then brings us to longer-term effects of the small-scale processes, such as possible by-passing of sediment around structures and time-varying behaviour of the coastal cells. Sources of information used in this chapter consist mainly of satellite imagery, (aerial) photographs, profile measurement data and the numerical modelling results from the foregoing chapter.

6.2 Beach-structure interaction

Before addressing the analysis on sediment transport mechanisms, we will firstly qualitatively look at the interactions of some characteristic beaches along East Coast Park and the structures enclosing them. This is important when analysing coastal erosion along East Coast Park, because beach-structure interactions might vary significantly along the coast and thus also the processes driving erosion might be different for different coastal cells.

In Section 3.3 coastal cells had been identified along East Coast Park, and a simple classification had been made based on the types of beaches found in the coastal cells, being predominantly straight along the beach planform, symmetrically curved (pocket beach) or asymmetrically curved (J-shaped beach). Building upon this classification, the morphology in each of the three distinguished cell types might be subject to different morphodynamic processes, irrespective of the same wave and tide environment affecting all the cells. For each cell type, then, different processes might be dominant in determining the beach morphology, which is important to realise when trying to assess the evolution of beaches along East Coast Park. As defined in the conceptual model of this study, the larger ECP system comprises a series of smaller systems, which may or may not interact, and do not necessarily all show the same beach planform or profile evolution.

Due to insufficient readily available data on exact locations along East Coast Park where erosion is significant, referred to as so-called *erosion hotspots,* the coastal processes will be assessed qualitatively in this chapter, so as to provide a basic understanding of the system from a coastal engineering point of view and to form a basis for future research. The main parameters determining the evolution within a coastal cell are found to be mainly dependent on three factors, namely (1) the spacing in between the headlands, (2) the orientation of the headlands and (3) the sediment characteristics within a cell. These aspects will be dealt with below, for each of the three identified cell types. In chapter 3.3 we found the coastline along East Coast Park to comprise 20 straight beaches, 2 pocket beaches and 8 J-shaped beaches.

Using the extent of the active zone we defined in the foregoing chapter, Figure 6.3 is adapted from Figure 5.23 and shows the inclusion of structures in the profile.

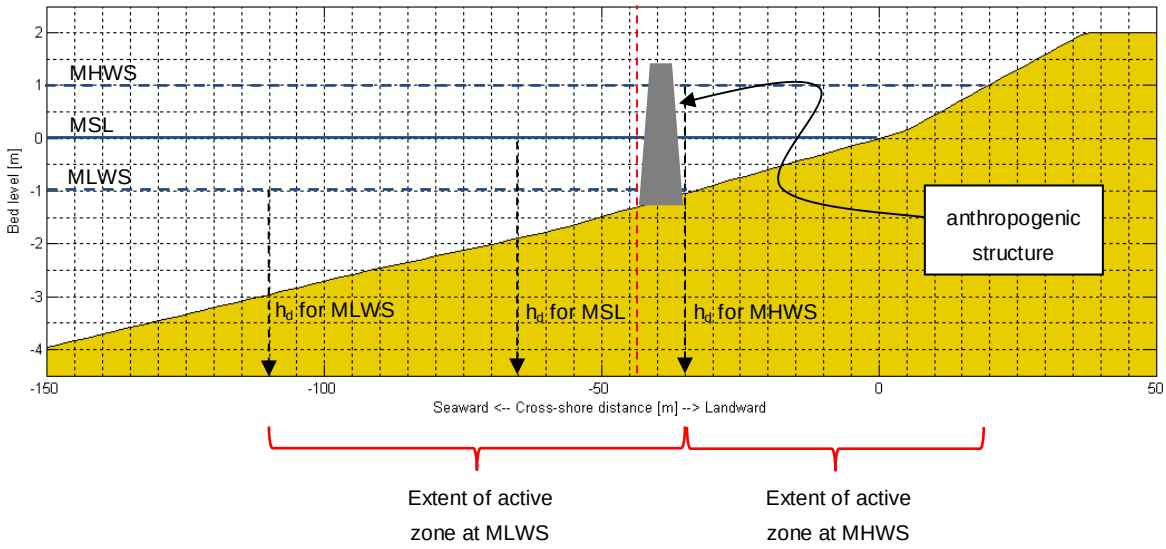

Figure 6.3 Extent of active width for a typical cross-shore profile along East Coast Park, representing ***profile 10****. This profile lies in the area where the sediment samples have been collected (Appendix C), in the vicinity of headland 10. The water lines for MHWS, MSL and MLWS are indicated, as well as the cross-shore locations of the corresponding closure depths (black arrows). In addition to Figure 5.23, here the presence of structures is included, with the vertical red dashed line referring to the approximate average location of the toe.*

In the description of the following beaches it is important to be aware that the formation of salient and or tombolos behind structures is also characteristic of the spacing in between structures and their orientation, but also of the location with respect to the shoreline. In analyses of salient and tomobolo formation, sediment input is an important parameter. Due to the fact that along East Coast Park and the (southeast) coast of Singapore sediment input is negligible, such an analysis applied to East Coast Park is impeded and is not treated in further detail.

6.2.1 Straight beaches (symmetric)

Straight beaches are the most abundant type of beaches along East Coast Park. They are defined as having a predominant straight section along the beach planform, with curvature possibly occurring in the lee of the headlands. The relatively long, straight part of the beach planform is mainly caused by the large spacing in between the two adjacent headlands enclosing these beaches and to the nearly shore-parallel orientation of the headlands. Curvature in the lee of headlands can be attributed to the change in wave approach throughout the year as part of changing monsoons.

In Figure 6.4 a schematisation of a straight beach and some characteristic parameters is shown. In this figure it is seen that the shape of straight beaches are predominantly symmetric, due to the relatively large spacing in between the structures and the similar orientation of the structures and their distance from the coast. This symmetry comes back into the angle of wave incidence into the coastal cell.

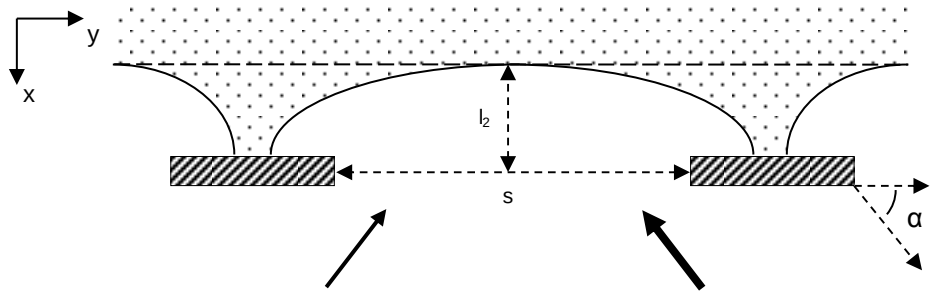

Figure 6.4 Schematic layout of a straight beach. The arrows indicate the possible angles of wave incidence, the dominant direction of wave incidence indicated by the thicker arrow. The dashed line indicates the average coastline position. The dashed arrows indicate significant parameters: s = spacing between headlands (length of control line), l_2 = distance from control line to the (average) coastline, α = structure orientation wrt angle of dominant wave incidence.

In Figure 6.5 a typical example of a straight beach along East Coast Park is shown for the S.W. monsoon. The beach is shown to be fairly symmetrical. Note also that the headlands are oriented almost parallel to the shore, and that the straight section of the beach is nearly parallel to the control line connecting the two headlands. The distance of the control line to the straight section of the beach is small compared to the length of the control line.

Figure 6.5 Example of a straight beach along East Coast Park.

6.2.2 Pocket beaches (symmetric)

In Figure 6.6 a schematisation of a pocket beach is shown. In this figure it is seen that the shape of pocket beaches are predominantly symmetric, although much more indented than straight beaches. The spacing between the structures is relatively small, but the orientation of the structures and their distance from the coast is similar. As with straight beaches, the symmetry comes back into the angle of wave incidence into the coastal cell.

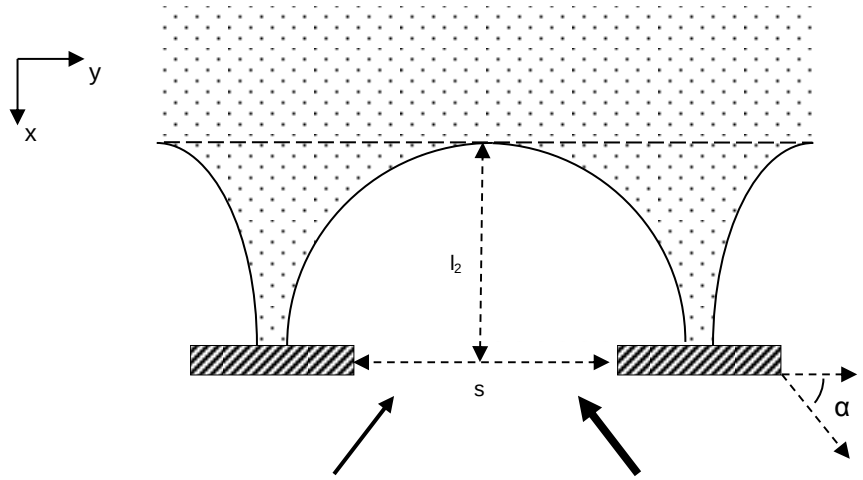

Figure 6.6 Schematic layout of a pocket beach. The arrows indicate the possible angles of wave incidence, the dominant direction of wave incidence indicated by the thicker arrow. The dashed line indicates the average coastline position. The dashed arrows indicate significant parameters: s = spacing between headlands (length of control line), l_2 = distance from control line to the (average) coastline, α = structure orientation wrt angle of dominant wave incidence.

Pocket beaches are found at two locations along East Coast Park only, namely in between headlands 8, 9 and 10, where also the collection of sediment samples was performed. Pocket beaches are characterised by a large curvature all around the beach planform, showing no or little straight sections. This formation is attributed to the relatively small spacing in between the headlands, in comparison with the distance from the control line to the centre of the beach. The headlands are shore-parallel oriented, and the beach planform is symmetrical. Due to this smaller spacing a relatively larger shadow zone is created and because the distance of the headlands to the shore is larger, waves reaching the waterline in the lee of the headlands are highly diminished due to diffraction.

An example of a pocket beach along East Coast Park is shown in Figure 6.7.

Figure 6.7 Example of a pocket beach along East Coast Park.

6.2.3 J-shaped beaches (asymmetric)

In Figure 6.8 a schematisation of a J-shaped beach is shown. In this figure it is seen that the shape of J-shaped beaches are predominantly asymmetric, in contrast to straight beaches and pocket beaches. The spacing between the structures is relatively large, just like for straight beaches, and the orientation of the structures is similar, as well as the distance of the structures from the (average) coastline. The main difference lies in the orientation of the structures, which is not shore-parallel. Therefore an asymmetry is induced by the incoming waves, which predominantly approach East Coast Park from the southeast.

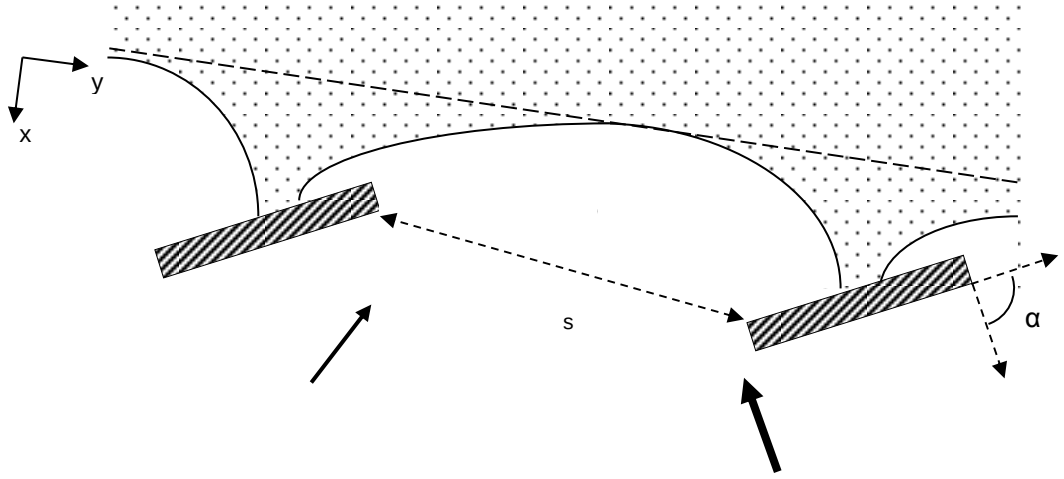

Figure 6.8 Schematic layout of a J-shaped beach. The arrows indicate the possible angles of wave incidence, the dominant direction of wave incidence indicated by the thicker arrow. The dashed line indicates the average coastline position. The dashed arrows indicate significant parameters: s = spacing between headlands (length of control line), l_2 = distance from control line to the (average) coastline, α = structure orientation wrt angle of dominant wave incidence.

Many of the beaches along East Coast Park are often referred to as having a J-shaped beach planform. Where we define beaches with predominantly straight sections and curvature only

in the lee of headlands as straight beaches, these type of beaches are sometimes referred to as *double* J-shaped beaches, having a J-shape in both the westward and the eastward section of a cell. The difference between original J-shaped beaches, however, lies in the orientation of the headlands enclosing them. They typically have a non-parallel orientation to the coast, whereas straight beaches are enclosed by (near) shore-parallel headlands. Due to this orientation a larger shadow zone exists behind the updrift headland, where updrift along East Coast Park is generally accepted to be according to the predominant angle of wave approach, which is from the southeast (see Section 2.2.4). In this way a relatively large straight beach in these cells is found as well, but due to the asymmetric planform this type is distinguished from straight beaches. Figure 6.9 shows an example of a J-shaped beach along East Coast Park.

Figure 6.9 Example of a J-shaped beach along East Coast Park.

6.2.4 Further analysis

In this study quantitative data has only been readily available for the two pocket beaches found along East Coast Park. For this reason quantitative analyses are only possible for these pocket beaches in the study before you. Nevertheless, based on the above schematisations and basic knowledge in coastal dynamics, we can still assess coastal processes qualitatively where data is lacking.

In the subsequent sections of this chapter the processes occurring on the cell scale are treated in more detail.

6.3 Sediment distribution within coastal cells

In Section 3.3.2 already the distribution of sediment in the two pocket beaches along East Coast Park were discussed, see Figure 3.10. In this figure we can regard a sediment distribution in both the cross-shore direction as along the beach planform.

Looking at the cross-shore distribution, we observed fine sediments above the high water mark, where the profile is nearly horizontal and large parts are still unaffected by the hydrodynamic forcing, but rather winds play a role. At mid-tide and the low water mark larger grains were found, which can be attributed to the fact that the fines on the beach face have already been washed out of this steep profile. Going further offshore, very fine sediments were found, consisting of a mixture of silt and clay. This seems to be caused by the presence of underlying marine clay layer, and the fact that silts are transported more easily offshore.

Along the beach planform coarser sediments were generally found in the lee of the headlands, which was also observed by Chew et al. (1974). A cause could be the use of coarser sediment in recent beach nourishment works, and poorer sorting behind the headlands due to limited wave action. As was explained earlier in this chapter, waves propagating into coastal cells diffract around the headlands, losing their energy. In the cells enclosed by headlands 8, 9 and 10 the waves diffract along a longer path, thus having lost much of their energy when reaching the back of the headland.

6.4 Cross-shore sediment transport

Along East Coast Park, waves primarily tend to break directly on the beach. This can be observed from both satellite imagery as from photographs, see Figure 6.11. This is caused by the fact that the waves approaching this coast are generally small. A basic rule of thumb is that waves start to feel the bottom at about 2 to 3 times the significant wave height, which in case of waves with an amplitude of about 0.25 m is very near the waterline at higher water levels.

Figure 6.10 Wave breaking at the waterline, East Coast Park

The above photograph is an example of waves which are commonly found during periods of larger winds, such as during the Sumatra squalls occurring during the S.W. monsoon. During low water levels the wave breaking is more of the spilling type, due to the gentler slope of the lower beach face. From the preliminary calculations of sediment transport *capacity* in the

previous chapter (see Section 5.4.2), we assume that wave energy is generally too low to move sediment upward on the beach face. Along East Coast Park, several possible contributing factors to erosion have been observed, at different locations along the beach face. In the following sections firstly erosion at the berm and upper beach face are treated, then erosion at the lower beach face, and finally the time-dependent evolution of the cross-shore profile is analysed.

The process of cross-shore sediment transport within coastal cells is illustrated schematically in Figure 6.11.

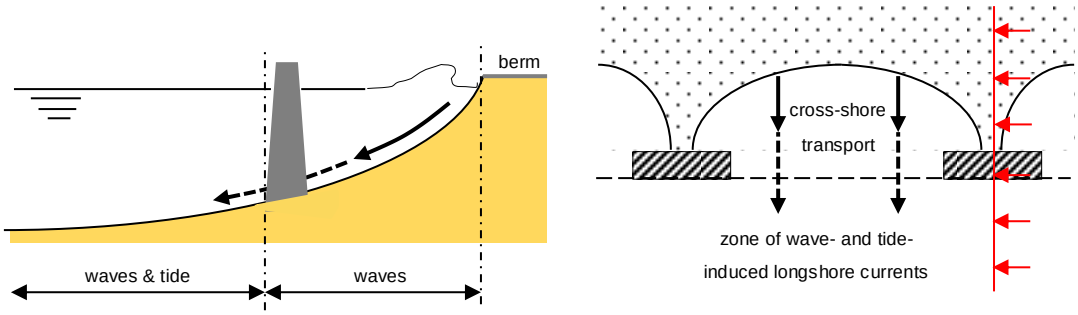

Figure 6.11 Schematic illustration of zones of cross-shore sediment transport. Left: cross-section indicating the sediment movement within and possibly out of a coastal cell. Right: top view of the same process, with the red line indicating the cross-sectional view of the left panel.

6.4.1 Forces driving cross-shore sediment transport

When it comes to cross-shore sediment transport within coastal cells, several causes are identified to contribute to cross-shore sediment transport, namely:

- swash motions along the waterline due to wave breaking and wave orbital velocities;
- excessive pore pressure due to wave run-up on the beach profile;
- undertow and gravity driven flow;
- rainfall (flash floods).

The distinction between wave breaking at the waterline and the orbital velocities in the surf zone is made to indicate the difference between waves directly affecting the waterline by the impact of breaking and the stirring up of sediment on the beach profile by wave orbital velocities. In the above drivers the effect of ship waves as described in Section 2.2.4, as well as the tide-induced water level fluctuations, are implicitly accounted for. The effect of (long) ship waves, if present, could contribute to wave run-up on the beach profile.

6.4.2 Observed sediment losses within coastal cells

In this section some observations of cross-shore directed sediment transport are shown. In order of discussion, these are:

- Scarp formation along the beach the berm;
- Gully formation along the beach berm;
- Liquefaction along the lower beach face.

The latter two observations have been made during the collection of sediment samples, in between headlands 8, 9 and 10, just after a so-called *flash flood* (short duration of intense rainfall).

Scarp formation along the beach berm

Erosion of the upper beach face and berm occurs during high water levels. This is usually expressed in the formation of beach scarps along the beach berm, see Figure 6.12. Beach scarp formation is usually recognised by near-vertical slopes occurring along the beach (berm). The size of the scarp formation is mainly dependent on the wave energy reaching the waterline. It is a common phenomenon around the world and often linked to more energetic wave conditions, such as storms (Schwartz, 2005). In the case of East Coast Park, then, beach scarp formation must be attributed to a combination of high water levels and more energetic waves, and not to the waves that occur predominantly throughout the year. Also, rising sea levels and lowering land surfaces contribute to waves affecting higher parts of the cross-shore profile.

Figure 6.12 Beach scarps along East Coast Park, in 2012 (left) and 1973 (right).

Gully formation along the beach berm

During the collection of sediment samples for this study, an unexpected phenomenon was observed along berm of the studied coastal cells. In Figure 6.13 a series of photos of this phenomenon is shown. Along the berm of the considered beaches deep cuts in the berm were found, on various locations along the berm at an irregular interval.

The cuts were on average about 50 cm deep, measured using a sediment tube of 30 cm long, see Figure 6.13d. The cuts all reached from the berm of the beach and extended to around mid-tide or even the lower beach face, where sediment was seen to be accumulated. Unaware of what was going on initially, it seemed unlikely for waves to create such irregular cuts in a similar fashion as with liquefaction (which is described hereafter), also because the slope of the beach becomes gradually gentle towards the berm.

Figure 6.13 Sliding off of upper beach berm during flash floods, East Coast Park. Figures (c) shows the cuts into the beach berm and the path followed during washing out of sediment. In (d) the size of the cut is indicated, being about 50 centimetres deep in all of the cuts. Figures (e) and (f) show the accumulation of rain water above the beach berm, and the flow of this water towards the beach, respectively. The phenomenon was observed in between headlands 8, 9 and 10 on 13 December 2012. No records have been found of similar observations at other locations, yet.

After taking a closer look, water still seemed to stream from above the berm into the cut, revealing large puddles of water landward of the berm line. This water had most probably accumulated during the intense rainfall that day, which is very common during that time of the year (N.E. monsoon). Due to inadequate drainage of the land surface, the water thus accumulates and flows off the beach face in case it reaches there. This occurs when either the land surface above berm height slopes towards the beach or is locally lower so that water is able to accumulate there. The upper beach face becomes saturated and the seaward flow of water creates streams which in turn form small funnels that eventually cause instability of the berm, after which sliding off of the sediment occurs.

Liquefaction along lower beach face

At the same time the aforementioned beach berm instability was observed, another unexpected phenomenon was observed, this time along the lower beach face. As water levels lowered at MLWS, some cuts along the beach became clearly visible, see Figure 6.14. The beach cuts were all on average around 20 centimetres deep. The most probable cause for this phenomenon is the relatively quick lowering of the water level during MLWS and the steep beach profile, in combination with an up and down movement due to wave run-up. This most oftenly occurs for loosely packed sediments, where the pores get filled with water during higher water levels. If the water movement due to wave run-up on the beach is relatively fast up and down, especially with waves rushing up and down the beach, an underpressure is created when both the water level and water table in the soil quickly drop. If this occurs, the pressure in the pores, which are filled with water, becomes too high and an outward directed flow of pore water occurs, turning the sediment into a fluid mud which then flows seaward. This is referred to as liquefaction.

Figure 6.14 Soil liquefaction along the lower beach berm of the beach enclosed by headlands 8 and 9.

What is remarkable about the aforementioned phenomena is that neither the liquefaction, nor the sliding off of beach berms along East Coast Park during so-called flash floods (periods of intense rainfall) have been reported before. The interesting fact of the latter phenomenon is that wave action might not have necessarily been the main contributor, but instead heavy

rainfall. This adds another perspective to the analysis, in which initially only hydrodynamic forces were considered, and not meteorological ones. With knowledge on the amount of yearly rainfall in Singapore and the intensities in which it occurs, see Chapter 2, it then seems very likely for such 'extreme' rain events to occur on a rather frequent basis and should thus not be neglected in any of the analyses regarding beach erosion along East Coast Park.

6.4.3 Time-varying cross-shore sediment distribution

Now that we have identified some processes contributing to cross-shore transport of sediment along the beach profiles of East Coast Park, it is interesting to investigate whether a time dependency exists in the morphology of the cross-shore profile, which could possibly be attributed to the varying wave climates throughout the year (due to different monsoons). For the beaches enclosed by headlands 8, 9 and 10 along East Coast Park profile data has been provided by the Tropical Marine Science Institute (TMSI) of profile measurements performed over a period of two years, making a total of about 8 measurements with an interval of 3 months each. Despite the short time span and relatively large interval of these measurements, they have been analysed and the results are presented below.

In total 5 profiles were analysed, 3 profiles behind each headland (8, 9 and 10) 2 profiles in the centre of the beach cells enclosed by the headlands, see also Figure 6.15.

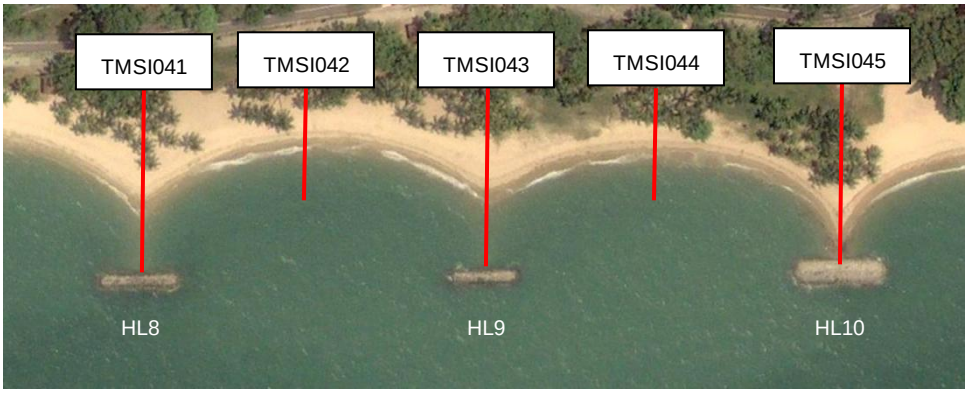

Figure 6.15 Rays of cross-shore profiles along which measurements have been performed by the TMSI. Locations are approximate, going from a landward benchmark to either the structure or the low water line.

In Figure 6.16 an example is shown of two profiles, profiles TMSI041 and TMSI042 (hereafter simply referred to as profile 041, 042 etc). These profiles are used to represent both a profile behind a breakwater and a beach profile. The other profile results can be found in Appendix D. In Figure 6.16 the horizontal displacement as a function of time is plotted for the two beach profiles. On the left profile measurements for different times are shown, plotted over each other. The adjacent figures to the right then show for each consecutive time interval the horizontal displacement along the vertical of the profile. So in case of advance a rightward displacement is shown, and a leftward displacement for retreat of the profile.

In profile 041 we observe prominent horizontal displacement in both the upper and lower parts of the profile, whereas in profile 042 we observe prominent horizontal displacement mainly in the upper part of the profile. Besides that, in profile 041 much larger displacements

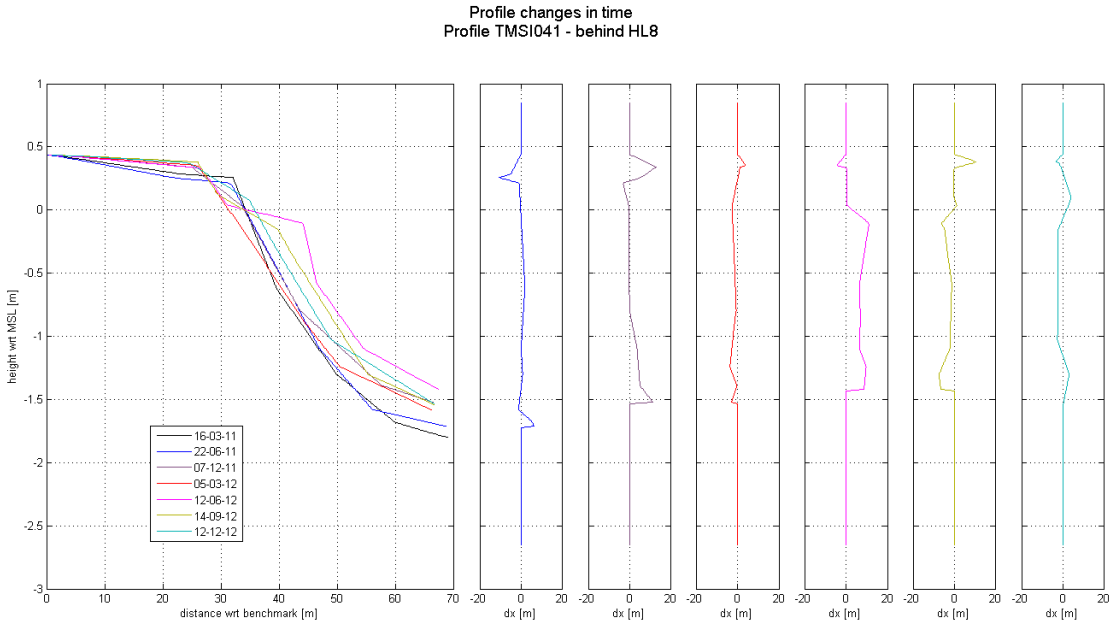

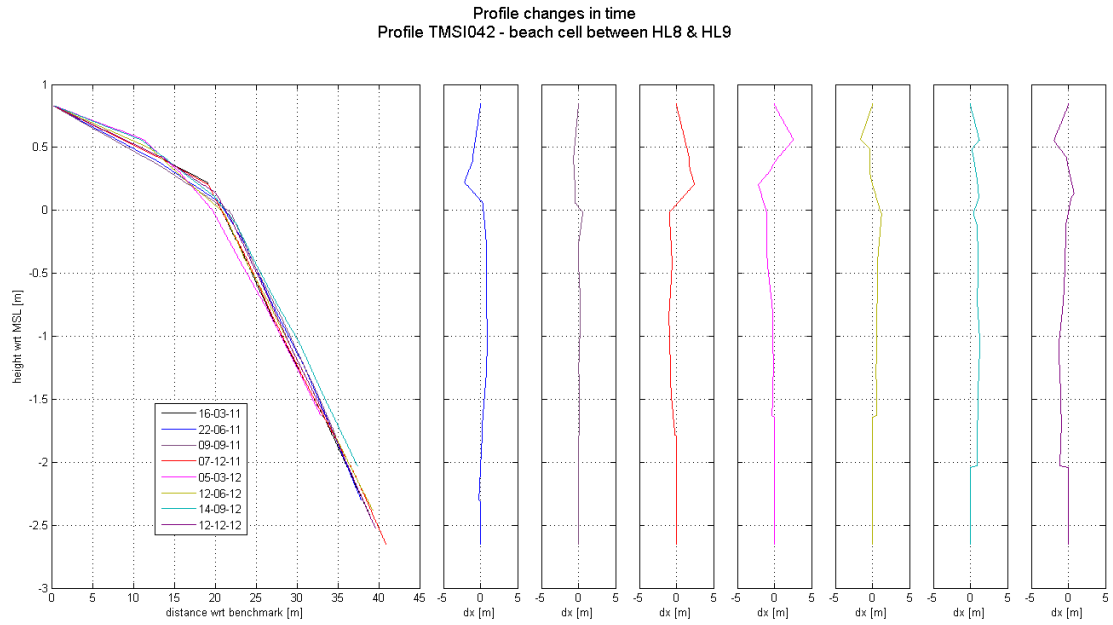

Figure 6.16 Profile changes in time for profiles TMSI041 and TMSI042 (Appendix D). On the left the profile measurements are shown, and right the profile changes of consecutive profile measurements, each with an interval of 3 months during the years of 2011 and 2012.

are found throughout the year. It should be remarked, however, that occasionally nourishment works are performed along East Coast Park, of which currently no data is readily available. Such nourishments works might be a contribution to these large displacements. Disregarding that, however, it is still noticeable that most of the transport occurs at the upper part of the profile. A probable cause for this is the fact that around this part of the profile sediments are poorly sorted due to the less frequent exposure to hydrodynamic forces. Sediment variability

at the upper part is also larger, so that fines found in the upper part of the profile (see Section 6.3) contribute to much of the sediment transport there. This also explains the transition in the profile slope, which becomes more gentle towards the upper part of the profile, just around the area where the largest transports occur. On the lower part, where sediment is coarse, a beach profile equilibrium then seems to have been (nearly) reached already.

Besides the causes and location of sediment transport within a beach profile, the time-dependency of this sediment transport is analysed. The initial idea of the profile analysis was to find a possible trend in the cross-shore movement of the beach profile, which would possibly substantiate the occurrence of structural erosion along the coast, rather than local erosion. As mentioned before however, the amount of profile data is too limited for a relatively short time period. It is thus difficult to draw valid conclusions on long-term trends in erosion.

Nevertheless, it is still interesting to regard any erosional patterns as a function of time. Looking at Figure 6.16 it is somewhat difficult to see clear patterns of profile retreat or advance throughout the measured time periods. Therefore we have chosen to illustrate the profile evolution differently, as is shown in Figure 6.17, which shows the evolution of each of the profiles in time. For larger image resolution reference is made to Appendix D. In the left column of Figure 6.17 the evolution is plotted for the profiles behind the breakwaters (041, 043 and 045), while in the right column the profiles in the coastal cells (042 and 044) are plotted. For each profile 4 points along the profile are chosen, at CD + 1.5 m (MSL – 0.152 m), CD + 1.0 m (MSL – 0.652 m), CD + 0.5 m (MSL – 1.152 m) and CD + 0 m (MSL – 1.652 m). For each period these points are then plotted and contour lines are drawn to illustrate the profile development as a function of time.

At first sight the lines seem rather chaotic, but when looking more carefully we can identify certain phenomena. Regarding the profiles behind the breakwaters, changes seem quite significant in comparison with the profile changes in the coastal cells. As mentioned before, because of the fact that nourishment works are performed at unknown time intervals throughout the years, it is difficult to draw solid conclusions for the profiles behind the breakwaters. However, when looking at the black and red line in profile 043 it looks as if retreat in the upper profile occurs when advance in the lower profile occurs, and vice versa (note the third and fourth period).

Profiles 042 and 044 seem more interesting, especially since profile 042 seems to support a seasonally dependent pattern in the profile evolution. Despite the short time period over which this data has been obtained, it can be seen that during the S.W. monsoon a seaward translation of the profile occurs and during the N.E. monsoon a shoreward translation. The same is found for profile 044, although less prominent. If these observations can be directly extrapolated to longer time periods, this observation could imply a building up of a steeper cross-shore profile during the calmer S.W. monsoon and the formation of a more gently sloping profile during the more energetic N.E. monsoon, which is a phenomenon often observed in more temperate climates with typical summer and winter profiles.

Similar observations have also been made by Chew et al. (1974), who performed profile measurements along a section of East Coast Park during three different periods from 1972 to 1973, see Figure 6.18. From these measurements the presence of a seasonality in the profile development seems to be substantiated. In the figure can be seen how an offshore directed translation of the contour lines occurs in between October 1972 and April 1973 (N.E. monsoon), while there is a shoreward translation in between April 1973 and October 1973 (S.W. monsoon), which is in accordance with what we observed in profile 042.

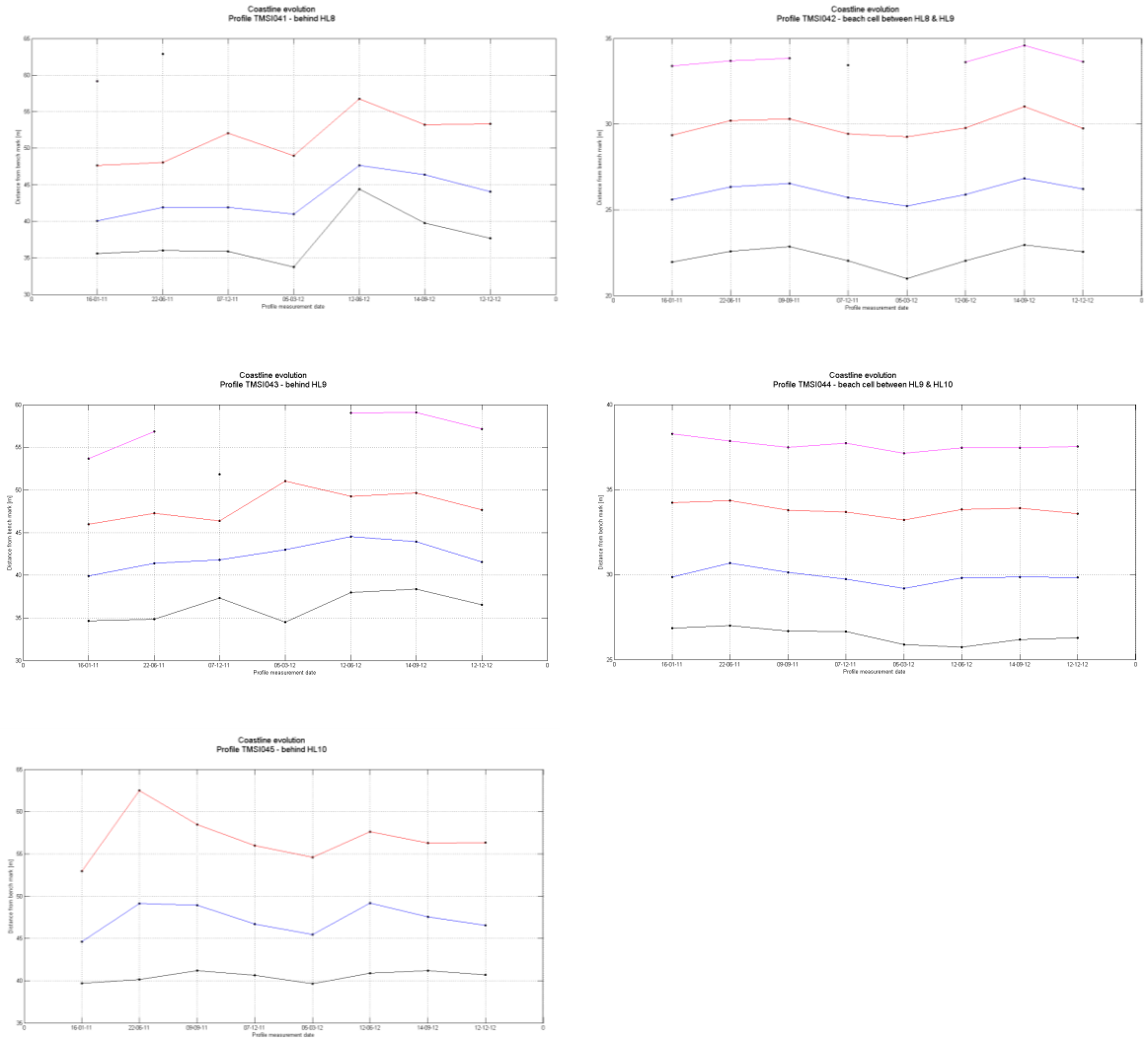

Figure 6.17 Profile evolution along several points in the cross-shore direction. From left to right and from top to bottom: profile 041, 042, 043, 044 and 045. Each measurement period is plotted on the x-interval, and the horizontal distance from the benchmark is plotted on the y-axis. The lines connect characteristic points along the profile, chosen at CD +1.5 m (black), CD +1.0 m (blue), CD +0.5 m (red) and CD + 0 m (magenta). Chart Datum is defined as MSL + 1.652 m. Missing lines or gaps indicate missing data points for that depth.

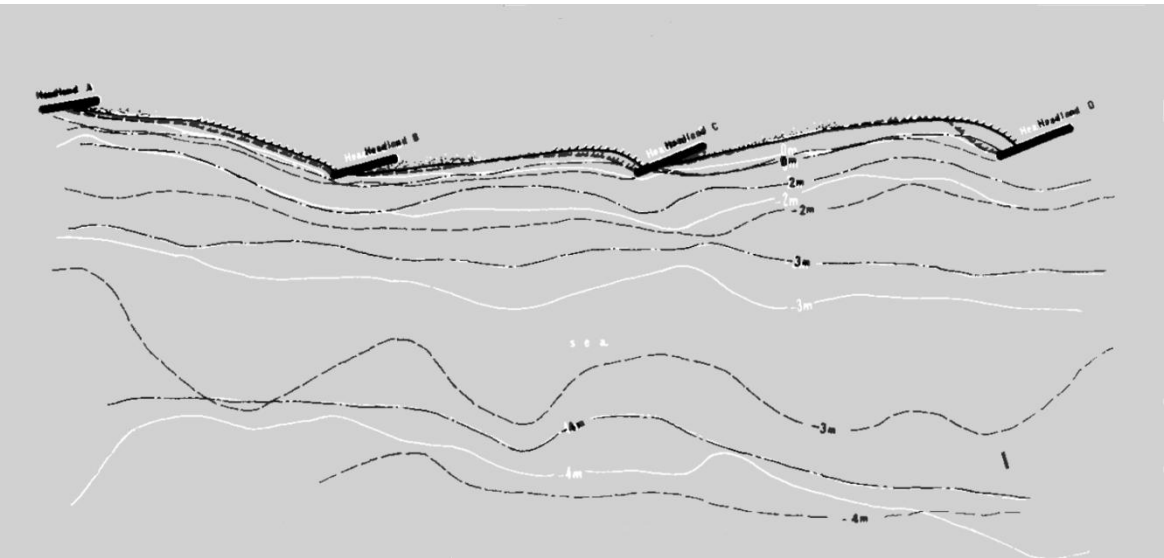

Figure 6.18 Contour lines as a function of time, measured by Chew et al. (1974). The dashed black line indicates contour lines measured in October 1972; the dashed-dot black lines are contour lines measured in April 1973; the white lines are contour lines measured in October 1973.

6.4.4 Cell type dependency

For cross-shore sediment transport the amount of *wave penetration* into the coastal cell is significant. From the description of beach-structure interaction for the different types of coastal cells, we have seen that waves need to penetrate further into the pocket beaches than into the other cells, for which they dissipate more towards the shoreline. It should be kept in mind, however, that this is also dependent on the water level. During high water levels waves will be able to penetrate deeper into the coastal cells and affect the waterline more directly, increasing the effect on sediment transport. In general, however, the effect of waves on the beach profile is less for pocket beaches due to the fact that high water levels occur for limited time periods only. On top of that, because of a larger distance of the control line between the headlands to the coast, sediments will be transported less far within the coastal cell and the chance of these reaching the zone where wave- and tide-induced longshore currents occur becomes smaller as well, in comparison to the other cell types.

Nevertheless, in the next section it is shown that disregarding the limited wave penetration into pocket beaches a significant amount of sediment loss in cross-shore direction can still be expected.

6.4.5 Overview

Along East Coast Park, cross-shore sediment transport is caused by a variety of factors, both hydrodynamic and meteorological ones. At the berm we find waves to affect the berm directly during high water levels, cutting out the berm, but we also observe the formation of gullies due to an excess of water on the land surface on top of the beach berm after flash floods. At the lower beach face the results of soil liquefaction have been observed, resulting from relatively rapid water movements up and down the beach due to wave run-up and tide-

induced water level fluctuations. This wave run-up might be enhanced by the presence of long waves or due to large wind-driven water level setup.

Regarding the flash floods, mention should be made on future predictions investigated in the climate scenarios of the IPCC (2007). According to their findings, global average temperatures have risen by about 0.74 °C in the last 100 years, and continue to rise. Despite periods of draught occurring during El Niño events, the frequency of heavy rainfall events is expected to increase in tropical regions, see also NCCS (2008).[xv]

Once sediment is stirred up on the beach profile it is transported into offshore direction due to undertow or gravity driven flow, which is enhanced by the large steepness of the beach profiles along East Coast Park. Due to the large steepness and the mild wave climate the onshore transport of these coarse-grained beach sediments is negligible. Depending on the coastal cell type, then, the eroded sediments will end up offshore of the beach, be it still within the coastal cell or seaward of the enclosing structures. Looking back at Figure 6.2, the sediment might then be moved in alongshore direction if the wave climate and water levels allow. The aspect of longshore sediment transport will be treated in the next section.

6.5 Longshore sediment transport

In Chapter 5 the influence of wave- and tide-induced longshore currents had already been accounted for (semi-)quantitatively. In this section we will build upon those results and qualitatively assess the influence of these forces on the longshore sediment transport within coastal cells or seaward of the structures, including the presence of structures in the cross-shore and longshore profiles. This analysis will make use of satellite imagery and literature so substantiate conclusions drawn.

6.5.1 Forces driving longshore sediment transport

When it comes to long-shore sediment transport within coastal cells or seaward of the enclosing structures (in the zone dominated by both waves and tide, see Figure 6.2), two main drivers are found for long-shore sediment transport, namely:

- (monsoon-generated swell / local wind) waves;
- tidal currents.

Again, the influence of water level fluctuations is implicitly accounted for. Similar to cross-shore sediment transport, waves breaking at the beach can also induce swash motions stimulating a longshore drift along the waterline. Generally a distinction is made in the zone of longshore sediment transport:

- the zone where both waves and the tide induce longshore currents, seaward of the structures;
- the zone where only (obliquely incoming) waves induce currents, along the waterline within a coastal cell.

These zones are schematically illustrated in

Figure 6.19.

[xv] *More recent versions of the NCCS can be found on http://app.nccs.gov.sg/page.aspx?pageid=123*

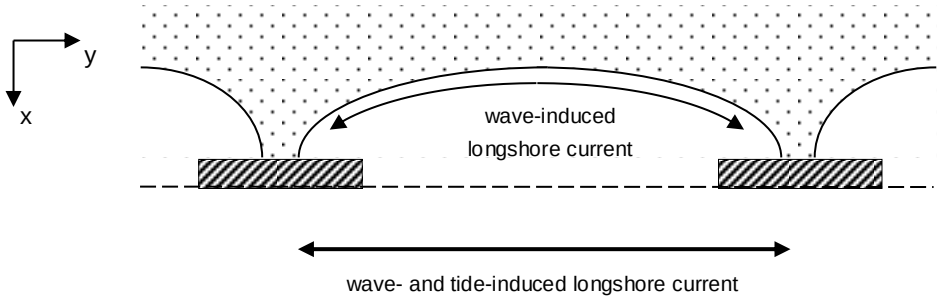

Figure 6.19 Schematic illustration of zones of longshore sediment transport. Seaward of the structures longshore currents are induced by both waves and the tide. Along the waterline longshore drift is stimulated by swash motions.

6.5.2 Role of structures in longshore sediment transport

In Section 5.4.2 the influence of waves on the nearshore morphology was assessed semi-quantitatively. Numerical models (Unibest-TC and –LT) had been used to determine current velocity distributions along the coastal profile. In Figure 6.20 the presence of structures is now

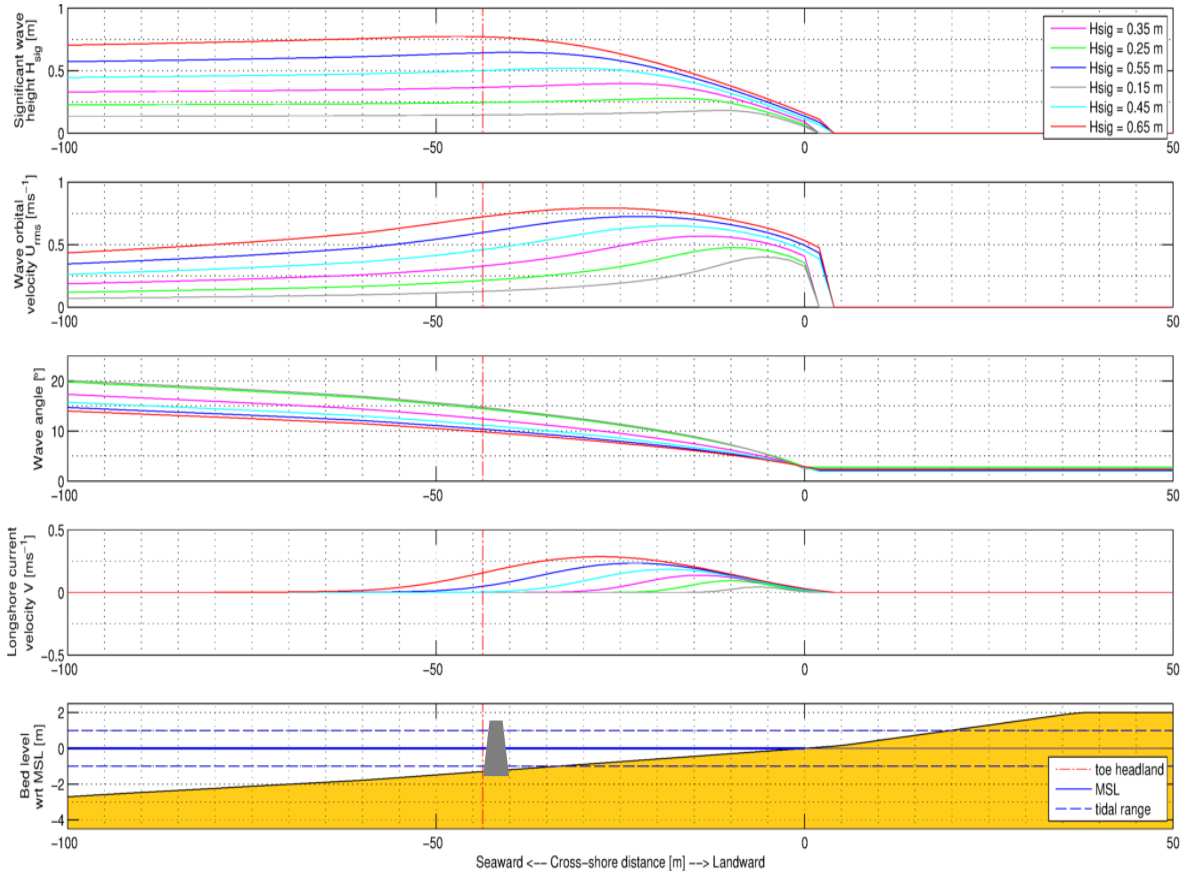

Figure 6.20 Cross-shore distribution of wave(-induced) parameters. According to Figure 5.24, with the inclusion of the structure position. The location of the toe of the structures is indicated by the vertical red dashed line.

included, and a vertical line is drawn along the toe of the structure. The location of this toe is on average at about MSL – 1.3 m. Already for maximum current velocities, it was found that tide- and wave induced longshore currents are too small to transport sediments alongshore. In Figure 6.20 it can be seen that these maximum velocities would occur near the waterline, which is within the beach cell for water levels around MSL and MHWS. In that case the actual current velocity is much smaller seaward of the structures, in the zone of wave- and tide-induced longshore currents. At MLWS the maximum current velocities *can* occur seaward of the structures, however. The found velocities might not influence the coarse-grained sediments much, but can contribute to longshore drift of finer sediments.

6.5.3 Time-varying longshore sediment distribution

A common feature of beaches around the world is the re-orientation of the beach planform due to a redistribution of sediment along the beach under changing wave climates. In a study by Daly et al. (2011) the effect of waves approaching embayments under different angles has been modelled quite accurately, showing how a longshore drift is created within a coastal cell with waves arriving at an angle to the cell. Waves approaching East Coast Park generally reach the shoreline under different angles throughout the year, as was shown in Section 2.2.4. Therefore it is interesting to see whether rotational features are present along East Coast Park due to changing wave angles. Using satellite imagery obtained from Google Earth, several beach planforms for different periods have been analysed to check this.

In Figure 6.21 several examples are shown of coastal cells at different dates. Each row shows the same coastal cell, but at different times. What is seen in the figures is that in the left column the beaches show patterns of accretion on the westward side and erosion on the eastward side of the coastal cell, while in the right column these patterns are reversed. At first sight it seems fairly obvious that the effect of beach rotation is also applicable to East Coast Park, where we already observed time-varying cross-shore profiles in Section 6.4.3. This then indicates that sediment is transported back and forth along the beach planform throughout the year. The only remaining uncertainty is then the time scale on which beaches respond to changes in wave climate. The upper beach in between headlands 4 and 5 in Figure 6.21 shows changes during the *same period* of the year, during the S.W. monsoon. The other beaches show such variability for *both* the S.W. and the N.E. monsoon. Due to a restricted amount of available satellite images, time scales of the beach rotations cannot be verified at this stage.

Following the results for longshore sediment transport, the observations made here seem to be in contrast with what was found earlier, when the possibility of longshore sediment transport was annulled. However, the main difference is that earlier we considered initiation of motion under wave-induced currents in a water depth of about 1.3 m (neglecting water level variations), where the bottom is composed of mud and clay. Here, on the other hand, we consider waves breaking directly on the beach, inducing turbulent motions that, slowly but surely, stir up the sediment and carry it alongshore. Note also the high wave orbital velocities at and near the waterline in Figure 6.20. The headlands in turn make sure that the sediment is retained within the coastal cell. Important to note is that this phenomenon is only observed along straight and J-shaped beaches, and not in the two pocket beaches along East Coast Park. This can be explained by the fact that the beaches need to be sufficiently exposed in order for waves to penetrate far enough into the cell, while maintaining its wave energy. The spacing between headlands 8, 9 and 10 is too small to let waves penetrate the cell undisturbed.

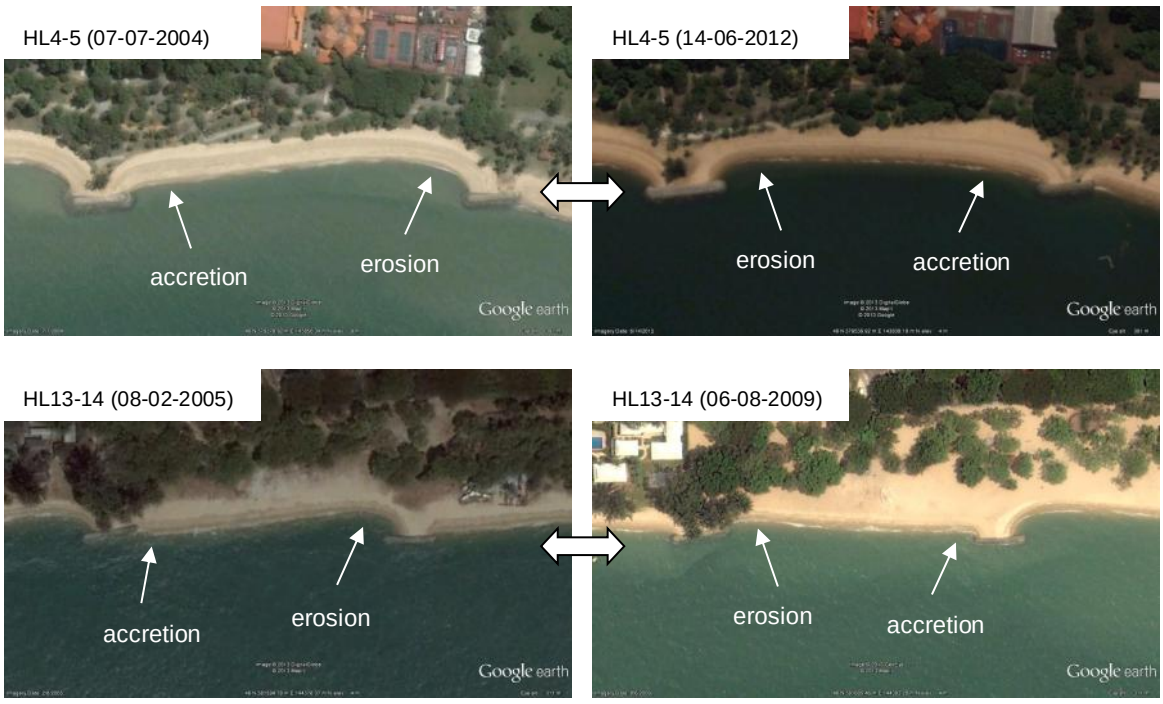

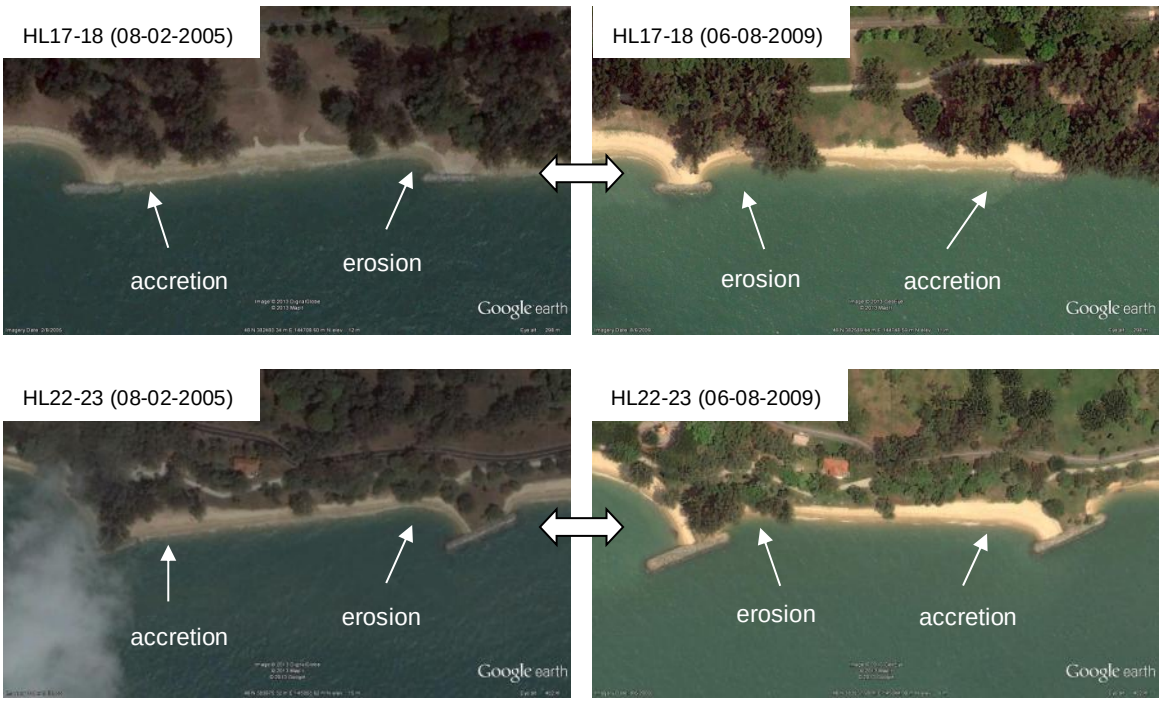

Figure 6.21 Beach rotation in coastal cells along East Coast Park, for beaches in between headlands 4-5, 13-14, 17-18 and 22-23 (Google Earth imagery).

Beach rotation in some of the above illustrated cells leads to downcoast parts accreting quite far in seaward direction. In some cases, as on 08-02-2005 for HL13-14, HL17-18 and HL22-23, the shoreline at the western end almost surpasses the seaward extent of the headland. This leads one to wonder whether by-passing of sediment around the structures is then possible. This will be addressed in Section 6.6.

6.5.4 Beach planform equilibrium

In analogy with the rotational behaviour of beaches, in this section brief attention is given to analyses of beach planform equilibria within coastal cells applied to East Coast Park. Many successful attempts have been made in the past to analyse static equilibrium for embayed beaches, all building upon the ideas by J. R. C. Hsu and Evans (1989), who came up with a parabolic equation to assess the equilibrium planform. This equation has been applied and improved along the years, in order to increase the general applicability. Tan et al. (2007) have applied the method to beaches along East Coast Park, concluding that many of the beaches studied have not reached static equilibrium yet, indicating that erosion might be expected to continue in the future.

Following our findings on seasonally dependent sediment distribution within coastal cells, or simply *beach rotation*, the application of simple methods to assess the static equilibrium planform of these beaches becomes less trivial. Amongst others, Ojeda and Guillén (2008) and Klein et al. (2010) have studied the complex nature of beach morphology and morphodynamic processes within embayed beaches. Besides the requirements for the applicability of the parabolic equation, the largest uncertainty then becomes the response of beaches along East Coast Park to changing wave climates. Assuming normal wave conditions throughout the year, the phenomenon of beach rotation is expected to occur on a relatively large time scale. If one tries to assess the static stability of these beaches using the parabolic equation given by J. R. C. Hsu and Evans (1989), which assumes a beach to be in static equilibrium, the validity of the results should be regarded with care. The dynamic behaviour of rotational (straight) beaches will limit the time that is needed for a beach to reach a certain equilibrium, and results obtained using a static equilibrium approach could then under- or overestimate the actual planform to be reached, as these are based on constant wave conditions and do not include the impacts of short-term events (Ojeda & Guillén, 2008).

6.5.5 Cell type dependency

Similar to the analysis of cross-shore sediment transport, the effect of cell type on longshore sediment transport will be addressed briefly.

There are several aspects contributing to the effect of waves on longshore sediment transport within or seaward of coastal cells, among which the most important ones are:

- the water level;
- the angle of wave incidence;
- coastal cell-specific parameters;
- the sediment type present in the littoral zone.

During higher water levels, waves can reach further into the coastal cell. The presence of structures then determines the amount of wave energy that will be carried into the cell. For example, in pocket beaches diffraction of waves is more prominent and thus also dissipation

of wave energy towards the beach. Longshore currents occur in case waves approach the coast obliquely. In case of low water levels, currents will be induced seaward of the headlands, driving the current downdrift along the coastal cells. In case of high water levels, waves might reach the waterline and induce a longshore drift due to swash motions along the beach. The magnitude of this drift is then determined by the wave climate and the sediment at the waterline.

Along straight beaches, such longshore drift along the waterline is more prominent, as is shown in Figure 6.21, where we observed beach rotation for several beaches along East Coast Park. This is then caused by the fact that straight beaches are more exposed to the incoming waves. In pocket beaches this effect is expected to be much less, whereas in J-shaped beaches besides unidirectional wave-induced longshore sediment transport also setup-driven longshore currents occur. This is illustrated in Figure 6.22. The balance between these updrift and downdrift forces then determines the predominant direction of sediment transport. From Figure 6.9 it then seems that the sediment transport due to wave breaking dominates over transport by setup-driven currents, see also Daly et al. (2011). For the observed predominant wave climate, however, these setup-driven currents are assumed to be minor in comparison with the already small swash motions in the other direction.

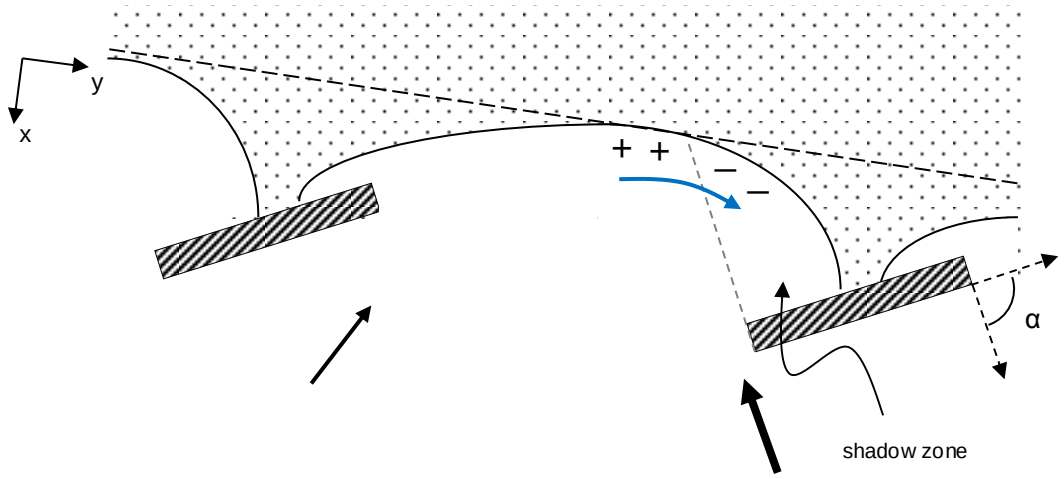

Figure 6.22 Illustration of wave-induced water level setup differences along the waterline in a J-shaped beach. The blue arrow indicates the corresponding direction of the current induced by gradients in setup.

6.5.6 Overview

Along East Coast Park, longshore sediment transport is mainly dependent on water level fluctuations and the wave climate. Generally, wave-driven longshore currents occur seaward of the headlands, but depending on the coastal cell type wave penetration might be sufficiently large to reach the beach and induce a longshore drift along the waterline due to swash motions. For pocket and J-shaped beaches this drift along the waterline is less prominent than for straight beaches, where we observed time-varying beach rotation.

Having analysed both cross-shore and longshore sediment transport separately, the question arises whether the combined effect of these transports contributes to longer-term sediment losses or distribution along the coast, in the form of sediment by-passing around structures. This is addressed in the following section.

6.6 By-passing of sediment around structures

When it comes to by-passing of sediment around a structure, several requirements need to be fulfilled in order for sediment to be able to be transported around a structure:

1 the cross-shore or alongshore transport of sediment within a cell needs to bring the sediment far enough seaward, beyond the headland, in order to reach the littoral zone where longshore currents are present;
2 water levels need to be such that wave- and tide-induced longshore currents are present just seaward of the headlands;
3 these currents should be strong enough to carry the offshore deposited sediment in alongshore direction;
4 assuming that coarse grains will be less easily transported when they lie in the cohesive bottom material further offshore, longshore sediment transport of coarse grains is expected only to be possible when sufficient sand has covered the cohesive layer, so that transport of sand over a non-cohesive sandy layer occurs.

This combined effect of cross-shore and longshore transport is illustrated in Figure 6.23 below.

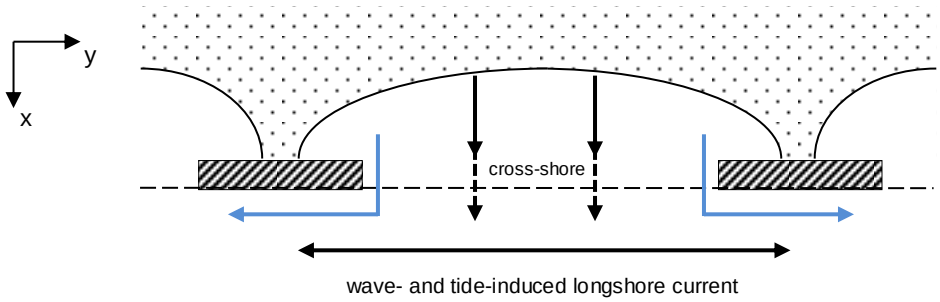

Figure 6.23 Sediment by-passing (blue line), as a result of the combined effect of cross-shore and longshore sediment transport.

From findings on cross- and longshore sediment transport in the previous sections, by-passing of sediment seems to be absent for coarse sediment grains due to the lack of strong enough currents to carry the sediment alongshore. For finer sediment, however, it is still possible to be transported alongshore. For example, for a sediment diameter of 0.2 mm the critical current velocity is approximately 0.2 m/s (Bosboom & Stive, 2011). From the sediment analysis performed during this study sediment beyond the headlands was found to be much smaller. With wave- and tide-induced longshore currents reaching maxima of about 0.23 to 0.33 m/s, see Section 5.4.2, transport of medium or fine sediments then seems likely to occur for lower water levels. The effect of an additional friction factor caused by the muddy bottom should be taken into account, however, as the transport of non-cohesive grains is impeded by the cohesive sub-layer.

During observations along East Coast Park, one location has been found where by-passing of beach sediments seems to be initiated, at the western end of headland 6, see Figure 6.24. Considering this, it can then be said that by-passing might occur if beach sediments surpass the toe of the headlands. However, in order to do so a sufficient amount of sediment needs to

be available. Regarding the fact that there is no natural source for the supply of coarse sediments along the coast, sediment input is then only stimulated through beach nourishment works. Also, as mentioned under point 4 of the prerequisites, transport of sand will be impeded by the presence of a cohesive bed surface. Therefore by-passing of sediment around structures will only occur on longer time scales, and can then be regarded as the long-term residual effect of cross- and longshore sediment transport.

Figure 6.24 Straight beach west of headland 6. The dashed red circle indicates the location and direction of the photos below. The lower left photo shows sand surpassing the headland, and the lower right photo shows the retreat of the water line seaward of the headland.

In some cases, it might be possible that the tombolo in the lee of the structure is inundated during high water levels. Clear examples are the tombolos behind headlands 8, 9 and 10, which were found to be inundated during high water levels before the tombolos were raised through beach nourishment works. In case such a scenario continues to prevail for a certain time, it is possible for sediment to be transported to adjacent beach cells via the lee of the headland, see Figure 6.25 below.

There are two factors making such transport of sediment not likely to happen for short time scales, however. The first is the fact that sufficient time is necessary for significant movement of sediment to occur. During events of large waves in combination with high water levels, the time necessary is less. The second factor is related to the regular beach management works

Figure 6.25 Pocket beaches enclosed by headlands 8, 9 and 10, prior to 2009 when the tombolos were raised through nourishment works. The blue arrows indicate the possible movement of sediment in the lee of the headlands during high water.

that are performed along East Coast Park, frequently raising the land to the level of the backshore, and recently also adjusting the layout of the headlands in Figure 6.25 by increasing the horizontal dimensions and crest level. If relative sea level rise continues in the same rate as it has until now, future sand replenishments will be necessary to prevent lowering of the tombolos and possible sediment transport in the lee of headlands.

6.7 Discussion and conclusions

Whereas in the previous chapter we addressed larger temporal and spatial morphological scales, using a semi-quantitative approach, in this chapter we have regarded smaller scale processes in a more qualitative way. From observations and basic knowledge of coastal dynamics we have been able to assess processes within coastal cells along East Coast Park. From the analysis we are now able to validate the hypotheses we defined earlier in Chapter 4. Below the research questions are repeated in accordance with their numbering.

4 Are waves able to stir up and transport sand? If so, where in the profile?

In the hypothesis we assumed the mild wave climate in the coastal waters of Singapore to contain too little energy to produce significant orbital and current velocities to transport sediment. In Chapter 5 numerical modelling tools were applied to assess such velocities and the transport capacity quantitatively, from which a cross-shore distribution of the longshore current followed. The maximum wave-induced velocities in this current distribution were found to be around 0.13 – 0.18 m/s, which together with the tide-induced amounts for about 0.23 to 0.33 m/s. For grains found on the beach profiles (~1.3 mm) such currents are too small for effective transport. In the analysis the presence of structures in the cross-shore profile was neglected.

In reality, however, structures are present and therefore the nearshore region is divided into a zone where only waves are dominant (within coastal cells) and a zone where both waves and the tide are effective (seaward of the structures). Seaward of the structures the currents are then found to be even smaller than the maximum current velocity we used in Chapter 5, making the transport of *coarse* sediments even less likely. Fine sediments however are more

likely to be transported, especially during lower water levels when the maximum velocities occur farther offshore.

Within the coastal cells a variety of processes occur, both in cross-shore direction as in longshore direction. These processes are dependent on the type of cell, of which three types had been classified, namely straight beaches, pocket beaches and J-shaped beaches.

Cross-shore transport of sands occurs only on the beach profile. In the upper part of the beach profile, at the berm, waves erode the berm during high water levels and energetic wave climates. During flash floods drainage of the coastal area can be affected and water will accumulate above the beach berm, leading to erosive gullies once this water reaches the beach and runs off the beach profile. In the lower part of the beach profile, or generally along the water line, liquefaction of sediment can occur in case of rapid up- and backrush on the beach, causing excessive pore pressures which lead to the outflow out of large volumes of sand into offshore direction. The wave-induced phenomena might be less in pocket beaches than in the other cell types, because of more wave energy dissipation within pocket beaches.

Wave-induced longshore sediment transport only occurs in case of obliquely incident waves to the coast. During high water levels waves reach the beach and cause swash motions leading to a longshore drift of sediment along the waterline. During low water levels waves will affect the zone seaward of the headlands and transport fines in alongshore direction.

5 What is the seasonal effect of monsoons on the coastal morphology?

The monsoon periods affect both the character of the wave climate as the predominant angle of wave incidence to the coast. During the N.E. monsoon more energetic waves prevail, approaching the coast from the southeast. During the S.W. monsoon waves are milder and the angle of approach lies predominantly between the southeast and the south. From the analysis it was seen that this monsoon-dependent variability in wave climate can affect both the coastal profile as the beach planform.

For the analysis of the beach profile 8 measured profiles over a period of 2 years (intervals of 3 months) were used. Despite the fact that from these profiles the largest profile changes occurred in the upper part of the beach profile, a rough profile evolution analysis showed that the profiles are subject to time-variability. The same had been observed in literature, where during the N.E. monsoon more mildly sloping upper foreshores developed, while during the S.W. monsoon these were found to be steeper.

Regarding the beach planform, satellite observations show that these tend to rotate in time. Typically profiles are found to be reversed during the N.E. and S.W. monsoon periods, but such rotation was even seen on a shorter timescale within a monsoon period. Beach rotation is driven by the angle of wave incidence, which can vary throughout the year not only due to monsoon-generated swell waves, but also due to short-term changes such as the occurrence of Sumatra squalls during the S.W. monsoon. The phenomenon has so far only been seen to occur along straight beaches.

6 Are waves able to by-pass sand around headlands to adjacent coastal cells?

The combined effect of cross- and longshore sediment transport can in some cases lead to by-passing of sediment around structures. This can only occur if sediment is being transported beyond the toe of the structures to end up in a zone where currents are strong enough to carry the sediment alongshore. In case of coarse sand we had already concluded that this longshore transport seems unlikely, whereas for fines the possibility is much more probable. At one location along East Coast Park, however, coarse beach sands had been found to cover part of the (seaward) toe of the structure. The assumption is then that such by-passing might only occur for sand over sandy material, because cohesive bottom material will create additional shear stresses on the grains, reducing the possibility of being carried alongshore. On top of that, sediment by-passing depends largely on sediment availability within a coastal cell. Since there are no natural sources of sediment input, by-passing can only be enhanced by human-induced sediment inputs such as through beach nourishments works.

Having answered all the previously defined research questions, we can now complete our conceptual model and draw some final conclusions in the last chapter by answering the main research question of this study, which was defined in Chapter 1.

7 Conclusions and recommendations

7.1 Discussion and conclusions

In our conceptual model in Chapter 4 we defined two morphological scales, of which the large-scale ECP system was treated in Chapter 5 and the small-scale cell system in Chapter 6. On these scales also the processes affecting the morphological evolution of the coast had been included, see Figure 7.1.

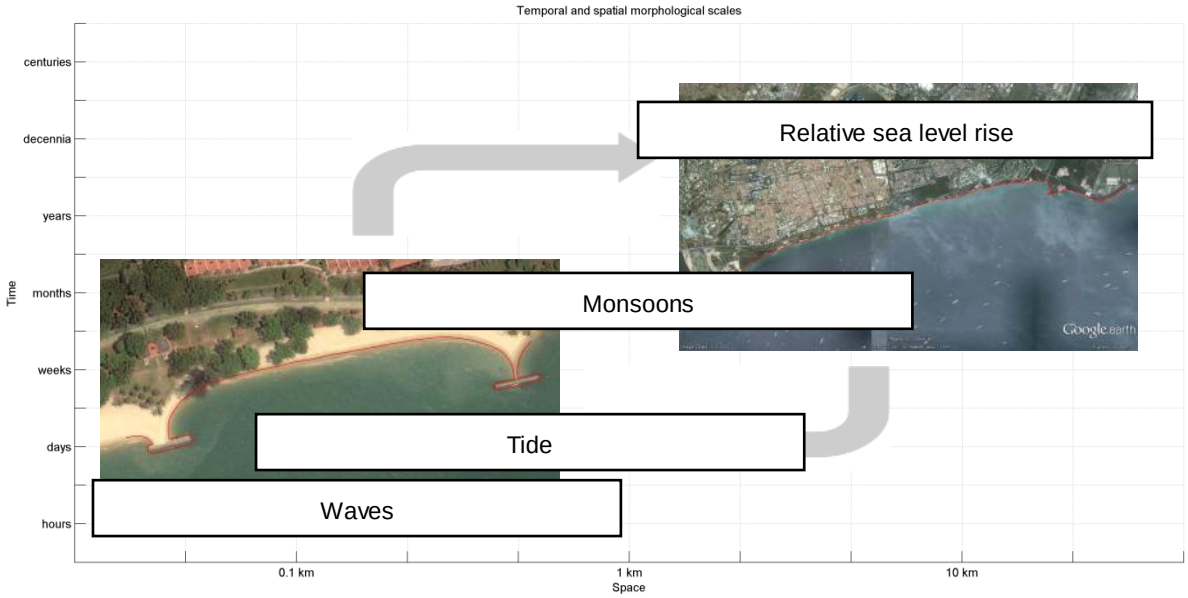

Figure 7.1 Spatial and temporal morphological scales of the coastal system in front of East Coast Park, including the interactions between the different scales, indicated by the arrows and the processes affecting the morphological evolution of the coast.

Resulting from our findings throughout this analysis we can now draw conclusions regarding the influence of these different processes on the coastal morphology and fill in their relative significance in Table 4.1. In the next section firstly the different processes contributing to morphological evolution along the coast are addressed for both the past, i.e. before the land reclamations, as for the present. In this way the relations between the different scales are assessed using a process-based approach, which can then be compared to indicate how the significance of processes on coastal morphology has changed over time. Throughout this description reference is made to the hypotheses that were defined based on our conceptual model.

Thereafter the interaction of the scales in Figure 7.1 is treated, after which the study objectives and research question of this study as defined in Chapter 1 are discussed.

7.1.1 Driving forces

Waves

Before the land reclamations the intertidal zone used to extend much further offshore from the shoreline than is the case today. Therefore waves only affected the coast at high water levels, during which these approached the coast under a larger angle than we observe nowadays, enhancing the longshore transport of fines. At intermediate and low water levels the presence of an intertidal flat caused dissipation of wave energy towards the coast.

Due to the land reclamations the intertidal zone has decreased from several hundreds of metres to about a mere 60 metres. The new beach profile consists of coarse sediments and has a steep slope, because of which it is exposed to wave action and wave breaking directly on the beach for longer time durations. During high water levels in combination with more energetic wave climates, waves affect the upper beach berm, carving it out and leaving behind scarps. (Coarse) Sediments stirred up on the beach are either transported offshore due to undertow and/or gravity driven flow, or are transported *along the waterline* due to wave-induced swash motions. Further offshore finer sediments are found, which are carried both alongshore as in cross-shore direction. Longshore transport of coarse sediments seaward of the headlands is less likely, due to insufficient transport capacity of the longshore currents and the presence of a cohesive bottom surface, adding an additional shear stress to the grains.

Tide

With the interpretation of the effect of tides on the morphology a distinction should be made between tide-induced water level variation and tidal currents. The effect of the former is implicitly included in the effect of waves, whereas the latter was regarded separately in the analysis.

With the intertidal zone being much narrower and relatively deep in the nearshore region since the land reclamations, the effect of tidal currents on the nearshore morphology is assumed to have been larger *before* the reclamations than is the case today. Using a simple expression and the numerical modelling tool Delft3D we have shown that tidal currents are too small to cause transport of *coarse* sediments, while transport of *fine* sediments might still be possible. In cross-shore direction, the influence of tidal currents is neglected, for the reason that the direction of tidal flow is alongshore and the small nearshore currents are presumed to be inadequate to form significant turbulent eddies, which could enhance cross-shore sediment transport.

Monsoons

The effect of monsoons is mainly accounted for by the changing direction and intensity of the incoming waves throughout the year. We have shown that the N.E. monsoon lead to more energetic waves and flattening of the coastal profile, whereas during the S.W. monsoon steepening of the coastal profile occurs. During the N.E. monsoon waves approach the coast mainly from the (south)east, while during the S.W. monsoon they approach the coast from a variety of angles, with Sumatra squalls occasionally causing waves to approach from the southwest.

Before the land reclamations waves are assumed to have approach the southeast coast under a larger angle normal to the coast. Since the reclamation of Changi in the east this angle of wave incidence has decreased, due to the fact that waves refract more to the coast now that the nearshore bathymetry in the eastern part of Singapore has changed rather drastically. This angle of wave incidence can be linked to longshore sediment transport through the so-called S-Φ curve, which then states that with a smaller angle of wave incidence we observe smaller longshore sediment transport rates today. Nevertheless, by analysing satellite imagery we have observed that the angle of wave incidence is still significant in the reorientation of the beach planform. Although wave directions might change on smaller time scales than the duration of the monsoons, the influence of monsoons is regarded to be dominating the coastal planform and profile.

Relative sea level rise

Relative sea level rise consists of eustatic sea level rise and local land subsidence. Based on observations over the past decades, the effect of relative sea level rise has been found to be noticeable, especially due to lowering of land surfaces along East Coast Park. This effect has been larger in the years just after the land reclamations and decreases in time due to the asymptotic decay of the rate of land subsidence. Nevertheless, the influence of land subsidence was found to be the same order of magnitude as eustatic sea level rise at present-day, for which the effect of *relative* sea level rise is still assumed to be significant on the long-term (several years to decades). Relative sea level rise along East Coast Park will mainly contribute to losses of sediment in cross-shore direction.

Other

Besides the aforementioned driving forces, during this study some other phenomena had been observed that contribute to losses of beach sediments. Along the upper beach berm we observed the formation of gullies due to runoff of excessive rainwater, leading to losses of relatively large volumes of sediment. Along the lower beach berm the result of liquefaction was observed, also causing significant losses of sediment, although less than along the upper beach berm. The latter phenomenon is the result of relatively rapid up- and downrush of waves on the beach, which might be caused by longer waves. However, at the present day no information is readily available on the effects of these phenomena on sediment losses along East Coast Park. Since they are dependent on ‘extreme’ events, which are here defined as a combination of high water levels, large waves and heavy rainfall, it is difficult to draw valid conclusions on their net effect.

7.1.2 Relative significance of coastal processes

Based on the influence of the driving forces on the coastal morphology as described in the foregoing section we can now fill in Table 4.1, which indicates the relative significance of the coastal processes. In this way the research questions and hypotheses defined in Chapter 4 are accounted for as well.

The influence is assessed for both the past, i.e. before the land reclamations, and the present, in order to indicate how the relative influence of the different driving forces and resulting morphological processes has changed since the land reclamations. As mentioned earlier, the use of pluses and minuses to assess the significance of the various processes is

one of many (subjective) ways to do so, and is merely to quantify the results and indicate their relative significance.

In Table 7.1 firstly the significance of processes *prior to the land reclamations* is shown.

Table 7.1 Significance of coastal processes in the morphological evolution prior to the land reclamations.

		cross-shore transport	longshore transport
ECP scale	RSLR	+ +	– –
	monsoons	+ +	+ +
cell scale	tidal currents	– –	+
	waves	–	+

Indication of significance, negative less significant: – – , – , + , + +

In Table 7.2 the significance of *present-day* coastal processes is indicated.

Table 7.2 Significance of present-day coastal processes in the morphological evolution

		cross-shore transport	longshore transport
ECP scale	RSLR	+	– –
	monsoons	+ +	+ +
cell scale	tidal currents	– –	– –
	waves	+ +	–

Indication of significance, negative less significant: – – , – , + , + +

From the above tables we can observe that the changes have occurred mostly for cross-shore sediment transport. The influence of relative sea level rise has decreased in time, but is still relevant. Due to the narrow intertidal zone, waves affect the beach more nowadays. In the longshore direction, the effect of tidal currents and waves has decreased, with waves still contributing more to longshore currents than the tide does. The effect of monsoon-induced variability in wave energy and direction is assumed to be the same now as it was in the past. For more detailed information reference is made to Section 7.1.1.

7.1.3 Interaction of scales

Looking back at Figure 7.1, we can now assess the interaction of scales which is indicated by the arrows linking both the small- and large-scale systems. Resulting from the above conclusions we can now state that wave-induced coastal processes are significant on the short-term, but can be felt on the long-term and large scale as well. By-passing of coarse sediment around structures might be negligible, but re-distribution of sediment in the coastal profile has become noticeable throughout the year(s) at various locations along East Coast Park. On the other hand, longer-term effects caused by relative sea level rise and monsoons affect the small-scale coastal cells directly as well.

7.1.4 Main research question and study objectives

Finally, getting back to the main research question of this study, which was defined in Chapter 1, we can now draw some final conclusions resulting from the analysis.

Research question

What are the dominant physical processes causing erosion along the coastline of East Coast Park, Singapore?

Objectives

- To identify the alongshore variation of coastline retreat
- To qualitatively assess the causes of this alongshore variation
- To qualitatively assess what happens to eroded material

The answer to the research question has been touched upon already in the first sections of this chapter, where the relation of different system scales was assessed based on the processes occurring on these scales.

With this study some more insight has been provided into the seasonal variation of coastal profiles and planforms. Considering the fact that the only substantial amount of shoreline retreat was observed at the location of the bulge, it can be concluded that this is merely a sign of the physical system working towards an equilibrium. Whether the system has reached this equilibrium or not is difficult to say with much certainty, because the coast we observe is still relatively young, showing signs of dynamic evolution patterns throughout the years.

When assessing the physical processes causing erosion along the coastline of East Coast Park a distinction is made into (1) extreme events, and (2) seasonal variability.

1. Extreme events are characterised by high water levels, wind-induced water setup and locally induced wind waves, possibly in combination with intense rainfall, all leading to large erosional impacts where beach stability is not guaranteed. These events are periodical and mainly contribute to local shoreline retreat where no input of sediment is guaranteed.

2. Monsoon-induced seasonal variability determines the overall layout of the coastal profile and planform on the long-term. Erosion on this scale is then a sign of long-term sediment redistribution and of the dynamic equilibrium state of the coast. With waves containing too little energy to bring all of the offshore deposited sediment back onshore, the result is a slowly receding coastline.

Overall, the evolution of the coastline along East Coast Park seems to follow the seasonal variability, rather than the local erosion patterns found after extreme events. Combined with eustatic sea level rise and land subsidence this leads to a relatively slow shoreward translation of the coast.

7.2 Recommendations

Below some recommendations are made for future research.

- *Accurate, up-to-date wave measurements*

  The availability of accurate and up-to-date wave data is important in assessing the present-day coastal processes. During this study such data was not readily available, and therefore it is recommended that more accurate wave measurements are performed in case nearshore coastal processes are to be analysed in more detail. In this way, also the effect of ship waves might be included, since present-day models do not include this effect (yet).

- *Long-term profile data*

  At the moment profile data is available for several years only, being measured by the Tropical Marine Science Institute over relatively large time intervals (of three months). To make a proper assessment of profile evolution along the coast, it is recommended to keep performing these profile measurements, preferably at more locations along the coast. More locations along the coast would mean for more locations within coastal cells, so that distribution of sediment within coastal cells can be assessed more accurately. Besides that, profile measurements should be extended further offshore, in order to be able to make an analysis of the entire coastal profile, rather than just the beach.

  Obtaining long-term profile data is also related to the fact that the new coastal profile is relatively new, so that an equilibrium might not yet have been reached.

- *Gully formation and liquefaction*

  During the study the formation of gullies and the result of liquefaction had been observed. So far, none of these phenomena has been found recorded. In case erosion is regarded as a continuing issue, it is therefore recommended to account for these (periodical) ‘extreme’ events as well, so that an analysis of coastal erosion along East Coast Park becomes more complete.

- *Research on the influence of mixed sediments*

  In this analysis we have mainly looked at the mobility of a mean grain diameter, which corresponds to coarse sand on the beach. In reality, however, a large range of sediment particles is found along the coastal profile. In order to make a proper analysis, it is then recommended to take the effect of mixed sediments into account, rather than using one mean particle size as a reference for the entire profile.

All of the above recommendations are the basis for a proper insight into the coastal processes along East Coast Park. This can then be used for proper beach management, applying long-term solutions which might reduce costs of present-day solutions.

8 Bibliography

Amos, C. L., Villatoro, M., Helsby, R., Thompson, C. E. L., Zaggia, L., Umgiesser, G., . . . Rizzetto, F. (2010). The measurement of sand transport in two inlets of Venice lagoon, Italy. *Estuarine, Coastal and Shelf Science, 87*(2), 225-236. doi: http://dx.doi.org/10.1016/j.ecss.2009.05.016

Arulrajah, A., & Bo, M. W. (2008). Characteristics of Singapore Marine Clay at Changi. *Geotechnical and Geological Engineering, 26*(4), 431-441. doi: 10.1007/s10706-008-9179-2

Battjes, J. A. (1974). *Surf similarity.* Paper presented at the Proceedings of the 14th International Conference on Coastal Engineering, Copenhagen.

Bird, E. (2010). *Encyclopedia of the World's Coastal Landforms*: Springer.

Bosboom, J., & Stive, J. F. (2011). *Coastal Dynamics I: Lecture Notes CT4305*: VSSD.

Bowman, D., Guillén, J., López, L., & Pellegrino, V. (2009). Planview Geometry and morphological characteristics of pocket beaches on the Catalan coast (Spain). *Geomorphology, 108*(3–4), 191-199. doi: http://dx.doi.org/10.1016/j.geomorph.2009.01.005

Bruun, P. (1954). Coast erosion and the development of beach profiles, U.S. Army Beach Erosion Board Technical Memorandum No. 44.

Bruun, P. (1962). Sea-level Rise as a Cause of Shore Erosion. *Journal of Waterways Harbors Division, American Society of Civil Engineers*(88), 117-130.

Bruun, P. (1988). The Bruun Rule of erosion by sea-level rise: a discussion on large-scale two- and three-dimensional usages. *Journal of Coastal Research, 4*(4), 627-648.

Chang, C. P., Liu, C. H., & Kuo, H. C. (2003). Typhoon Vamei: An equatorial tropical cyclone formation. *Geophysical Research Letters, 30*(3), 1150. doi: 10.1029/2002gl016365

Changsha, Z. (2011a). *Sharing coastal experience: beaches don't be fooled by what you see on the surface, especially in Singapore*. Retrieved from http://geogallers.com/geo/geoteachers.php

Changsha, Z. (2011b). *Where in Singapore: land surface lowering*. Retrieved from http://geogallers.com/geo/geoteachers.php

Cheng, N. S. (1997). A simplified settling velocity formula for sediment particle. *Journal of Hydraulic Engineering, ASCE, 2*(123), 149-152.

Chew, S. Y., & Wei, J. (1980). *Major reclamation scheme for Marina City, Singapore*.

Chew, S. Y., Wong, P. P., & Chin, K. K. (1974). *Beach development between headland breakwaters*.

Chia, L. S., & Chou, L. M. (1991). *Urban Coastal Area Management: The Experience of Singapore : Proceedings of the Singapore National Workshop on Urban Coastal Area Management, Republic of Singapore, 9-10 November 1989*: International Center for Living Aquatic Resources Management.

Chia, L. S., Khan, H., & Chou, L. M. (1988). *The Coastal Environmental Profile of Singapore*: International Center for Living Aquatic Resources Management.

Chia, L. S., Rahman, A., & Tay, D. B. H. (1991). *The Biophysical Environment of Singapore*: Singapore University Press.

Chong, P. T. (2004). *Characterisation of Singapore lower marine clay.* (Doctor of Philosophy), National University of Singapore. Retrieved from http://scholarbank.nus.edu.sg/handle/10635/13784

Church, J. A., & White, N. J. (2006). A 20th century acceleration in global sea-level rise. *Geophysical Research Letters, 33*(1), L01602. doi: 10.1029/2005gl024826

Cooper, J. A. G., & Pilkey, O. H. (2004). Sea-level rise and shoreline retreat: time to abandon the Bruun Rule. *Global and Planetary Change, 43*(3–4), 157-171. doi: http://dx.doi.org/10.1016/j.gloplacha.2004.07.001

Daly, C. J., Bryan, K. R., Roelvink, J. A., Klein, A. H. F., Hebbeln, D., & Winter, C. (2011). *Morphodynamics of embayed beaches: The effect of wave conditions.* Paper presented at

the Journal of Coastal Research, SI 64 (Proceedings of the 11th International Coastal Symposium).

Dean, R. G. (1973). *Heuristic Models of Sand Transport in the Surf Zone*. Paper presented at the First Australian Conference on Coastal Engineering, 1973: Engineering Dynamics of the Coastal Zone., Sydney, N.S.W.: Institution of Engineers, Australia, 1973. http://books.google.nl/books?id=DqPfGwAACAAJ

Dean, R. G. (1987). *Coastal sediment processes: Toward engineering solutions.* Paper presented at the Proceedings of Coastal Sediments '87.

Department of Statistics, M. o. T. I. (2012). Yearbook of Statistics Singapore (pp. 320).

Gonzalez, M., Medina, R., & Losada, M. (2010). On the design of beach nourishment projects using static equilibrium concepts: Application to the Spanish coast. *Coastal Engineering, 57*(2), 227-240. doi: 10.1016/j.coastaleng.2009.10.009

Gupta, A. (2005). *The Physical Geography of Southeast Asia*: OUP Oxford.

Hallermeier, R. J. (1980). A profile zonation for seasonal sand beaches from wave climate. *Coastal Engineering, 4*(0), 253-277. doi: http://dx.doi.org/10.1016/0378-3839(80)90022-8

Hallermeier, R. J. (1983). *Sand Transport Limits in Coastal Structure Designs*: USA, Army. Coastal Engin. Res. Center.

Hilton, M. J., & Manning, S. S. (1995). Conversion of Coastal Habitats in Singapore: Indications of Unsustainable Development. *Environmental Conservation, 22*(04), 307-322. doi: doi:10.1017/S0376892900034883

Holthuijsen, L. H. (2007). *Waves in Oceanic And Coastal Waters*: Cambridge University Press.

Hsu, J., Silvester, R., & Xia, Y. (1989). Applications of Headland Control. *Journal of Waterway, Port, Coastal, and Ocean Engineering, 115*(3), 299-310. doi: doi:10.1061/(ASCE)0733-950X(1989)115:3(299)

Hsu, J. R. C., & Evans, C. (1989). Parabolic bay shapes and applications. *ICE Proceedings, 87*, 557-570. http://www.icevirtuallibrary.com/content/article/10.1680/iicep.1989.3778

Hsu, J. R. C., Yu, M. J., Lee, F. C., & Benedet, L. (2010). Static bay beach concept for scientists and engineers: A review. *Coastal Engineering, 57*(2), 76-91. doi: http://dx.doi.org/10.1016/j.coastaleng.2009.09.004

Ibad-Zade, Y. A. (1987). Movement of sediments in open channels. 364.

IPCC. (2007). Climate Change 2007: Synthesis Report. Contribution of Working Groups I, II and III to the Fourth Assessment Report of the Intergovernmental Panel on Climate Change (pp. 104). Geneva, Switzerland.

Katoh, K., & Yanagishima, S.-i. (1992). *Berm formation and berm erosion*.

Kirkegaard, J., Kofoed-Hansen, H., & Elfrink, B. (1998). *Wake wash of high-speed craft in coastal areas*.

Klein, A. H. F., Ferreira, Ó., Dias, J. M. A., Tessler, M. G., Silveira, L. F., Benedet, L., . . . De Abreu, J. G. N. (2010). Morphodynamics of structurally controlled headland-bay beaches in southeastern Brazil: A review. *Coastal Engineering, 57*(2), 98-111. doi: http://dx.doi.org/10.1016/j.coastaleng.2009.09.006

Knight Frank Research. (2012). The Wealth Report 2012 - A Global Perspective on Prime Property and Wealth.

Leuliette, E. W., Nerem, R. S., & Mitchum, G. T. (2004). Calibration of TOPEX/Poseidon and Jason Altimeter Data to Construct a Continuous Record of Mean Sea Level Change. *Marine Geodesy, 27*(1), 79. doi: 10.1080/01490410490465193

Maritime Navigation Commission. (2003). *Guidelines for managing wake wash from high-speed vessels: report of Working Group 41 of the Maritime Navigation Commission*: International Navigation Association, PIANC.

Masselink, G. A., & Hughes, M. G. A. (2003). *An Introduction to Coastal Processes and Geomorphology*: Arnold.

Moore, B. D. (1982). *Beach profile evolution in response to changes in water level and wave height*. Unpublished M.S. thesis. University of Delaware, Newark, DE.

Muñóz-Pérez, J. J., Tejedor, L., & Medina, R. (1999). Equilibrium beach profile model for reef-protected beaches. *Journal of Coastal Research, 15*(4), 950-957.

NCCS. (2008). Singapore National Climate Change Strategy.

NCCS. (2012). Singapore National Climate Change Strategy.

Ojeda, E., & Guillén, J. (2008). Shoreline dynamics and beach rotation of artificial embayed beaches. *Marine Geology, 253*(1–2), 51-62. doi: http://dx.doi.org/10.1016/j.margeo.2008.03.010

Ooi, S. K., Sisomphon, P., Kurniawan, A., & Gerritsen., H. (2011). *Modelling of Sea Level and Current Anomalies in the Singapore Region*. Paper presented at the Proceedings of the 34th World Congress of the International Association for Hydro- Environment Research and Engineering: 33rd Hydrology and Water Resources Symposium and 10th Conference on Hydraulics in Water Engineering, Brisbane, Australia.

Pilkey, O. H., Young, R. S., Riggs, S. R., Smight, A. W. S., Wu, H., & Pilkey, W. D. (1993). The concept of shoreface profile of equilibrium: A critical review. *Journal of Coastal Research, 9*(1), 255-278.

Qu, X., Meng, Q., & Suyi, L. (2011). Ship collision risk assessment for the Singapore Strait. *Accident Analysis & Prevention, 43*(6), 2030-2036. doi: http://dx.doi.org/10.1016/j.aap.2011.05.022

Raju, D. K., Santosh, K., Chandrasekar, J., & Tiong-Sa, T. (2010). *Coastline change measurement and generating risk map for the coast using geographic information system.* Paper presented at the Joint International Conference on Theory, Data Handling and Modelling in GeoSpatial Information Science, Hong Kong.

Schiereck, G. J. (2004). *Introduction to bed, bank and shore Protection*. Delft, The Netherlands: VSSD.

Schroevers, M., Huisman, B. J. A., Van der Wal, M., & Terwindt, J. (2011, 20-23 March 2011). *Measuring ship induced waves and currents on a tidal flat in the Western Scheldt estuary.* Paper presented at the Current, Waves and Turbulence Measurements (CWTM), 2011 IEEE/OES 10th.

Schwartz, M. (2005). *Encyclopedia of Coastal Science*: Springer.

Shields, A. (1936). Anwendung der Ähnlichkeitsmechanik und der Turbulenzforschung auf die Geschiebebewegung. *Mitteilung der Preussischen Versuchsanstalt fur Wasserbau und Schiffbau, Heft 26, Berlin*, 26.

Silvester, R. (1960). Stabilization of sedimentary coastlines. *Nature, 188*(4749), 467-469. doi: 10.1038/188467a0

Silvester, R., & Ho, S. K. (1972). *Use of crenulate shaped bays to stabilize coasts*.

Silvester, R., & Hsu, J. R. C. (1993). *Coastal stabilization: innovative concepts*: PTR Prentice Hall.

Silvester, R., & Hsu, J. R. C. (1997). *Coastal Stabilization*: World Scientific.

Silvester, R., Tsuchiya, Y., & Shibano, Y. (1980). *Zeta bays, pocket beaches and headland control.* Paper presented at the Proc. 17th Int. Conf. Coastal Eng., Sydney, N.S.W.

Tan, S. K., Goh, K. W., & Wang, Z. (2007). Engineering study on the proposed restoration of shoreline along East Coast Park and Pasir Ris Park (pp. 148).

Tay, S. H. X. (2010). *Typhoon-induced extreme water levels near Singapore: a numerical model investigation.* (MSc Master thesis), Delft University of Technology. Retrieved from http://repository.tudelft.nl/view/ir/uuid%3A3ae5ad50-c75e-4a60-a2dc-19970acfa0bc/

Torsvik, T., & Soomere, T. (2008). Simulation of patterns of wakes from high-speed ferries in Tallinn Bay. *Estonian Journal of Engineering, 14*(3), 232-254. doi: 10.3176/eng.2008.3.04

Turki, I., Medina, R., Gonzalez, M., & Coco, G. (2012). Natural variability of shoreline position: Observations at three pocket beaches. *Marine Geology*(0). doi: http://dx.doi.org/10.1016/j.margeo.2012.10.007

Valdemoro, H. I., & Jiménez, J. A. (2006). The influence of shoreline dynamics on the use and exploitation of Mediterranean tourist beaches. *Coastal Management, 34*(4), 405-423. doi: 10.1080/08920750600860324

Van Ieperen, H. J. (1987). The fall velocity of grain particles (Vol. 83, pp. 17): Department of Hydraulics and Catchment Hydrology, Agricultural University Wageningen.

Van Maren, D. S., & Gerritsen, H. (2012). Residual flow and tidal asymmetry in the Singapore Strait, with implications for resuspension and residual transport of sediment. *Journal of Geophysical Research: Oceans, 117*(C4), C04021. doi: 10.1029/2011jc007615

Van Rijn, L. C. (1990). *Sediment transport by currents and waves* (2nd ed. ed.). Delft, The Netherlands: Delft Hydraulics.

Vanoni, V. A. (1975). *Sedimentation Engineering*. New York: ASCE.

Wang, Z., Tan, S. K., & Cheng, N. (2009). Design of Headland Control, Beach Protection Scheme *Advances in Water Resources and Hydraulic Engineering* (pp. 1299-1304): Springer Berlin Heidelberg.

Waterman, R. E. (2010). *Integrated coastal policy via Building with Nature.* (PhD Dissertation), Delft University of Technology, the Netherlands. Retrieved from http://repository.tudelft.nl/view/ir/uuid%3Afa9a36f9-7cf8-4893-b0fd-5e5f15492640/

Wong, P. P. (1973). Beach formation between breakwaters, southeast coast, Singapore. *Journal of Tropical Geography, 37*, 68-73.

Wong, P. P. (1985). Artificial coastlines: the example of Singapore. *Zeitschrift für Geomorphologie, 57*, 175-192.

Wong, P. P. (1992). Impact of a sea level rise on the coasts of Singapore: preliminary observations. *Journal of Southeast Asian Earth Sciences, 7*(1), 65-70. doi: http://dx.doi.org/10.1016/0743-9547(92)90016-5

Wright, L. D., & Short, A. D. (1984). Morphodynamic Variability of Surf Zones and Beaches - A Synthesis. *Marine Geology, 56*(1-4), 93-118. doi: 10.1016/0025-3227(84)90008-2

A Wave characteristics

During this study recent wave data has not been readily available. Therefore, wave characteristics used throughout this analysis are based on a paper published by Chew et al. (1974), dating several decades ago, see also Figure A.1 below. From these data an overview is created which is used in numerical calculations. This overview is presented below in Table A.1.

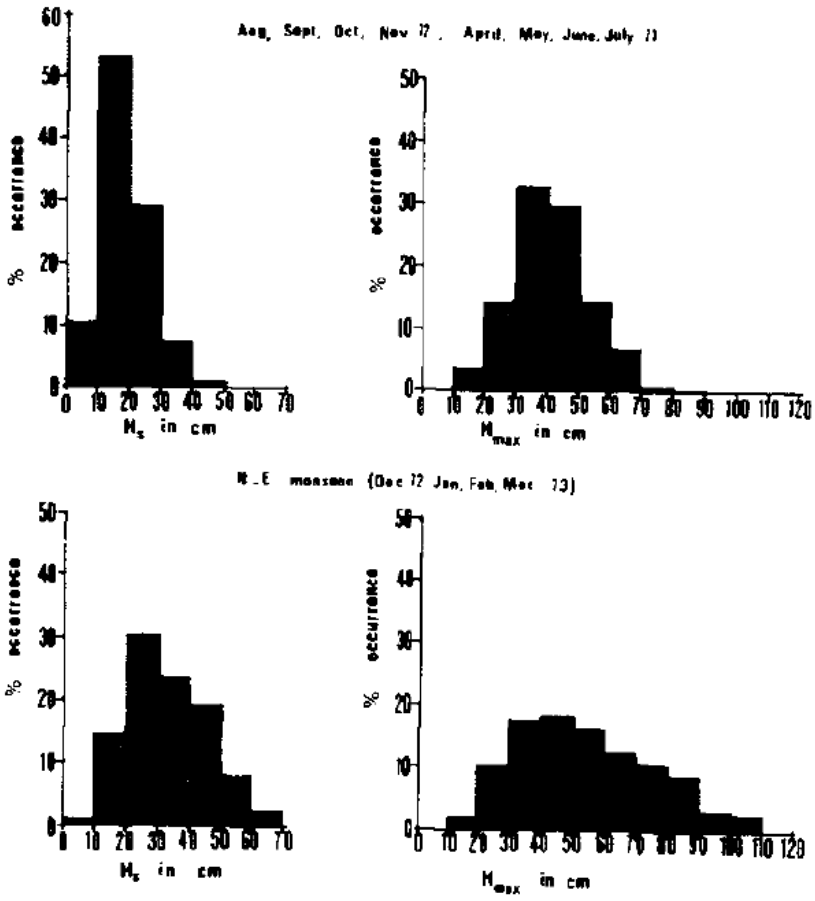

Figure A.1 Frequency distribution of significant wave height Hs and maximum wave height Hmax during the S.W. monsoon (upper graphs) and N.E. monsoon (lower graphs). From Chew et al. (1974).

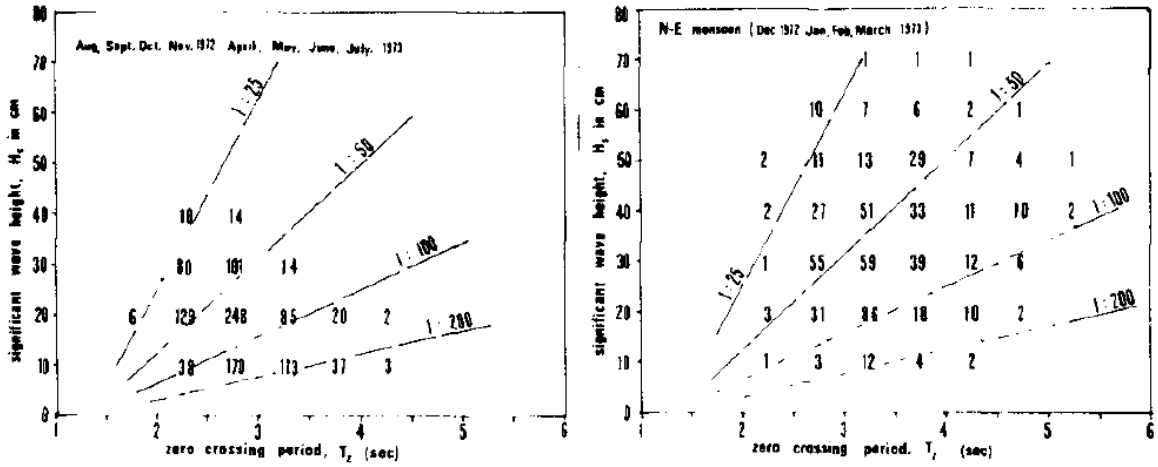

Figure A.2 Scatter plot of significant wave height Hs vs zero-crossing wave period Tz for the S.W. monsoon (left panel) and the N.E. monsoon (right panel). From Chew et al. (1974).

During the Unibest-LT calculations some numerical instabilities were observed, which seemed to be caused by the smallest wave heights and periods. For that reason, the smallest wave heights had been excluded in further calculations, and the wave period of 3.16 s had been adapted to 4 s.

The root mean square wave height H_{rms} is calculated through

$$H_{rms} = 0.5\sqrt{2} \cdot H_s \qquad A.1$$

Table A.1 Wave climate characteristics along East Coast Park, retrieved and adapted from Chew et al. (1974)

ORIGINAL WAVE CLIMATE								
wave characteristics			occurrence in days				occurrence in %	
			original		scaled to 1 year			
Hs [m]	Hrms [m]	T [s]	NE	SW	NE	SW	NE	SW
0.07	0.05	2.16	2.43	24.33	7.29	36.50	2	10
0.15	0.11	3.16	18.25	124.1	54.75	186.15	15	51
0.25	0.18	4.08	36.5	70.57	109.51	105.86	30	29
0.35	0.25	4.83	29.2	17.03	87.60	25.55	24	7
0.45	0.32	5.47	21.9	6.08	65.70	9.12	18	2.5
0.55	0.39	6.05	9.73		29.19		8	0
0.65	0.46	6.58	3.65	1.22	10.95	1.83	3	0.5
		total	121.66	243.33	365.00	365.00	100	100
		years	0.33	0.67	1.00	1.00		
ADAPTED WAVE CLIMATE								
wave characteristics			occurrence in days				occurrence in %	
			original		scaled to 1 year			
Hs [m]	Hrms [m]	T [s]	NE	SW	NE	SW	NE	SW
0.15	0.11	3.16	18.25	124.1	55.87	206.83	15.31	56.67
0.25	0.18	4.08	36.5	70.57	111.74	117.62	30.61	32.22
0.35	0.25	4.83	29.2	17.03	89.39	28.38	24.49	7.78
0.45	0.32	5.47	21.9	6.08	67.04	10.13	18.37	2.78
0.55	0.39	6.05	9.73		29.79		8.16	0
0.65	0.46	6.58	3.65	1.22	11.17	2.03	3.06	0.56
		total	119.23	219	365.00	365.00	100	100
		years	0.33	0.60	1.00	1.00		

B Coastal cell and structure characteristics

For one of the methods used to classify the coastal cells and their enclosing headlands some specific parameters of both cells and structures were identified. In this way, an overview could be created and patterns were ought to be found based on cell-structure relations. The results of this analysis are presented below. All graphs result from Table B.1, which are values measured manually using Google Earth for the satellite images of 06-08-2009. Anomalies should for this reason be neglected.

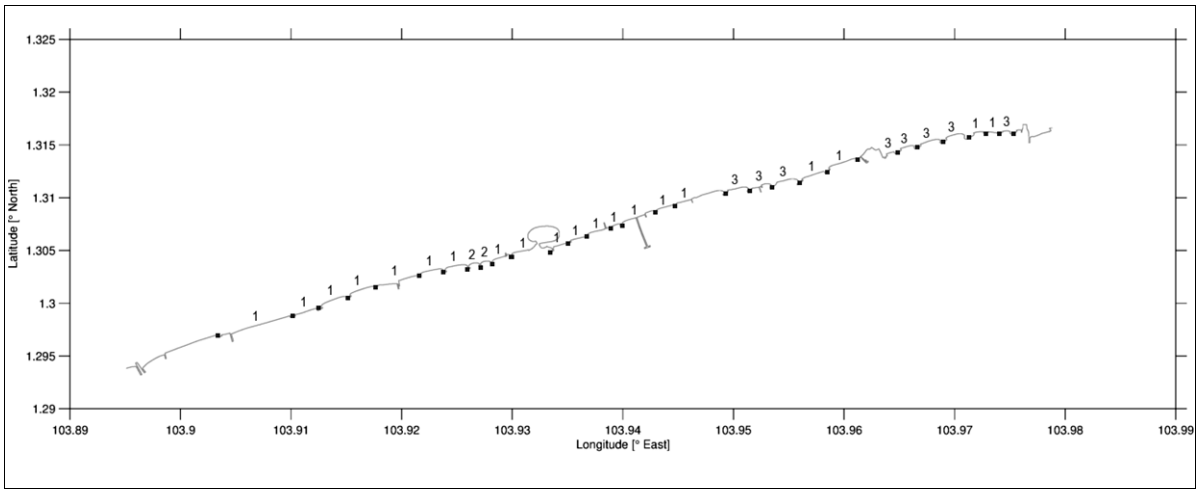

Figure B.1 Coastal cell types along East Coast Park, Singapore. Headlands are indicated with black cubes, and the enclosed cells are classified according to their type, namely straight beaches (1), pocket beaches (2) or J-shaped beaches (3)

In Figure B.2 below some characteristic parameters of coastal cells and structure types are illustrated.

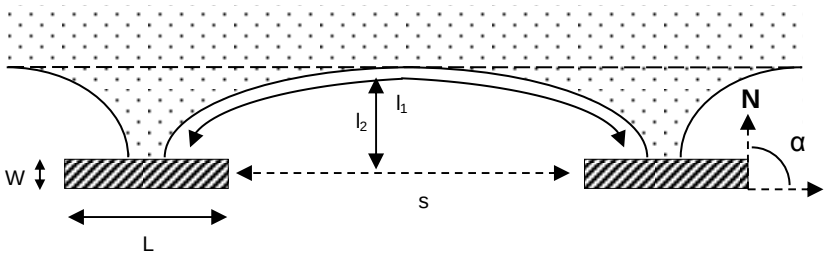

Figure B.2 Characteristic parameters for coastal cells and their enclosing structures. W is the structure width, L is the structure length, S is the spacing in between the structures, l_1 is the length along the beach line, l_2 is the distance from the control line of the structures (defined by S) to the (average) coastline, α is the orientation angle with respect to the Nautical North.

B.1 Structure characteristics

Regarding structures, the main parameters that have been analysed are length, width and orientation. These data have been plotted below, starting with headland 1 in the west and ending with headland 31 in the east. From these data it is obvious that dimensions vary considerably, but when looking at the lengths it seems that a couple segments can be considered. There is a large range of headlands with lengths around 30 m, and a large range ranging from 60 to 80 m. The larger lengths of more eastward located headlands can be explained due to the fact that the length is measured along the crest of the headland and headlands 25 to 31 have a considerable curvature. Also the widths of these headlands are substantially larger.

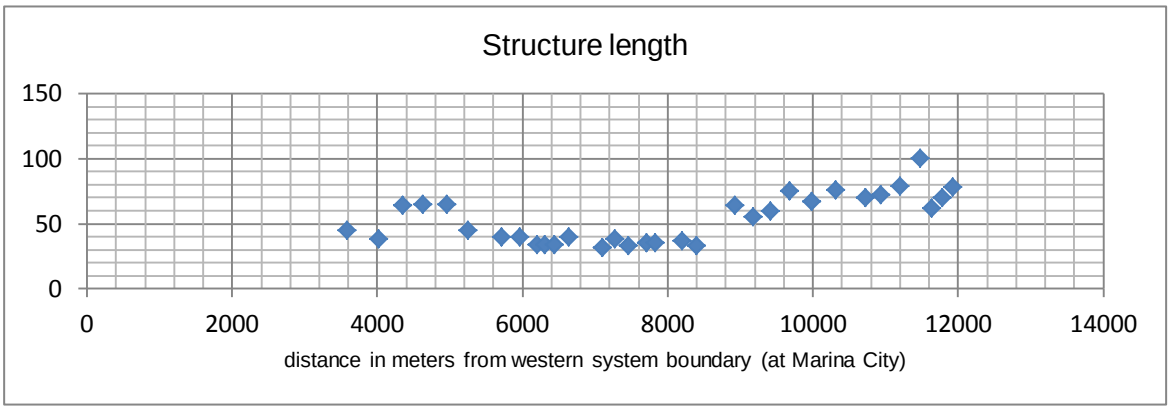

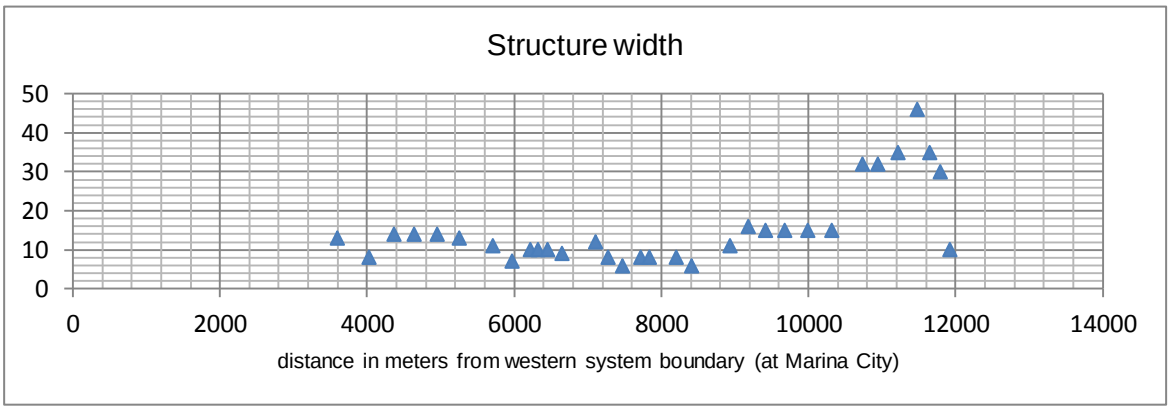

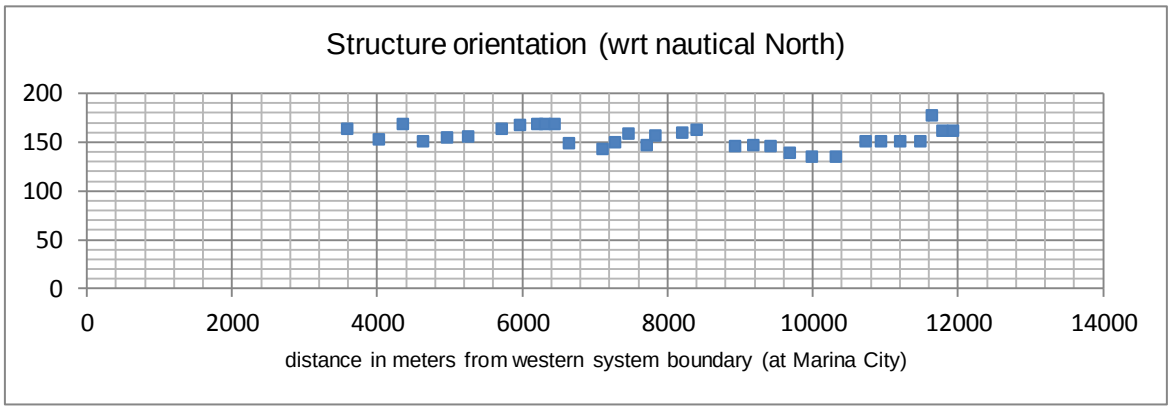

Looking at the orientation of the structures, a clear pattern again is found for headlands 19 to 24, which seem to share almost the same orientation. More towards the west the orientations change more significantly.

B.2 Coastal cell characteristics

Regarding coastal cells, the three analysed parameters are the indent ratio of the cell, which is basically the ratio between the beach perimeter and the length of the control line of (spacing between) the structures, the orientation of the coastal cell, which is based on the straight or middle sections of the cell, and the type of cell.

The cell types are defined as follows:

1 straight beach
2 pocket beach
3 J-shaped beach

The orientation of the cells seems to be more or less in accordance with the orientation of the structures. Note that these orientations are based on one date, and that orientations might change over the year. The indent ratio and the cell type are more or less related, where coastal cells with indent ratios larger than 1 or 1.1 are generally found to be pocket beaches or asymmetric, or of the type 2 and 3, respectively (see the legend in Table B.1). The larger part of the coastal cells consists of straight beaches, although quite some asymmetric and pocket beaches are found. What is obvious is that these deviating cells are typically adjacent to each other.

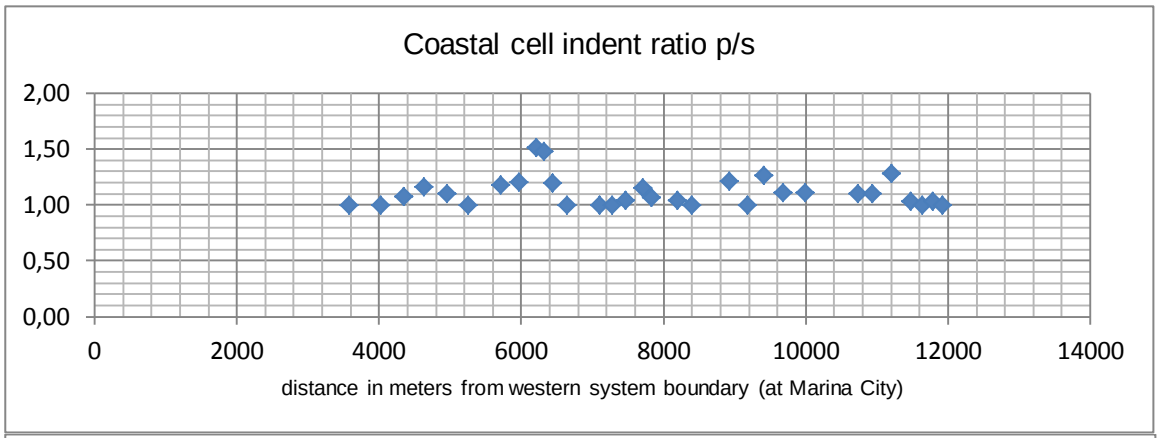

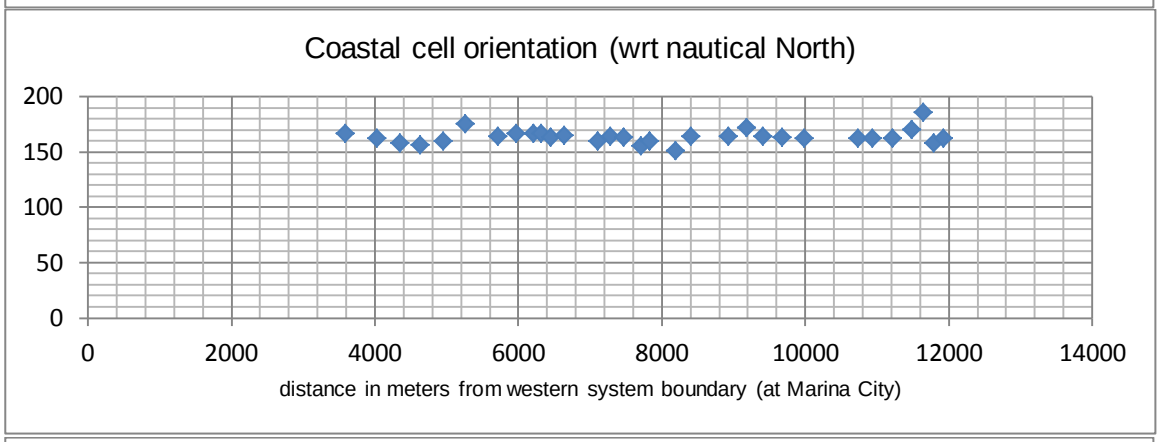

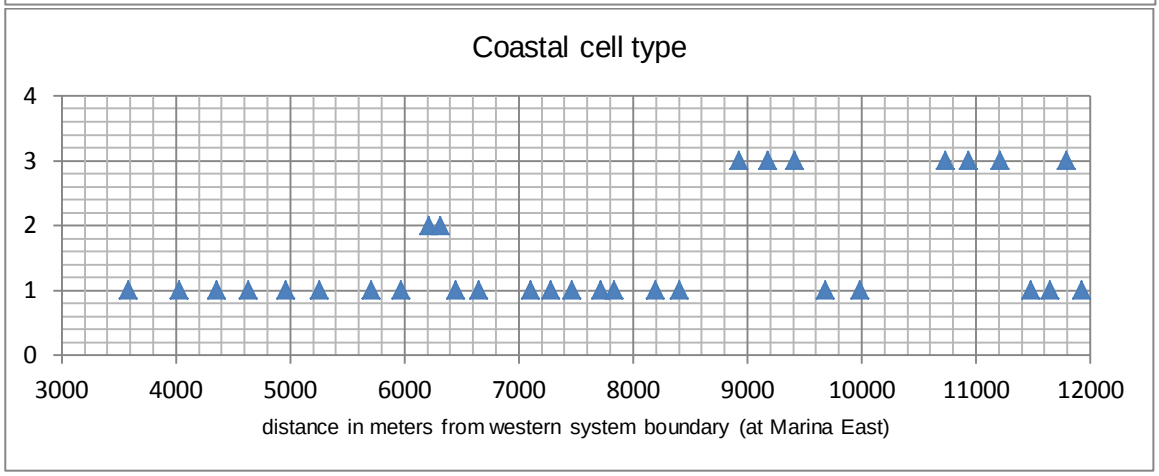

See also Figure B.1.

B.3 Overview

See Table B.1 on the next page.

Table B.1 An overview of characteristic parameters for structures and coastal cells along East Coast Park

Structure characteristics							Coastal cell characteristics								
									enclosing struct. #						
X-value to center structure [m]	struct #	headland	type	length [m]	width [m]	orientation [in ° wrt nautical North]	X-value to begin cell [m]	cell #	west	east	spacing s (tip-to-tip) [m]	berm peri-meter p [m]	ratio p/s	orientation [°]	type
3590	14	HL1	pbw	45	13	163	3620	8	14	15	86	86	1.00	167	1
4030	16	HL2	pbw	38	8	152	4050	10	16	17	288	288	1.00	162	1
4360	17	HL2'	pbw	64	14	168	4390	11	17	18	225	242	1.08	158	3
4640	18	HL3	pbw	65	14	150	4645	12	18	19	246	286	1.16	156	2
4960	19	HL4	pbw	65	14	154	4970	13	19	20	243	268	1.10	160	2
5260	20	HL5	pbw	45	13	155	5270	14	20	21	196	196	1.00	175	1
5715	22	HL6	pbw	40	11	163	5730	16	22	23	210	247	1.18	164	2
5970	23	HL7	pbw	40	7	167	5975	17	23	24	204	245	1.20	167	2
6215	24	HL8	pbw	34	10	168	6220	18	24	25	88	133	1.51	167	2
6320	25	HL9	pbw	34	10	168	6325	19	25	26	85	126	1.48	167	2
6450	26	HL10	pbw	34	10	168	6455	20	26	27	134	160	1.19	163	1
6650	28	HL11	pbw	40	9	148	6660	22	28	30	75	75	1.00	165	1
7110	33	HL12	pbw	32	12	142	7110	24	33	34	155	155	1.00	160	1
7280	34	HL13	pbw	38	8	149	7285	25	34	35	152	152	1.00	164	1
7470	35	HL14	pbw	33	6	158	7475	26	35	36	202	210	1.04	163	1
7720	37	HL15	pbw	35	8	146	7730	28	37	38	93	107	1.15	155	1
7835	38	HL16	pbw	35	8	156	7845	29	38	39	151	161	1.07	160	1
8200	40	HL17	pbw	37	8	159	8205	31	40	41	187	194	1.04	151	1
8410	41	HL18	pbw	33	6	162	8415	32	41	42	165	165	1.00	164	1
8930	45	HL19	pbw	64	11	145	8940	34	45	46	190	230	1.21	164	3

9180	46	HL20	pbw	55	16	146	9190	35	46	48	105	105	1.00	172	1
9420	49	HL21	pbw	60	15	145	9430	37	49	50	210	265	1.26	164	3
9685	50	HL22	pbw	75	15	139	9695	38	50	51	235	260	1.11	163	1
9990	51	HL23	pbw	67	15	135	10000	39	51	52	275	305	1.11	162	1
10320	52	HL24	pbw	76	15	135									
10735	57	HL25	pbw	70	32	150	10770	42	57	59	134	148	1.10	162	3
10940	59	HL26	pbw	72	32	150	10970	43	59	60	195	215	1.10	162	3
11215	60	HL27	pbw	79	35	150	11240	44	60	61	165	212	1.28	162	3
11485	61	HL28	pbw	100	46	150	11520	45	61	62	115	119	1.03	170	1
11650	62	HL29	pbw	62	35	177	11660	46	62	63	97	97	1.00	186	1
11790	63	HL30	pbw	70	30	161	11800	47	63	64	99	102	1.03	158	3
11930	64	HL31	pbw	78	10	161	11935	48	64	65	72	72	1.00	162	1

Legend

Breakwater types:

pbw = parallel breakwater - attached

Coastal cell types:

1 = straight (uninterrupted) coastline

2 = pocket beach (symmetric)

3 = J-shaped beach (asymmetric)

Remarks

1 The x-value to the center of the structures or the begin (western boundary) of the coastal cells is a mere indicator used in the analysis to roughly measure locations from a chosen reference point, in this case the westernmost coastal tip of Marina East. All measurements are made using Google Earth;

2 Structure lengths are measured along the crest, also taking the submerged toes into account where visible;

3 Dimensions and orientations might vary along a structure or beach cell in reality. In this case only those dimensions and orientations have been noted that seem of relevance to the littoral drift and the incoming waves;

4 The marked values indicate non-breakwater structures, enclosing the particular beach (e.g. drains, jetties)

C Fieldwork

C.1 Introduction

The fieldwork was to be performed in order to obtain accurate sediment parameters, most importantly grain size diameter values (D_{50}), because of no readily available information on present-day sediment parameters. Simultaneously, visual observations would be made of the coastline along East Coast Park, in order to clarify certain knowledge gaps as much as possible. The results of this fieldwork are presented below, starting with the set-up and results of the sediment sampling.

To make the collection of sediment samples feasible, considering the restricted time available, a specific area of interest was chosen, namely the coastal cells enclosed by headlands 8, 9 and 10, see also Figure C.1. The reason for this choice was related to the fact that these cells seemed most interesting as a study case for the BwN design pilot. The results of the samples would serve as an indication for sediment present along all of East Coast Park, assuming similar fill material is used everywhere. Due to the fact that these structures are very closely located, in comparison with other headlands along East Coast Park, this location seemed like an interesting study case for the Building with Nature design pilot. In this way, questions resulting from knowledge gaps on sediment characteristics could be answered.

Namely,

1. What is the present-day alongshore variation of sediment grain size?
2. What is the present-day cross-shore variation of sediment grain size?
3. Where along the beach profile does the transition from sand to the clay substratum occur?
4. At this transition, does sand encroach the clay layer or vice versa?
5. Can the distribution of sediment in cross-shore direction directly be related to the water level variation due to the tide?

Question 4 results from the fact that the type of encroachment might say something about the morphological processes occurring along the profile. In case of sand encroaching the clay layer, cross-shore processes seem more likely to be dominant, while if the clay would encroach the sand, longshore processes seem more likely to be dominant.

Another reason for the sediment analysis resulted from the fact that preliminary calculations were made using numerical models, in which grain sizes of 200 µm and 600 µm were used. In literature, however, mention was made of grain sizes larger than 1000 µm. To be able to perform proper sediment transport or profile development calculations, accurate input data is necessary. The results from this analysis therefore also serve as a basis for future research.

C.2 Sediment sampling

C.2.1 Setup

The first step in the fieldwork was choosing an adequate date, which was dependent on the tide. As sediment samples were planned to be taken just offshore of the headlands as well, Low Water Spring was preferred in order not to be obstructed by high water levels. Tide times were retrieved from the website of the National Environmental Agency of Singapore (http://app2.nea.gov.sg/tidetime.aspx) and the 12th, 13th and 14th of December 2012 had the lowest expected water levels, of CD + 0.3 m, CD + 0.2 m and CD + 0.1 m respectively. Thursday 13 December 2012 was chosen as the day sediment samples would be collected.

Considering the fact that only surface sediment was to be collected, the material used for collection consisted of a hand corer sampler and a plastic tube from a sediment corer. The hand corer sampler was used to collect samples above the waterline, whereas the tube was used to collect samples below the waterline. A GPS tracker was used to mark the collection locations, and plastic Ziploc bags were used to store the samples.

The idea was to take several samples along 5 profiles, of which 3 transects through the headlands and 2 transects through the centre of the enclosed beaches. Each of the collections would be located at a regular interval, with at least one location seaward of the structures in every profile. In this way a total of 17 samples would be collected. The idea was illustrated according to Figure C.1.

Figure C.1 Suggestive cross-shore locations of sediment samples to be collected within the beach cells enclosed by headlands 8, 9 and 10

C.2.2 Data collection and analysis

Collection

After discussing the previously suggested locations for sediment sampling with experts from the Tropical Marine Science Institute (TMSI), they proposed for the rays crossing the center of both beach cells to take the first three samples along the steep beach slope, where the variety in sediment distribution is largest, and to take one sample offshore as suggested in

Figure C.1. This idea is depicted by the profiles TMSI 42 and TMSI 44 in Figure C.2. The profile numbers refer to profiles as used by the TMSI for their own surveys.

In this way, along the transects crossing the headlands two samples were taken in the lee of the structure, at the high and low water marks, and one sample just seaward of the structure. Along the transects crossing the centre of the beaches three samples were taken on the beach face, consecutively at or above the high water mark, at mid-range and at the low water mark. The last sample was taken seaward of the waterline, at a location parallel to the other seaward locations.

Figure C.2 Sediment samples collected on 13 December 2012, at and in between headland numbers 8, 9 and 10 (from left to right). The green lines indicate the profiles or transects that are used by researchers from the Tropical Marine Science Institute (TMSI) for regular profile measurements. The red dots indicate the locations of the sediment samples collected on this date, and their corresponding numbering. The figure is illustrative and the exact locations might deviate slightly.

During execution of the fieldwork we noticed that the intended lowest points behind the headlands were not located along the profiles intersecting the headlands, as expected from Figure C.1, but more towards the sides, as can be seen by location numbers 41-2, 43-2 and 45-2 in Figure C.2. The lines connecting sample locations 41-1, 43-1 and 45-1 with the corresponding headlands were nearly horizontal and thus equal to the high water mark, and sediment characteristics along this line seemed to be similar. A possible reason for this could be that this area has recently been nourished. Therefore it was chosen to take samples 41-2, 43-2 and 45-2 a bit to the side, roughly at the low water line behind the headlands.

In the end a total of 16 surface sediment samples have been collected, leaving out one sample seaward of headland 8. The reason for this was related to the difficulty of the execution. All underwater samples were taken by hand, using only a sediment tube. As the soil became more muddy in offshore direction, it made walking without getting stuck in the mud incredibly difficult. But from the collection of samples 42-4, 43-3, 44-4 and 45-3 already sufficient insight was obtained in the sediment distribution.

Analysis

The analysis of the collected sediment samples was performed by Setsco Services Pte Ltd [xvi] in Singapore. The determination of particle size distribution is done through a standard sieving method. The method basically consists of a series of steps, consecutively:

(1) Drying of the sediment specimen at 105 ± 5 °C until a constant mass is reached (within 0.1%), after which it is cooled and weighed (M1);
(2) placing the specimen in a container, which is then filled up with water until half full, after which the contents are agitated and the suspension of fine solids poured onto a guarded 63 µm sieve with a 1.18 mm sieve nesting on top of it;
(3) washing of the coarse residue until water passing through the sieve is clear. All residues from the container and sieves are washed into the tray;
(4) The specimen is again oven dried at 105 ± 5 °C until a constant mass is reached, cooled and weighed (M2);
(5) Then the clean and dry sieves are nested on a fitting receiver in order of increasing aperture size, from bottom to top, and the dry sediment specimen is placed on top of the coarse sieve, after which the distribution of particles can be obtained.

The methods used by Setsco Services Pte Ltd follow the standards described by the American Society for Testing and Materials (ASTM) and the British Standards Institution (BSI).

C.2.3 Results

The results of the analysis are found in Table C.1 and Figure C.3. The particle sizes D_{50} and D_{90} have been determined from the results provided by Setsco Services Pte Ltd.

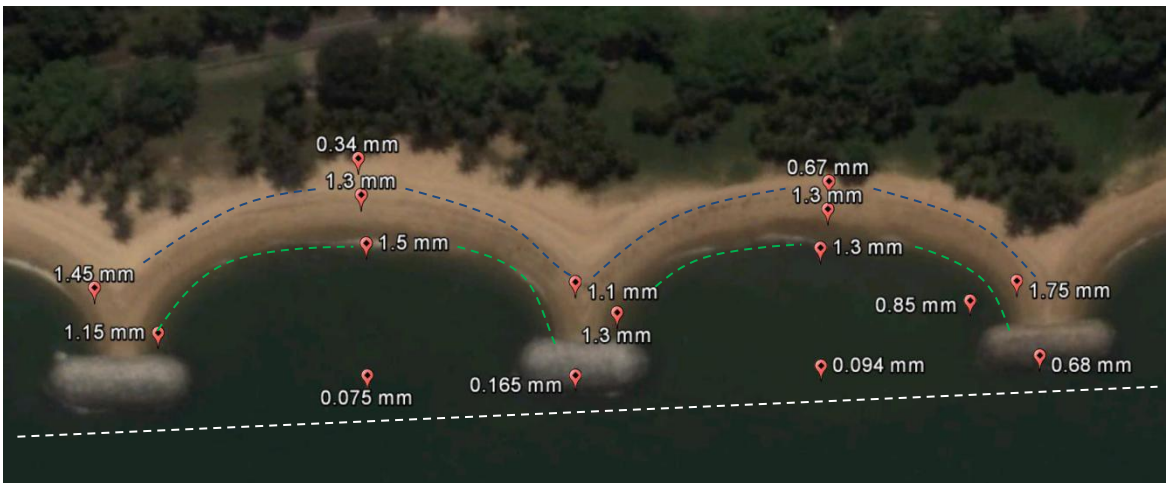

Figure C.3 Mean sediment grain sizes (D_{50}) and the locations where sediment samples were collected in between headlands 8, 9 and 10 at East Coast Park, on 13 December 2012 during Low Water Spring tide. The blue dashed line indicates the high water line, the green dashed line indicates the low water line, and the white dashed line indicates the upper shoreface. In the centre of the coastal cells, samples were also collected at mid-tide. Indicated locations might deviate from exact locations.

[xvi] *http://www.setsco.com*

Table C.1 Sediment characteristics resulting from sediment analysis performed by Setsco, Singapore. Samples were collected on 13 December 2012, during Low Water Spring.

Sample #	[mg/m^3]		Grain size analysis (%)				Particle size distribution [mm]				[-]		Particle size [mm]	
	Bulk density	Particle density	Gravel	Sand	Silt	Clay	D_{60}	D_{30}	D_{10}	D_{MAX}	C_U	C_C	D_{50}	D_{90}
041-1	1.98	2.66	31	65	2	2	1.7	0.89	0.47	4.76	4	1	1.45	3.5
041-2	1.95	2.66	17	77	3	3	1.4	0.82	0.55	6.73	3	1	1.15	2.7
042-1	1.89	2.68	4	91	3	2	0.4	0.25	0.13	6.73	3	1	0.34	0.7
042-2	1.92	2.67	29	67	1	3	1.7	0.83	0.13	6.73	13	3	1.3	3.7
042-3	1.92	2.66	28	69	1	2	1.7	1	0.64	4.76	3	1	1.5	3.5
042-4	1.81	2.64	1	55	27	17	0.12	0.012	-	2	-	-	0.075	0.21
043-1	2	2.65	18	78	1	3	1.3	0.75	0.38	4.76	3	1	1.1	2.65
043-2	1.91	2.66	25	66	5	4	1.6	0.66	0.072	4.76	22	4	1.3	3
043-3	1.96	2.63	2	81	7	10	0.18	0.094	0.0028	4.76	64	18	0.165	0.25
044-1	1.93	2.68	13	83	1	3	0.84	0.47	0.18	4.76	5	1	0.67	2.35
044-2	1.95	2.66	20	76	1	3	1.6	0.9	0.56	4.76	3	1	1.3	2.9
044-3	1.96	2.67	16	79	2	3	1.5	0.91	0.61	4.76	2	1	1.3	2.5
044-4	1.99	2.61	4	66	18	12	0.13	0.064	-	3.36	-	-	0.094	0.215
045-1	1.91	2.64	39	58	1	2	2.1	1.3	0.54	4.76	4	1	1.75	3.4
045-2	1.94	2.63	25	54	8	13	1.4	0.27	-	4.76	-	-	0.85	3.5
045-3	1.9	2.65	23	64	6	7	1.1	0.28	0.017	4.76	65	4	0.68	3

D Cross-shore profiles HL8, HL9 & HL10

For insight in the cross-shore profile development along East Coast Park, some cross-shore profiles were provided by the Tropical Marine Science Institute (TMSI) in Singapore. Researchers at the TMSI have studied the shoreline of East Coast Park for more than a decade, and only since 2011 have they started to measure cross-shore profiles along the coast with more spatial resolution. Continuing from the chosen area of interest, enclosed by headlands 8, 9 and 10, profile measurements for 2011 – 2012 (4 times a year with an interval of about 3 months) were provided for 5 profiles coinciding with the profiles used as described in Appendix C, of which the figure is repeated below. The profile measurements do not fully coincide with the lengths of the rays in figure below, but start from a bench mark to either the low water line within the beach cells or to the structures behind the headlands. These profiles have been provided below to substantiate the study in a most complete manner.

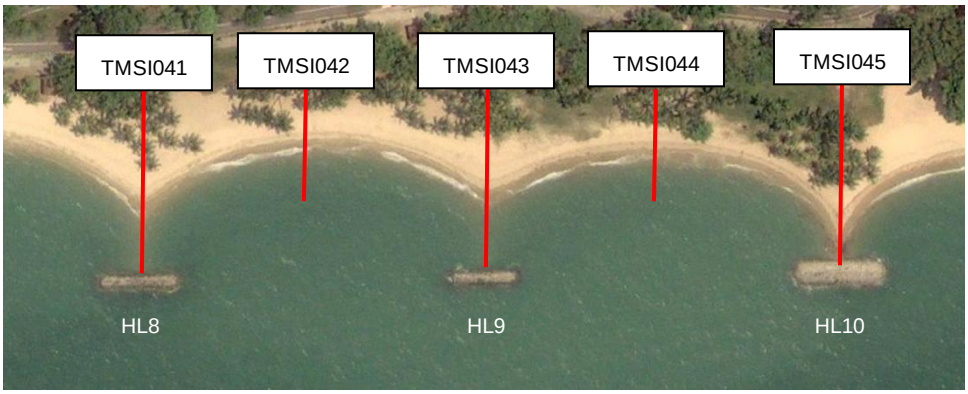

Figure D.1 Rays of cross-shore profiles along which measurements have been performed by the TMSI. Locations are approximate, going from a landward benchmark to either the structure or the low water line.

D.1 Profiles TMSI

Profile TMSI 041

TMSI 041 is the profile that transects headland 8, see Figure C.2. For this profile only 7 measurements have been executed, excluding the 9th of September 2011, due to ongoing renovations at that time at headland 8.

Looking at the consecutive periods, TMSI had distinguished several periods of accretion and erosion, where the calculated monthly rate of change (RoC) was defined according to the horizontal displacement of the profile:

- high retreat: RoC < -0.5 m
- low retreat: -0.5 m < RoC < -0.05 m
- no change: -0.05 m < RoC < +0.05 m
- low advance: +0.05 m < RoC < +0.5 m
- high advance: RoC > +0.5 m

In this way the following periods were distinguished for profile TMSI 041. During the reversal of the monsoons for both years, from Mar '11 - Jun '11 and Mar '12 - Jun '12, periods of high advance had been noticed. After the renovation of the headland, no change in profile was observed, possibly due to sand replenishments. During Dec '11 - Mar '12 and Jun '12 - Sep '12 low retreat occurred, and from Sep '12 - Dec '12 the retreat was high. See also Figure D.1.

Profile TMSI 042

TMSI 042 is the transect through the centre of the beach enclosed by headlands 8 and 9.

For this profile only periods of low advance and low retreat were observed. Low advance was observed for the S.W. monsoon periods Mar '11 - Sep '11 and Mar '12 - Sep '12, whereas low retreat was observed during the N.E. monsoon periods, from Sep '11 - Mar '12 and Sep '12 - Dec '12. See Figure D.2.

Profile TMSI 043

TMSI 043 is the transect through headland 9.

From Mar '11 - Jun '12 periods of low advance have been observed only. The reason for this is most probably because of renovation of headland 9 that was performed during the N.E. monsoon, around Dec '11. From Jun '12 - Sep '12 low retreat was observed, and from Sep '12 - Dec '12 high retreat. See also Figure D.3.

Profile TMSI 044

TMSI 044 is the transect through the centre of the beach enclosed by headlands 9 and 10.

From Mar '11 - Jun '11 and Dec '11 - Mar '12 low advance was observed. From Jun '11 - Dec '11 low retreat occurred, and for the remaining period no changes were observed. See Figure D.4.

Profile TMSI 045

TMSI 045 is the transect through headland 10.

Periods of high advance occurred from Mar '11 - Jun '11 and Mar '12 - Jun '12, during the S.W. monsoon. Low retreat then occurred during reversal of monsoons, from Jun '11 - Sep '11, Dec '11 - Mar '12 and Sep '12 - Dec '12. The remaining periods experienced high retreat, from Sep '11 - Dec '11 and Jun '12 - Sep '12. See Figure D.5.

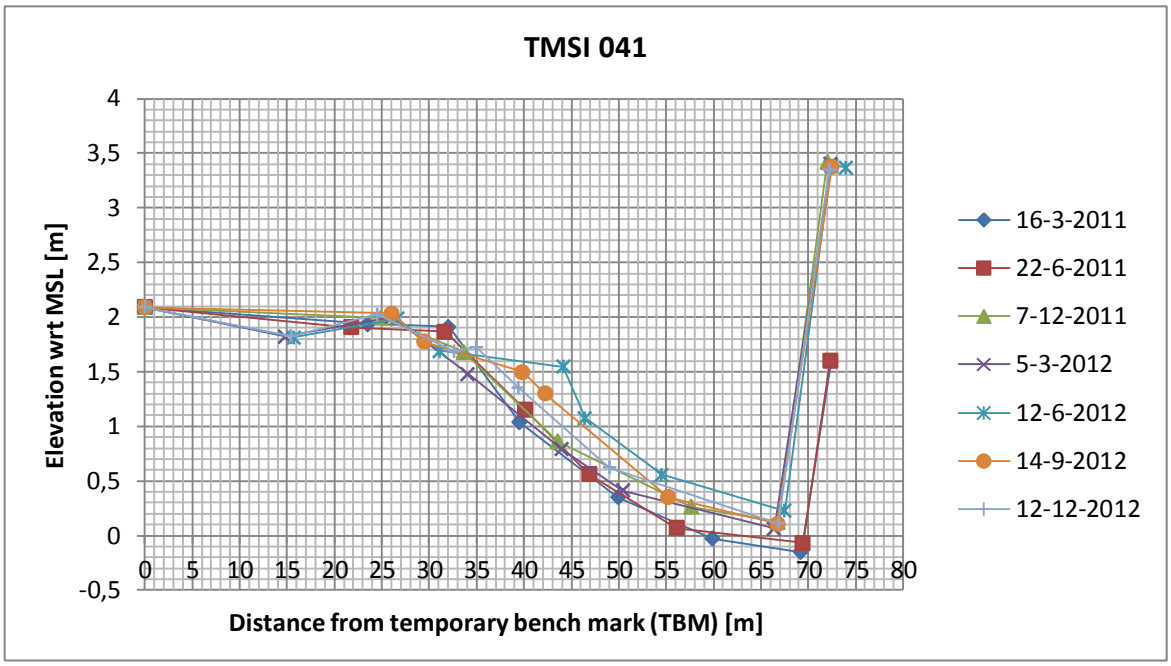

Figure D.2 Profile measurements for TMSI 041

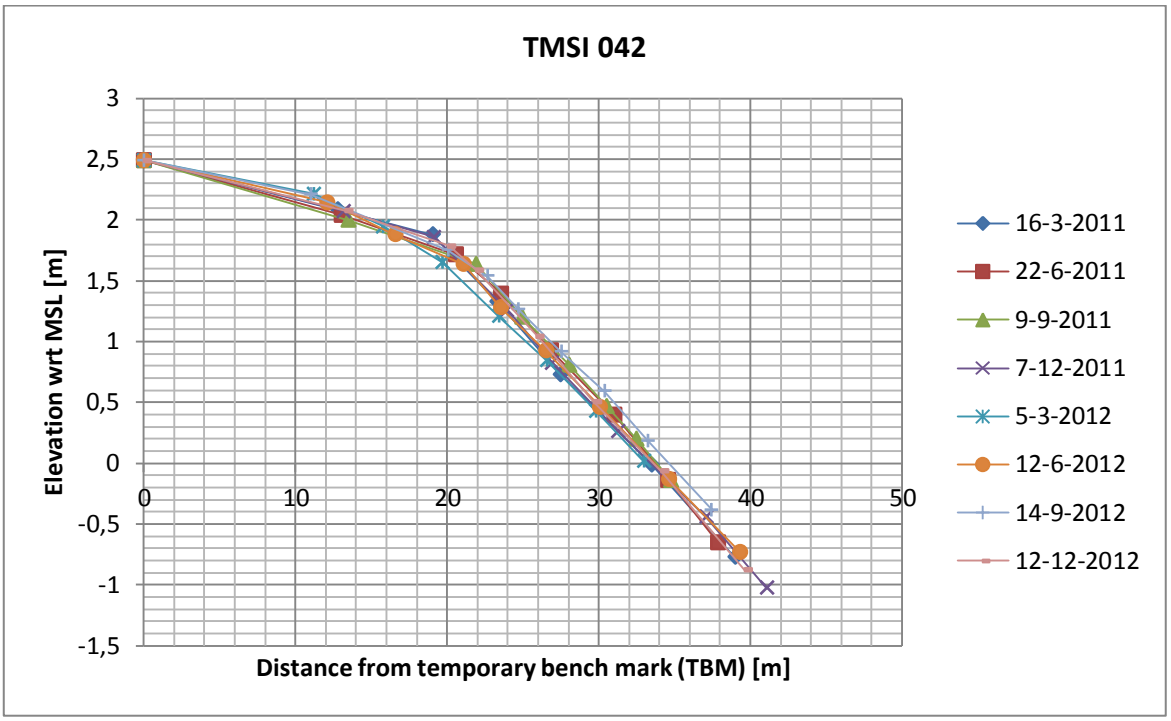

Figure D.3 Profile measurements for TMSI 042

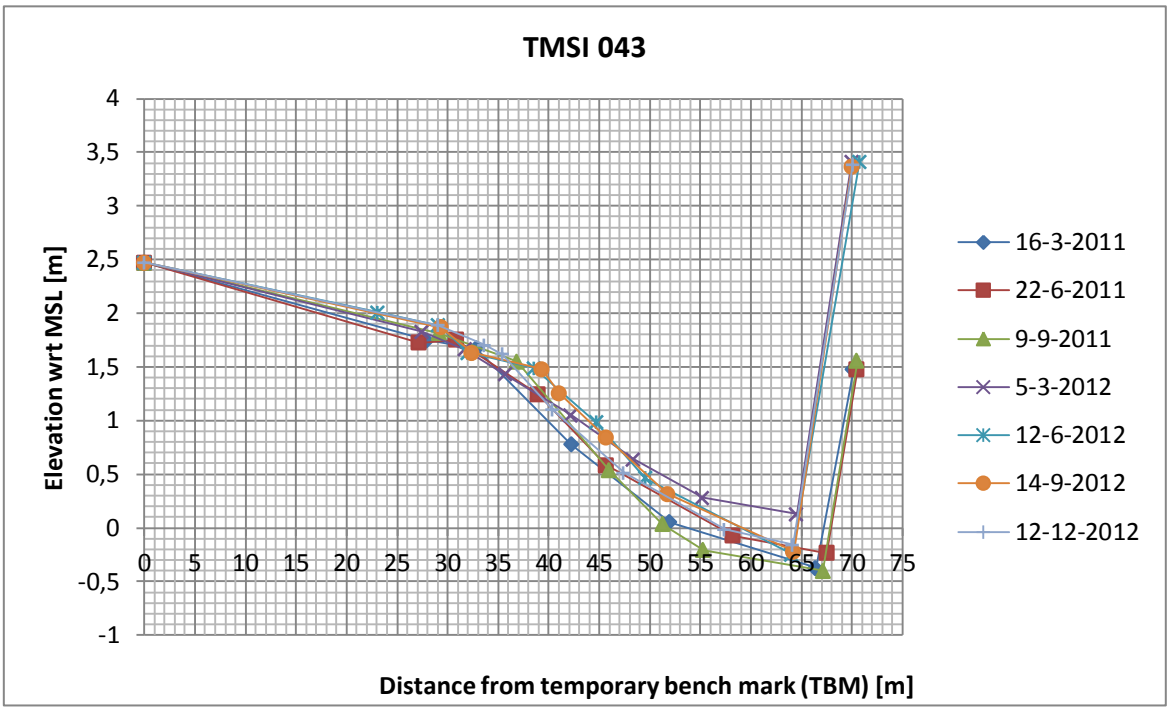

Figure D.4 Profile measurements for TMSI 043

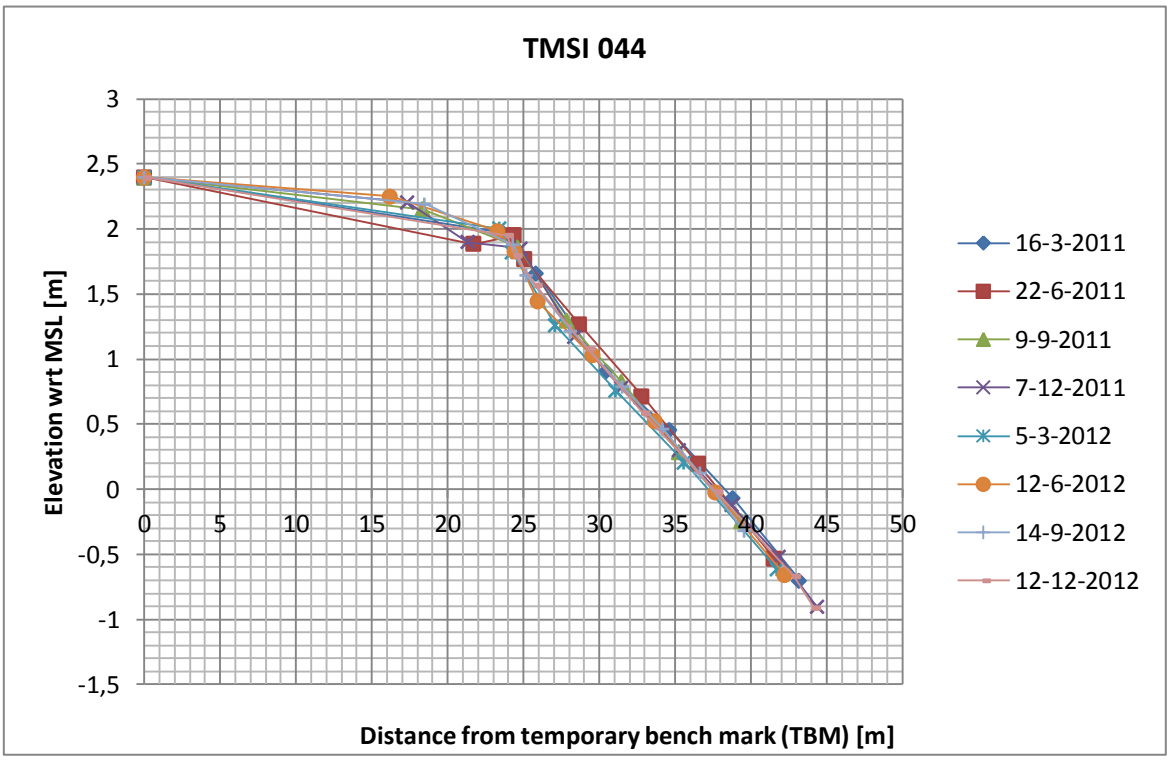

Figure D.5 Profile measurements for TMSI 044

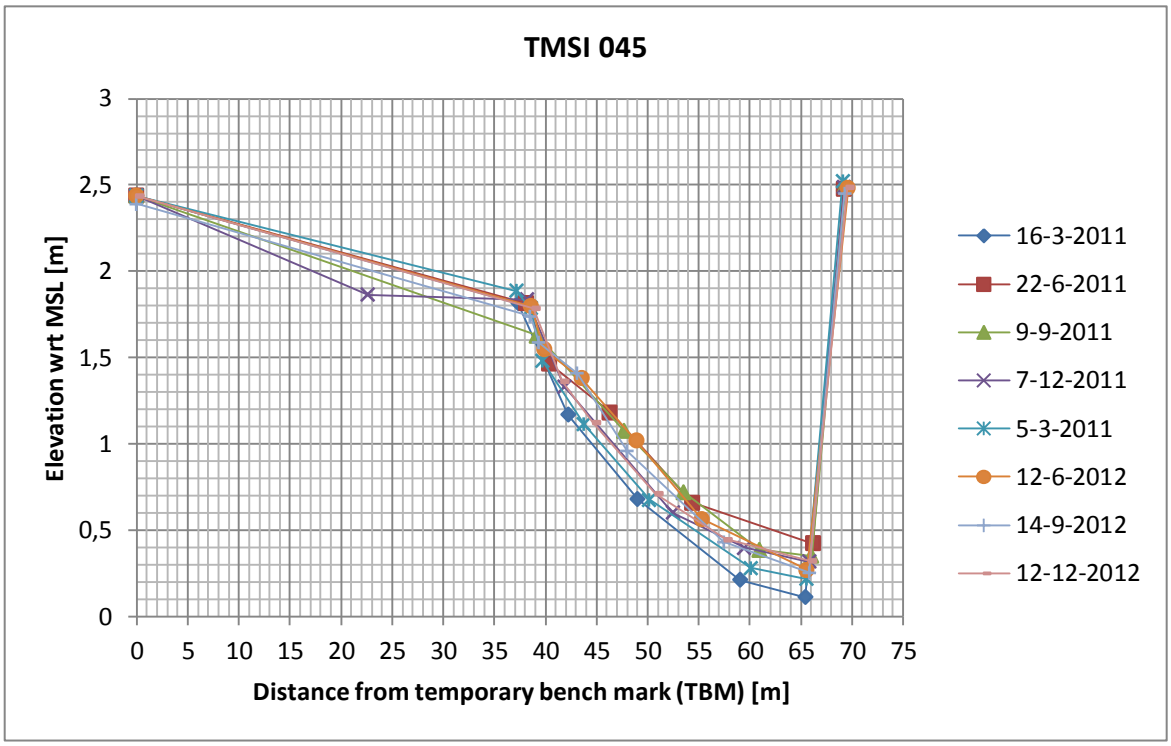

Figure D.6 Profile measurements for TMSI 045

D.2 Profile analysis

D.2.1 Cross-shore profile variation

In Figure D.6, Figure D.7 and Figure D.8 on the next pages the differences per measured profile have been illustrated, indicating locations of retreat and/or advance. From these illustrations it is seen that behind the headlands (TMSI041, 043 and 045) noticeable differences occur both in the upper and lower part of the profile, whereas in the other profiles TMSI042 andTMSI044) differences occur largely in the upper part of the profile only.

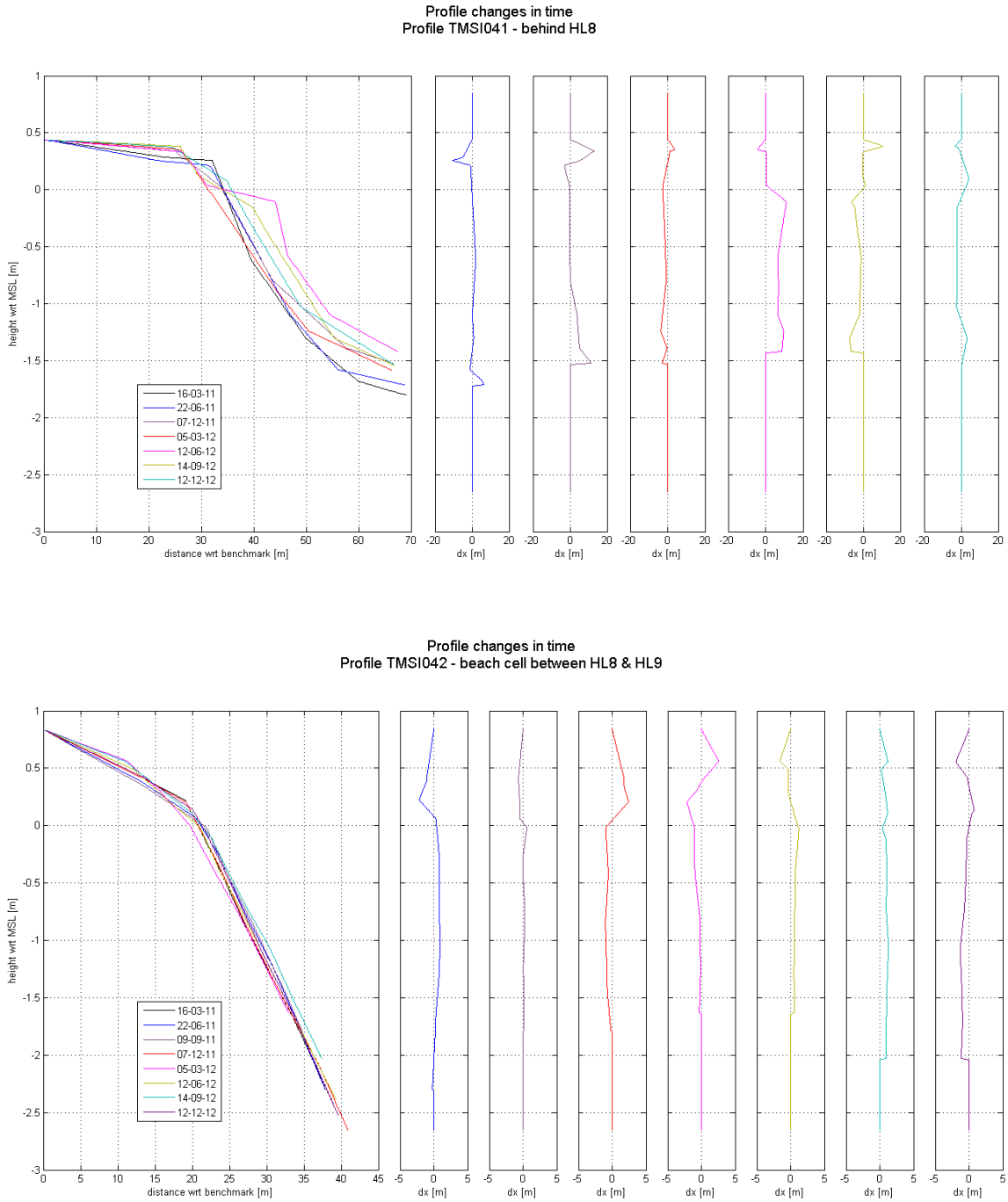

Figure D.7 Profile changes in time for profiles TMSI041 and TMSI042. Left the profile measurements are shown, and right the profile changes of consecutive profile measurements, each with an interval of 3 months during the years of 2011 and 2012.

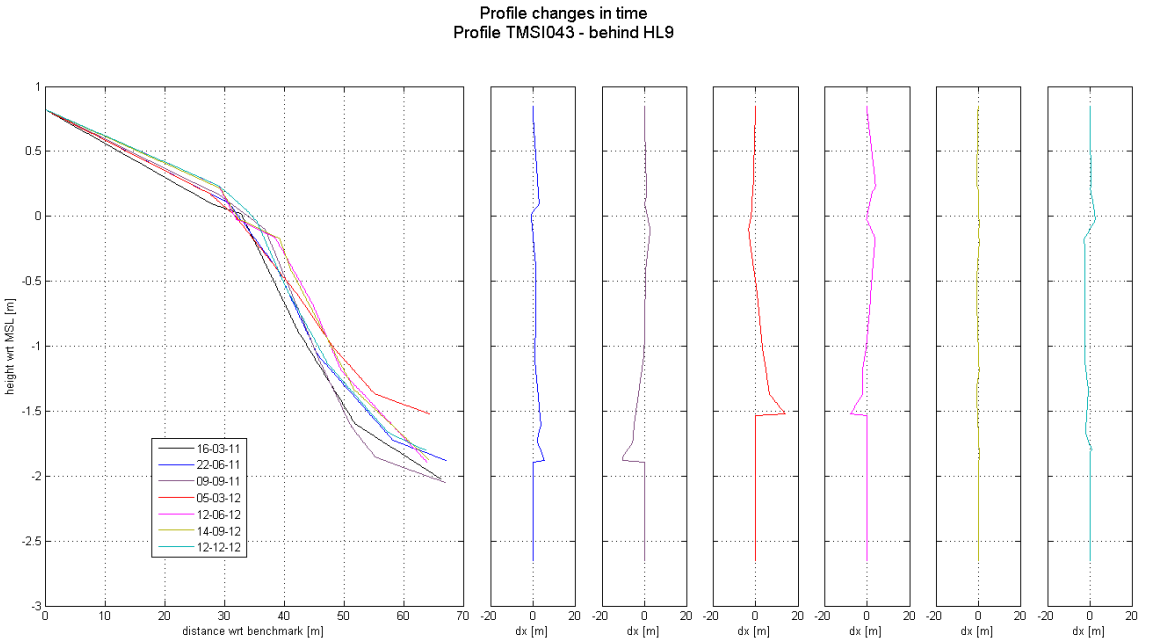

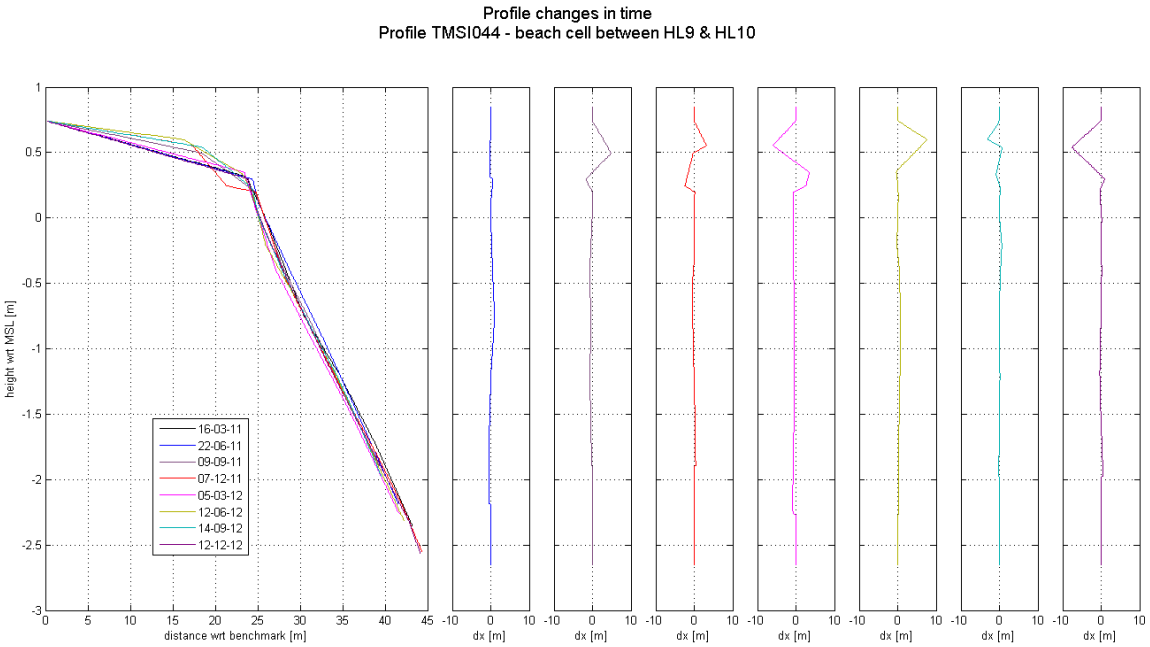

Figure D.8 Profile changes in time for profiles TMSI043 and TMSI044. Left the profile measurements are shown, and right the profile changes of consecutive profile measurements, each with an interval of 3 months during the years of 2011 and 2012.

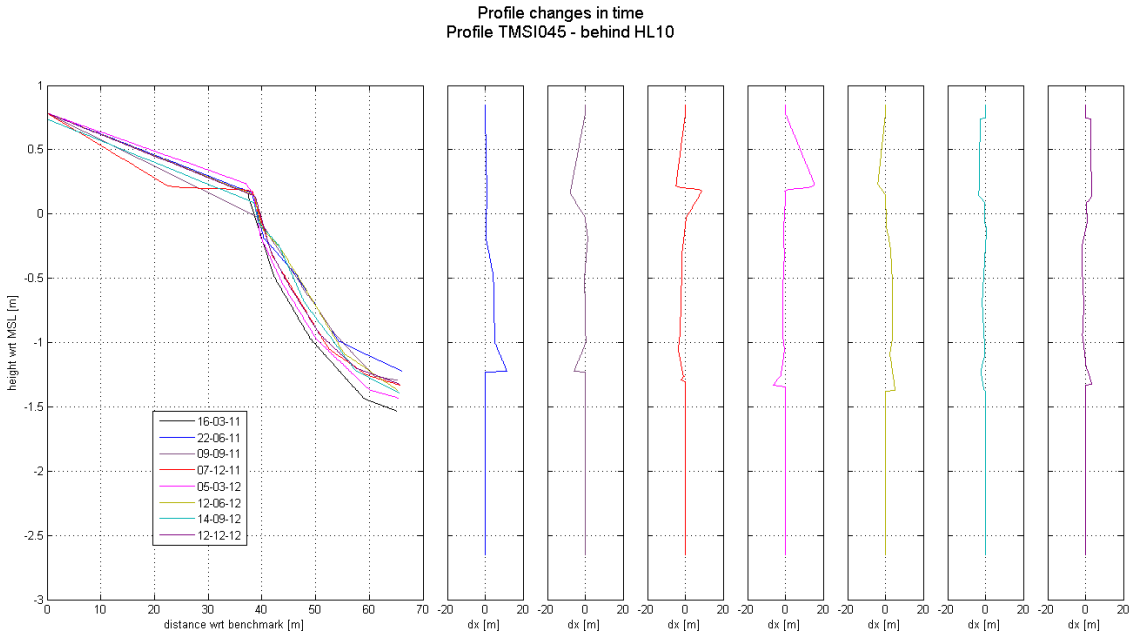

Figure D.9 Profile changes in time for profile TMSI045. Left the profile measurements are shown, and right the profile changes of consecutive profile measurements, each with an interval of 3 months during the years of 2011 and 2012.

D.2.2 Cross-shore profile evolution

In Figure D.9, Figure D.10 and Figure D.11on the next pages the coastline evolution along several locations of the cross-shore profiles have been illustrated, to indicate the time-dependent movement of the different positions of the coastal profile. From these illustrations it can only be seen in profile TMSI042 that a certain periodic behaviour in the profile seems to occur. However, considering the development in the other profiles, which are far more irregular, and the relatively short time period and thus limited amount of measurements it cannot be directly concluded whether this behaviour is also monsoon dependent.

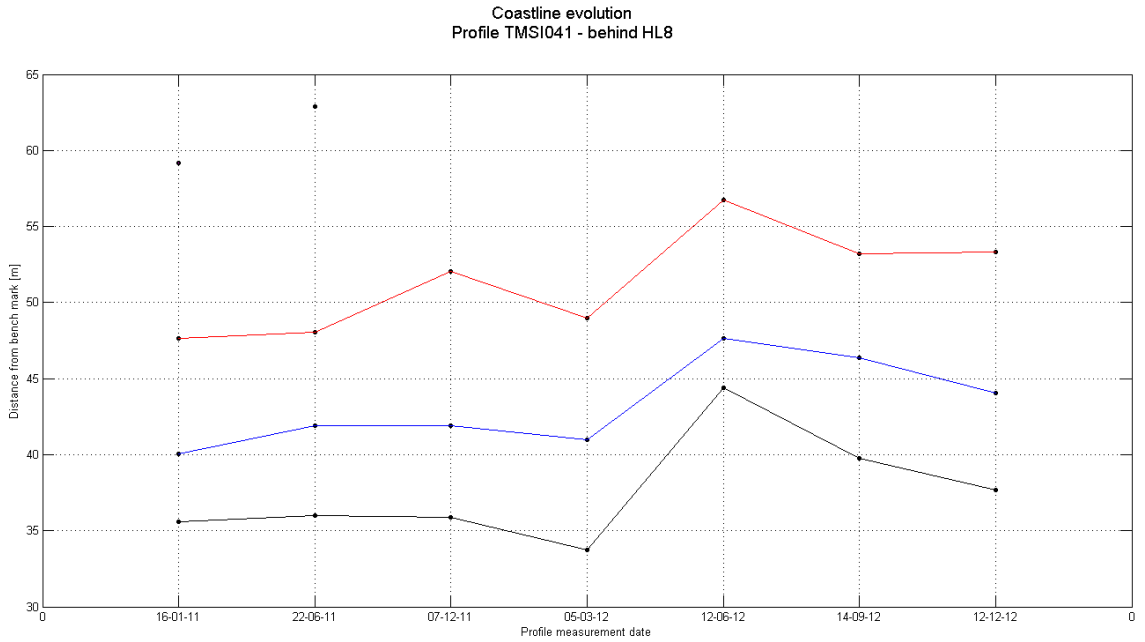

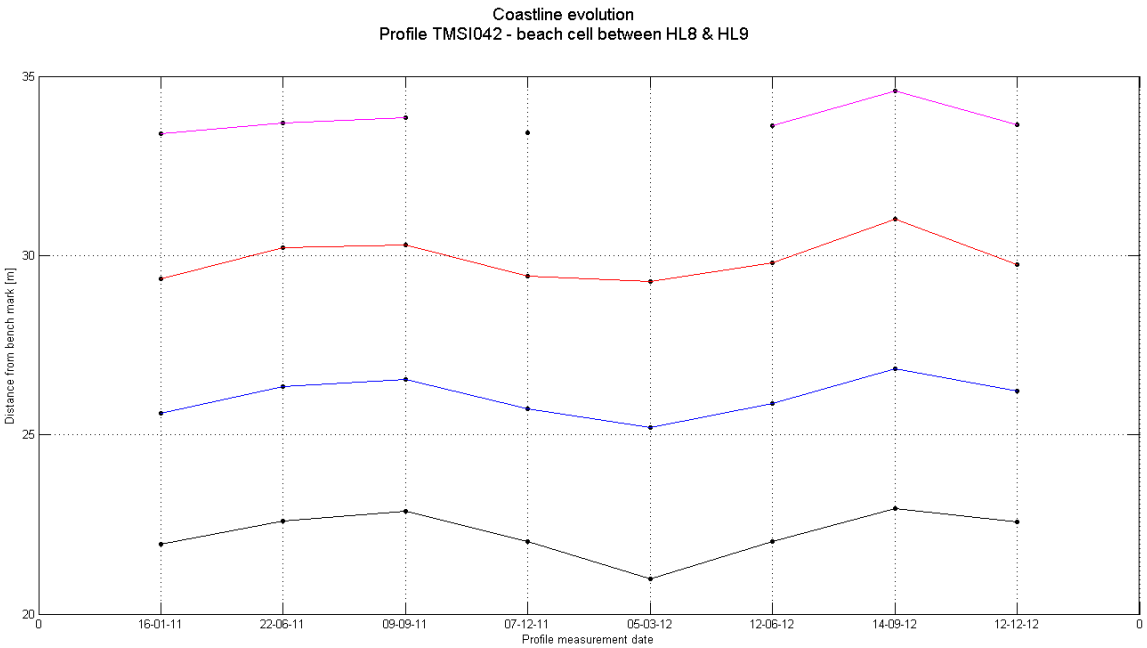

Figure D.10 Profile evolution along several points in the cross-shore direction of profiles TMSI041 and TMSI 042, for points at CD +1.5 m (black), CD +1.0 m (blue), CD +0.5 m (red) and CD + 0 m (magenta). Chart Datum is defined as MSL + 1.652 m. The latter evolution is interrupted due to missing points.

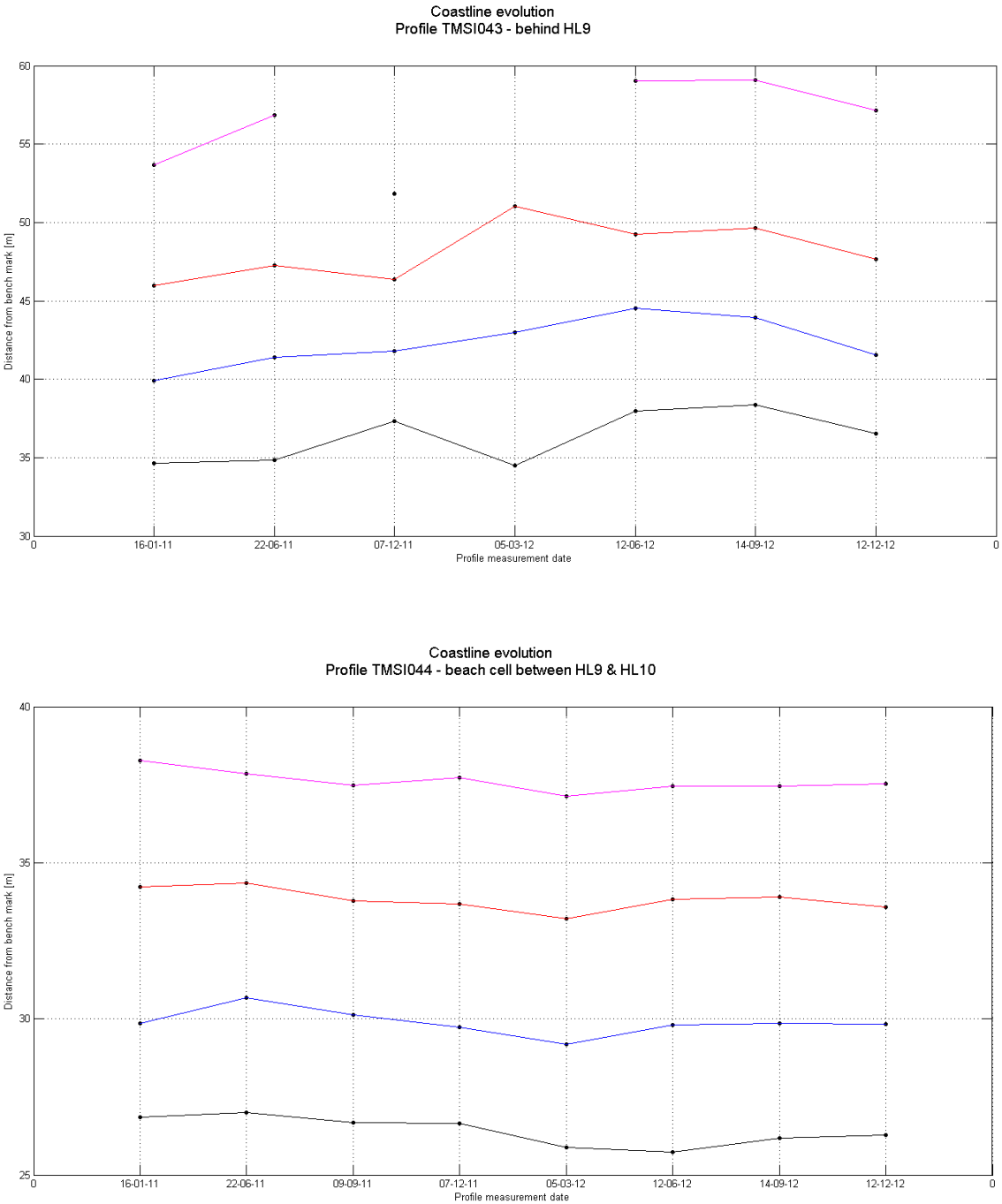

Figure D.11 Profile evolution along several points in the cross-shore direction of profiles TMSI043 and TMSI 044, for points at CD +1.5 m (black), CD +1.0 m (blue), CD +0.5 m (red) and CD + 0 m (magenta). Chart Datum is defined as MSL + 1.652 m. The latter evolution is interrupted due to missing points.

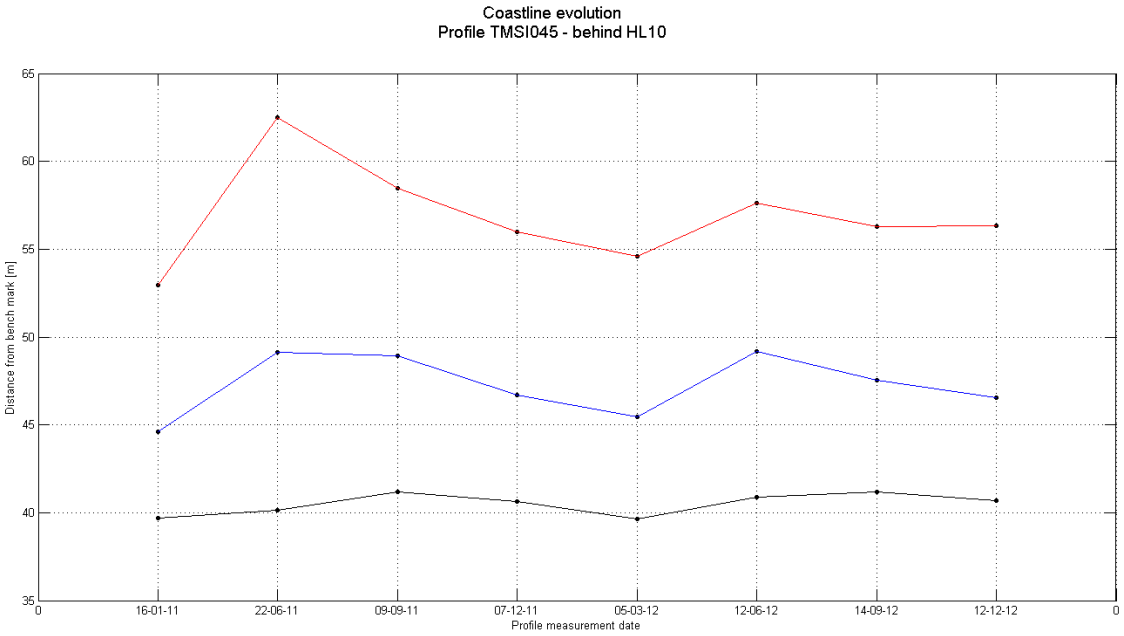

Figure D.12 Profile evolution along several points in the cross-shore direction of profile TMSI045, for points at CD +1.5 m (black), CD +1.0 m (blue), CD +0.5 m (red) and CD + 0 m (magenta). Chart Datum is defined as MSL + 1.652 m. The latter evolution is interrupted due to missing points.

E Unibest modelling results

In this appendix the modelling results of both the Unibest-TC and the Unibest-LT calculations are presented. In this study these models have merely been used to relatively quickly assess current velocities, sediment transports and profile developments. Considering the limited readily available input data for both models, calibration of the models with real-time measurements has not been possible. For that reason the model results have mainly been used to make a semi-quantitative assessment, rather than a fully quantitative one. For more background information on the models reference is made to the user guides of both models.

In both models several cross-shore rays have been chosen along East Coast Park to assess the desired parameters. In Figure E.1 these profiles have been illustrated. The difference in spacing between the first 7 profiles and the others is done intentionally, as the bathymetry in the eastern part along East Coast Park showed more uniformity. It should be stressed that due to the choice of fixed profile rays, wave focusing is excluded as a process in the nearshore region. It should be noted that the numbering of results might differ from Figure E.1, see also the description below the figure.

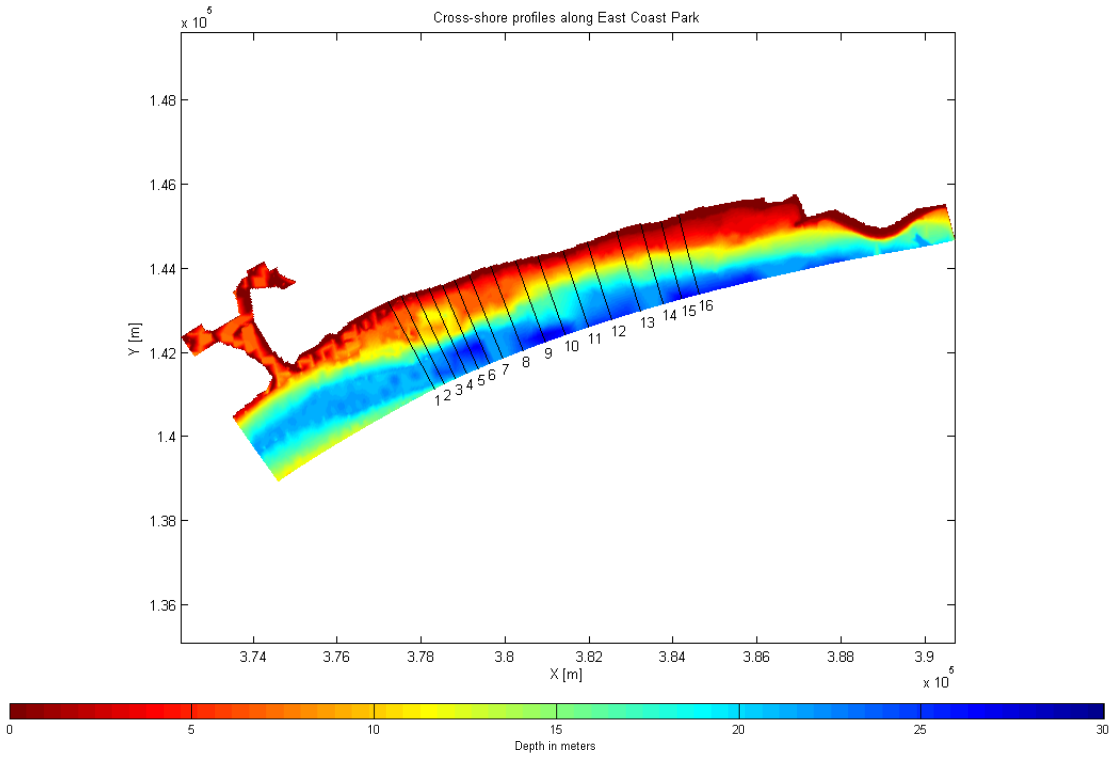

Figure E.1 Cross-sections of profiles along East Coast Park, as used in Unibest-TC and –LT. Due to the fact that more irregularity in the nearshore bathymetry was found in the western part along East Coast Park, between the first 7 profiles a smaller interval had been chosen than in between the other profiles. Because initially profiles were chosen along the whole southeast coast, the numbers of profiles might differ from the numbering presented here. Instead, profile 1 in this figure might be profile 9 in the model results, and profile 16 in the above figure then corresponds with profile 24 in the model results.

E.1 Unibest-TC

Using Unibest-TC we have been able to model cross-shore profile evolution as a function of time, and an indication has been obtained of sediment transports.

E.1.1 Profile development and sediment transports

Due to insufficiently readily available data for calibration of the model, model results should be regarded with much care as there are too many uncertainties influencing these results. What is tried to illustrate here is the shape of the profile development, regardless of the values obtained of coastal retreat or advance. The same holds for the results for the sediment transports, of which the main interest lies in the shape of the cross- and longshore sediment transport curves and their position, rather than the actual values.

In the graphs on the subsequent pages only some examples have been shown for the N.E. monsoon calculations, in which, however, the aforementioned magnitudes are not neglected from the images. Instead the reader is expected to regard these with care. Due to instabilities when trying to model larger grain sizes, the model results shown are for a grain diameter of 0.6 mm, with an angle of repose $\tan\varphi$ of 0.25. The latter parameter formed one of the uncertainties in the model, since the angle of repose is amongst others dependent on the grain size diameter. A larger angle of repose then implies a larger possible profile slope. However, a for these calculations a default value was chosen. The calculations were performed for a period of one year for both the (upscaled) N.E. and S.W. monsoon.

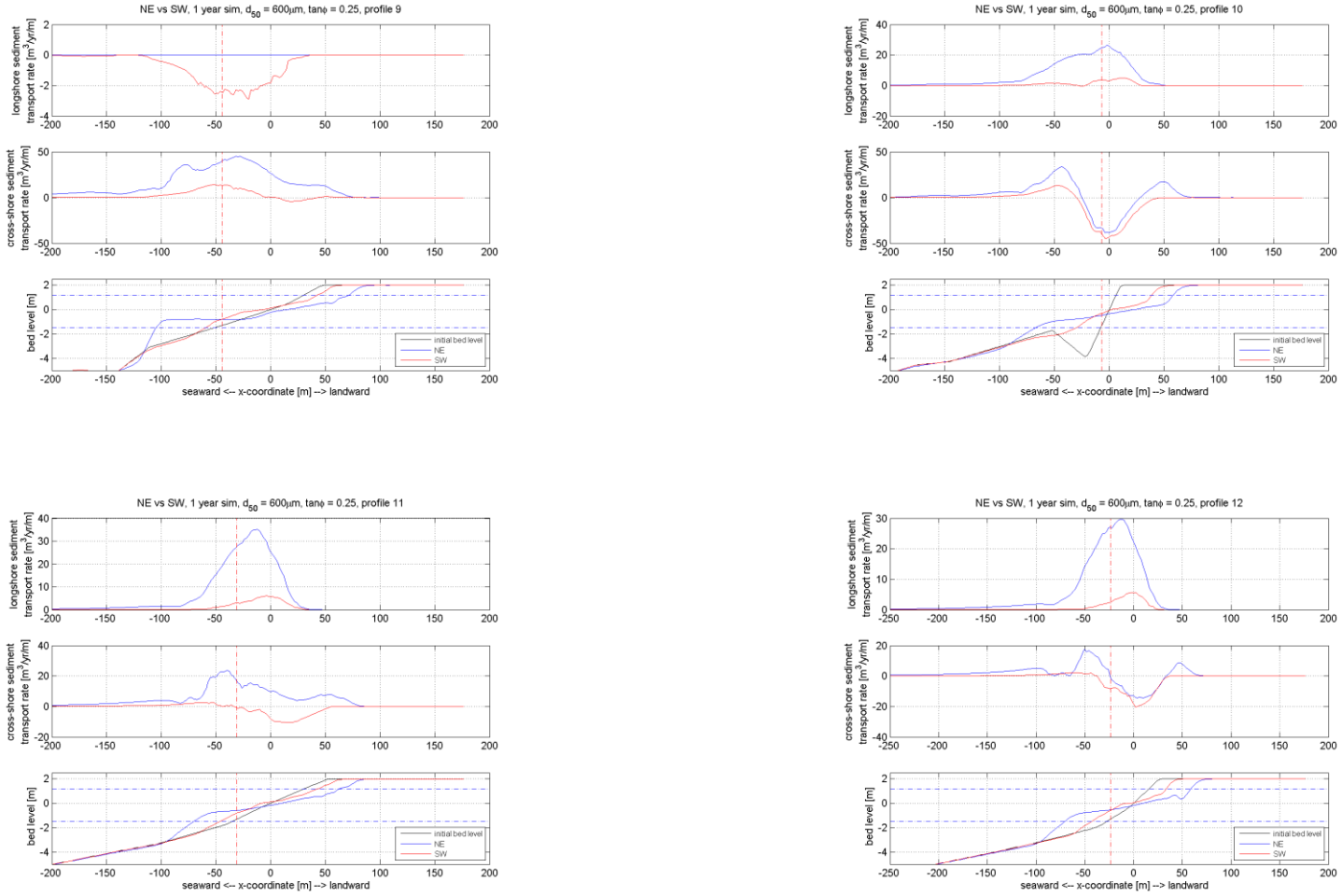

Figure E.2 Cross-shore profile development and sediment transports for both the N.E. and S.W. monsoon during 1 year for profiles 1 (upper left), 2 (upper right), 3 (lower left) and 4 (lower right) for a sediment diameter of 0.6 mm.

E.1.2 Timescale to morphological equilibrium

Besides the profile development we wanted to know how long it would approximately take for the profile to reach a certain morphological equilibrium, be it static or dynamic. To do so some other illustrations were made, as shown in the figures on the subsequent pages. Similar to the model results from before, also here care should be taken when looking at values.

Some examples of model results are shown for both the N.E. and S.W. monsoon, for a grain diameter of 0.6 mm, with an angle of repose tanφ of 0.25. The latter parameter formed one of the uncertainties in the model, since the angle of repose is amongst others dependent on the grain size diameter. A larger angle of repose then implies a larger possible profile slope. However, a for these calculations a default value was chosen. The calculations were performed for a period of one year for both the (upscaled) N.E. and S.W. monsoon. In the figures on the next pages firstly results are shown for the N.E. monsoon calculations, thereafter for the S.W. monsoon.

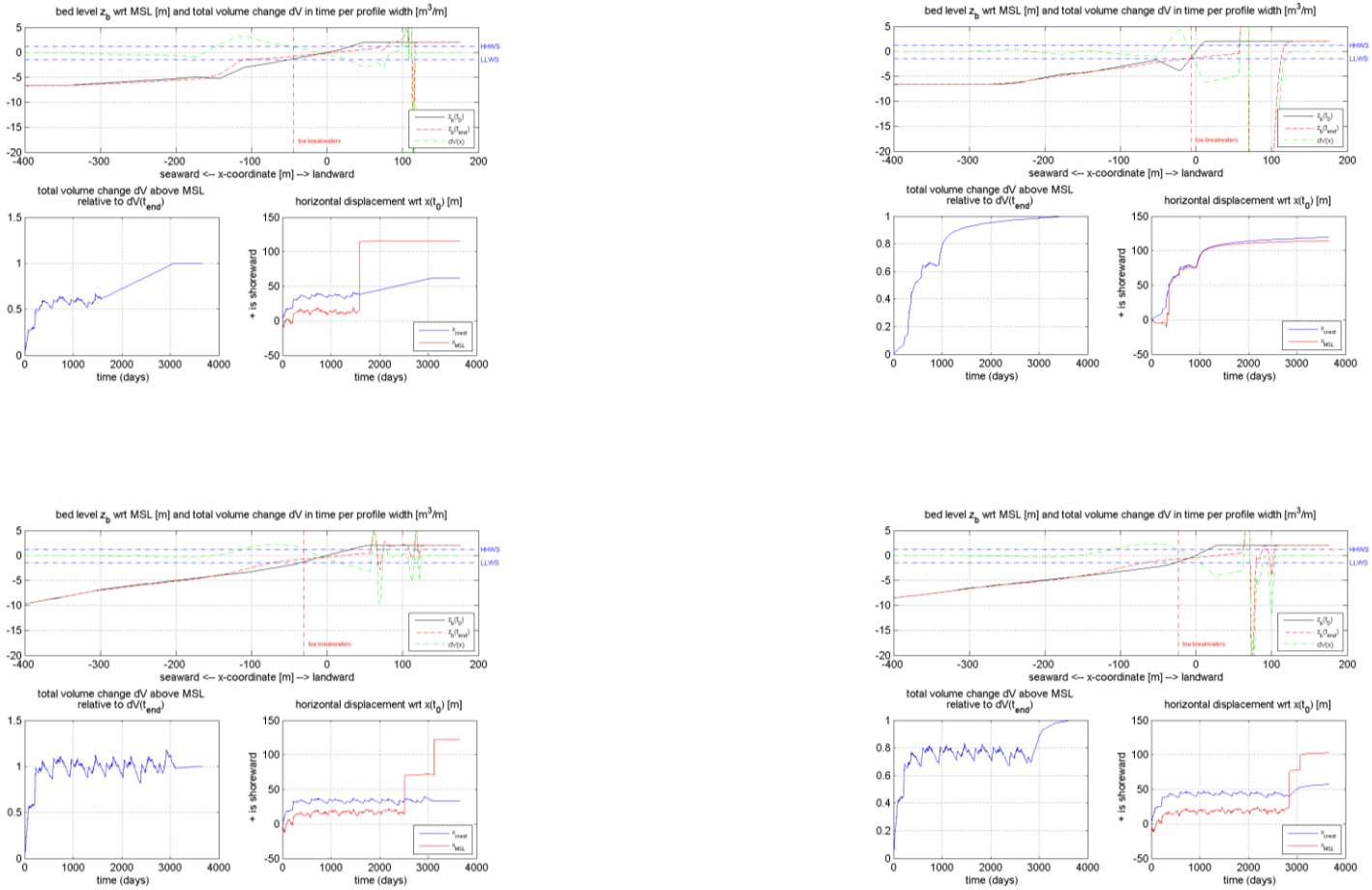

*Figure E.3 Timescale of morphological equilibrium for total volume change dV above MSL relative to $dV(t_{end})$. Modelling time is 10 years of a **N.E. monsoon** wave climate, for sediment diameter of 0.6 mm. Upper from left to right: profiles 1 and 2; Lower from left to right: profiles 3 and 4.*

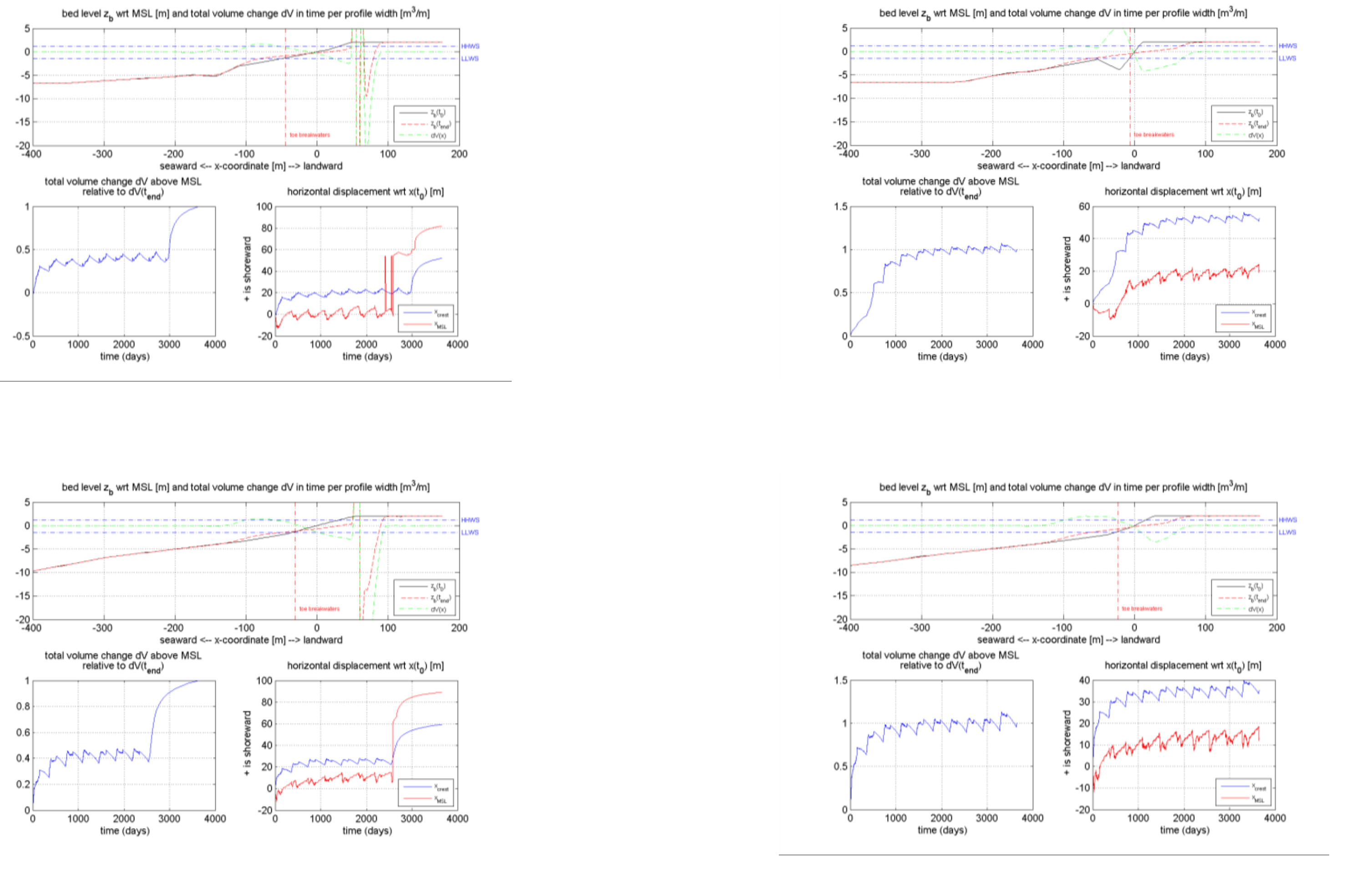

*Figure E.4 Timescale of morphological equilibrium for total volume change dV above MSL relative to dV(t_{end}). Modelling time is 10 years of a **S.W. monsoon** wave climate, for sediment diameter of 0.6 mm. Upper from left to right: profiles 1 and 2; Lower from left to right: profiles 3 and 4.*

E.2 Unibest-LT

Using Unibest-LT we have been able to obtain parameters related to (longshore) sediment transport, by modelling the cross-shore wave transformation for each profile.

For illustration purposes some example results are shown in Figure E.5 and Figure E.6 on the next pages, for both the N.E. and S.W. monsoon, respectively. What can be seen is that during the S.W. monsoon the wave-induced longshore current caused by the predominant significant wave height of 0.35 m, an eastward current occurs.

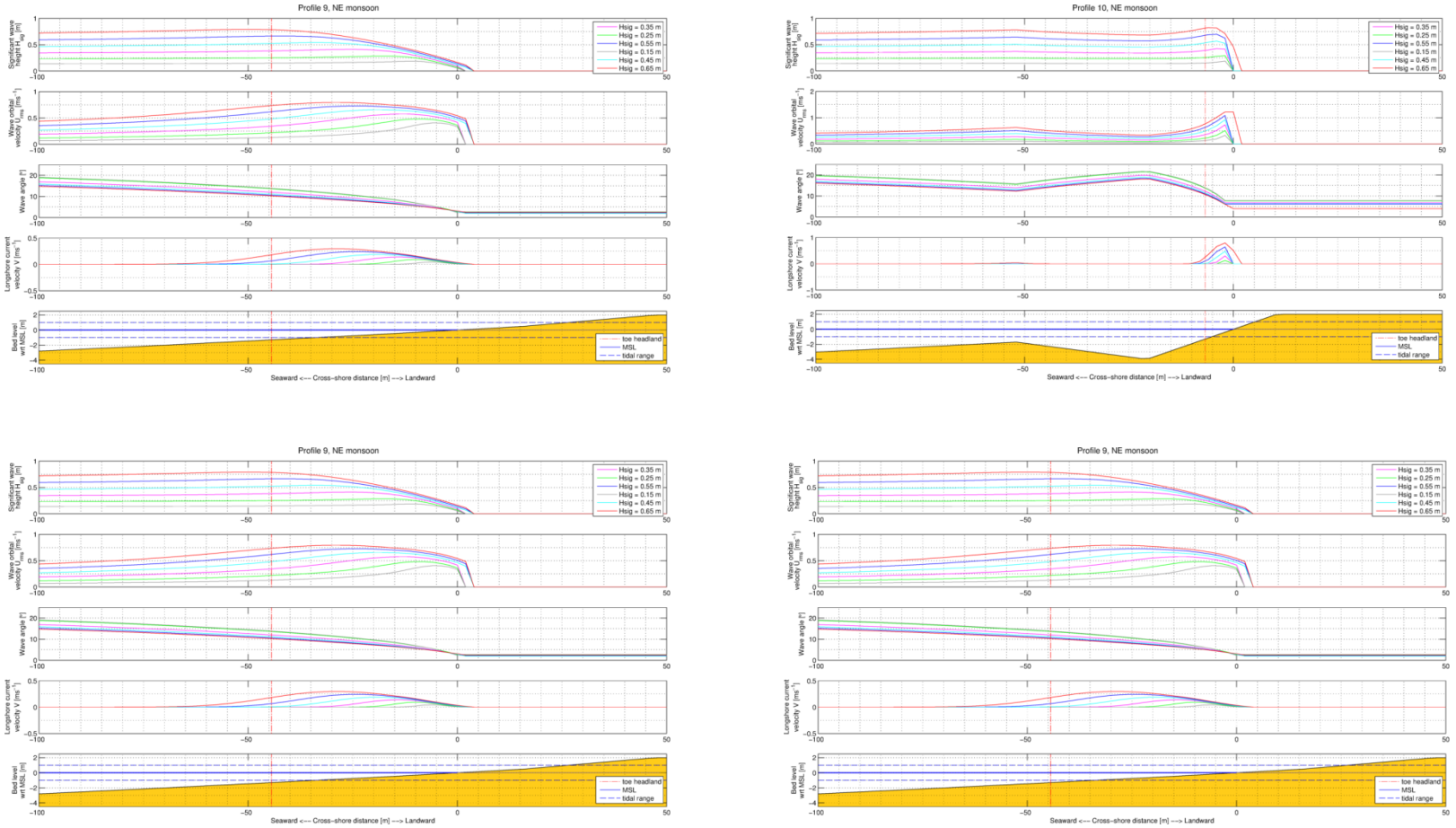

*Figure E.5 Wave transformation and resulting current along profiles 1 (upper left), 2 (upper right), 3 (lower left) and 4 (lower right) for H_s = 0.65 (red), 0.55 (navy), 0.45 (light blue), 0.35 (magenta), 0.25 (green) and 0.15 (grey) m during the **N.E. monsoon**. From top to bottom: the significant wave height H_s, the wave orbital velocity U_{rms}, the wave angle, the longshore current velocity V and the bed level. The vertical red line indicates the average location of the toe of headlands along East Coast Park.*

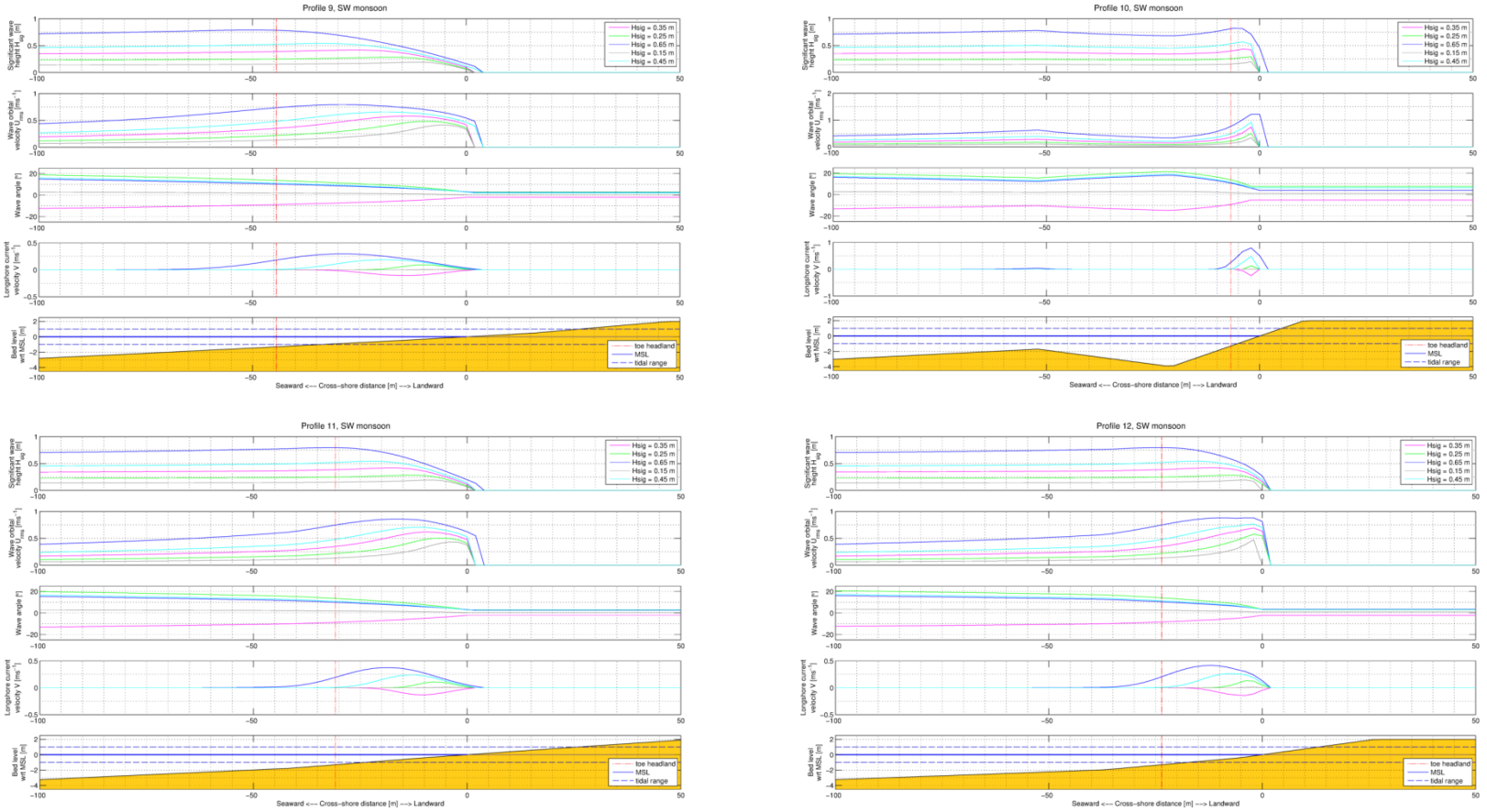

*Figure E.6 Wave transformation and resulting current along profiles 1 (upper left), 2 (upper right), 3 (lower left) and 4 (lower right) for H_s = 0.65 (navy), 0.45 (light blue), 0.35 (magenta), 0.25 (green) and 0.15 (grey) m during the **S.W. monsoon**. From top to bottom: the significant wave height H_s, the wave orbital velocity U_{rms}, the wave angle, the longshore current velocity V and the bed level. The vertical red line indicates the average location of the toe of headlands along East Coast Park.*

F Delft3D modelling results

In this section the model results of the flow velocities and sediment transports during the N.E. monsoon (December and January) are presented.

The results were obtained by Julia Vroom by nesting a 2D model in the 2D Singapore Regional Model (SRM), of which the bathymetry was obtained from the 3D SRM. The computational grid of the nested model has cells of 30 by 30 m.

Firstly the results are presented from a bird view, showing the velocity and transport vectors in the coastal waters of East Coast Park. Afterwards, several cross-sections are presented of both cross-shore and longshore components of flow velocity and sediment transport.

F.1 Vector results

F.1.1 Flow velocities

On the next pages the results for the flow velocities for the months June (S.W. monsoon), December and January (N.E. monsoon) are presented in Figure F.1 to Figure F.3. Note that the differences in flow velocities between the monsoons are minor.

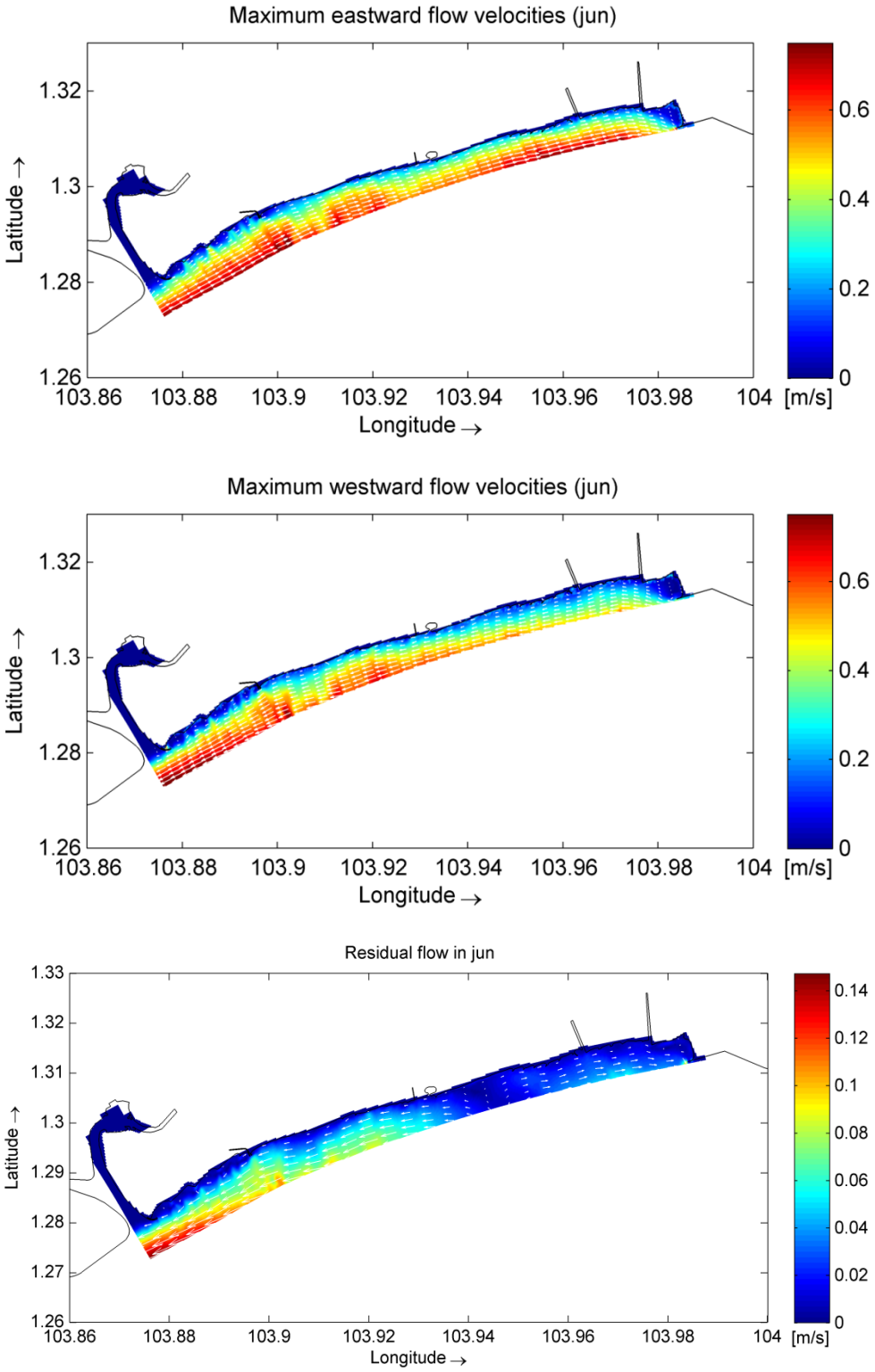

Figure F.1 Flow velocity vectors of tidal currents southeast of Singapore for June, representing the S.W. monsoon. The velocities have been computed using a nested Delft3D model in the 2D Singapore Regional Model. The results show maximum eastward and westward directed flow velocities in the upper and middle panel, respectively. The lower panel shows the residual flow velocities. The model results were obtained from Julia Vroom at Deltares.

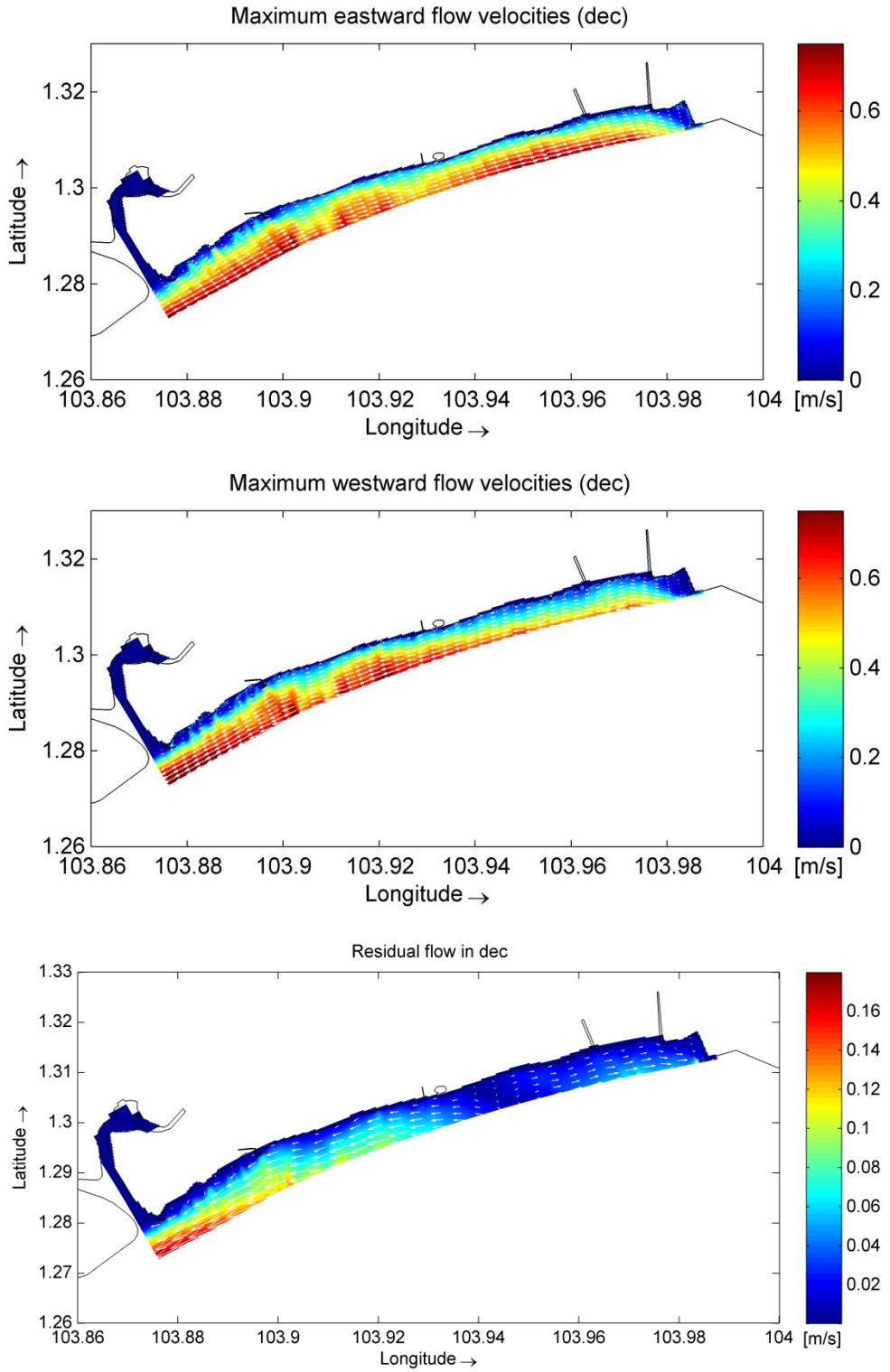

Figure F.2 Flow velocity vectors of tidal currents southeast of Singapore for December, representing the N.E. monsoon. The velocities have been computed using a nested Delft3D model in the 2D Singapore Regional Model. The results show maximum eastward and westward directed flow velocities in the upper and middle panel, respectively. The lower panel shows the residual flow velocities. The model results were obtained from Julia Vroom at Deltares.

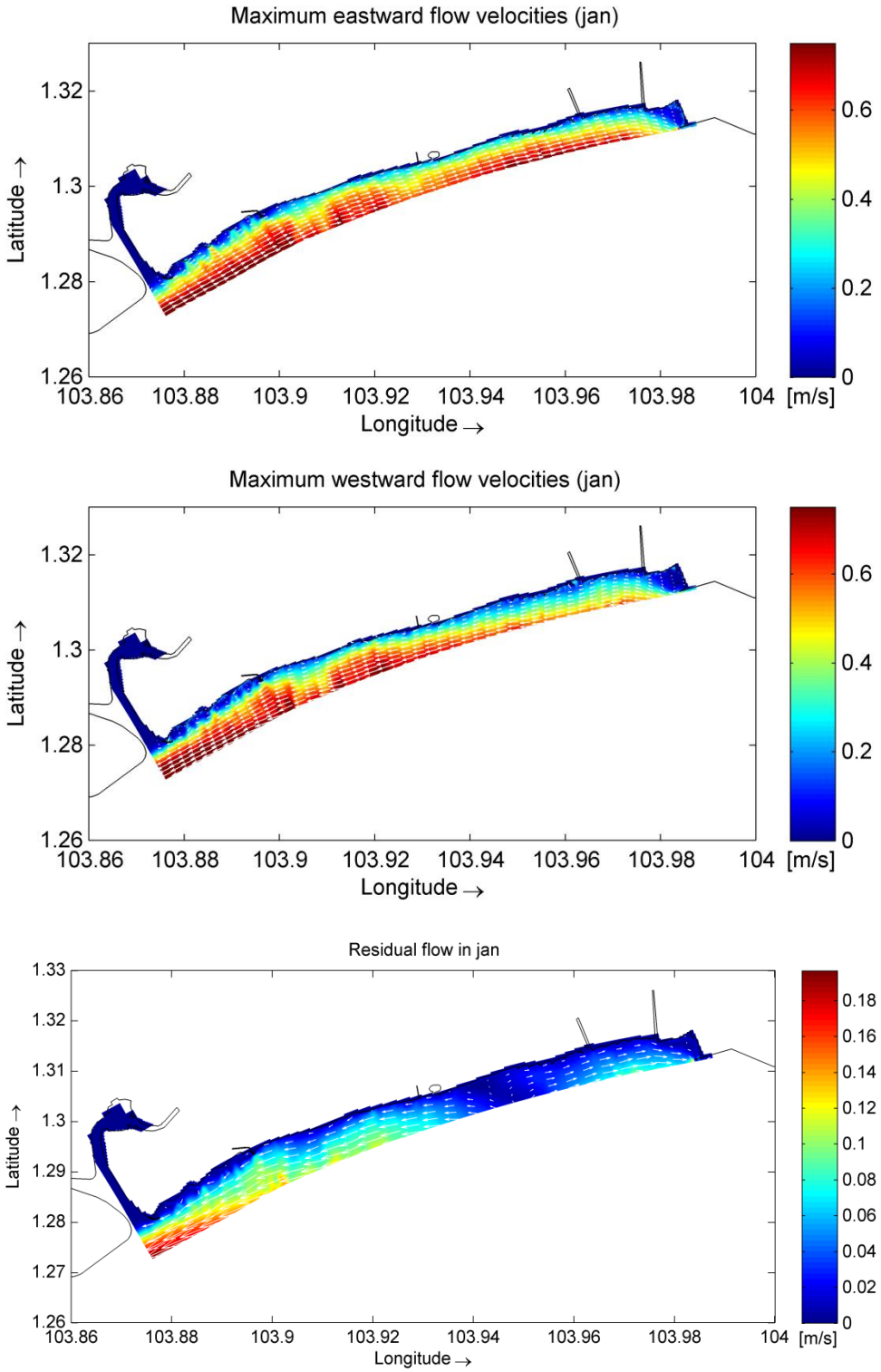

Figure F.3 Flow velocity vectors of tidal currents southeast of Singapore for January, representing the N.E. monsoon. The velocities have been computed using a nested Delft3D model in the 2D Singapore Regional Model. The results show maximum eastward and westward directed flow velocities in the upper and middle panel, respectively. The lower panel shows the residual flow velocities. The model results were obtained from Julia Vroom at Deltares.

F.1.2 Sediment transports

On the next page, in Figure F.4, modelling results are shown for all three modelled periods (June, December and January) for ease of comparison. Note how in June most of the transport is eastward directed, in December a large part along the western shore of East Coast Park is directed westward, while in January eastward directed sediment transport seems to take over the westward directed transport in the west.

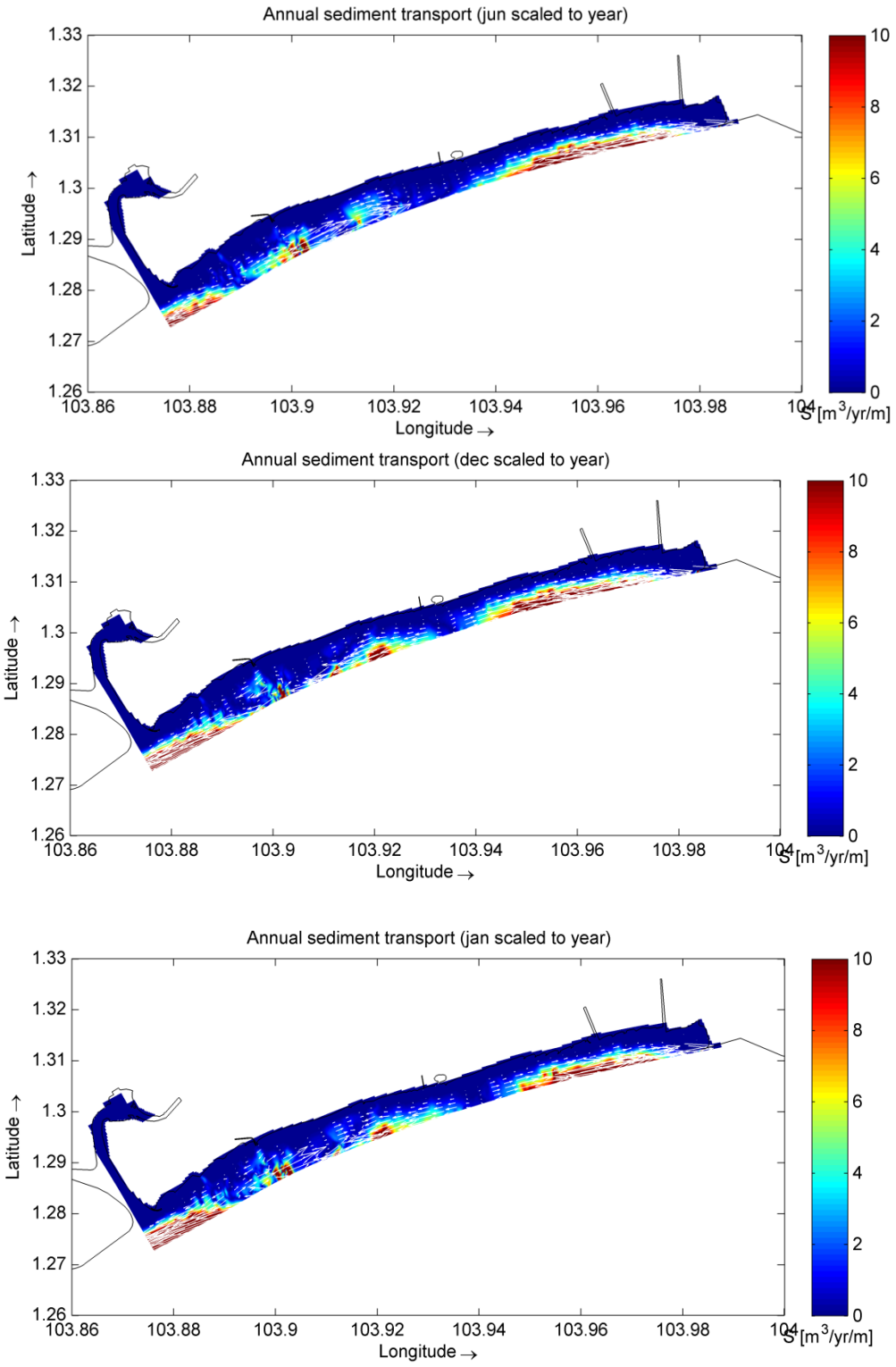

Figure F.4 Sediment transport vectors due to tidal currents southeast of Singapore for June (upper panel), representing the S.W. monsoon, and December (middle panel) and January (lower panel), representing the N.E. monsoon. The model results were obtained from Julia Vroom at Deltares.

F.2 Cross-shore distribution of X- and Y-components

In this section finally the aforementioned results are shown along several rays along the coastline, as shown in Figure F.5. The rays that are relevant to East Coast Park are cross-sections 200, 300 and 400 and therefore only these have been presented in this section.

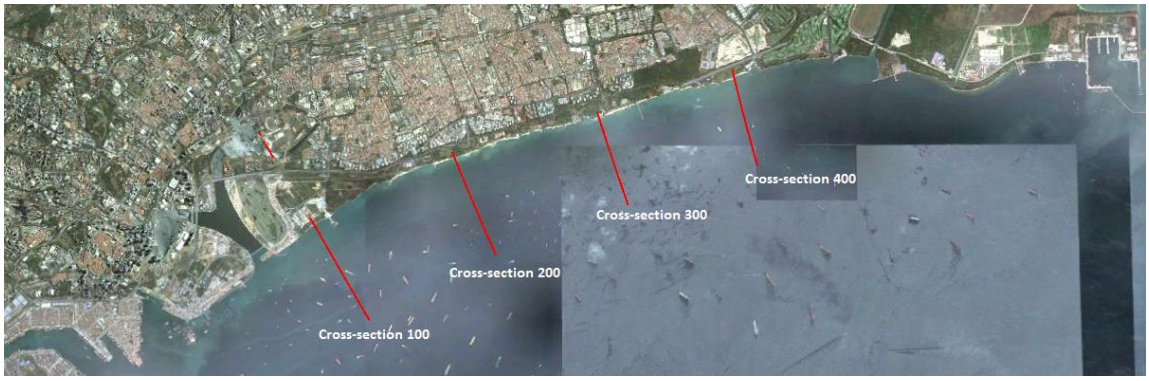

Figure F.5 Several cross-sectional rays along the southeast coast of Singapore, where Cross-sections 200, 300 and 400 are along East Coast Park.

In the western part of East Coast Park (Figure F.6) sediment transport seems to pick up at about the 6 m depth contour. Looking at the longshore component of the sediment transport, firstly the sediment transport is eastward directed, but this reverses to a westward directed transport further offshore. During the S.W. monsoon eastward directed transport is most prominent, whereas during the N.E. monsoon westward directed transport is most prominent. Regarding the cross-shore component of the sediment transport, a northward (onshore) directed transport occurs during the S.W. monsoon and a southward (offshore) directed transport during the N.E. monsoon.

In the central part of East Coast Park (Figure F.7), sediment is seen to be picked up from about the 5 m depth contour. Alongshore, eastward directed transport is found during June and December, but in January westward directed transport occurs as well. In cross-shore direction, the sediment is transported southwards (offshore) during June and December, but northwards (onshore) in the nearshore region during January.

Finally, in the eastern part of East Coast Park (Figure F.8), sediment is seen to be picked up at about the 3 m depth contour (note that water depths become shallower further offshore in eastward direction). In alongshore direction sediment transport is directed eastward for all of the modeled periods, while in cross-shore direction it is directed northwards (onshore) for all periods.

In all of the model results it can be seen that tide-induced sediment transport near the shoreline is negligible. Keeping in mind that sediment transports have been obtained using a D_{50} of 0.2 mm, it seems plausible to conclude that the contribution of the tide-induced flow velocities to (short-term) sediment transport is insignificant along East Coast Park.

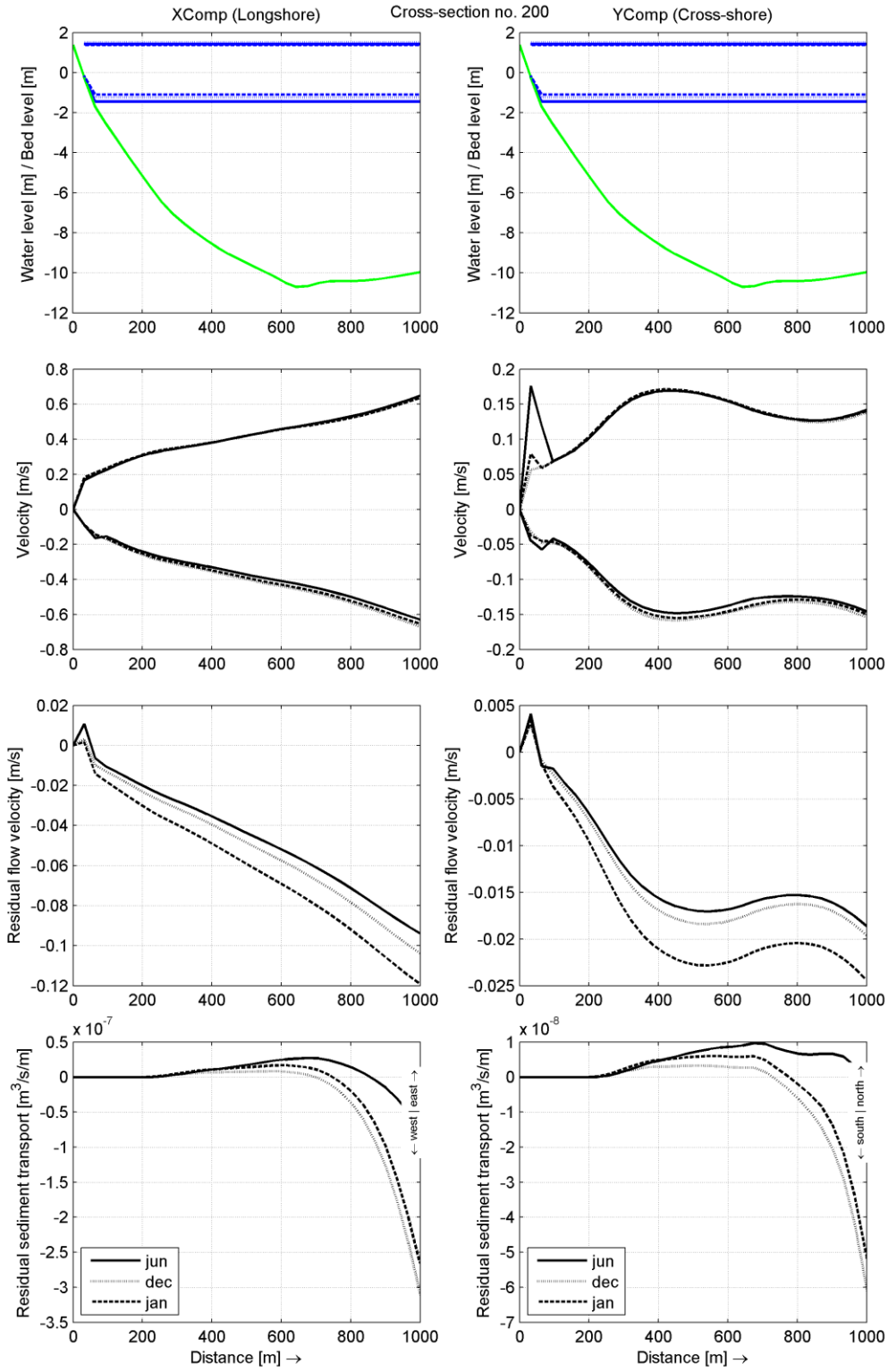

Figure F.6 Cross-section 200: cross-shore distribution of in cross- and longshore flow velocities and sediment transport rates for the months June (S.W. monsoon), December and January (N.E. monsoon). In the left column the longshore components are illustrated, and in the right the cross-shore components.

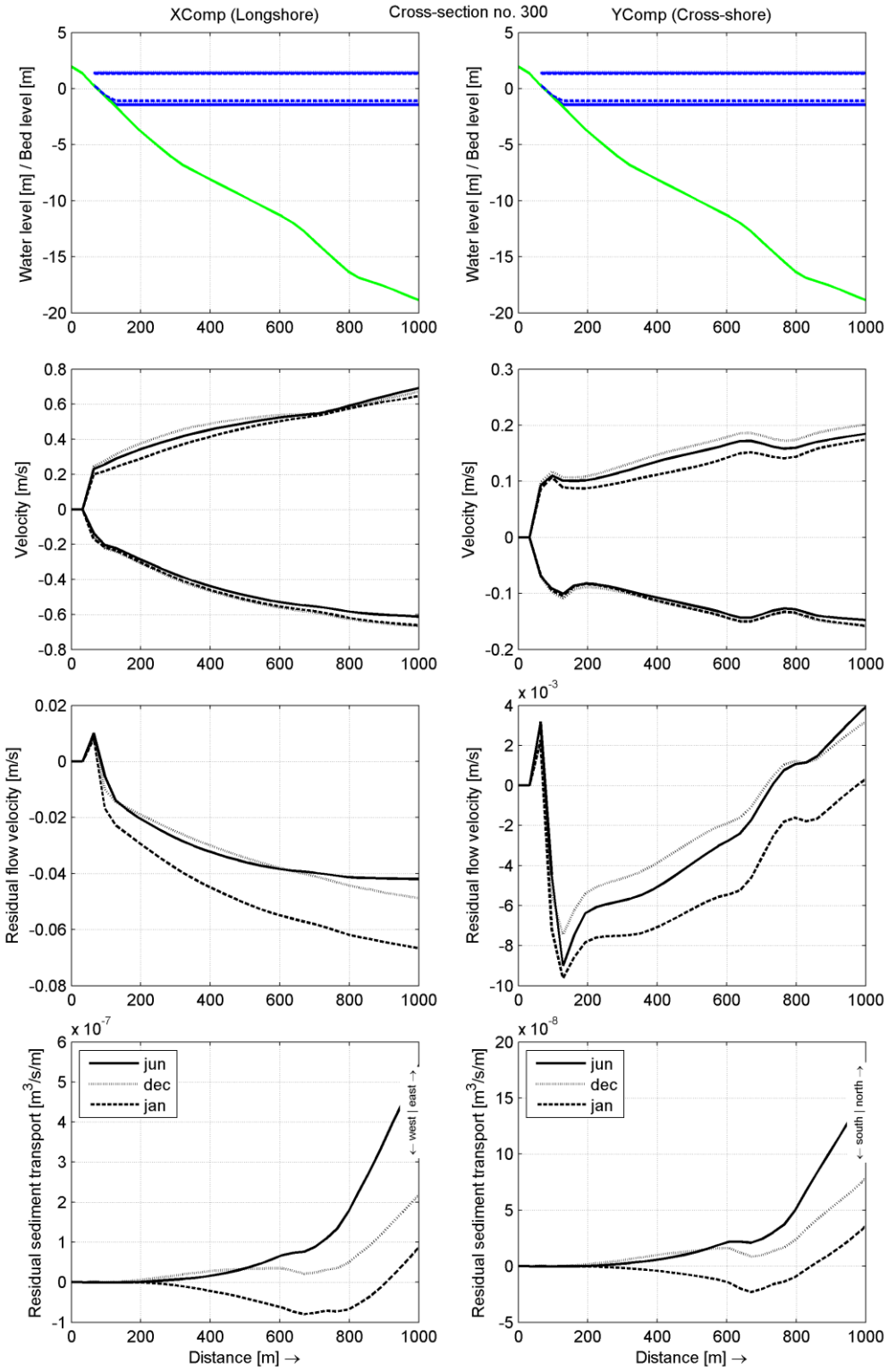

Figure F.7 Cross-section 300: cross-shore distribution of in cross- and longshore flow velocities and sediment transport rates for the months June (S.W. monsoon), December and January (N.E. monsoon). In the left column the longshore components are illustrated, and in the right the cross-shore components.

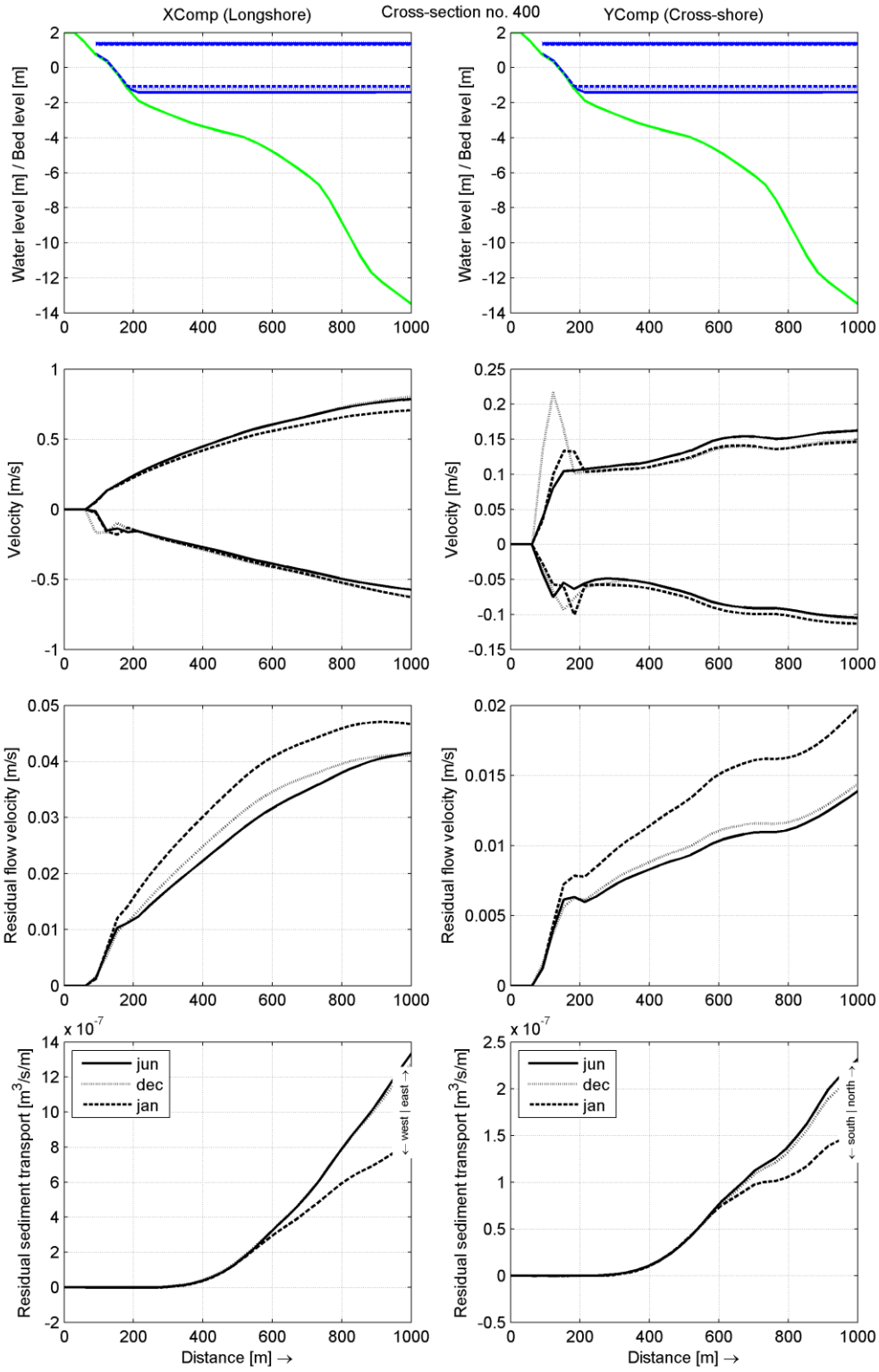

Figure F.8 Cross-section 400: cross-shore distribution of in cross- and longshore flow velocities and sediment transport rates for the months June (S.W. monsoon), December and January (N.E. monsoon). In the left column the longshore components are illustrated, and in the right the cross-shore components.